

Thermodynamic Properties of Alkali Metal Hydroxides. Part II. Potassium, Rubidium, and Cesium Hydroxides

Cite as: Journal of Physical and Chemical Reference Data **26**, 1031 (1997); <https://doi.org/10.1063/1.555996>

Submitted: 21 July 1995 . Published Online: 15 October 2009

L. V. Gurvich, G. A. Bergman, L. N. Gorokhov, V. S. Iorish, V. Ya. Leonidov, and V. S. Yungman



View Online



Export Citation

ARTICLES YOU MAY BE INTERESTED IN

[Thermodynamic Properties of Alkali Metal Hydroxides. Part I. Lithium and Sodium Hydroxides](#)

Journal of Physical and Chemical Reference Data **25**, 1211 (1996); <https://doi.org/10.1063/1.555982>

[JANAF Thermochemical Tables, 1974 Supplement](#)

Journal of Physical and Chemical Reference Data **3**, 311 (1974); <https://doi.org/10.1063/1.3253143>

[Thermodynamic Properties of the Group IA Elements](#)

Journal of Physical and Chemical Reference Data **23**, 385 (1994); <https://doi.org/10.1063/1.555945>

Where in the **world** is AIP Publishing?
Find out where we are exhibiting next



Thermodynamic Properties of Alkali Metal Hydroxides. Part II. Potassium, Rubidium, and Cesium Hydroxides

L. V. Gurvich,^{a)} G. A. Bergman, L. N. Gorokhov, V. S. Iorish, V. Ya. Leonidov, and V. S. Yungman

Thermocenter of the Russian Academy of Sciences, Izhorskaya st. 13/19, IVTAN, Moscow 127412, Russia

Received July 21, 1995; revised manuscript received February 21, 1997

The data on thermodynamic and molecular properties of the potassium, rubidium and cesium hydroxides have been collected, critically reviewed, analyzed, and evaluated. Tables of the thermodynamic properties [C_p° , $\Phi^\circ = -(G^\circ - H^\circ(0))/T$, S° , $H^\circ - H^\circ(0)$, $\Delta_f H^\circ$, $\Delta_f G^\circ$] of these hydroxides in the condensed and gaseous states have been calculated using the results of the analysis and some estimated values. The recommendations are compared with earlier evaluations given in the JANAF Thermochemical Tables and Thermodynamic Properties of Individual Substances. The properties considered are: the temperature and enthalpy of phase transitions and fusion, heat capacities, spectroscopic data, structures, bond energies, and enthalpies of formation at 298.15 K. The thermodynamic functions in solid, liquid, and gaseous states are calculated from $T=0$ to 2000 K for substances in condensed phase and up to 6000 K for gases. © 1997 American Institute of Physics and American Chemical Society. [S0047-2689(97)00204-3]

Key words: bond energy, dissociation energy, enthalpy, enthalpy of formation, entropy, fusion, heat capacity, hydroxides, molecular (vibrational) constants and structure, phase transition, thermodynamic properties.

Contents

1. Introduction.	1033	4. Cesium Hydroxide.	1082
1.1. References for Introduction.	1034	4.1. Cesium Hydroxide in Condensed Phases.	1082
2. Potassium Hydroxide.	1034	4.1.1. Heat Capacity and Enthalpy	
2.1. Potassium Hydroxide in Condensed Phases.	1034	Measurements of CsOH(cr&liq).	1082
2.1.1. Heat Capacity and Enthalpy		4.1.2. Enthalpy of Formation of CsOH(cr).	1085
Measurements of KOH(cr&liq).	1034	4.1.3. Appendix. Tables of Experimental	
2.1.2. Enthalpy of Formation of KOH(cr).	1039	and Evaluated Data for CsOH(cr).	1086
2.1.3. Appendix. Tables of Experimental		4.2. Cesium Hydroxide in Gaseous Phase.	1091
and Evaluated Data for KOH(cr).	1040	4.2.1. Cesium Hydroxide Monomer.	1091
2.2. Potassium Hydroxide in Gaseous Phase.	1046	4.2.2. Appendix. Tables of Experimental	
2.2.1. Potassium Hydroxide Monomer.	1046	and Evaluated Data for CsOH(g).	1097
2.2.2. Appendix. Tables of Experimental		4.2.3. Cesium Hydroxide Dimer.	1100
and Evaluated Data for KOH(g).	1055	4.2.4. Appendix. Tables of Experimental	
2.2.3. Potassium Hydroxide Dimer.	1059	and Evaluated Data for [CsOH] ₂ (g).	1103
2.2.4. Appendix. Tables of Experimental		5. Recommendations for Future Measurements.	1106
and Evaluated Data for [KOH] ₂ (g).	1065	6. Acknowledgments.	1106
3. Rubidium Hydroxide.	1068	7. References for Potassium, Rubidium, and	
3.1. Rubidium Hydroxide in Condensed Phases.	1068	Cesium Hydroxides.	1106
3.1.1. Heat Capacity and Enthalpy			
measurements of RbOH(cr&liq).	1068		
3.1.2. Enthalpy of Formation of RbOH(cr).	1070		
3.1.3. Appendix. Tables of Experimental			
and Evaluated Data for RbOH(cr).	1071		
3.2. Rubidium Hydroxide in Gaseous Phase.	1073		
3.2.1. Rubidium Hydroxide Monomer.	1073		
3.2.2. Appendix. Tables of Experimental			
and Evaluated Data for RbOH(g).	1076		
3.2.3. Rubidium Hydroxide Dimer.	1078		
3.2.4. Appendix. Tables of Experimental			
and Evaluated Data for [RbOH] ₂ (g).	1081		

List of Tables

1. Smoothed heat capacity of KOH [70STU/HIL].	1040
2. Experimental heat capacity of KOH [88WHI/PER].	1041
3. Experimental enthalpy values $H^\circ(T) - H^\circ(273.15 \text{ K})$ of KOH [54POW/BLA].	1041
4. Smoothed heat capacity and enthalpy values of KOH [71GIN/GUB], [71GIN].	1042
5. Comparison of the heat capacity, enthalpy, entropy, and enthalpy of formation values for KOH(cr) at 298.15 K.	1042
6. Temperature of transitions of KOH.	1042
7. Temperature of fusion of KOH.	1043
8. Enthalpy of $\beta - \gamma$ transformation of KOH.	1043
9. Enthalpy of fusion of KOH.	1043

^{a)}Deceased.

- | | | | |
|---|------|---|------|
| 10. Thermal functions of KOH(cr) below 298.15 K. | 1043 | 36. Bond lengths (\AA), angle (deg), and vibrational frequencies (cm^{-1}) of RbOH in the ground electronic state. | 1074 |
| 11. Differences ($\text{J K}^{-1} \text{mol}^{-1}$) between the thermal functions of KOH(cr&liq) calculated in the present work and in [82GUR/VEI, 85CHA/DAV]. | 1043 | 37. Differences ($\text{J K}^{-1} \text{mol}^{-1}$) between the thermal functions of RbOH(g) calculated in the present work and in [82GUR/VEI]. | 1075 |
| 12. The enthalpy of formation of KOH(cr) from measurements of the enthalpies of solution of potassium hydroxide in water. | 1044 | 38. Results of determination of $\Delta_f H^\circ(\text{RbOH}, \text{g}, 0 \text{ K})$, kJ mol^{-1} | 1076 |
| 13. Thermodynamic properties at 0.1 MPa: KOH(cr&liq). | 1045 | 39. Thermodynamic properties at 0.1 MPa: RbOH(g). | 1077 |
| 14. Bond lengths (\AA), bond angle (deg), and frequencies (cm^{-1}) of KOH in the ground electronic state. | 1046 | 40. Bond lengths (\AA), angles (deg), and vibrational frequencies (cm^{-1}) of $\text{Rb}_2\text{O}_2\text{H}_2$ in the ground electronic state. | 1079 |
| 15. Differences ($\text{J K}^{-1} \text{mol}^{-1}$) between the thermal functions of KOH(g) calculated in the present work and in [82GUR/VEI, 85CHA/DAV]. | 1050 | 41. Differences ($\text{J K}^{-1} \text{mol}^{-1}$) between the thermal functions of $\text{Rb}_2\text{O}_2\text{H}_2(\text{g})$ calculated in the present work and in [82GUR/VEI]. | 1080 |
| 16. Partial pressure of KOH(g) over KOH(liq), [82FAR/SRI]. | 1055 | 42. Results of determination of $\Delta_f H^\circ(\text{Rb}_2\text{O}_2\text{H}_2, \text{g}, 0 \text{ K})$, kJ mol^{-1} | 1081 |
| 17. Partial pressures of KOH(g), K(g), and OH(g) for the reaction $\text{KOH}(\text{g}) = \text{K}(\text{g}) + \text{OH}(\text{g})$, [82FAR/SRI]. | 1055 | 43. Thermodynamic properties at 0.1 MPa: $\text{Rb}_2\text{O}_2\text{H}_2(\text{g})$ | 1081 |
| 18. Partial pressure of KOH(g) over KOH(liq), [84HAS/ZMB]. | 1056 | 44. Smoothed heat capacity of CsOH [87JAC/MAC2]. | 1086 |
| 19. Total vapor pressure over potassium hydroxide, [21WAR/ALB]. | 1056 | 45. Experimental heat capacity values of CsOH [90KON/COR]. | 1087 |
| 20. Apparent vapor pressure of potassium hydroxide, [74KUD]. | 1056 | 46. Experimental enthalpy values $H^\circ(T) - H^\circ(298.15 \text{ K})$ of CSOH [90KON/COR]. | 1087 |
| 21. Apparent vapor pressure over potassium hydroxide, [88KON/COR2]. | 1056 | 47. Comparison of the heat capacity, enthalpy, entropy, and enthalpy of formation values for CsOH(cr) at 298.15 K. | 1088 |
| 22. Results of experimental determination of $\Delta_f H^\circ(\text{KOH}, \text{g}, 0 \text{ K})$, kJ mol^{-1} | 1057 | 48. Temperatures of phase transformations of CsOH. | 1088 |
| 23. Thermodynamic properties at 0.1 MPa: KOH(g). | 1058 | 49. Temperature of fusion of CsOH. | 1088 |
| 24. Bond lengths (\AA), angles (deg), and vibrational frequencies (cm^{-1}) of $\text{K}_2\text{O}_2\text{H}_2$ in the ground electronic state. | 1061 | 50. Enthalpy of $\beta - \gamma$ transition of CsOH. | 1088 |
| 25. Differences ($\text{J K}^{-1} \text{mol}^{-1}$) between the thermal functions of $\text{K}_2\text{O}_2\text{H}_2(\text{g})$ calculated in the present work and in [82GUR/VEI, 85CHA/DAV]. | 1062 | 51. Enthalpy of fusion of CsOH. | 1088 |
| 26. Partial pressure of $\text{K}_2\text{O}_2\text{H}_2(\text{g})$ over KOH(liq), [84HAS/ZMB]. | 1065 | 52. Thermal functions of CsOH(cr) below 298.15. | 1089 |
| 27. Results of experimental determination of $\Delta_f H^\circ(\text{K}_2\text{O}_2\text{H}_2, \text{g}, 0 \text{ K})$, kJ mol^{-1} | 1066 | 53. Differences ($\text{J K}^{-1} \text{mol}^{-1}$) between the thermal functions of CsOH(cr&liq) calculated in the present work and in [82GUR/VEI, 85CHA/DAV]. | 1089 |
| 28. Thermodynamic properties at 0.1 MPa: $\text{K}_2\text{O}_2\text{H}_2(\text{g})$ | 1067 | 54. The enthalpy of formation of CsOH(cr) from measurements of the enthalpies of solution of cesium hydroxide in water. | 1089 |
| 29. Comparison of the heat capacity, enthalpy, entropy, and enthalpy of formation values for RbOH(cr) at 298.15 K. | 1071 | 55. Reaction scheme and results of determination of the enthalpy of formation of CsOH(cr), obtained in the study [88KON/COR] (second method). | 1090 |
| 30. Temperature of phase transformation of RbOH. | 1071 | 56. Thermodynamic properties at 0.1 MPa: CsOH(cr&liq). | 1091 |
| 31. Temperature of fusion of RbOH. | 1071 | 57. Bond lengths (\AA), angle (deg), and vibrational frequencies (cm^{-1}) of CsOH in the ground electronic state. | 1094 |
| 32. Enthalpy of $\beta - \gamma$ transformation of RbOH. | 1072 | 58. Differences ($\text{J K}^{-1} \text{mol}^{-1}$) between the thermal functions of CsOH(g) calculated in the present work and in [82GUR/VEI, 85CHA/DAV]. | 1094 |
| 33. Enthalpy of fusion of RbOH. | 1072 | 59. Equilibrium constant values for the reaction $\text{Cs}(\text{g}) + \text{KOH}(\text{g}) = \text{K}(\text{g}) + \text{CsOH}(\text{g})$, [69GOR/GUS]. | 1097 |
| 34. Differences ($\text{J K}^{-1} \text{mol}^{-1}$) between the thermal functions of RbOH(cr,liq) calculated in the present work and in [82GUR/VEI]. | 1072 | 60. Partial pressure of CsOH(g) over CsOH(liq), [88BLA/JOH]. | 1097 |
| 35. Thermodynamic properties at 0.1 MPa: RbOH(cr&liq). | 1072 | | |

61. Apparent vapor pressure over cesium hydroxide, [88KON/COR2].	1097
62. Results of determination of $\Delta_f H^\circ(\text{CsOH}, \text{g}, 0 \text{ K})$, kJ mol^{-1}	1098
63. Thermodynamic properties at 0.1 MPa: $\text{CsOH}(\text{g})$	1099
64. Bond lengths, angles (deg) and vibrational frequencies (cm^{-1}) of $\text{Cs}_2\text{O}_2\text{H}_2$ in the ground electronic state.	1101
65. Differences ($\text{J K}^{-1} \text{ mol}^{-1}$) between the thermal functions of $\text{Cs}_2\text{O}_2\text{H}_2(\text{g})$ calculated in the present work and in [82GUR/VEI, 85CHA/DAV].	1102
66. Partial pressure of $\text{Cs}_2\text{O}_2\text{H}_2(\text{g})$ over $\text{CsOH}(\text{liq})$ [88BLA/JOH].	1103
67. Results of determination of $\Delta_f H^\circ(\text{Cs}_2\text{O}_2\text{H}_2, \text{g}, 0 \text{ K})$, kJ mol^{-1}	1104
68. Thermodynamic properties at 0.1 MPa: $\text{Cs}_2\text{O}_2\text{H}_2(\text{g})$	1105

List of Figures

1. Heat capacity of KOH at 15–100 K.	1034
2. Heat capacity of KOH at 110–350 K.	1034
3. Enthalpy $H^\circ(T) - H^\circ(298.15 \text{ K})$ for solid KOH at 298–679 K.	1035
4. Enthalpy $H^\circ(T) - H^\circ(298.15 \text{ K})$ for liquid KOH at 679–1228 K.	1035
5. Heat capacity of KOH at 300–800 K.	1036
6. Partial pressure of $\text{KOH}(\text{g})$ over $\text{KOH}(\text{liq})$	1053
7. Total and apparent pressure over $\text{KOH}(\text{liq})$	1053
8. Partial pressure of $\text{K}_2\text{O}_2\text{H}_2(\text{g})$ over $\text{KOH}(\text{liq})$	1064
9. Heat capacity of CsOH at 5–100 K.	1064
10. Heat capacity of CsOH at 100–340 K.	1082
11. Heat capacity of CsOH at 298–700 K.	1082
12. Enthalpy $H^\circ(T) - H^\circ(298.15)$ for solid and liquid CsOH at 298–700 K.	1083
13. Partial pressures of monomer and dimer over $\text{CsOH}(\text{liq})$ [88BLA/JOH].	1095
14. Apparent pressure of $\text{CsOH}(\text{g})$ over $\text{CsOH}(\text{liq})$ [88KON/COR2].	1096

1. Introduction

The thermodynamic properties [$C_p^\circ, \Phi^\circ = -(G^\circ - H^\circ(0))/T, S^\circ, H^\circ - H^\circ(0), \Delta_f H^\circ, \Delta_f G^\circ$] of condensed and gaseous lithium, sodium, potassium, rubidium, and cesium hydroxides in standard states have been reevaluated. This activity was stimulated by the existence of new data since the time of publication of four critical reviews containing analogous information [82GUR/VEY], [82MED/BER], [82WAG/EVA], [85CHA/DAV].

This review is divided into two parts: Part I was published earlier [96GUR/BER] and was devoted to the compounds of Li and Na; Part II (this article) is devoted to the compounds of K, Rb, and Cs. The review for each compound contains a brief description of all experimental and theoretical studies of thermodynamic and molecular constants linked with the calculations of tables of thermodynamic properties. The

technique used, the impurities in the samples studied, the results obtained, and the accuracy of the data are discussed in these reviews. Unfortunately, the literature includes several reports which were not available to the authors. We assume that the absence of these sources does not influence the accuracy of the adopted values and the calculated thermodynamic properties. In all cases, special attention was devoted to estimating the uncertainties of adopted values and calculated thermodynamic properties. The selected constants and calculated properties are compared with similar quantities in earlier reviews [82WAG/EVA], [82MED/BER], [82GUR/VEY] and [85CHA/DAV]. Some recommendations are tentative due to the lack of reliable information. Recommendations for future measurements are given in Section 5.

The principal difficulty in providing reliable properties of the alkali metal hydroxides is the lack of precise experimental information on (1) the crystalline phase transition, (2) heat capacity data for the liquid state, (3) vibrational frequencies of monomeric and dimeric molecules of the hydroxides, (4) structural parameters for the dimeric molecules and data for the more complex species, (5) the composition of the vapor over the crystal and liquid phases, and (6) the enthalpies of formation for the gaseous molecules.

All crystalline hydroxides of the alkali metals except LiOH possess polymorphism. See Table 1, Part I [96GUR/BER]. All hydroxides have several other modifications at high pressures.

General comments:

- (1) The units used throughout the text and tables are: temperature in K; Gibbs energy of formation and enthalpy of formation in kJ mol^{-1} ; enthalpy, entropy, Gibbs energy function, and heat capacity in J K mol^{-1} .
- (2) In general, the literature coverage extends from the end of the last century to 1994.
- (3) The temperature scale used for the recommended values is ITS-90. Many of the data known in the literature were obtained using earlier temperature scales. Oftentimes the scale is not mentioned in the papers, so it was necessary to guess the approximate corrections. It should be noted that below $T = 1000 \text{ K}$, the corrections between all temperature scales are less than 1 K, while from 1000 K to 2000 K the corrections are always less than 2 K and are well within the uncertainty of the temperature measurements.
- (4) The following relative atomic masses are adopted [93IUP]: O, 15.9994; Cs, 132.90543; H, 1.00794; K, 39.0983; Rb, 85.4678.
- (5) In the Appendices for each hydroxide, the experimental values of enthalpy, heat capacity, and equilibrium constants obtained in the cited studies are given.
- (6) Tables of ‘‘Thermodynamic properties at 0.1 MPa’’ are calculated, using thermal functions for reference substances $\text{K}(\text{cr and liq and g})$, $\text{Rb}(\text{cr and liq and g})$, $\text{Cs}(\text{cr and liq and g})$, H_2 , and $\text{O}_2(\text{g})$ from [82GUR/VEY]. The transition from condensed to gaseous occurs for potassium at 1039 K [$\Delta_s H^\circ(\text{K}, 0 \text{ K}) = 89.891 \text{ kJ mol}^{-1}$], for

rubidium at 977 K [$\Delta_s H(\text{Rb}, 0 \text{ K}) = 82.192 \text{ kJ mol}^{-1}$], and for cesium at 948 K [$\Delta_s H(\text{Cs}, 0 \text{ K}) = 78.014 \text{ kJ mol}^{-1}$]. The uncertainties of the standard enthalpy and Gibbs energy of formation are estimated using uncertainties in the thermal functions adopted in this work and in [82GUR/VEY].

- (7) The fundamental constants used in the statistical mechanical calculations are taken from the CODATA recommendations [88COH/TAY].

1.1. References for Introduction

- 82GUR/VEY L. V. Gurvich, I. V. Veyts, V. A. Medvedev, G. A. Bergman, V. S. Yungman, and G. A. I. Khachkuruzov, *Termodinamicheskie svoystva individual'nykh veshchestv. Spravoschnoe izdanie v 4-kh tomakh*. Moskva: Nauka **4**(1), (1982).
- 82MED/BER V. A. Medvedev, G. A. Bergman, V. P. Vasil'ev *et al.*, *Termicheskie konstanty veshchestv* (VINITI, Moscow, 1982), Vol. 10.
- 82WAG/EVA D. D. Wagman, W. H. Evans *et al.*, "The NBS Tables of Thermodynamic Properties. Selected Values for Inorganic C_1 and C_2 Organic Substances on SI Units," *J. Phys. Chem. Ref. Data* **11**, Suppl. 2 (1982).
- 85CHA/DAV M. W. Chase, C. A. Davies, J. R. Downey, D. J. Frurip, R. A. McDonald, and A. N. Syverund, *J. Phys. Chem. Ref. Data* **14**, Suppl. 1 (1985).
- 88COH/TAY E. R. Cohen and B. N. Taylor, *J. Phys. Chem. Ref. Data* **17**, 1795 (1988).
- 93IUP "Atomic Weights of the Elements 1991, IUPAC Commission on Atomic Weights and Isotopic Abundances," *J. Phys. Chem. Ref. Data* **22**, 1571 (1993).
- 96GUR/BER L. V. Gurvich, G. A. Bergman, L. N. Gorokhov, V. S. Iorish, V. Ya. Leonidov, and V. S. Yungman, *J. Phys. Chem. Ref. Data* **25**, 1211 (1996).

2. Potassium Hydroxide

2.1. Potassium Hydroxide in Condensed Phases

At atmospheric pressure, KOH exists in three crystal phases: a low temperature monoclinic modification (0–226.7 K), space group $P2_1/a$, with antiferroelectric ordering (α -KOH); a room temperature monoclinic modification (226.7–517 K), space group $P2_1/m$ (β -KOH); and a high temperature cubic modification (517–679 K), space group $Fm3m$ (γ -KOH). See Table 1, Part I [96GUR/BER]. The α - β transition at 226.7 K was not known before 1986 [86BAS/ELC]. Thus, in many earlier studies the transition at 517 K was denoted as α - β transition.

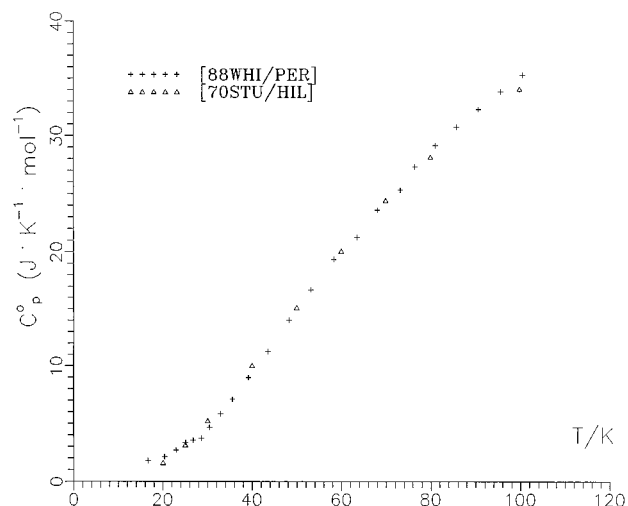


FIG. 1. Heat capacity of KOH at 15–100 K.

2.1.1. Heat Capacity and Enthalpy Measurements of KOH(cr&liq)

Temperatures below 298.15 K

[70STU/HIL]

Stull *et al.* measured the heat capacity in adiabatic calorimeter at 20–298 K. A commercial sample of KOH ("reagent grade") was dried under vacuum at 425 °C. Analysis by acid titration indicated 97.8% KOH and 2.2% K_2CO_3 . No information concerning other impurities was given. The low temperature adiabatic calorimeter was described in [63OET/MCD]. The calorimeter was calibrated using the benzoic acid standard; measurements agreed with the standard values in the limit of 3% below 20 K, 0.5% from 30 to 80 K, and 0.3% from 80 to 300 K. The heat capacity values for KOH were corrected for the presence of 2.2% K_2CO_3 . Stull *et al.* only reported smoothed heat capacity values (see Table 1 and Figs. 1 and 2). They detected a

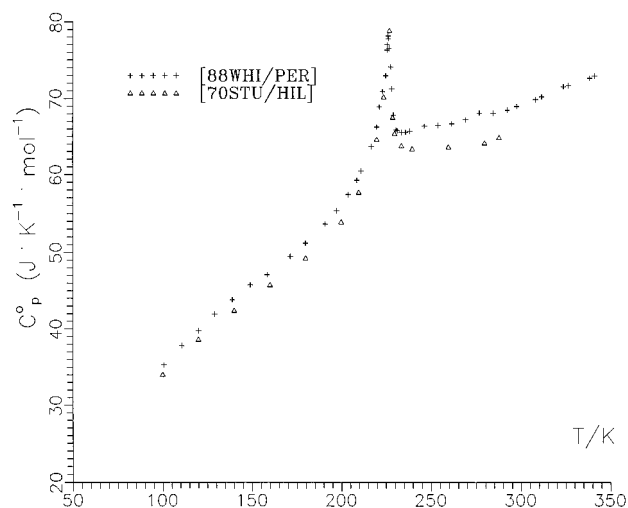


FIG. 2. Heat capacity of KOH at 100–350 K.

broad λ -type transition with a heat capacity peak at 227.5 K, but the value of the enthalpy of transition was not given. The extrapolation of the heat capacity below 20 K by the T^3 -Law led to $S^\circ(20\text{ K}) = 0.54\text{ J K}^{-1}\text{ mol}^{-1}$ and $H^\circ(20\text{ K}) - H^\circ(0) = 7.9\text{ J mol}^{-1}$. Stull *et al.* calculated the values $S^\circ(298.15\text{ K}) = 18.85\text{ cal K}^{-1}\text{ mol}^{-1} = 78.87\text{ J K}^{-1}\text{ mol}^{-1}$ and $H^\circ(298.15\text{ K}) - H^\circ(0) = 2904\text{ cal mol}^{-1} = 12.15\text{ kJ mol}^{-1}$.

[88WHI/PER]

White *et al.* measured the heat capacity at the temperatures from 16.65 to 341.71 K. The sample was prepared by drying of KOH ("Alpha ultrapure") in vacuum at 160 °C in a zirconium crucible. The sample contained 0.05 mass % H_2O and 2.8 mass % K_2CO_3 as impurities (the level of carbonate impurity was determined by x-ray powder diffraction). The heat capacity of powdered KOH (20.6911 g) was measured in a heat-pulse adiabatic calorimeter [84WHI] with an accuracy 1%; 130 experimental values were obtained (see Table 2 and Figs. 1 and 2). The authors determined a wide λ -anomaly in the heat capacity curve between 210 and 235 K centered at $226.7 \pm 0.2\text{ K}$. The enthalpy of the transition was derived from integration of the excess heat capacity; the results were $\Delta_{\text{trs}}H = 222 \pm 3\text{ J mol}^{-1}$ and $\Delta_{\text{trs}}S = 1.01\text{ J K}^{-1}\text{ mol}^{-1}$. White *et al.* have not calculated the thermodynamic functions.

Temperatures above 298.15 K

[51VED/SKU]

Vedenev and Skuratov measured the enthalpy between 19 and 100 °C. A commercial sample of KOH ("Kahlbaum"), containing about 15% H_2O , was dehydrated in a dry stream of N_2 by heating in a silver container at 400–420 °C, then in vacuum ($p = 2\text{--}3\text{ mm Hg}$) during 24–28 h. The chemical analysis of the sample gave 98.51% KOH, 1.48% K_2CO_3 and 0.01% H_2O . The six enthalpy measurements were made in a massive copper drop-calorimeter calibrated by the heat capacity of water. The average value of "mean heat capacity" was calculated as $C_p^\circ(19\text{--}100\text{ °C}) = 0.2996 \pm 0.0006\text{ cal K}^{-1}\text{ g}^{-1}$. After correction for K_2CO_3 impurities, the value $0.3009\text{ cal K}^{-1}\text{ g}^{-1}$ was obtained, and then $H^\circ(373.15\text{ K}) - H^\circ(292.15\text{ K}) = 5721\text{ J mol}^{-1}$ and $H^\circ(373.15\text{ K}) - H^\circ(298.15\text{ K}) = 5318\text{ J mol}^{-1}$.

[54POW/BLA]

Powers and Blalock measured the enthalpy $H(T) - H(273.15\text{ K})$ of solid and liquid KOH from 435 to 1228 K. The capsule material was nickel. Chemical analysis of the sample of KOH carried out after measurements of enthalpy showed an increase of K_2CO_3 impurity from 0.12% up to 0.28% and a decrease of the total alkalinity from 100% to 98.68%.

A Bunsen ice calorimeter was used [51RED/LON]. The calorimeter was calibrated with alumina ($\alpha\text{-Al}_2\text{O}_3$) in the range 700–1200 K; the results were in agreement with the US NBS data [47GIN/COR] to within 3%. Powers and Blalock made four measurements of β -KOH enthalpy (435–491 K), seven measurements for γ -KOH (532–571 K), and 69

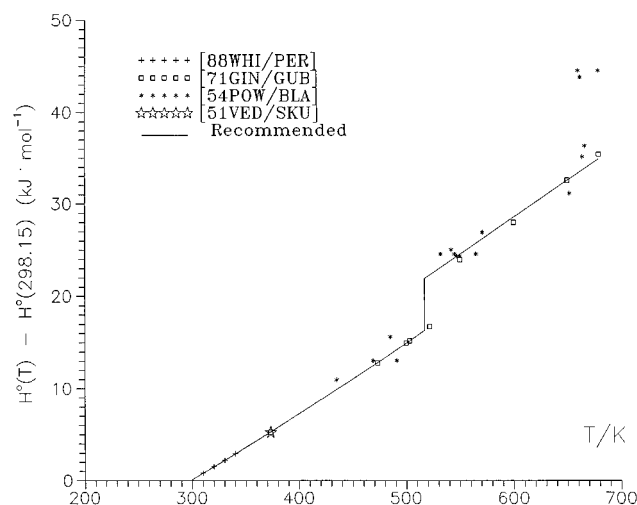


FIG. 3. Enthalpy $H^\circ(T) - H^\circ(298.15\text{ K})$ for solid KOH at 298–679 K.

measurements for liquid KOH (691–1228 K). These data are listed in Table 3 and shown in Figs. 3 and 4. Twelve enthalpy measurements were not used in the least-squares analysis.

The enthalpy values for β -KOH and liquid KOH were represented by linear equations (in cal g^{-1}):

$$\beta\text{-cr,}(273\text{--}522\text{ K}):H^\circ(T) - H^\circ(273\text{ K}) = 0.32(T - 273.15\text{ K}),$$

$$\text{liq,}(673\text{--}1228\text{ K}):H^\circ(T) - H^\circ(273\text{ K})$$

$$= 52.5 + 0.354(T - 273.15\text{ K}).$$

Thus, constant values for heat capacity of β -KOH and KOH(liq) were recommended: $C_p^\circ = 0.32\text{ cal K}^{-1}\text{ g}^{-1} = 75.1\text{ J K}^{-1}\text{ mol}^{-1}$ and $C_p^\circ = 0.35 \pm 0.02\text{ cal K}^{-1}\text{ g}^{-1} = 82.2 \pm 4.7\text{ J K}^{-1}\text{ mol}^{-1}$, respectively. Note that this latter value was rounded by Powers and Blalock from 0.354 to $0.35\text{ cal K}^{-1}\text{ g}^{-1}$. In view of the poor reproducibility of the

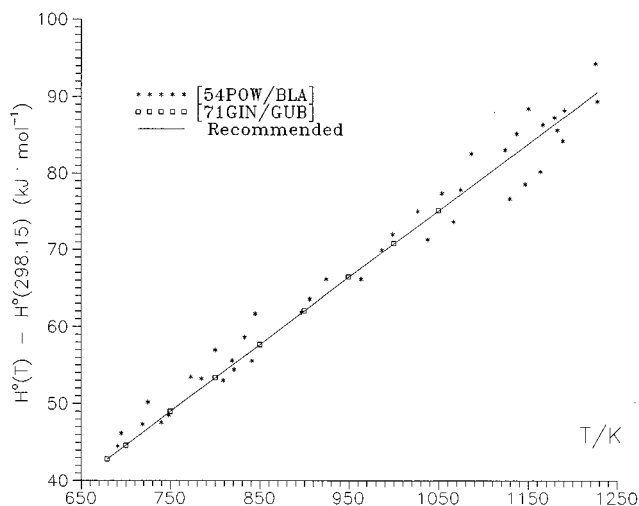


FIG. 4. Enthalpy $H^\circ(T) - H^\circ(298.15\text{ K})$ for liquid KOH at 679–1228 K.

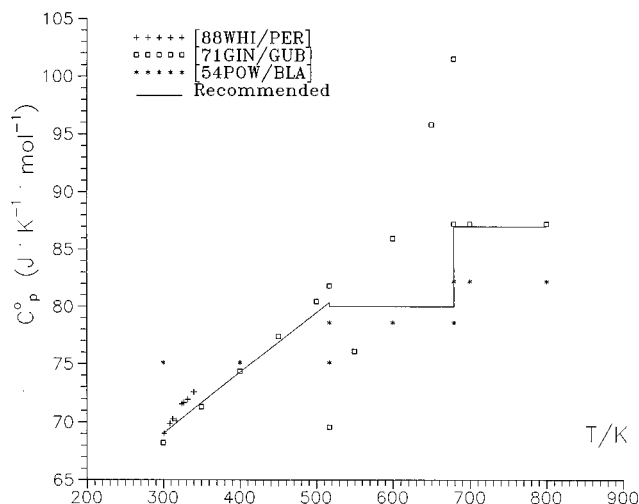


FIG. 5. Heat capacity of KOH at 300–800 K.

enthalpy values for β -KOH, the authors did not use these results for calculations. The heat capacity of γ -KOH, $C_p^\circ = 0.335 \text{ cal K}^{-1} \text{ g}^{-1} = 78.6 \text{ J K}^{-1} \text{ mol}^{-1}$ was estimated as an average value between the values for β KOH and liquid KOH. The enthalpy of transition $\Delta_{tr}H(249^\circ\text{C}) = 24 \text{ cal g}^{-1} = 5.63 \text{ kJ mol}^{-1}$ and the enthalpy of fusion $\Delta_{fus}H(406^\circ\text{C}) = 40 \text{ cal g}^{-1} = 9.39 \text{ kJ mol}^{-1}$ were calculated.

[71GIN/GUB], [71GIN]

Ginzburg *et al.* measured the enthalpy (“mean heat capacity”) by drop calorimetry from 373 to 1073 K. The sample was prepared from commercial KOH containing 15% H_2O . Dehydration of the sample was carried out by heating of the melt in vacuum at 450–470 $^\circ\text{C}$ for 1.5 h. According to the chemical analysis, the sample contained 98.5% KOH, 1.5% K_2CO_3 and the traces of Cl^- , SO_4^{2-} and PO_4^{3-} . Nickel capsules were used. The authors carried out 51 measurements of the enthalpy at 19 temperatures. The enthalpy values were corrected for the 1.5% K_2CO_3 impurity. The experimental data were given in graphical form and equations only. The smoothed values of heat capacity and enthalpy are listed in Table 4 and shown in Figs. 3 and 4.

The following enthalpy of transition values and equations for the heat capacity (in $\text{cal K}^{-1} \text{ mol}^{-1}$) were recommended by Ginzburg *et al.*:

$$\beta\text{-cr, (298.15–522.15 K): } C_p^\circ = 11.933 + 14.59 \cdot 10^{-3}T,$$

$$\gamma\text{-cr, (522.15–683.15 K): } C_p^\circ = -7.735 + 47.13 \cdot 10^{-3}T,$$

$$\text{liq, (683.15–1300 K): } C_p^\circ = 20.845,$$

$$\Delta_{tr}H(522.15 \text{ K}) = 1229.7 \text{ cal mol}^{-1}$$

$$\Delta_{fus}H(683.15 \text{ K}) = 1744.1 \text{ cal mol}^{-1}.$$

Discussion of Heat Capacity and Enthalpy Data

Figures 1 and 2 show the low temperature heat capacity values [70STU/HIL] (20–298 K) and [88WHI/PER] (16.65–

342 K). The data of these two studies are in poor agreement. Below 40 K the deviations are about 30%. In the range 50–100 K the heat capacity values obtained in [70STU/HIL] lie 0.5%–2% lower than those from [88WHI/PER]. Above 120 K the deviations increase up to 4% at 200 K and up to 6% at 298 K. It is difficult to explain these discrepancies. Apparently, the sample of KOH used in [70STU/HIL] was not pure; the K_2CO_3 impurity was determined as 2.2%, but the other impurities (including H_2O) were not specified. In the [88WHI/PER] study, the K_2CO_3 impurity was slightly larger (2.8%), but impurity of H_2O was very small (0.05%). This latter value was determined from the DSC endothermic effect due to fusion of the eutectic KOH - $\text{KOH} \cdot \text{H}_2\text{O}$ at 377 K.

The data of White *et al.* [88WHI/PER] were adopted based on the good agreement between the heat capacity below 342 K [88WHI/PER] and the enthalpy measurements at 373.15 K [51VED/SKU] and in the range 373–503 K [71GIN/GUB]. The data [70STU/HIL] do not agree with the enthalpy measurements mentioned above; the deviations are –5% for the enthalpy increment $H^\circ(373 \text{ K}) - H^\circ(298.15 \text{ K})$ and more than 10% for the heat capacity at 373 K (apparently the heat capacity data [70STU/HIL] were extrapolated to 373 K).

Calculation of the thermal functions in the range 5–298.15 K (see Table 10) was made by the spline method [94LUT/GUR] using the data of White *et al.* [88WHI/PER]. At 298.15 K it results in the following values:

$$C_p^\circ(298.15 \text{ K}) = 68.93 \pm 0.7 \text{ J K}^{-1} \text{ mol}^{-1},$$

$$S^\circ(298.15 \text{ K}) = 81.25 \pm 0.8 \text{ J K}^{-1} \text{ mol}^{-1},$$

$$H^\circ(298.15 \text{ K}) - H^\circ(0) = 12600 \pm 100 \text{ J mol}^{-1}.$$

These values are compared with those recommended in different reviews (based on the data [70STU/HIL]) in Table 5. The uncertainties of the adopted values are due to the discrepancies of data mentioned above.

Figure 3 shows the enthalpy $H^\circ(T) - H^\circ(298.15 \text{ K})$ of solid KOH measured in [51VED/SKI], [54POW/BLA], and [71GIN/GUB]. The values of $H^\circ(T) - H^\circ(298.15 \text{ K})$ at 310, 320, 330 and 340 K calculated by integration of the heat capacity data [88WHI/PER] are also given on Fig. 3. All these data for β -KOH agree satisfactorily with each other within about 0.5%, except those by Powers and Blalock [54POW/BLA]. The latter are inaccurate because of low reproducibility of experimental results, especially for solid KOH. An average deviation in this case was about 10% for β - and γ -KOH. In addition, the measurements [54POW/BLA] appear to have systematic error which yielded in overestimation of the results. This conclusion is made on the basis of comparison of their measurements with the enthalpy values of alumina used as a standard; the values obtained in [54POW/BLA] are 2%–3% higher than those recommended in [47GIN/COR].

The equation for heat capacity of the monoclinic β -modification of KOH:

$$C_p^\circ / \text{J K}^{-1} \text{ mol}^{-1} = 53.864 + 51.415 \cdot 10^{-3}T - 0.234 \cdot 10^5 T^{-2}$$

was derived by analysis of the data [51VED/SKU], [71GIN/GUB], and [88WHI/PER]. The following values were used:

four points of the enthalpy increments [71GIN/GUB] (373–503 K), one point at 373.15 K which is an average value of six measurements of the enthalpy [51VED/SKU], and eight points of $H^\circ(T) - H^\circ(298.15 \text{ K})$ at 260–340 K obtained by integration of the heat capacity measured in [88WHI/PER].

There are only two works devoted to the measurements of the enthalpy increments for γ -KOH and liquid KOH - [54POW/BLA] (below 1228 K) and [71GIN/GUB] (below 1073 K). However, the data [54POW/BLA] are not accurate and have systematic errors (see above). In the data of Ginzburg *et al.*, the values for γ -KOH were fitted by an equation which gives a rise to the heat capacity, from $C_p^\circ(522 \text{ K}) = 71 \text{ J K}^{-1} \text{ mol}^{-1}$ to $C_p^\circ(683 \text{ K}) = 102 \text{ J K}^{-1} \text{ mol}^{-1}$. The comparison of the heat capacities for γ -NaOH and γ -CsOH shows that for γ -KOH the constant value close to $80 \text{ J K}^{-1} \text{ mol}^{-1}$ might be more reliable. The heat capacity of γ -KOH then becomes equal to the heat capacity of β -KOH at $T_{\text{trs}}(\beta-\gamma)$. For the internal consistency of data for liquid KOH and γ -KOH it is necessary to introduce corrections in the values of $\Delta_{\text{trs}}H$ and $\Delta_{\text{fus}}H$ obtained in [71GIN/GUB]. These corrections are calculated using the equation:

$$\begin{aligned} [H^\circ(683.15 \text{ K}) - H^\circ(522.15 \text{ K})] - C_p^\circ(\gamma\text{-KOH}) \\ - (T_{\text{fus}} - T_{\text{tr}}) = (35860 - 21937) - 80(683.15 - 522.15) \\ = 1.05 \text{ kJ mol}^{-1} \end{aligned}$$

and dividing the value 1.05 kJ mol^{-1} into two parts (0.45 and 0.6 kJ mol^{-1}). These values are added to the values of $\Delta_{\text{trs}}H$ and $\Delta_{\text{fus}}H$ obtained in [71GIN/GUB]:

$$\begin{aligned} \Delta_{\text{trs}}H &= 5.15 + 0.45 = 5.6 \text{ kJ mol}^{-1}, \\ \Delta_{\text{fus}}H &= 7.3 + 0.6 = 7.9 \text{ kJ mol}^{-1}. \end{aligned}$$

Figure 4 shows the enthalpy increments for liquid KOH measured in [54POW/BLA] (691–1228 K) and in [71GIN/GUB] (700–1073 K). Constant values, $C_p^\circ = 82.2 \pm 4.7 \text{ J K}^{-1} \text{ mol}^{-1}$ and $87.2 \text{ J K}^{-1} \text{ mol}^{-1}$, were calculated from these data, respectively. As was mentioned, the data obtained by Powers and Blalock are less accurate than the data of Ginzburg *et al.* A value of $87.0 \text{ J K}^{-1} \text{ mol}^{-1}$ for the heat capacity of the liquid was adopted, based on the data from Ginzburg *et al.*

Phase Equilibrium Data

[10HEV2]

Hevesy determined the temperatures and enthalpies of a polymorphic transition and fusion by a thermal analysis method. A commercial sample of KOH (“Merck”) that contained about 0.4% K_2CO_3 was dehydrated in a silver container at $\sim 450^\circ\text{C}$ “for many hours.” The cooling curves were made with the rate $12^\circ\text{C}/\text{min}$. The transition and fusion temperatures, $248 \pm 0.5^\circ\text{C} = 521 \text{ K}$ and $360.4 \pm 0.7^\circ\text{C} = 633.55 \text{ K}$, were obtained from these measurements. The enthalpy of transition ($27.1 \text{ cal g}^{-1} = 6.36 \text{ kJ mol}^{-1}$) and the enthalpy of fusion ($28.6 \text{ cal g}^{-1} = 6.71 \text{ kJ mol}^{-1}$) were obtained by a quantitative thermal analysis.

[15SCA2]

Scarpa studied the system KOH - KCl and determined $T_{\text{trs}} = 266^\circ\text{C} = 539 \text{ K}$ and $T_{\text{fus}} = 3800^\circ\text{C} = 653 \text{ K}$ by DTA. The sample of KOH contained 1.47% K_2CO_3 as an impurity.

[23EWL]

Ewles obtained a value for the KOH transition temperature, $T_{\text{trs}} = 242^\circ\text{C} = 515 \text{ K}$, by the disappearance of fluorescence.

[49SEW/MAR]

Seward and Martin determined $T_{\text{trs}} = 249^\circ\text{C} = 522 \text{ K}$ and $T_{\text{fus}} = 410 \pm 1^\circ\text{C} = 683 \text{ K}$ by DTA. The KOH sample (the “reagent” quality) was dehydrated in a nickel container at $475\text{--}500^\circ\text{C}$ during 10–12 hours.

[51DIO], [52RES/DIO]

Diogenov *et al.* studied the systems KOH - KNO_3 and KOH - K_2CrO_4 and determined $T_{\text{trs}} = 256^\circ\text{C} = 529 \text{ K}$ and $T_{\text{fus}} = 403^\circ\text{C} = 676 \text{ K}$ by the visual method of thermal analysis (observation of crystal appearance upon slow decreasing of the melt temperature).

[52BER/KHI], [53KHI/KHI], [54KHI]

Khitrov and co-authors determined $T_{\text{trs}} = 240^\circ\text{C} = 513 \text{ K}$ and $T_{\text{fus}} = 406^\circ\text{C} = 679 \text{ K}$ by thermal analysis. The KOH sample was dehydrated by heating in a silver container at 500°C in a stream of H_2O and CO_2 -free air for 6 h. A chemical analysis showed that the sample of KOH contained the traces of H_2O and K_2CO_3 only.

[54BER/RES]

Bergman and Reshetnikov determined the fusion temperature, $T_{\text{fus}} = 404 \pm 1^\circ\text{C}$, by the visual method of thermal analysis.

[54POW/BLA]

Powers and Blalock obtained $\Delta_{\text{trs}}H = 5.63 \text{ kJ mol}^{-1}$ and $\Delta_{\text{fus}}H = 9.39 \text{ kJ mol}^{-1}$ (see discussion of the enthalpy data).

[56COH/MIC]

Cohen-Adad and Michaud investigated the system KOH - H_2O and determined by thermal analysis the transition ($242^\circ\text{C} = 515 \text{ K}$) and fusion temperatures ($401 \pm 1^\circ\text{C} = 674 \text{ K}$). Chemical analysis indicated the sample of KOH contained about 1.5% K_2CO_3 .

[58RES/VIL]

Reshetnikov and Vilutis obtained by DTA the transition and fusion temperatures $250^\circ\text{C} = 523 \text{ K}$ and $404^\circ\text{C} = 677 \text{ K}$.

[59RES/UNZ]

Reshetnikov and Unzhakov measured the fusion temperatures $401^\circ\text{C} = 674 \text{ K}$ by DTA and $403^\circ\text{C} = 676 \text{ K}$ by a visual method of thermal analysis. The dehydration of KOH samples was made by heating at $450\text{--}500^\circ\text{C}$.

[59ROL/COH]

Rollet *et al.* prepared a sample of KOH by electrolysis of K_2CO_3 water solution in a stream of H_2 . After purification and dehydration the sample of KOH contained about 0.1% K_2CO_3 only. For cooling and heating curves, the values

$T_{\text{trs}}=242\text{ }^{\circ}\text{C}=515\text{ K}$ and $T_{\text{fus}}=404\text{ }^{\circ}\text{C}=677\text{ K}$ were obtained.

[61MIC], [61COH/MIC]

Michaud *et al.* investigated the systems KOH-H₂O and KOH-K₂CO₃ and determined by DTA $T_{\text{trs}}=242\pm 0.3\text{ }^{\circ}\text{C}=515\text{ K}$ and $T_{\text{fus}}=404\text{ }^{\circ}\text{C}=677\text{ K}$ for KOH.

[61RES/ROM]

Reshetnikov and Romanova studied the system KOH - KNO₂ and obtained by DTA $T_{\text{trs}}=248\pm 1\text{ }^{\circ}\text{C}=521\text{ K}$ and $T_{\text{fus}}=404\text{ }^{\circ}\text{C}=677\text{ K}$ for KOH.

[63LUX/BRA]

Lux and Brandl studied the system KOH - H₂O and obtained $T_{\text{trs}}=248\text{ }^{\circ}\text{C}=521\text{ K}$ and $T_{\text{fus}}=416\text{ }^{\circ}\text{C}=689\text{ K}$ for KOH.

[66MIT/GRO]

Mitkevich and Grot investigated the system KOH-K and obtained by DTA: $T_{\text{trs}}=242\text{--}247\text{ }^{\circ}\text{C}=515\text{--}520\text{ K}$ and $T_{\text{fus}}=399\text{--}404\text{ }^{\circ}\text{C}=672\text{--}677\text{ K}$ for a KOH sample containing 98.9% KOH and 0.5% K.

[67MIC], [68MIC]

Michaud studied the system KOH-LIOH and obtained the values $T_{\text{trs}}=244\text{ }^{\circ}\text{C}=517\text{ K}$ and $T_{\text{fus}}=405.2\pm 0.3\text{ }^{\circ}\text{C}=678.35\text{ K}$ by DTA for a KOH sample that was dehydrated at 500 °C during 2 h.

[67RES/BAR], [69RES/BAR]

Reshetnikov and Baranskaya investigated a sample of KOH that contained about 0.3% K₂CO₃ and 0.1 H₂O. They obtained the values $T_{\text{trs}}=242\text{ }^{\circ}\text{C}=515\text{ K}$ and $T_{\text{fus}}=406\text{--}407\text{ }^{\circ}\text{C}=679\text{--}680\text{ K}$ by the thermal analysis. The enthalpy of transition $\Delta_{\text{trs}}H=1.54\text{ kcal mol}^{-1}=6.44\text{ kJ mol}^{-1}$ and enthalpy of fusion $\Delta_{\text{fus}}H=1.98\text{ kcal mol}^{-1}=8.28\text{ kJ mol}^{-1}$ were determined by quantitative DTA; $\Delta_fH^{\circ}=6.59\text{ kJ mol}^{-1}$ for NaOH was adopted as a standard.

[67RUB], [68RUB/SEB]

Ruby studied the system KOH - KF and obtained $T_{\text{trs}}=244\text{ }^{\circ}\text{C}=517\text{ K}$ and $T_{\text{fus}}=404\text{ }^{\circ}\text{C}=677\text{ K}$ by DTA. Ruby *et al.* [68RUB/SEB] investigated the system KOH - KCl and obtained $T_{\text{fus}}=405\text{ }^{\circ}\text{C}=678\text{ K}$.

[67TSE/ROG]

Tsentsiper *et al.* studied the system KOH - K₂O and obtained by DTA: $T_{\text{trs}}=245\text{ }^{\circ}\text{C}=518\text{ K}$ and $T_{\text{fus}}=401\text{ }^{\circ}\text{C}=674\text{ K}$ for the KOH sample containing 0.7% K₂CO₃ and the traces of H₂O.

[71GIN/GUB]

Ginzburg *et al.* obtained for KOH $\Delta_{\text{trs}}H=5.15\text{ kJ mol}^{-1}$ and $\Delta_{\text{fus}}H=7.30\text{ kJ mol}^{-1}$ (see discussion of the enthalpy data).

[74BEC/COU]

Using a KOH commercial sample, Bec *et al.* obtained a transition temperature $244\text{ }^{\circ}\text{C}=517\text{ K}$ by DTA. The authors made an x-ray investigation of the various KOH modifications and observed that this temperature corresponds to a monoclinic to cubic transition.

[80BAI], [80BAI/SHA], [83BAI], [88BAI/NIK]

Baikov *et al.* obtained $T_{\text{trs}}=515\text{ K}$ by DTA and by a kinetic investigation (the anomalous temperature dependence of a separation coefficient for hydrogen isotopes in the KOH crystal-gas system).

[86BAS/ELC]

Bastow *et al.* investigated the low-temperature phase transition in KOH (and KOD). The KOH sample was prepared by heating a commercial sample in a nickel foil boat under dry N₂. Information concerning purity of the samples was not given. The DSC measurements with slow heating rates ($\sim 0.4\text{ K/min}$ near the transition) gave the λ -curve with the maximum at 233 K. The same transition temperature was derived from the temperature dependence of the dielectric constant. For KOD the transition temperature was determined as 257 K.

The structures of KOH at 77 K and 293 K have been determined from high resolution neutron powder diffraction data. Both modifications of KOH were monoclinic; the low-temperature modification had a space group P2₁/a, and the high-temperature one had a space group P2₁/m. The phase transition KOH at 233 K was described as an order-disorder transition; the crystal adopted an ordered antiferroelectric arrangement.

[87MAC/JAC]

Mach *et al.* determined by DSC the temperature of a phase transition of KOD at 251 K.

[88WHI/PER]

White *et al.* measured low-temperature heat capacity of KOH (see discussion of heat capacity data) and obtained the λ -anomaly centered at $226.7\pm 0.2\text{ K}$. From integration of the excess heat capacity in the range 210–235 K the authors calculated $\Delta_{\text{trs}}H=222\pm 3\text{ J mol}^{-1}$.

Discussion of Phase Equilibrium Data

The low-temperature α - β phase transformation of KOH is a transition into an ordered antiferroelectric state. This transition is accompanied by the λ -anomaly of heat capacity. Bastow *et al.* [86BAS/ELC] determined the maximum of λ -curve at 233 K by DSC. More precise data were obtained by the heat capacity measurements made by Stull *et al.* [70STU/HIL] (227.5 K) and by White *et al.* [88WHI/PER] ($226.7\pm 0.2\text{ K}$) (see discussion of heat capacity data). The latter value is adopted in present review.

The measurements of the temperature of β - γ transition (monoclinic - cubic) are listed in Table 6. The results of these measurements are in the range from 513 to 539 K. The comparatively high scatter of these data probably may be explained by the rather low purity of the samples used for investigations and by the errors of the thermal analysis method. The best measurements of transition temperature were fulfilled by [67MIC, 67RUB, 67TSE/ROG, 69RES/BAR, 74BEC/COU] and values in the range 515–518 K were obtained. The average value, $T_{\text{trs}}=517\pm 3\text{ K}$, is adopted in the present review.

The results of numerous measurements of the melting

point of KOH are listed in Table 7. The underestimated values of T_{fus} were obtained in the older studies [10HEV2, 14NAI/BER, 15SCA] because the investigated samples of KOH were not completely dehydrated. The values of T_{fus} , obtained in the other studies, are in the range 672–689 K. In the present review, $T_{\text{fus}} = 679 \pm 2$ K is adopted. This value is an average of the results of the six best studies: [67MIC, 68RUB, 61KOH/MIC, 67RES/BAR, 71DIO/RES, 54KHI].

The enthalpy of the α - β transition of KOH ($\Delta_{\text{trs}}H = 222 \pm 3$ J mol $^{-1}$) was calculated by integrating the excess of heat capacity of KOH made in [88WHI/PER] (see discussion of heat capacity data). This value and the entropy of transition ($\Delta_{\text{trs}}S = 1.01$ J K $^{-1}$ mol $^{-1}$) was used in the calculation of the thermodynamic functions of KOH below 298.15 K.

The data for the enthalpy of β - γ transition and the enthalpy of fusion of KOH are listed in Tables 8 and 9. The adopted values for the enthalpy of liquid KOH, from the data [71GIN/GUB], must be in agreement with the adopted values of the heat capacity and the enthalpies of transformations of KOH. To achieve this, we made corrections in the enthalpies of β - γ transition and fusion of KOH [71GIN/GUB] (see discussion on enthalpy data) and adopted the following values: $\Delta_{\text{trs}}H = 5.6 \pm 0.6$ kJ mol $^{-1}$ and $\Delta_{\text{fus}}H = 7.9 \pm 0.8$ kJ mol $^{-1}$.

Calculation of Thermal Functions of KOH(cr&liq)

The thermal functions of KOH(cr) for the temperatures 20–298.15 K (see Table 10) were calculated using the data [88WHI/PER] and spline technique [94LUT/GUR]. The thermal functions of KOH(cr&l) for the temperatures 0–2000 K (Table 13) are calculated using the adopted values and equations presented in the previous section and the data from Table 10. The uncertainties of the tabulated values are given in Table 13.

The following values are adopted:

$$\begin{aligned} C_p^\circ(298.15 \text{ K}) &= 68.93 \pm 0.7 \text{ J K}^{-1} \text{ mol}^{-1}, \\ S^\circ(298.15 \text{ K}) &= 81.25 \pm 0.8 \text{ J K}^{-1} \text{ mol}^{-1}, \\ H^\circ(298.15 \text{ K}) - H^\circ(0) &= 12600 \pm 100 \text{ J mol}^{-1}. \end{aligned}$$

Heat Capacity Equations (in the following temperature ranges):

$$\begin{aligned} \beta\text{-cr, (298.15–517 K): } C_p^\circ/\text{J K}^{-1} \text{ mol}^{-1} \\ = 53.864 + 51.415 \cdot 10^{-3} T - 0.234 \cdot 10^5 T^{-2}, \end{aligned}$$

$$\gamma\text{-cr, (517–679 K): } C_p^\circ/\text{J K}^{-1} \text{ mol}^{-1} = 80,$$

$$\text{liq, (679–2000 K): } C_p^\circ/\text{J K}^{-1} \text{ mol}^{-1} = 87.$$

Phase Equilibrium Data:

$$\alpha\text{-}\beta \text{ transition: } T_{\text{trs}}/\text{K} = 226.7 \text{ and } \Delta_{\text{trs}}H/\text{J mol}^{-1} = 222,$$

$$\begin{aligned} \beta\text{-}\gamma \text{ transition: } T_{\text{tr}}/\text{K} = 517 \pm 3 \text{ and } \Delta_{\text{trs}}H/\text{J mol}^{-1} \\ = 5600 \pm 600, \end{aligned}$$

$$\begin{aligned} \text{Fusion: } T_{\text{fus}}/\text{K} = 679 \pm 2 \text{ and } \Delta_{\text{fus}}H/\text{J mol}^{-1} \\ = 7900 \pm 800. \end{aligned}$$

The calculated values of the thermal functions of KOH(cr, liq) differ from those listed in earlier reviews [82GUR/VEI] and [85CHA/DAV] (see Table 11), due to the use in this study of the new experimental data [88WHI/PER] for the low-temperature heat capacity of KOH. These differences are about 2 and 4 J K $^{-1}$ mol $^{-1}$ in the values of $\Phi^\circ(T)$ and

$S^\circ(T)$ at 500 K, respectively. For liquid KOH the differences increase up to 3 and 5 J K $^{-1}$ mol $^{-1}$ due to the use in this study of different data for the enthalpies of transition and fusion and for the heat capacity of the liquid.

2.1.2. Enthalpy of Formation of KOH(cr)

The enthalpy of formation of crystalline potassium hydroxide can be obtained from its enthalpy of solution in water and appropriate auxiliary data. The enthalpy of solution of KOH(cr) in water has been determined by the various investigators. These data are summarized in Table 12 and discussed below.

Experimental Studies

[1875BER]^a

Berthelot (see also [1875BER2]) measured the enthalpy of solution of KOH(cr) in water in a calorimeter at 284.55 K (one experiment). The precision of the calibration and temperature measurements, the sample purity, and the method of analysis of final solution was not indicated. Therefore it is difficult to evaluate the uncertainty of Berthelot's results.

[1886THO]^a

Thomsen measured the enthalpy of solution of KOH(cr) in water at 290.42 K in an isoperibol calorimeter (one experiment). The calorimeter energy equivalent was determined by a sum of heat capacities of all substances and part of the calorimeter. This method is not precisely correct. No information regarding the purity of the KOH sample was given.

[01FOR]^a

Forcrand measured the enthalpies of solution of KOH(cr) in water (one experiment) and a series of solids containing various amounts of water in the range KOH-(0.25–1.55)H₂O (five experiments) in an isoperibol calorimeter. We treated the [01FOR] data for KOH-nH₂O using a least-squares method and obtained the corresponding equation $\Delta_{\text{aq}}H/\text{kJ mol}^{-1} = f(n)$. The $\Delta_{\text{aq}}H$ value was found to be equal -48.9 kJ mol $^{-1}$ for $n=0$ (see Table 12). Some essential details of measurements were not given (e.g., the purity of samples, the precision of temperature measurements).

[46VOS/PON]

The enthalpy of solution of KOH(cr) in water was measured in a calorimeter at 298.15 K (two experiments). Essential details of measurement (purity of the KOH sample, precision of temperature measurements) were not given. The result of this work is about 23–27 kJ mol $^{-1}$ less negative than the $\Delta_{\text{aq}}H^\circ_\infty$ value obtained by other authors (see Table 12). The reason for this could be attributed to the presence of a significant amount of H₂O impurity in the KOH sample as was indicated by the authors [46VOS/PON].

^aThe data obtained by Berthelot [1875BER, 1875BER2], Thomsen [1886THO] and Forcrand [01FOR] [measurements with KOR(cr)] were recalculated by Parker [65PAR] taking into account the changes of atomic weights and the corrections for transition to the standard temperature and infinite dilution. Her recommendations are listed in Table 12, column 6.

[61RES]

Reshetnikov measured the enthalpy of solution of KOH (cr) in water at 298.15 K using an isoperibol calorimeter. The temperature was recorded on a platinum resistance thermometer with precision of ± 0.0005 K. The energy equivalent of the calorimeter was determined electrically. The calorimeter was tested by measuring the enthalpy of solution of KCl; the results obtained were in good agreement with the best literature data (see [82MED/BER]). The author declared that his KOH sample was pure, but did not quantitatively specify its purity. All preparative handlings as well as loading the calorimeter sample holder were made in a nitrogen-filled glove box.

[88KON/COR]

Konings *et al.* measured the enthalpy of solution of KOH(cr) in water in a precise isoperibol calorimeter at 298.15 K. The energy equivalent of the calorimeter was determined by an electrical method. The precision of temperature measurements was ± 0.0002 K. The KOH sample had a rather high purity. It was prepared from potassium metal (trade mark "Baker"), that was heated at 570 K in argon saturated with water vapor. Potassium content in the KOH sample was 69.74 ± 0.12 mass % (the calculated value is 69.68 mass %). The x-ray powder-diffraction analysis showed that no other crystalline phases except KOH detected. The chemical analy-

sis [titration with HCl(aq)] indicated that the sample contained the K_2CO_3 impurity (0.24 ± 0.01 mass %). The correction for this impurity was taken into account.

Discussion of the Enthalpy of Formation Data

The results of the older studies ([1875BER], [1875BER2], [1886THO], (01FOR)) have only historical interest because at that time experimental techniques, methods, and materials were of poor quality. Moreover, many important details of measurements were not recorded in these papers. It is also obvious (see experimental studies section) that data of [46VOS/PON] are erroneous.

The $\Delta_f H^\circ(\text{KOH,cr,298.15 K})$ values based on the data of Reshetnikov [61RES] and Konings *et al.* [88KON/COR] are more accurate. The precise isoperibol calorimeters and purer KOH samples were used in these studies, but the sample used by Konings *et al.* was more carefully characterized. The enthalpy of solution of KOH(cr), determined by Konings *et al.*, is 1.2 kJ mol^{-1} more negative than value obtained by Reshetnikov, who did not specify the purity of his KOH sample. Thus the $\Delta_f H^\circ(\text{KOH,cr,298.15 K})$ value obtained by Konings *et al.* [88KON/COR] is taken to be more reliable.

$$\Delta_f H^\circ(\text{KOH,cr,298.15 K}) = -423.4 \pm 0.2 \text{ kJ mol}^{-1}.$$

This value and similar values, as recommended in other reviews, are compared in Table 5.

2.1.3. Appendix. Tables of Experimental and Evaluated Data for KOH(cr)

TABLE 1. Smoothed heat capacity of KOH [70STU/HIL]

T/K	C_p°	
	cal K ⁻¹ mol ⁻¹	J K ⁻¹ mol ⁻¹
20	0.387	1.619
25	0.756	3.163
30	1.25	5.23
40	2.40	10.04
50	3.62	15.15
60	4.80	20.08
70	5.84	24.43
80	6.73	28.16
100	8.15	34.10
120	9.25	38.70
140	10.15	42.47
160	10.95	45.81
180	11.78	49.29
200	12.89	53.93
210	13.80	57.74
220	15.45	64.64
224	16.79	70.25
227.4	18.85	78.87
229	16.15	67.57
230	15.63	65.40
234	15.25	63.81
240	15.15	63.39
260	15.21	63.64
280	15.34	64.18
298.15	15.51	64.89

TABLE 2. Experimental heat capacity of KOH [88WHI/PER]

N	T/K	$C_p^\circ/\text{J K}^{-1} \text{mol}^{-1}$	N	T/K	$C_p^\circ/\text{J K}^{-1} \text{mol}^{-1}$
1	16.65	1.781	51	201.64	56.32
2	20.39	2.128	52	203.98	57.31
3	22.90	2.702	53	204.09	57.42
4	25.02	3.342	54	206.36	58.26
5	26.74	3.575	55	208.77	59.27
6	28.56	3.710	56	210.64	60.36
7	30.43	4.670	57	211.21	60.45
8	32.90	5.853	58	212.36	61.24
9	35.56	7.117	59	213.63	61.86
10	39.14	9.004	60	213.67	62.05
11	43.55	11.27	61	216.16	63.50
12	48.31	14.03	62	217.09	63.67
13	53.23	16.71	63	217.80	64.84
14	58.38	19.36	64	218.50	65.41
15	63.58	21.25	65	218.57	65.47
16	68.14	23.60	66	218.67	64.93
17	73.27	25.33	67	219.22	65.92
18	76.56	27.30	68	220.02	66.27
19	81.09	29.17	69	221.15	67.76
20	85.84	30.78	70	221.61	68.93
21	90.72	32.33	71	222.83	68.89
22	95.67	33.87	72	223.43	70.93
23	100.68	35.34	73	223.66	71.50
24	105.72	36.55	74	225.24	73.01
25	110.78	37.85	75	225.30	73.71
26	115.57	39.01	76	226.05	76.28
27	120.07	39.78	77	226.07	77.00
28	124.58	40.76	78	226.70	78.15
29	127.64	41.74	79	226.83	77.81
30	129.10	41.95	80	227.21	76.52
31	133.64	42.75	81	227.61	75.18
32	139.07	43.54	82	228.02	74.14
33	139.11	43.83	83	228.06	74.02
34	141.87	44.53	84	228.68	71.29
35	145.53	45.01	85	229.25	69.09
36	149.03	45.77	86	229.42	68.51
37	151.97	45.97	87	229.47	67.86
38	152.58	45.90	88	229.67	66.69
39	158.42	47.13	89	230.09	66.43
40	164.90	48.26	90	230.51	65.89
41	166.18	48.51	91	230.93	65.86
42	171.38	49.48	92	231.11	66.03
43	177.89	51.14	93	231.68	65.76
44	179.87	51.17	94	233.97	65.56
45	184.43	52.21	95	236.27	65.57
46	185.11	52.83	96	238.57	65.68
47	190.98	53.67	97	244.41	65.84
48	192.37	54.23	98	246.68	66.38
49	193.61	54.28	99	249.20	66.25
50	197.53	55.37	100	254.24	66.47
101	254.42	66.53	117	300.84	69.09
102	258.41	66.49	118	300.99	69.02
103	259.02	66.71	119	308.78	69.89
104	261.83	66.70	120	311.68	69.90
105	268.70	67.46	121	312.29	70.27
106	269.49	67.27	122	315.41	69.92
107	271.91	67.39	123	316.75	70.11
108	272.50	67.25	124	324.40	71.55
109	277.22	68.14	125	325.25	71.47
110	283.14	68.20	126	327.04	71.68
111	285.00	68.09	127	332.17	71.94
112	285.04	67.97	128	338.96	72.66
113	286.70	68.06	129	339.97	72.58
114	292.91	68.49	130	341.71	72.96
115	297.65	68.93			
116	298.27	69.01			

TABLE 3. Experimental enthalpy values $H^\circ(T) - H^\circ(273.15 \text{ K})$ of KOH [54POW/BLA]

N	T/K	$H^\circ(T) - H^\circ(273.15 \text{ K})$	
		cal g ⁻¹	J mol ⁻¹
1	435	54	12680
2	469	63	14790
3	485	74	17370
4	491(sol, β)	63	14790
5	532(sol, γ)	112	26290
6	542	114	26760
7	545	112	26290
8	547	111	26060
9	550	111	26060
10	565	112	26290
11	571(sol, γ)	122	28640
12	691(liq)	197	46240
13	693	203	47650
14	695	204	47890
15	719	209	49060
16	723	205	48120
17	725	221	51880
18	739	215	50470
19	740	210	49300
20	748	214	50240
21	773	235	55170
22	785	234	54930
23	800	250	58690
24	801	234	54930
25	809	233	54700
26	819	244	57280
27	821	239	56100
28	830	251	58920
29	833	257	60330
30	841	244	57280
31	845	270	63380
32	847	246	57750
33	897	271	63620
34	900	286	67140
35	906	278	65260
36	925	289	67840
37	949	300	70420
38	954	296	69480
39	964	289	67840
40	965	281	65960
41	987	305	71600
42	987	307	72070
43	999	314	73710
44	1027	327	76760
45	1038	311	73010
46	1042	331	77700
47	1043	337	79110
48	1047	322	75590
49	1054	337	79110
50	1067	321	75350
51	1071	344	80750
52	1075	339	79580
53	1079	329	77230
54	1079	335	78640
55	1087	359	84270
56	1095	334	78410
57	1095	341	80050
58	1125	361	84740
59	1130	334	78410
60	1136	369	86620
61	1138	370	86860
62	1140	340	79810

TABLE 3. Experimental enthalpy values $H^\circ(T) - H^\circ(273.15 \text{ K})$ of KOH [54POW/BLA]—Continued

N	T/K	$H^\circ(T) - H^\circ(273.15 \text{ K})$	
		cal g ⁻¹	J mol ⁻¹
63	1147	342	80280
64	1151	384	90140
65	1153	367	86150
66	1153	346	81220
67	1159	366	85920
68	1159	375	88030
69	1164	349	81930
70	1166	359	84270
71	1167	375	88030
72	1180	379	88970
73	1183	383	89910
74	1183	372	87330
75	1185	382	89670
76	1189	379	88970
77	1189	366	85920
78	1191	383	89910
79	1226	409	96010
80	1228	388	91080

TABLE 4. Smoothed heat capacity and enthalpy values of KOH [71GIN/GUB], [71GIN]

T/K	$C_p^\circ(T)/\text{J K}^{-1} \text{ mol}^{-1}$	$H^\circ(T) - H^\circ(2908.15 \text{ K})/\text{J mol}^{-1}$
298.15	68.13	0
400	74.35	7256
500	80.45	14995
522.15(β)	81.80	16792
522.15(γ)	70.60	21937
600	85.95	28031
683.15(γ)	102.35	35860
683.15(liq)	87.22	43157
700	87.22	44626
800	87.22	53348
900	87.22	62069
1000	87.22	70791
1100	87.22	79512

TABLE 6. Temperature of transitions of KOH

Reference	$T_{\text{tr}}/^\circ\text{C}$	T_{tr}/K	Comments
$\alpha - \beta$ transition			
Original studies			
70STU/HIL		227.5	Heat capacity data
86BAS/ELC		233	DSC-method
88WHI/PER		226.7 ± 0.2	Heat capacity data
Adopted this study		226.7 ± 0.2	Based on 88WHI/PER
$\beta - \gamma$ transition			
Original studies			
10HEV2	248 ± 0.5	521	Thermal analysis
15SCA2	266	539	Thermal analysis (DTA)
23EWL	242	515	Thermal analysis (DTA)
49SEW/MAR	249	522	Thermal analysis (DTA)
51DIO	256	529	Thermal analysis
53KHI/KHI, 54KHI	240	513	Thermal analysis (DTA)
56COH/MIC, 61COH/MIC	242	515	Thermal analysis
58RES/VIL	250	523	Thermal analysis (DTA)
59ROL/COH	242	515	Thermal analysis
61MIC	242 ± 0.3	515.15	Thermal analysis (DTA)
61RES/ROM	248 ± 1	521	Thermal analysis (DTA)
63LUX/BRA	248	521	Thermal analysis
66MIT/GRO	242–247	515–520	Thermal analysis (DTA)
67MIC, 68MIC	244	517	Thermal analysis (DTA)
67TSE/ROG	245	518	Thermal analysis (DTA)
67RES/BAR, 69RES/BAR	242	515	Thermal analysis (DTA)
67RUB, 68RUB/SEB	244	517	Thermal analysis (DTA)
74BEC/COU	244	517	Thermal analysis (DTA)
80BAI, 88BAI/NIK	242	515	Thermal analysis (DTA)
Reviews			
82MED/BER		517 ± 4	Based on 5 studies
82GUR/VEI		520 ± 3	Based on 12 studies
85CHA/DAV		516	Based on 69RES/BAR and 67MIC
Adopted this study		517 ± 3	Based on 67MIC, 67RUB, 67TSE/ROG, 69RES/BAR, 74BEC/COU

TABLE 5. Comparison of the heat capacity, enthalpy, entropy, and enthalpy of formation values for KOH(cr) at 298.15 K

Reference	$C_p^\circ(298.15 \text{ K})/\text{J K}^{-1} \text{ mol}^{-1}$	$S^\circ(298.15 \text{ K})/\text{J K}^{-1} \text{ mol}^{-1}$	$H^\circ(298.15 \text{ K}) - H^\circ(0 \text{ K})/\text{J mol}^{-1}$	$\Delta_f H^\circ(298.15 \text{ K})/\text{kJ mol}^{-1}$
70STU/HIL	64.89	78.87	12208	...
82MED/BER	64.89 ± 0.4	78.87 ± 0.6	12150 ± 100	-424.67 ± 0.25
82WAG/EVA	64.9	78.9	12150	-424.764
82GUR/VEI	64.90	78.87 ± 0.4	12150 ± 80	-424.58 ± 0.25
85CHA/DAV	64.894	78.907 ± 0.84	12163	-424.72 ± 0.4
88WHI/PER	68.93	81.25 ^a	12600	...
89KON/COR	-423.40 ± 0.14
Adopted	68.93 ± 0.7	81.25 ± 0.8	12600 ± 100	-423.4 ± 0.2

^aCalculated in this review.

TABLE 7. Temperature of fusion of KOH

Reference	$T_{\text{fus}}/^{\circ}\text{C}$	T_{fus}/K	Comments
Original studies			
10HEV2	360.4±0.7	633.55	Thermal analysis
14NAI/BER	345	618	Thermal analysis
15SCA2	380	653	Thermal analysis (DTA)
49SEW/MAR	410±1	683	Thermal analysis (DTA)
51DIO, 52RES/DIO	403	676	Thermal analysis, visual method
52BER/KHI	406	679	Thermal analysis, visual method
53KHI/KHI, 54KHI	406	679	Thermal analysis (DTA)
54BER/RES	404±1	677	Thermal analysis, visual method
56COH/MIC	401±1	674	Thermal analysis
58RES/VIL	404	677	Thermal analysis (DTA)
59RES/UNZ	401–403	674–676	Thermal analysis, visual method
59ROL/COH	404	677	Thermal analysis
61COH/MIC, 61MIC	404	677	Thermal analysis
61RES/ROM	404	677	Thermal analysis (DTA)
63LUX/BRA	416	689	Thermal analysis (DTA)
66MIT/GRO	399–404	672–677	Thermal analysis (DTA)
67MIC,68MIC	405.2±0.3	678.35	Thermal analysis (DTA)
67RES/BAR	406–407	679–680	Thermal analysis, visual method
67RUB	404	677	Thermal analysis (DTA)
67TSE/ROG	401	674	Thermal analysis (DTA)
68RUB/SEB	405	678	Thermal analysis (DTA)
71DIO/RES	405	678	Thermal analysis
80BAI	407	680	Thermal analysis (DTA)
Reviews			
82MED/BER		678±3	Based on 14 studies
82GUR/VEI		678±2	Based on 20 studies
85CHA/DAV		679	Based on 67RES/BAR and 67MIC
Adopted this study		679±2	Based on 54KHI, 61KOH/MIC, 67MIC, 67RES/BAR, 68RUB, 71DIO/RES

TABLE 8. Enthalpy of β - γ transformation of KOH

Reference	$\Delta_{\text{trs}}H, \text{J mol}^{-1}$	Comments
Original studies		
10HEV2	6360	Thermal analysis (DTA)
54POW/BLA	5630	Enthalpy measurements
67RES/BAR	6440	Thermal analysis (DTA)
71GIN/GUB	5150	Enthalpy measurements
71GIN/GUB, with correction	5600	See Sec. 2.1
Reviews		
82MED/BER	5650 ± 420	Based on 54POW/BIA
82GUR/VEI	6450 ± 500	Based on 67RES/BAR
85CHA/DAV	6443 ± 630	Based on 67RES/BAR
Adopted	5600 ± 600	Based on 71GIN/GUB with correction

TABLE 9. Enthalpy of fusion of KOH

Reference	$\Delta_{\text{fus}}H, \text{J mol}^{-1}$	Comments
Original studies		
10HEV2	6710	Thermal analysis (DTA)
49SEW/MAR	7700	Calculation from system
54POW/BLA	9390	Enthalpy measurements
67RES/BAR	8280	Thermal analysis (DTA)
68MIC	8900	Calculation from system
71GIN/GUB	7300	Thermal analysis (DTA)
71GIN/GUB, with correction	7900	See Sec. 2.1
Reviews		
82MED/BER	9370±630	Based on 54POW/BLA
82GUR/VEI	9400±1200	Based on 54POW/BLA
85CHA/DAV	8619±630	Based on 67RES/BAR, 68MIC
Adopted this study	7900±800	Based on 71GIN/GUB with correction

TABLE 10. Thermal functions of KOH(cr) below 298.15 K

T/K	$C_p^{\circ}(T)$ $\text{J K}^{-1} \text{mol}^{-1}$	$H^{\circ}(T) - H^{\circ}(0 \text{ K})$ kJ mol^{-1}	$S^{\circ}(T)$ $\text{J K}^{-1} \text{mol}^{-1}$
20	2.073	0.0147	0.943
25	3.311	0.0279	1.524
30	4.294	0.0463	2.195
35	6.903	0.0747	3.066
40	9.365	0.115	4.139
45	12.21	0.169	5.407
50	14.93	0.237	6.836
60	19.96	0.412	10.010
70	24.48	0.634	13.432
80	28.50	0.900	16.969
90	32.03	1.203	20.534
100	35.08	1.539	24.071
120	39.99	2.292	30.921
140	43.90	3.132	37.387
160	47.48	4.045	43.483
180	51.33	5.033	49.293
200	56.10	6.104	54.935
210	59.86	6.683	57.755
220	66.56	7.311	60.679
225	74.21	7.659	62.241
226.7 ^a	78.16	7.789	62.816
230	66.70	8.029	63.870
240	65.73	8.686	66.662
260	66.81	10.012	71.970
280	67.81	11.358	76.957
298.15	68.93	12.600	81.250

^a α - β transition.TABLE 11. Differences ($\text{J K}^{-1} \text{mol}^{-1}$) between the thermal functions of KOH(cr&liq) calculated in the present work and in [82GUR/VEI, 85CHA/DAV]

T/K	[Present Work]-[82GUR/VEI]			[Present Work]-[85CHA/DAV] ^a		
	$\Delta C_p^{\circ}(T)$	$\Delta\Phi^{\circ}(T)$	$\Delta S^{\circ}(t)$	$\Delta C_p^{\circ}(T)$	$\Delta\Phi^{\circ}(T)$	$\Delta S^{\circ}(T)$
298.15	4.030	0.870	2.350	4.036	0.877	2.343
500	-0.522	1.782	3.399	-0.102	1.832	3.678
1000	4.0	1.494	1.375	3.893	2.004	2.828
1500	4.0	1.742	2.996	3.893	2.560	4.406
2000	4.0	2.207	4.148	3.893	3.168	5.527

^aThe values of $\Delta\Phi^{\circ}(T)$ tabulated in [85CHA/DAV] are adjusted to the reference temperature $T=0$ instead of 298.15 K.

TABLE 12. The enthalpy of formation of KOH(cr) from measurements of the enthalpies of solution of potassium hydroxide in water

Authors	Moles of H ₂ O, n ^a	T/K	No. of measurements	$\Delta_{\text{aq}}H^\circ$, ^a kJ mol ⁻¹	Δ_{aq}° , ^b at 298.15 K, kJ mol ⁻¹	$\Delta_f H^\circ(\text{KOH, cr},$ 298.15 K), ^c kJ mol ⁻¹
1875BER, 1875BER2	260	284.55	1	-52.1 ₃	-55.5 ₂	-426.7
1886THO	250	290.42	1	-55.6 ₁	-57.5 ₃	-424.6
01FOR	170	294.65	1	-54.2	-55.5	-426.7
	170	294.65	5	-48.9 ^d	-50.2 ± 2.0	-432.0
46VOS/PON	310	298.15	2	-31.4 ₄	-32.0	-450.2
61RES	620	298.15	6	-57.17	-57.6 ± 0.4 ^e	-424.5 ± 0.4
88KON/COR	6040	298.15	4	-58.59 ± 0.18 ^f	-58.8 ± 0.2	-423.4 ± 0.2 ^g

^aReaction is $\text{KOH(cr)} + n\text{H}_2\text{O(l)} = \text{KOH(soln, nH}_2\text{O)}$.

^bReaction is $\text{KOH(cr)} + \infty\text{H}_2\text{O(l)} = \text{KOH(soln, } \infty\text{H}_2\text{O)}$. Calculations were carried out by us with the exception of the Berthelot, Thomsen and Forcrand results (see Sec. 2.1). The enthalpies of dilution of KOH (soln, nH₂O) to infinite dilution were taken from Parker's book [65PAR].

^cThe CODATA values ($\Delta_f H^\circ(\text{OH}^-, \text{soln}, \infty\text{H}_2\text{O}, 298.15 \text{ K}) = -230.015 \pm 0.040 \text{ kJ mol}^{-1}$ and $\Delta_f H^\circ(\text{K}^+, \text{soln}, \infty\text{H}_2\text{O}, 298.15 \text{ K}) = -252.14 \pm 0.08 \text{ kJ mol}^{-1}$ [89COX/WAG]) were used in processing the experimental data. The uncertainty was calculated as a square root from the sum of squares of uncertainties of the $\Delta_{\text{aq}}H^\circ_\infty(298.15 \text{ K})$, $\Delta_f H^\circ(\text{OH}^-, \text{soln}, \infty\text{H}_2\text{O}, 298.15 \text{ K})$ and $\Delta_f H^\circ(\text{K}^+, \text{soln}, \infty\text{H}_2\text{O}, 298.15 \text{ K})$ values.

^dThe value was obtained by extrapolating the experimental data [01FOR] for the enthalpies of solution of the KOH·nH₂O samples containing different amounts of water (from n=0.25 to n=1.55) to zero moles of H₂O.

^eThe uncertainty was increased conditionally to ±0.4 kJ mol⁻¹ owing to the opportunity of presence of some impurities in the KOH sample.

^fThe uncertainty was recalculated using the Student's criterion. Author's [88KON/COR] uncertainty is ±0.11 kJ mol⁻¹.

^gAuthor's [88KON/COR] value is -423.57 ± 0.14 kJ mol⁻¹. It seems that these authors do not take into account a difference ($\Delta_{\text{aq}}H^\circ_\infty - \Delta_{\text{aq}}H^\circ$) (see columns 5 and 6 of Table 12).

TABLE 13. Thermodynamic properties at 0.1 MPa: KOH(cr&liq)

T/K	C_p°	$-(G^\circ - H^\circ(0\text{ K}))/T$	S°	$H^\circ - H^\circ(0\text{ K})$	$\Delta_f H^\circ$	$\Delta_f G^\circ$
	J K ⁻¹ mol ⁻¹			kJ mol ⁻¹		
0	0.000	0.000	0.000	0.000	-421.518	-421.518
25	3.311	0.410	1.524	0.028	-422.243	-419.739
50	14.928	2.097	6.836	0.237	-423.257	-416.849
75	26.430	5.032	15.192	0.762	-424.098	-413.450
100	35.080	8.681	24.071	1.539	-424.662	-409.809
150	45.692	16.614	40.477	3.580	-425.291	-402.225
200	56.100	24.415	54.935	6.104	-425.492	-394.496
250	66.331	31.974	69.359	9.346	-425.052	-386.787
300	69.028	39.251	81.677	12.728	-424.561	-379.177
350	71.668	46.101	92.516	16.245	-426.381	-371.562
400	74.284	52.522	102.257	19.894	-425.798	-363.769
450	76.885	58.549	111.157	23.673	-425.075	-356.058
500	79.478	64.227	119.392	27.582	-424.214	-348.435
517cr, β	80.358	66.085	122.064	28.941	-423.890	-345.864
517cr, γ	80.000	66.085	132.895	34.541	-418.290	-345.864
600	80.000	76.171	144.806	41.181	-416.702	-334.357
679cr, γ	80.000	84.744	154.702	47.501	-415.195	-323.610
679liq	87.000	84.744	166.336	55.401	-407.295	-323.610
700	87.000	87.232	168.986	57.228	-406.749	-321.031
800	87.000	98.193	180.603	65.928	-404.177	-308.961
900	87.000	107.931	190.851	74.628	-401.663	-297.211
1000	87.000	116.689	200.017	83.328	-399.236	-285.736
1100	87.000	124.647	208.309	92.028	-475.788	-269.883
1200	87.000	131.939	215.879	100.728	-472.480	-251.310
1300	87.000	138.667	222.843	109.428	-469.212	-233.012
1400	87.000	144.913	229.290	118.128	-465.980	-214.965
1500	87.000	150.740	235.292	126.828	-462.786	-197.146
1600	87.000	156.202	240.907	135.528	-459.627	-179.540
1700	87.000	161.342	246.182	144.228	-456.503	-162.131
1800	87.000	166.194	251.154	152.928	-453.414	-144.902
1900	87.000	170.791	255.858	161.628	-450.361	-127.848
2000	87.000	175.157	260.321	170.328	-447.344	-110.953
298.15	68.930	38.989	81.250	12.600	-424.580	-379.457
Uncertainties in Functions						
0	0.200	0.200
300	0.700	0.600	0.800	0.100	0.200	0.300
500	1.000	0.700	1.000	0.200	0.300	0.400
1000	3.000	1.200	2.000	0.700	0.700	1.000
1500	5.000	2.500	3.000	2.000	2.000	4.000
2000	7.000	4.000	4.500	5.000	5.000	8.000

2.2. Potassium Hydroxide in Gaseous Phase

2.2.1. Potassium Hydroxide Monomer

Molecular Constants of KOH(g)

The molecular constants of KOH, measured, calculated,

estimated, or accepted in the following studies, are listed in Table 14.

[53SMI/SUG]

Smith and Sugden estimated the molecular constants of KOH assuming a linear model of the molecule with

TABLE 14. Bond lengths (Å), bond angle (deg), and frequencies (cm^{-1}) of KOH in the ground electronic state

Reference	$r(\text{K-O})$	$r(\text{O-H})$	$\angle(\text{K-O-H})$	ν_1	$\nu_2(2)$	ν_3	Note
[53SMI/SUG]	2.27	0.97	180	400	340	...	a
[58SPI/MAR]	408	b
[59BUC]	3611	c
[60SNY/KUM]	3600	c
[61WIL]	3600	c
[66JEN/PAD]	2.48	0.96	112	401	1300	3610	d
[66KUC/LID]	2.18	0.97	180	e
[69TIM/KRA]	2.18	0.97	180	408	395	3740	f
[71BEL/DVO]	2.18	0.97	180	408	300	3600	g
[71KEL/PAD]	2.18	0.96	180	408	325	3600	f
[72KAM/MAE]	3561	c
[73PEA/TRU]	2.2115	0.9120	180	h
[75KUI/TOR]	2.2115	0.9120	180	390	320	...	i
[76PEA/WIN]	2.212	0.912	180	408	300	...	j
[78BEL]	180	407.5	300.5	...	k
[78BEL]	413	375.5	...	l
[78ENG]	2.2711	0.936	180	m
[78LOV]	2.2115	0.9120	180	n
[80NEM/STE]	2.23	0.96	180	401	783	3804	o
[80NEM/STE]	2.23	0.96	180	399	716	3804	p
[80PIE/LEV]	2.158	0.988	180	q
[82GUR/VEI]	2.2115	0.9120	180	408	300	3700	r
[84DEV/CAR]	412	s
[84KAM/KAW]	3542	t
[85CHA/DAV]	2.18	0.97	180	408	340	3610	u
[86BAU/LAN]	2.235	0.9472	180	455	v
[86BAU/IAN]	2.208	0.9472	180	467	w
[87ALI/VEN]	2.2115	0.912	180	408	300	3700	r
[90KON]	180	406	280	...	b
Adopted in the present work	2.212	0.912	180	408	300	3700	r

^aEstimated.

^bIR spectrum of vapor.

^cIR spectrum of solid.

^dTaken from the old JANAF Thermochemical Tables (before 1971) for nonlinear configuration; ν_2 is nondegenerate.

^eMicrowave spectrum.

^fThe data from [58SPI/MAR, 66KUC/LID] and estimates of ν_2 and ν_3 .

^g ν_1 and ν_2 from IR spectra in Ar matrix; ν_3 is estimated; bond lengths from [66KUC/LID].

^hMillimeter wave spectrum.

ⁱMicrowave spectrum; ν_1 and ν_2 are assumed.

^jMillimeter wave spectrum; ν_1 and ν_2 are assumed.

^kAr matrix IR spectra; assignment for a linear molecule.

^lAr matrix IR spectra; assignment for a bent molecule; ν_2 is nondegenerate.

^m*Ab initio* calculation.

ⁿBond lengths from [73PEA/TRU].

^oDiatomics-in-molecules method; parameters of potential surface are calculated using the [66BUE/PEY] approach.

^pDiatomics-in-molecules method; parameters of potential surface are calculated using an alternative approach.

^qSTO-3G theoretical calculation.

^rBond lengths from [76PEA/WIN], ν_1 from [58SPI/MAR], ν_2 from [71BEL/DVO], ν_3 estimated.

^sElectronic emission spectra of gas.

^tRaman spectra of crystal.

^uBond lengths from [66KUC/LID]; ν_1 from [58SPI/MAR]; ν_2 and ν_3 from [70JEN].

^vSCF *ab initio* calculation.

^wCI(SD) *ab initio* calculation.

$r(\text{O-H}) = 0.97 \text{ \AA}$. The value of $r(\text{K-O})$ was taken to be equal to that for the KO molecule as estimated by Brewer and Mastick [49BRE/MAS]. The value of $\nu(\text{K-O})$ was estimated by comparison with the vibrational frequencies for diatomic metal oxides listed by Herzberg [39HER]; the value of $\nu(\text{K-O-H})$ was calculated in the ionic model approximation.

[58SPI/MAR]

Spinar and Margrave studied the IR spectrum of the equilibrium vapor over potassium hydroxide at 690–900 °C and assigned an absorption at 405–410 cm^{-1} to $(\text{KOH})_x$ where $x = 1$ or 2. The authors tentatively attributed this absorption to the K–O stretching vibration of the linear KOH molecule with the uncertainty of 10 cm^{-1} . The ultraviolet and visible spectra were also observed from 2000 to 7400 \AA and no absorption of the KOH molecule was detected.

[59BUC]

Buchanan investigated the near IR spectrum of crystalline potassium hydroxide and assigned an absorption band at $3611 \pm 4 \text{ cm}^{-1}$ to ν_3 (the O–H stretching frequency) of KOH.

[59SCH/POR]

Schoonmaker and Porter assumed a linear structure for the KOH molecule but did not exclude a nonlinear one.

[60SNY/KUM]

Snyder *et al.* observed the vibrational spectrum of crystalline potassium hydroxide at 23 °C and assigned a wide band at 3600 cm^{-1} to ν_3 (the O–H stretching frequency) of KOH and a band at 643 cm^{-1} to a lattice mode.

[61WIL]

Wilmshurst investigated the IR reflection spectra of potassium hydroxide in the range 200–4200 cm^{-1} and assigned a band at 3600 cm^{-1} of the solid at 23 °C and a band at 3360 cm^{-1} (center) of the liquid at 440 °C to ν_3 (the O–H stretching frequency of KOH).

[66JEN/PAD]

Jensen and Padley adopted all molecular constants of KOH recommended in an earlier version of the JANAF Thermochemical Tables where a bent configuration of the molecule had been selected.

[66KUC/LID]

Kuczowski *et al.* carried out a preliminary analysis of the rotational transitions $J = 1 \rightarrow 2$ and $0 \rightarrow 1$ for the ground vibrational state of KOH in the microwave spectrum. The authors obtained the evidence for an effective linear structure, though they did not exclude the possibility of a quasi-linear structure with a small potential hump on the linear configuration. Assuming $0.97 \pm 0.05 \text{ \AA}$ for the O–H distance, they obtained the K–O distance as $2.18 \pm 0.01 \text{ \AA}$.

[69ACQ/ABR]

Acquista and Abramowitz made an unsuccessful attempt at obtaining the IR spectrum of Ar matrix-isolated monomeric KOH. They observed several bands below 350 cm^{-1} which could be ascribed only to polymeric species of KOH.

[69TIM/KRA]

Timoshinin and Krasnov listed the molecular constants of KOH using the data [58SPI/MAR, 66KUC/LID] and some estimates.

[70JEN]

Jensen estimated $\nu_3 = 3610 \text{ cm}^{-1}$ for a linear configuration of the KOH molecule and accepted the other molecular constants from literature data.

[71BEL/DVO]

Belyaeva *et al.* reported preliminary results of an investigation of the IR spectrum of KOH and KOD in Ar matrix at 4.2 K in the range 200–4000 cm^{-1} . The observed bands at 408 and 300 cm^{-1} were attributed, respectively, to ν_1 (the K–O symmetric stretching) and ν_2 (the K–O–H bending) fundamental frequencies of linear KOH. The force field calculation was made on the assumption that $\nu_3 = 3600 \text{ cm}^{-1}$.

[71KEL/PAD]

Kelly and Padley accepted the molecular constants for a linear configuration of KOH using literature data and some estimations.

[72KAM/MAE]

Kamisuki and Maeda observed the IR absorption spectrum of KOH films on a quartz carrier at $-165 \text{ }^\circ\text{C}$ and assigned a band at 3561 cm^{-1} to the O–H stretching frequency.

[73PEA/TRU]

In the millimeter wave spectral region, Pearson and Trueblood observed several rotational transitions of KOH and KOD in the ground vibrational state. The measured frequencies were interpreted in the terms of a linear model. The rotational constants in the ground state were found to be in disagreement with the microwave results of [66KUC/LID] which could be spurious as it had been privately communicated by one of the authors [66KUC/LID]. The authors [73PEA/TRU] recommended $B_0 = 8208.679(10) \text{ MHz}$ and $D_0^\circ = 12.18(6) \text{ kHz}$. The resulting interatomic distances were calculated as 0.9120 \AA for the O–H bond and 2.2115 \AA for the K–O bond.

[75KUI/TOR]

Kuijpers *et al.* measured more than 50 lines of the rotational transition $J = 6 \leftarrow 5$ for a large number of vibrational states in the microwave spectrum of ^{39}KOH and ^{41}KOH . The vibrational frequencies $\nu_1 = 390(40) \text{ cm}^{-1}$ and $\nu_2 = 320(30) \text{ cm}^{-1}$ were determined from the intensity ratios of the $(0,0^\circ,0)$, $(0,2^\circ,0)$, and $(1,0,0)$ transitions. The rotational constants B_0 and D_0° for linear ^{39}KOH were found in complete agreement with those reported in [73PEA/TRU]. The vibration-rotation and λ -type doubling constants were also obtained.

[76PEA/WIN]

In the millimeter wave spectral range, Pearson *et al.* measured rotational transitions for a number of excited vibrational states of KOH and KOD. The data obtained in [75KUI/TOR] were included in the analysis. As a result, the rotational and vibration-rotation constants of potassium hy-

dioxide were calculated for several vibrational states. The values $\nu_1 = 408 \text{ cm}^{-1}$ and $\nu_2 = 300 \text{ cm}^{-1}$ were assumed. For the ground state, the values $B_0 = 8208.691(17) \text{ MHz}$ (0.273812 cm^{-1}) and $D_0^\circ = 2.226(75) \text{ kHz}$ ($4.08 \cdot 10^{-7} \text{ cm}^{-1}$) were determined. The structural parameters were found as $r_o = 2.212(2) \text{ \AA}$ and $r_e = 2.196(2) \text{ \AA}$ for the K–O bond and $r_o = 0.912(10) \text{ \AA}$ and $r_e = 0.960(10) \text{ \AA}$ for the O–H bond. [78BEL] (see also [91BEL])

Belyaeva investigated IR spectra of KOH and KOD trapped in Ne, Ar, Kr, and Xe matrices at 8 K in the range 200–4000 cm^{-1} . Analysis of the spectra was carried out on the assumption that in gaseous phase there are both linear and bent monomeric molecules of potassium hydroxide. The assignment of the bands observed in the Ar matrix was made for the stretching K–O (ν_1) and bending K–O–H (ν_2) vibrational frequencies of both configurations. The bands at 407.5 and 302.5/298.5 cm^{-1} were assigned to ν_1 and ν_2 , respectively, of linear KOH; the bands at 413 and 375.5 cm^{-1} were assigned to ν_1 and ν_2 , respectively, of nonlinear KOH.

[78ENG] (see also [77ENG])

England calculated *ab initio* energies and dipole moments for linear geometry and obtained $r(\text{K–O}) = 4.2913 \text{ a.u.}$ (2.271 \AA) and $r(\text{O–H}) = 1.7688 \text{ a.u.}$ (0.935 \AA) with an accuracy about 2%, but decided that the calculations did not unambiguously establish the linearity of the KOH molecule.

[78LOV]

Lovas, in the review of microwave spectra data, recommended the structural parameters of KOH obtained in [73PEA/TRU].

[80NEM/STE]

Nemukhin and Stepanov applied the diatomics-in-molecules approach to calculating the geometry and vibrational frequencies. The structure of the molecule in the $^1\Sigma^+$ ground state was found to be linear. The values of the equilibrium bond lengths and vibrational frequencies were obtained using two sets of parameters for the potential surface. The authors noted some limitations of this method for predicting the bending frequency.

[80PIE/LEV]

Pietro *et al.* carried out *ab initio* calculation of the KOH molecular geometry using the STO-3G basis set and obtained for a linear structure ($C_{\infty v}$ symmetry) the values $r(\text{K–O}) = 2.158 \text{ \AA}$ and $r(\text{O–H}) = 0.988 \text{ \AA}$.

[82GUR/VEI]

Gurvich *et al.* adopted a linear molecular model for calculating the thermal functions of KOH(g) and selected the rotational constant B_0 from [76PEA/WIN], ν_1 from [58SPI/MAR], and ν_2 from [71BEL/DVO]. The value of ν_3 was estimated to be the same as in the other alkali metal hydroxides.

[84DEV/CAR]

Dever *et al.* observed the first electronic emission spectrum of KOH in the $\text{K}_2 + \text{H}_2\text{O}_2$ diffusion flame and esti-

mated from the short wavelength peak separations the ground state K–O stretching frequency ν_1 as $412 \pm 18 \text{ cm}^{-1}$.

[84KAM/KAW]

Kamesaka and Kawahara observed the Raman spectra of crystalline KOH and KOD at 77 K and at room temperature and assigned a double peak band at 3531/3553 cm^{-1} to the O–H stretching mode of KOH.

[85CHA/DAV]

Chase *et al.* adopted a linear structure of KOH for calculating the thermal functions and selected the bond lengths from [66KUC/LID]. ν_1 was taken from [58SPI/MAR]; ν_2 and ν_3 were estimates made by Jensen [70JEN].

[85KAN/HIR]

Kanno and Hiraishi investigated a Raman spectrum of aqueous solution of KOH in the glassy state and observed a band at about 285 cm^{-1} .

[86BAU/LAN]

Bauschlicher *et al.* calculated *ab initio* the values of $r(\text{K–O})$, $\nu(\text{K–O})$, and $D_0^\circ(\text{K–OH})$ of the KOH molecule in the linear ground electronic state assuming the rigid OH subunit with a fixed O–H bond distance 0.9472 \AA . The calculations were made using both the self-consistent field (SCF) and singles plus doubles configuration (CISD) levels and the extended Gaussian basis set of at least triple-zeta plus double polarization quality.

[87AL'VEN]

Al'tman *et al.* in the review of the geometry and vibrational frequencies for triatomic molecules recommended molecular constants of KOH selected from literature data.

[87RAW/YAM]

Raw *et al.* studied a hyperfine structure of the rotational transitions $J = 2 \leftarrow 1$ in the $(0, 0^\circ, 0)$, $(1, 0^\circ, 0)$, and $(0, 1^\circ, 0)$ vibrational states of ^{39}KOH in 32 GHz microwave region. The results provided additional support for a linear structure of the molecule.

[90KON]

Konings investigated the IR spectrum of KOH vapor at 1015 K in the region 50–600 cm^{-1} . Two strong absorption maxima at 406 ± 4 and $280 \pm 2 \text{ cm}^{-1}$ were assigned to ν_1 (the K–O stretch) and ν_2 (the K–O–H bend) fundamentals of linear KOH.

Discussion of the Molecular Constants of KOH(g)

Over a long period of time suppositions about the geometry of the KOH molecule have been rather controversial. Smith and Sugden [53SMI/SUG] assumed a linear structure, while Jensen and Padley [66JEN/PAD] adopted $\angle(\text{K–O–H}) = 112^\circ$ following the recommendation given in the early JANAF Thermochemical Tables. Later Jensen [70JEN] revised this opinion and adopted a linear model of KOH. The existence of both linear and bent molecules of KOH in gas phase was assumed by Belyaeva [73BEL].

The earliest attempt of the experimental determination of molecular structure of KOH was made by Kuczkowski *et al.* [66KUC/LID]. They reported preliminary results of the mi-

crowave investigation of KOH and came to the conclusion that the molecule was linear but did not exclude a possibility of a quasi-linearity. Later, Pearson and Trueblood [73PEA/TRU] declared that the work [66KUC/LID] did not appear to be reproducible. The spectral data, obtained in [73PEA/TRU, 75KUI/TOR, 76PEA/WIN] for a large number of the rotational transitions in several vibrational states, were successfully interpreted in terms of a linear structure of KOH. The rotational constants and bond lengths of the molecule were obtained with a high degree of accuracy by Pearson with co-workers [73PEA/TRU, 76PEA/WIN].

The investigation of the nuclear quadrupole structure of the $J = 2 \leftarrow 1$ transition [87RAW/YAM], as well as the results of theoretical calculations [78ENG, 80NEM/STE, 80PIE/LEV, 86BAU/LAN], provided additional support for a linear configuration of KOH. Nevertheless, in an *ab initio* investigation of the geometry and dipole moment of KOH [78ENG] a linearity of the molecule still was called in question though a promised study apparently was not published.

For linear KOH, there are three fundamental frequencies: K–O stretching (ν_1), K–O–H bending (ν_2), and O–H stretching (ν_3). The frequencies ν_1 and ν_3 are nondegenerate: ν_2 is doubly degenerate.

There are several spectral investigations of the vibrational frequencies KOH in gas phase [58SPI/MAR, 84DEV/CAR, 90KON] and in inert matrices [71BEL/DVO, 78BEL, 91BEL].

Spinar and Margrave [58SPI/MAR] detected in the IR spectrum of potassium hydroxide a vapor band at 405–410 cm^{-1} but could not definitely assign it to either monomeric or dimeric KOH molecule. In any case, a value $\nu(\text{K–O}) = 408 \pm 10 \text{ cm}^{-1}$, given in [58SPI/MAR], was still considered to be due to the monomer.

Dever *et al.* [84DEV/CAR] investigated the electronic emission spectra of the $\text{K}_2 + \text{H}_2\text{O}_2$ diffusion flames and estimated $\nu_1 = 412 \pm 18 \text{ cm}^{-1}$ from peak separations.

Konings [90KON] reported $\nu_1 = 406 \pm 4 \text{ cm}^{-1}$ and $\nu_2 = 280 \pm 2 \text{ cm}^{-1}$ from the analysis of IR spectrum of KOH vapors. However, in a subsequent publication Konings [94KON] stated that his assignment of ν_2 was not correct, and the band at 280 cm^{-1} should be attributed to the dimeric molecule.

In the preliminary publication of the IR spectrum of potassium hydroxide isolated in Ar matrix [71BEL/DVO], the assignment of $\nu_1 = 408 \text{ cm}^{-1}$ and $\nu_2 = 300 \text{ cm}^{-1}$ for linear KOH was made. Later Belyaeva [78BEL, 91BEL] obtained the spectra in the other inert matrices for H and D isotopomers and interpreted the obtained data in terms of both linear and bent configurations of the KOH(KOD) molecule. In Ar matrix spectra, the bands at 407.5 cm^{-1} and 302.5/298.5 cm^{-1} were assigned to, respectively, ν_1 and ν_2 , of linear KOH. A double-peak structure of the band attributed to ν_2 was convincingly explained by the removal of degeneracy of the deformation vibration in matrix. The assignment of the bands at 413 cm^{-1} and 375.5 cm^{-1} to ν_1 and ν_2 , respectively, of nonlinear KOH is objectionable not only because a linearity of KOH in the ground electronic state has

been proved experimentally (see above), but also because the value 375.5 cm^{-1} is too small for a deformation frequency in a bent triatomic molecule.

In addition to the above-mentioned spectral investigations, there are a number of IR and Raman spectra studies of KOH and KOD in a crystalline state and solutions (several examples are given in Table 14). From these studies one can see that ν_3 for KOH(cr) is in the vicinity of 3600 cm^{-1} . This frequency was not observed in IR spectra of gas or in matrix because of strong H_2O band overlapping.

The theoretical calculations [80NEM/STE, 86BAU/LAN] did not yield for reliable predictions of vibrational frequencies of KOH. Nemukhin and Stepanov [80NEM/STE] applied a diatomics-in-molecules method using two different sets of parameters for potential function. In both cases the values of ν_1 are in good agreement with the experimental data, but for ν_2 the calculated values are more than twice as large than known experimental or estimated values for a linear molecular configuration of KOH which had been shown in [80NEM/STE]. Bauschlicher *et al.* [86BAU/LAN] in *ab initio* calculations using different levels obtained obviously exaggerated values of ν_1 . The authors [86BAU/LAN] explained it by the fact that the theoretical values were derived assuming a rigid OH unit, which neglected any coupling between low-frequency bending and high-frequency stretching modes.

The ground electronic state of KOH is $^1\Sigma^+$. The existence of low-lying excited electronic states of the molecule is not expected. This was confirmed by Spinar and Margrave [58SPI/MAR] who did not observe any features in ultraviolet and visible spectra of potassium hydroxide vapors. Dever *et al.* [84DEV/CAR] assumed that a weakly bound excited electronic state of KOH with the energy about 25 000 cm^{-1} was responsible for the electronic emission spectrum of KOH observed in their study.

A linear configuration of KOH in the ground electronic state $^1\Sigma^+$ with $r_o(\text{K–O}) = 2.212 \pm 0.002 \text{ \AA}$ and $r_o(\text{O–H}) = 0.912 \pm 0.010 \text{ \AA}$ according to [76PEA/WIN] is adopted in the present work. The corresponding value of moment of inertia is calculated as $I = (10.233 \pm 0.010)10^{-39} \text{ g cm}^{-1}$. The value of ν_1 is taken as $408 \pm 5 \text{ cm}^{-1}$ which is consistent with all experimental data [58SPI/MAR, 71BEL/DVO, 78BEL, 84DEV/CAR, 90KON]. The selection of ν_2 is not so definitive. It is accepted in the present work that the value $\nu_2 = 300 \pm 10 \text{ cm}^{-1}$ based on the assignment made by Belyaeva *et al.* [71BEL/DVO, 78BEL, 91BEL] from the IR spectrum in Ar matrix. This value is consistent with those for the other alkali metal hydroxides. For ν_3 , a characteristic value 3700 $\pm 100 \text{ cm}^{-1}$ is taken similar to the other hydroxides.

The molecular constants of KOH adopted in the present work for calculation of the thermal functions are summarized below:

$$r_o(\text{K–O}) = 2.212 \pm 0.002 \text{ \AA};$$

$$r_o(\text{O–H}) = 0.912 \pm 0.010 \text{ \AA};$$

$$\angle(\text{K-O-H}) = 180^\circ;$$

$$I = (10.233 \pm 0.010) 10^{-39} \text{ g cm}^2;$$

symmetry number: $\sigma = 1$; statistical weight: $p_x = 1$;

$$\nu_1 = 408 \pm 10 \text{ cm}^{-1}, d_1 = 1;$$

$$\nu_2 = 300 \pm 10 \text{ cm}^{-1}, d_2 = 2;$$

$$\nu_3 = 3700 \pm 100 \text{ cm}^{-1}, d_3 = 1.$$

Calculation of the KOH(g) Thermal Functions

The thermal functions of KOH(g) in the standard state are calculated in the "rigid rotor-harmonic oscillator" approximation with low-temperature quantum corrections according to the equations given in [89GUR/VEY]. The molecular constants used in calculation of the thermal functions are given in the previous subsection. The calculated values of $C_p^\circ(T)$, $\Phi^\circ(T)$, $S^\circ(T)$, $H^\circ(T) - H^\circ(0)$ in the temperature range 0–6000 K are given in Table 23.

The uncertainties in the calculated thermal functions of KOH(g) are mainly due to uncertainties in the molecular constants. At high temperatures the uncertainties, because of the approximate method of calculation, become more substantial. These uncertainties are estimated on the basis of the differences between the thermal functions for the linear triatomic molecules (N_2O , CO_2 , CS_2 , OCS , HCN , FCN , and ClCN), calculated in [89GUR/VEY, 91GUR/VEY] in the "nonrigid rotor-anharmonic oscillator" approximation, and those calculated in the "rigid rotor-harmonic oscillator" approximation. Since the value of the constant of centrifugal distortion, D_0° , of KOH is known [76PEA/WIN], it is possible to estimate the corresponding contribution to the thermal functions. It amounts to from 0.005 to 0.1 J (K mol) $^{-1}$ in $\Phi^\circ(T)$ at $T = 298.15$ and 6000 K, respectively. The total uncertainties in the thermal functions of KOH(g) are presented in Table 23.

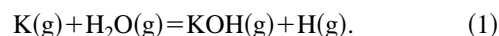
The thermal functions of KOH(g) were calculated earlier in [82GUR/VEI, 85CHA/DAV] in the range 100–6000 K. The differences between the thermal functions, calculated in the present work and those tabulated in [82GUR/VEI, 85CHA/DAV] are shown in Table 15. The thermal functions calculated in the present work and in [82GUR/VEI] practi-

cally coincide because the molecular constants used in both calculations are the same. The data tabulated in [85CHA/DAV] differ from those calculated in the present work due to the use of somewhat obsolete values of ν_2 and bond lengths in that review.

Enthalpy of Formation of KOH(g)—Experimental Investigations of Equilibria in Flames

[66JEN/PAD], [70JEN]

Jensen and Padley performed photometric measurements of potassium hydroxide formation in $\text{H}_2 + \text{O}_2 + \text{N}_2$ flames. It was found that the logarithmic plot of potassium first resonance doublet emission intensity against $1/T$ deviated from linearity at temperatures exceeding 2250 K. Part of this deviation was caused by formation of K^+ ions. Ionization of potassium atoms was partly suppressed by means of addition of a high concentration of cesium chloride to the atomizer solution. Unlike measurements with sodium, in the case of potassium it was not possible to attribute the remaining deviation from linearity entirely to formation of KOH molecules. It was found that a fraction (0.15) of the remaining deviation from linearity for the principal flame with the temperature $T = 2475 \pm 15$ K arose from unsuppressed ionization. The remainder, 0.85, was attributed to hydroxide formation. Finally the value $[\text{KOH}]/[\text{K}] = 0.22 \pm 0.06$ was calculated. To this value corresponds the equilibrium constant value $K^\circ(2475 \text{ K}) = 6.7 \cdot 10^{-3}$ for the reaction



Third-law calculation performed in [66JEN/PAD], using a bent hydroxide molecule model, resulted in the value $D_0^\circ(\text{K-OH}) = 81 \pm 2 \text{ kcal mol}^{-1}$ ($339 \pm 8 \text{ kJ mol}^{-1}$). Later Jensen [70JEN] recalculated the $D_0^\circ(\text{K-OH})$ value from the equilibrium data obtained by Jensen and Padley using a linear model. The results of calculations for both models were close and a value $D_0^\circ(\text{K-OH}) = 339 \pm 9 \text{ kJ mol}^{-1}$ was finally recommended.

[68FEU/QUE]

Feugier and Queraud measured attenuation (A, decibel) of microwave ($\lambda = 4.16 \text{ mm}$) and intensity (I) of potassium resonance line emission at 7665 Å in the butane-oxygen-

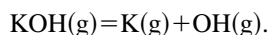
TABLE 15. Differences (J K $^{-1}$ mol $^{-1}$) between the thermal functions of KOH(g) calculated in the present work and in [82GUR/VEI, 85CHA/DAV]

T/K	[Present Work]-[82GUR/VEI] ^a			[Present Work]-[85CHA/DAV] ^b		
	$\Delta C_p^\circ(T)$	$\Delta \Phi^\circ(T)$	$\Delta S^\circ(T)$	$\Delta C_p^\circ(T)$	$\Delta \Phi^\circ(T)$	$\Delta S^\circ(T)$
298.15	0.001	0.006	0.004	0.654	1.067	1.908
1000	0.001	0.004	0.004	-0.026	1.828	2.210
2000	0.001	0.005	0.005	-0.104	2.005	2.149
3000	0.001	0.005	0.006	-0.069	2.046	2.114
4000	0.001	0.005	0.005	-0.044	2.060	2.097
5000	0.001	0.005	0.006	-0.030	2.067	2.089
6000	0.000	0.005	0.006	-0.022	2.070	2.085

^aThe values of $\Phi^\circ(T)$ and $S^\circ(T)$ tabulated in [82GUR/VEI] are recalculated to standard pressure 0.1 MPa.

^bThe values of $\Phi^\circ(T)$ tabulated in [85CHA/DAV] are adjusted to the reference temperature $T = 0$ instead of 298.15 K.

nitrogen flames seeded with potassium compounds. The flames used were of the fuel to oxygen stoichiometry of 1.00 and 0.80. Attenuation A depends on the electron concentration in a flame. Under operating conditions, a linear relation between I and A was found. Using this experimental evidence, an expression was derived for intensity of emission I as a function of total potassium concentration in a flame and equilibrium constant for the reaction



The equilibrium constant values were calculated using statistical thermodynamics for a set of $D_0^\circ(\text{K-OH})$ values. For every pair of temperatures, the value $D_0^\circ(\text{K-OH})$ was found fitting the experimental ratio of emission intensity. The values $D_0^\circ(\text{K-OH}) = 3.40 \pm 0.13$ eV (328 ± 13 kJ mol⁻¹) and $D_0^\circ(\text{K-OH}) = 3.20 \pm 0.10$ eV (309 ± 10 kJ mol⁻¹) were obtained for the flames with 1.00 and 0.80 stoichiometry, respectively.

[69COT/JEN]

Cotton and Jenkins determined the dissociation energy $D_0^\circ(\text{K-OH})$ using measurements of the concentration of potassium atoms as a function of hydrogen atom concentration in hydrogen-rich, hydrogen oxygen-nitrogen flames. A set of six isothermal flames ($T = 1800$ K) of varying composition was used for the measurements. The equilibrium constant for reaction (1) was evaluated from the slope-to-intercept ratio of a linear fit of relative metal atom versus hydrogen-atom concentration. The mean value $K^\circ(1800) = 8.5 \cdot 10^{-4}$ was obtained for the equilibrium constant of the reaction (1). Third-law calculations were made with the data from the 1961 JANAF Tables (see [71STU/PRO]) for a bent model of KOH molecule. The following value of dissociation energy with the total error limit was obtained: $D_0^\circ(\text{K-OH}) = 85.2 \pm 2$ kcal mol⁻¹ (356.5 ± 8 kJ mol⁻¹).

[71KEL/PAD]

Kelly and Padley made flame photometric studies of K emission in $\text{H}_2 + \text{O}_2 + \text{CO}_2$ and $\text{H}_2 + \text{O}_2 + \text{N}_2$ flames in the temperature range 1950–2750 K. To suppress ionization of potassium atoms, cesium chloride was introduced in flames together with the potassium salt. Thirty-two values of the equilibrium constant for reaction (1) were obtained. The data were presented in the graph which showed pronounced deviation from linearity for six points at temperatures exceeding ≈ 2500 K. The authors attributed this deviation to unsuppressed ionization of potassium atoms. They fitted the equilibrium constant values for the reaction (1) with the equation

$$K^\circ(T) = A \exp[-\Delta_r H^\circ(2350\text{K})/RT],$$

where $\log A = 1.61$, $-\Delta_r H^\circ(2350\text{K}) = 168$ kJ mol⁻¹. They regarded this equation as appropriate for the temperature range 1950–2750 K.

From the enthalpy of reaction (1) at the mean temperature of the range, $T = 2350$ K, Kelly and Padley calculated the 2nd- and 3rd-law values of dissociation energy $D_0^\circ(\text{KOH})$ for linear and bent models of this molecule (kJ mol⁻¹): 351

± 10 (2nd law, linear); 352 (3rd law, linear); 344 (2nd law, bent); 335 (3rd law, bent). They recommended as the best value $D_0^\circ(\text{K-OH}) = 352$ kJ mol⁻¹ based on the 2nd- and 3rd-law treatment for the linear model.

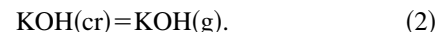
Enthalpy of Formation of KOH(g)—Mass Spectrometric Studies of Equilibria in Flames

[58POR/SCH], [58POR/SCH2]

Porter and Schoonmaker [58POR/SCH2] carried out a mass spectrometric study of potassium hydroxide vaporization (preliminary account was published in [58POR/SCH]). The effusion cell consisted of a metal crucible with the interior walls lined with a pressed layer of magnesia. Most of the data were obtained in the temperature range between 300 and 400 °C.

The major ions observed in the mass spectrum were K^+ , KOH^+ , and K_2OH^+ . Under “slightly reducing” conditions, when the outer crucible was made of stainless steel, K^+ was the major ion observed, with appearance energy in agreement with the ionization energy of potassium atoms. Under “near neutral” conditions, when the outer crucible was made of platinum, K^+ ion intensity was greatly diminished. It was concluded that at least at reducing conditions K^+ was formed in the process of ionization of potassium atoms. K_2OH^+ ions were attributed to ionization of $\text{K}_2\text{O}_2\text{H}_2$ molecules.

In contrast to sodium hydroxide, the ratio of K_2OH^+ to KOH^+ ion intensity remained substantially constant for variations in cell temperatures and experimental conditions. From these observations Porter and Schoonmaker came to the conclusion that at least a large fraction of the KOH^+ ions was formed by dissociative ionization of the dimer molecules, $\text{K}_2\text{O}_2\text{H}_2$. From the total KOH^+ ion current taken as an upper limit on the amount of KOH formed from KOH(g) , the authors [58POR/SCH2] calculated an upper limit for KOH partial pressure at $T = 626$ K: $P(\text{KOH}) < 1.4 \cdot 10^{-6}$ atm. Using an estimated value $-\Delta_{\text{sub}}[G^\circ(T) - H^\circ(298)]/T = 37$ cal K⁻¹ mol⁻¹ the authors [58POR/SCH2] calculated a lower limit $\Delta_r H^\circ(298) > 40$ kcal mol⁻¹ (> 167 kJ mol⁻¹) on the enthalpy of reaction



[58POR/SCH3]

In studying the NaOH–KOH system, Porter and Schoonmaker presented sufficiently conclusive evidence that the primary source of KOH^+ ions must be simple ionization of KOH molecules, because $\text{KOH}^+/\text{K}_2\text{OH}^+$ ion intensity ratio was dependent upon composition of the system. For the KOH–NaOH system of unspecified composition, the following partial pressures were obtained: $T = 641$ K, $P(\text{KOH}) = 6.2 \cdot 10^{-8}$ atm, $P(\text{K}_2\text{O}_2\text{H}_2) = 3.1 \cdot 10^{-8}$ atm; $T = 666$ K, $P(\text{KOH}) = 9.7 \cdot 10^{-8}$ atm, $P(\text{K}_2\text{O}_2\text{H}_2) = 5.4 \cdot 10^{-8}$ atm. These values were used in [58POR/SCH3] to calculate the enthalpy of dimer dissociation into monomers, $\Delta_r H^\circ(650\text{K}) = 46.5 \pm 5$ kcal mol⁻¹ (see previous subsection). Combining this value with the enthalpy of sublimation of the dimer, 36 ± 2 kcal mol⁻¹ [58POR/SCH], Porter and Schoonmaker ob-

tained the enthalpy of sublimation of KOH: $\Delta_{\text{sub}}H^\circ(626) = 41.3 \pm 3 \text{ kcal mol}^{-1}$ ($172.8 \pm 12 \text{ kJ mol}^{-1}$). Using an estimated value $\Delta C_p = -10 \text{ cal K}^{-1} \text{ mol}^{-1}$ for the sublimation process, they found the value $\Delta_{\text{sub}}H^\circ(298.15) = 44.6 \pm 3 \text{ kcal mol}^{-1}$ ($186.6 \pm 12 \text{ kJ mol}^{-1}$).

[68GUS/GOR]

Gusarov and Gorokhov carried out a mass spectrometric study of potassium hydroxide vaporization. The effusion cell was made of platinum. Mass spectra were obtained at ionizing electron energy of 50 eV. The ions detected were K^+ , KOH^+ , K_2O^+ , and K_2OH^+ ; K^+ ions were the most abundant. K_2O^+ and K_2OH^+ ions were attributed to fragmentation of $\text{K}_2\text{O}_2\text{H}_2$ molecules. K^+ ion intensity was ascribed mainly to ionization of K atoms. At the end of the sample vaporization, a slow fall of ion intensities was detected, due to decrease of potassium hydroxide activity because of accumulation of less volatile impurities, e.g., K_2CO_3 . At this stage of the experiment, the ratio of ion intensities $\text{KOH}^+ / (\text{K}_2\text{OH}^+)^{1/2}$ remained nearly constant at constant temperature, indicating that the KOH^+ ions were formed in the process of simple ionization of KOH molecules.

To remove atomic potassium from the vapor, potassium superoxide was added to the sample of hydroxide. It was concluded that under oxidizing conditions, K^+ ions originated from fragmentation of KOH and $\text{K}_2\text{O}_2\text{H}_2$ molecules. Attributing all K^+ ions either to monomer or to dimer, an estimate of lower and upper bounds of the ratio of dimer and monomer pressure was obtained for the mean temperature 646 K: $0.32 \leq P(d)/P(m) \leq 0.66$ [the value $\sigma(d)/\sigma(m) = 2$ was assumed for the ratio of ionization cross sections of dimer to monomer]. Comparison of $\text{K}_2\text{OH}^+ / \text{KOH}^+$ ion intensity ratio under oxidizing conditions, with that without potassium superoxide added, demonstrated that addition of superoxide led to the decrease in the potassium hydroxide activity by a factor of 1.82. For the hydroxide of unit activity, the lower and upper bounds of dimer to monomer pressure ratio were calculated to be $0.58 \leq P(d)/P(m) \leq 1.20$. With the uncertainties in ionization cross sections estimated as a factor of 1.5, it was finally accepted: $\log[P(d)/P(m)] = -0.08 \pm 0.34$ ($T = 646 \text{ K}$).

Results of KOH^+ ion intensity measurements in the temperature range 598–653 K were used for calculation of the second-law enthalpy of sublimation of the monomer. The third-law enthalpy of sublimation was calculated using the value $\log[P(\text{KOH})/\text{atm}] = -2.16 \pm 0.12$ for $T = 1068 \text{ K}$, obtained from the data of Jackson and Morgan [21JAC/MOR] on the total vapor pressure of potassium hydroxide. The value $\log[P(d)/P(m)] = -0.40 \pm 0.40$ extrapolated from $T = 646 \text{ K}$ was employed to calculate the monomer pressure. The results of calculations for reaction (2) with total error estimates are summarized below:

$$\Delta_{\text{sub}}H^\circ(625) = 43.5 \pm 1.7 \text{ kcal mol}^{-1} (182.0 \pm 7 \text{ kJ mol}^{-1}),$$

Second law:

$$\Delta_{\text{sub}}H^\circ(0) = 47.0 \pm 1.7 \text{ kcal mol}^{-1} (196.6 \pm 7 \text{ kJ mol}^{-1}),$$

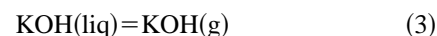
Third law:

$$\Delta_{\text{sub}}H^\circ(0) = 44.8 \pm 0.6 \text{ kcal mol}^{-1} (1.87.4 \pm 2.5 \text{ kJ mol}^{-1}).$$

To calculate the $\Delta_{\text{sub}}H^\circ(0)$ values, thermal functions from the 1965 JANAF Tables (see [71STU/PRO]) were used for $\text{KOH}(\text{cr})$. For $\text{KOH}(\text{g})$, results of calculation for a linear model were used (calculations were carried out by Dr. V. Yungman).

[82FAR/SRI], see also [83FAR/SRI]

Farber *et al.* conducted a mass spectrometric study of potassium hydroxide vaporization and $\text{KOH}(\text{g})$ thermal dissociation using a quadrupole mass spectrometer with a "double-boiler" high temperature assembly. The reaction



was investigated in the temperature range 703–853 K. An alumina effusion cell was used. The measurements were made at an electron energy 1–2 eV above the appearance energy of the ions. The authors [82FAR/SRI] stated that the mole fraction of the dimer $\text{K}_2\text{O}_2\text{H}_2$ was less than 10% and any contribution to the KOH^+ intensity was negligible. Ion intensities obtained were converted to partial pressures and the second- and third-law values of enthalpy of vaporization and enthalpy of formation were calculated using data from JANAF Tables [74CHA/CUR]:

$$\Delta_{\text{vap}}H^\circ(298.15 \text{ K}) = 185.4 \pm 4.0 \text{ kJ mol}^{-1};$$

$$\Delta_f H^\circ(\text{KOH}, \text{g}, 298.15 \text{ K}) = -227.2$$

$$\pm 4.0 \text{ kJ mol}^{-1} \text{ (2nd law);}$$

$$\Delta_{\text{vap}}H^\circ(298.15 \text{ K}) = 184.2 \pm 0.5 \text{ kJ mol}^{-1};$$

$$\Delta_f H^\circ(\text{KOH}, \text{g}, 298.15 \text{ K}) = -228.0$$

$$\pm 2.0 \text{ kJ mol}^{-1} \text{ (3rd law).}$$

The partial pressure values for $\text{KOH}(\text{g})$ are presented in Table 16 and are included in Fig. 6.

The dissociation reaction



was investigated using a double-boiler experiment in the temperature range 1200–1375 K (14 points). The KOH sample was heated first in the low-temperature part of the apparatus and the vapor was then introduced into the effusion cell with substantially higher temperature, necessary to dissociate $\text{KOH}(\text{g})$ into K and OH. The third-law value $\Delta_f H^\circ(298.15) = 355.6 \pm 2.0 \text{ kJ mol}^{-1}$ was obtained for reaction (4). The values of partial pressures for the dissociation reaction (4) are listed in Table 17.

[84HAS/ZMB]

Hastie *et al.* carried out a study of vaporization of potassium hydroxide with a transpiration mass spectrometric apparatus, described in detail in [79BON/HAS]. The apparatus consisted of a chamber for transpiration and a second chamber in which modulation of the molecular beam and mass

spectrometric analysis were performed. A quadrupole mass filter was used. In addition, the mass of sample transported could be determined gravimetrically and the carrier gas volume could be calculated from the gas flow rate and transport time. A sample container was made of platinum.

In the mass spectrum of the vapor of potassium hydroxide supersonic molecular beam obtained at 30 eV electron energy, K^+ , KOH^+ , K_2OH^+ , and K_2O^+ ions were detected, in decreasing order of ion intensity. The first two ions were assigned to KOH and the latter two ions to $K_2O_2H_2$ molecules. KOH^+ and K_2OH^+ ion intensities were used as measures of the monomer and dimer partial pressures. Small ion signals corresponding to $K_3O_2H_2^+$ were tentatively attributed to the trimer species $K_3O_3H_3$; at 1000 K the partial pressure ratio of trimer to dimer was ≈ 0.05 . The ratio of dimer to monomer remained constant during isothermal total vaporization experiments. Thus the $KOH(liq)$ activity remained at unity throughout experiments.

For calibration of apparatus sensitivity, the weight loss measurement at $T = 1024$ K was conducted. The absolute vapor pressures of monomer and dimer, $P(KOH) = 2.8 \times 10^{-3}$ atm, $P(K_2O_2H_2) = 1.2 \cdot 10^{-3}$ atm, were calculated using the value $P(d)/P(m) = 0.42$ extrapolated from the data [68GUS/GOR]. Two separate experiments were performed on potassium hydroxide vaporization as a function of temperature with fixed N_2 pressure: Run 1, $P(N_2)$ 0.2 atm, $T = 840$ – 1060 K (25 points); Run 2, $P(N_2) = 0.16$ atm, $T = 955$ – 1066 K (26 points). From the second-law analysis the authors [84HAS/ZMB] obtained the following enthalpy of vaporization values:

$$\text{Run 1, } \Delta_{\text{vap}}H^\circ(1000 \text{ K}) = 39.2 \pm 1 \text{ kcal mol}^{-1} \\ (1674.0 \pm 4 \text{ kJ mol}^{-1});$$

$$\text{Run 2, } \Delta_{\text{vap}}H^\circ(1000 \text{ K}) = 40.7 \pm 2 \text{ kcal mol}^{-1} \\ (170.3 \pm 8 \text{ kJ mol}^{-1}).$$

The authors [84HAS/ZMB] recommended $\Delta_{\text{vap}}H^\circ(1000 \text{ K}) = 164.0 \pm 4 \text{ kJ mol}^{-1}$ and calculated corresponding value $D_0^\circ(K-OH) = 84.1 \pm 1 \text{ kcal mol}^{-1}$ ($351.9 \pm 4 \text{ kJ mol}^{-1}$). The data obtained for KOH pressure are listed in Table 18 and included in Fig. 6.

Enthalpy of Formation of $KOH(g)$ —Experimental Determinations of the Total or Apparent Vapor Pressure

In the papers annotated below, results of boiling point, transpiration, and Knudsen effusion measurements are presented. For the two latter techniques the results represent not total pressures, but apparent pressures, calculated assuming presence of only one species (usually monomer) in vapor. For the case of monomer and dimer, the apparent pressure $P(\text{app})$ is related to the true monomer pressure $P(m)$ through following expressions:

$$\text{transpiration, } P(\text{app}) = P(m)[1 + 2P(d)/P(m)]$$

$$\text{Knudsen effusion, } P(\text{app}) = P(m)[1 + 2^{0.5}P(d)/P(m)].$$

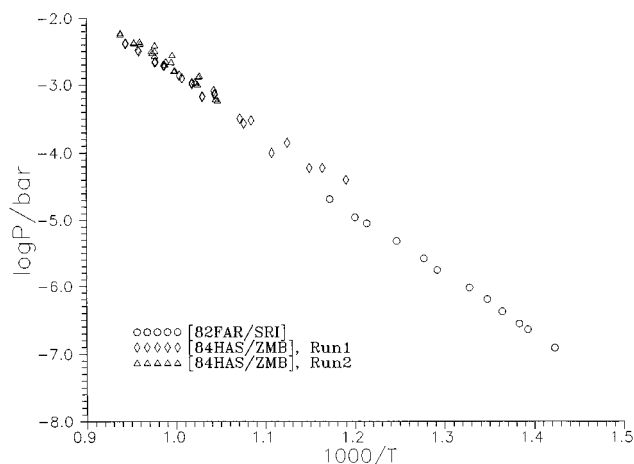


FIG. 6. Partial pressure of $KOH(g)$ over $KOH(liq)$.

[21WAR/ALB]

Von Wartenberg and Albrecht measured the total vapor pressure over liquid potassium hydroxide with the boiling point method at different pressures of nitrogen in the temperature range 1170 – 1327 °C. A platinum tube with closed lower end was used in the measurements. The lower part of the tube was made of Pt–Ir alloy and the temperature was measured with a thermocouple calibrated against melting point of sodium chloride. The temperature dependence of the vapor pressure was approximated by the equation:

$$\log(P/\text{atm}) = -32450/4.57T + 4.4467.$$

The normal boiling point, corresponding to this equation, was found to be 1324 °C. The results are listed in Table 21 and are presented in Fig. 7.

[21JAC/MOR]

Jackson and Morgan measured vapor pressure of potassium hydroxide with a transpiration technique. A sample

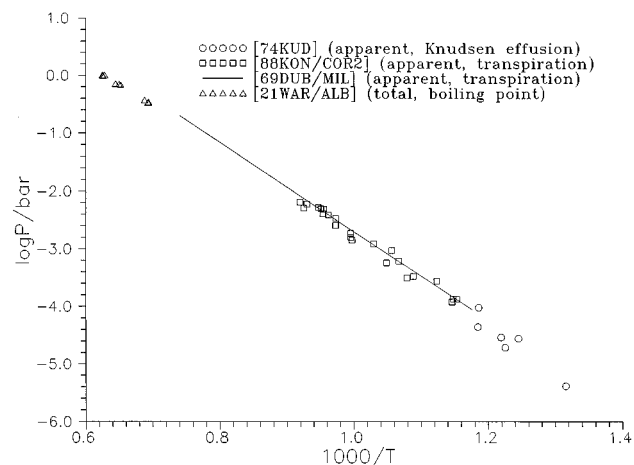


FIG. 7. Total and apparent pressure over $KOH(liq)$.

(weighted) of KOH was placed in a boat of silver foil. This inner boat was placed in an outer boat also of silver foil. The temperature was measured with a thermocouple with an accuracy of $\pm 10^\circ\text{C}$. The weight loss of sample was measured at different nitrogen flow rates and the KOH pressure calculated was extrapolated to zero flow rate. The value of KOH pressures so obtained was 8 mm Hg at 795°C (an averaged value from nine measurements at 793–795 K). Jackson and Morgan believed that the error was not more than 25%.

[69DUB/MIL]

Dubois and Millet determined the potassium hydroxide vapor pressure using transpiration technique. Details of the experiment were described in [68DUB/MIL]. The flow rates of carrier gas (argon) were in the range $12\text{--}35\text{ cm}^3\text{ min}^{-1}$. Assuming KOH(g) to be present, the results obtained in the temperature range 850–1350 K were presented in a graph and were approximated with the equation:

$$\log(P/\text{atm}) = 4.993 - 0.7692 \cdot 10^4/T.$$

The graph corresponding to this equation is included in Fig. 7.

[74KUD]

Kudin measured the potassium hydroxide vapor pressure in the temperature range 760–844 K using Knudsen effusion method. The amount of substance vaporized was determined from the weight loss measurements. Employing $P(d)/P(m)$ value of 0.68 derived from [68GUS/GOR], he calculated a third-law value of the enthalpy of sublimation for the monomer: $\Delta_{\text{sub}}H^\circ(0) = 46.2 \pm 1.5\text{ kcal mol}^{-1}$ ($193.3 \pm 6\text{ kJ mol}^{-1}$). Total (apparent) vapor pressure values calculated assuming presence of monomer are listed in Table 20.

[88KON/COR2]

Konings and Cordfunke measured vapor pressure of potassium hydroxide using the transpiration method. The KOH sample contained K_2CO_3 as the major impurity (0.6 mass %). The transpiration apparatus consisted of a silica reaction tube, a silver boat, a silica thermocouple pocket, and a nickel condenser tube which were placed in a temperature-controlled furnace. The temperature was measured with a calibrated Pt–PtRh thermocouple to within 0.1 K. In several experiments the carrier gas (argon) was saturated with water vapor. 23 measurements were carried out in the range 866.8–1087.0 K. The authors indicated that the presence of water vapor had no influence on the KOH vapor pressure, thus indicating the congruent vaporization of the hydroxide. Assuming only gaseous monomeric species to be present, the vapor pressure over liquid KOH was represented by the equation:

$$\log(P/\text{Pa}) = -(7586 \pm 243) \cdot (T/\text{K})^{-1} + (9.838 \pm 0.025).$$

The third-law enthalpy of sublimation was calculated in [88KON/COR2] using thermal functions from [82GUR/VEI]: $\Delta_{\text{sub}}H^\circ(298.15) = 189.6 \pm 0.8\text{ kJ mol}^{-1}$. The total (apparent) vapor pressure values are listed in Table 21 and are presented in Fig 7.

Enthalpy of Formation of KOH(g)—Miscellaneous Data

[69GOR/GUS], [70GOR/GUS]

Gorokhov, Gusarov, and Panchenkov [69GOR/GUS] carried out mass spectrometric measurements of the appearance energy of ions in mass spectra of potassium and cesium hydroxides (an abstract of deposited paper [69GOR/GUS] was published in [70GOR/GUS]). Partially hydrolyzed superoxide samples were used to obtain vapors of hydroxides free from atomic potassium and cesium (see [68GUS/GOR]). Vaporization of the potassium hydroxide sample was performed from effusion cells made of silver. The appearance energy of K^+ ions was found to be $\text{AE}(\text{K}^+/\text{KOH}) = 7.80 \pm 0.15\text{ eV}$. Combining this value with the ionization energy of potassium atom, 4.34 eV, the following value was obtained: $D_0^\circ(\text{K-OH}) = 80 \pm 3\text{ kcal mol}^{-1}$ ($335 \pm 12\text{ kJ mol}^{-1}$); the uncertainty presents an estimate of the total error. Combining this value of dissociation energy with that from the paper [68GUS/GOR], $84.7 \pm 2\text{ kcal mol}^{-1}$, the authors [69GOR/GUS] recommended the value $D_0^\circ(\text{K-OH}) = 82 \pm 3\text{ kcal mol}^{-1}$ ($343 \pm 12\text{ kJ mol}^{-1}$) as the most reliable.

[84DEV/CAR]

Dever *et al.* obtained electronic emission spectra of KOH(g) in a study of gaseous reactions of potassium vapor with hydrogen peroxide over a wide pressure range, from “single collisions” to “diffusion flame” conditions. From the short-wave length limit of the KOH^+ chemiluminescent spectra, they found a lower bound for the dissociation energy: $D_0^\circ(\text{K-OH}) \geq 88.2\text{ kcal mol}^{-1}$ ($\geq 369\text{ kJ mol}^{-1}$).

[86BAU/LAN]

Bauschlicher *et al.* calculated dissociation energies of the alkali hydroxide molecules MOH into M^+ and OH^- ions by *ab initio* methods at both the self-consistent-field (SCF) and singles plus doubles configuration-interaction level (CI(SD)) using extended Gaussian basis sets of at least triple zeta plus double polarization quality. The following values of the dissociation energy were obtained for KOH: $D_e(\text{K-OH}) = 3.56\text{ eV}$ (SCF), $D_e(\text{K-OH}) = 3.66\text{ eV}$ (CI(SD)). As the “best,” $D_0^\circ(\text{K-OH}) = 3.61 \pm 0.10\text{ eV}$ ($348 \pm 10\text{ kJ mol}^{-1}$) was chosen, as calculated with zero-point correction taken equal to -0.07 eV and a correction of 0.02 eV based upon the errors in the computed bond lengths (the computed bond lengths were slightly too long and bond energies were underestimated).

Discussion of the Enthalpy of Formation of KOH(g)

The authors of this review have recalculated all equilibria from the papers annotated in the enthalpy of formation subsections with the thermal functions from this work and with auxiliary data from [82GUR/VEI] and [89GUR/VEY]. The recalculated values of enthalpies of reactions and the values of enthalpy of formation of KOH(g) are collected in Table 22. For the enthalpies of reactions, results of the 2nd-law and 3rd-law treatment are presented; error assessments represent statistical uncertainty (95% confidence level). If both the 2nd- and 3rd-law values of the enthalpy of a reaction are available, the 3rd-law enthalpy of formation is presented in Table 22. Error assessments for the enthalpy of formation

values represent total uncertainty estimates, obtained on the basis of all error constituents (statistical uncertainty, estimate of systematic error in equilibrium constant values, uncertainty of thermal functions and auxiliary thermochemical data).

Flame photometric studies ([66JEN/PAD], [69COT/JEN], [71KEL/PAD]) are to be regarded as an important source of information on the stability of KOH(g). However, the very high temperatures employed in flame photometric studies result in substantial increase of uncertainties for the 3rd-law enthalpies of reactions. Results of the condensed phase-gas equilibria studies, performed at substantially lower temperatures, seem to be more appropriate in evaluating the enthalpy of formation. The mass spectrometric studies by Porter and Schoonmaker [58POR/SCH, 58POR/SCH2, 58POR/SCH3] provide insight into the main features of the alkali hydroxide vaporization. However, the quantitative aspects are weak.

For selection of the KOH(g) enthalpy of formation, two mass spectrometric studies, [68GUS/GOR] and [84HAS/ZMB], appear to be the most important. The main result of the work [68GUS/GOR] consists in evaluation of the dimer to monomer pressure ratio over KOH(cr). Later the results of the paper [68GUS/GOR] were used for interpretation of experiments with transpiration mass spectrometry [84HAS/ZMB]. In this work the partial pressures of monomer and dimer over KOH(liq) cover a wide temperature range. Using the data from both papers, the enthalpy $\Delta_f H^\circ(0\text{ K}) = 16.0 \pm 3\text{ kJ mol}^{-1}$ for the reaction



was obtained and monomer and dimer partial pressures for the data of the boiling point measurements [21WAR/ALB], Knudsen effusion [74KUD] and transpiration experiments [21JAC/MORJ], [69DUB/MIL], [88KON/COR2] were calculated. The enthalpy of formation values for KOH(g), obtained from the enthalpies of sublimation so calculated, are in agreement with the flame photometric data.

Results obtained by Farber and Srivastava [82FAR/SRI] are in agreement with the data discussed above. Nevertheless, they cannot be regarded as reliable because dimer molecules were not detected in this work, possibly due to interaction of the sample with the effusion cell material, alumina [84HAS/ZMB]. It is possible to assume that transfer of ionization cross sections estimated for the maxima of ionization efficiency curves, to the ion currents measured 1–2 eV above corresponding appearance energy, resulted in significant overestimation of the KOH(g) partial pressure. This overestimation compensated for the decreased KOH activity and resulted in “correct” P(KOH) values. It is to be expected that the appearance energy of the K⁺ ions [69GOR/GUS] and corresponding $D_0^\circ(\text{K-OH})$ value is too low by an amount of the order kT , due to the thermal excitation of neutral KOH molecules.

Results obtained by Feugier and Queraud [68FEU/QUE] are in reasonable agreement with the mass spectrometric and total vapor pressure data. However, they cannot be regarded as accurate at least on two reasons: (i) any proofs that mea-

surements were fulfilled under equilibrium conditions are lacking; (ii) vibrational components of the KOH and OH partition functions were not taken into account in derivation of an analytical expression for equilibrium constant of KOH dissociation.

Spectroscopic evidence for a lower bound value $D_0^\circ(\text{K-OH}) = 369\text{ kJ mol}^{-1}$ [84DEV/CAR] seems to be erroneous; other chemiluminescent pathways than those considered in [84DEV/CAR] cannot be excluded [84HAS/ZMB]. The only quantum-mechanical calculation of the KOH dissociation energy [86BAU/LAN] is in agreement with the most reliable experimental values.

From the papers annotated, results [84HAS/ZMB] (Run 1), [21WAR/ALB], [69DUB/MIL], and [88KON/COR2] seem to be the most reliable. An average value of the KOH enthalpy of sublimation from these papers is $\Delta_{\text{sub}} H^\circ(\text{KOH,cr}, 0\text{ K}) = 192.45 \pm 3\text{ kJ mol}^{-1}$. To this value corresponds $\Delta_{\text{sub}} H^\circ(\text{KOH,cr}, 298.15\text{ K}) = 191.5 \pm 3\text{ kJ mol}^{-1}$. Combining this latter value with the adopted value for the enthalpy of formation of the KOH(cr), the value $\Delta_f H^\circ(\text{KOH,g}, 298.15\text{ K}) = -231.9 \pm 3\text{ kJ mol}^{-1}$ is obtained.

On the basis of the above discussion, the values

$$\Delta_f H^\circ(\text{KOH,g}, 298.15\text{ K}) = -232.0 \pm 3\text{ kJ mol}^{-1}$$

and

$$D_0^\circ(\text{K-OH}) = 357.0 \pm 3\text{ kJ mol}^{-1}$$

are adopted in this review.

2.2.2. Appendix. Tables of Experimental and Evaluated Data for KOH(g)

TABLE 16. Partial pressure of KOH(g) over KOH(liq), [82FAR/SRI]

No.	T/K	P/Pa	No.	T/K	P/Pa
1	703	$1.23 \cdot 10^{-2}$	7	774	$1.76 \cdot 10^{-1}$
2	718	$2.29 \cdot 10^{-2}$	8	783	$2.64 \cdot 10^{-1}$
3	723	$2.79 \cdot 10^{-2}$	9	802	$4.84 \cdot 10^{-1}$
4	733	$4.20 \cdot 10^{-2}$	10	824	$8.95 \cdot 10^{-1}$
5	742	$6.36 \cdot 10^{-2}$	11	833	1.10
6	753	$9.54 \cdot 10^{-2}$	12	853	2.06

TABLE 17. Partial pressures of KOH(g), K(g), and OH(g) for the reaction $\text{KOH(g)} = \text{K(g)} + \text{OH(g)}$, [82FAR/SRI]

No.	T/K	10^2P(KOH)/Pa	10^3P(K)/Pa	10^3P(OH)/Pa
1	1200	4.63	0.800	0.761
2	1210	4.66	0.984	0.958
3	1240	4.78	1.28	1.28
4	1253	4.83	1.57	1.58
5	1270	4.90	2.07	1.91
6	1273	4.91	2.16	2.12
7	1275	4.92	2.26	2.22
8	1285	4.95	2.47	2.44
9	1293	4.99	2.87	2.67
10	1300	5.01	2.98	2.98
11	1323	5.10	3.91	4.19
12	1343	5.18	4.97	5.32
13	1362	5.25	6.55	6.48
14	1375	5.30	8.14	7.08

TABLE 18. Partial pressure of KOH(g) over KOH(liq), [84HAS/ZMB]

Run 1			Run 2		
No.	T/K	P/atm 10^{-3}	No.	T/K	P/atm 10^{-3}
1	870	0.06	1	955	0.58
2	903	0.10	2	957	0.61
3	929	0.27	3	976	1.01
4	933	0.32	4	978	1.06
5	971	0.65	5	979	1.11
6	971	0.67	6	1002	1.59
7	993	1.24	7	1002	1.58
8	996	1.35	8	1001	1.61
9	1023	2.17	9	1001	1.62
10	1024	2.14	10	1012	1.99
11	1059	4.12	11	1011	2.22
12	1060	4.12	12	1024	2.70
13	1044	3.23	13	1024	3.20
14	1043	3.15	14	1024	3.87
15	1014	1.90	15	1041	4.11
16	1013	1.89	16	1042	4.42
17	982	1.01	17	1066	5.99
18	982	1.06	18	1066	5.73
19	959	0.80	19	1049	4.21
20	958	0.73	20	1049	4.34
21	958	0.70	21	1028	3.16
22	922	0.30	22	1027	2.99
23	889	0.14	23	1005	2.16
24	859	0.06	24	1004	2.76
25	840	0.04	25	975	1.31
			26	974	1.36

TABLE 19. Total vapor pressure over potassium hydroxide, [21WAR/ALB]

No.	P/mm Hg	t/°C
1	250.9	1170
2	255.0	1168
3	277.5	1180
4	513.1	1260
5	524.1	1265
6	534.6	1278
7	744.0	1324
8	755.4	1318
9	7600	1327

TABLE 20. Apparent vapor pressure of potassium hydroxide, [74KUD]

No.	T/K	P/atm
1	760	$4.06 \cdot 10^{-6}$
2	816	$1.92 \cdot 10^{-5}$
3	820	$2.90 \cdot 10^{-5}$
4	803	$2.77 \cdot 10^{-5}$
5	844	$4.41 \cdot 10^{-5}$
6	843	$9.44 \cdot 10^{-5}$

TABLE 21. Apparent vapor pressure over potassium hydroxide, [88KON/COR2]

No.	T/K	P/Pa
1	866.8	13.38
2	871.1	13.42
3	872.3	11.95
4	889.9	27.44
5	918.4	33.31
6	937.0	61.80
7	946.3	94.25
8	953.6	57.22
9	971.3	122.72
10	1002.3	142.28
11	1004.4	187.94
12	1027.2	340.31
13	1027.6	256.20
14	1039.1	388.88
15	1046.9	488.98
16	1051.3	498.69
17	1055.3	523.55
18	1075.2	602.57
19	1080.5	512.23
20	1087.0	650.39
21	926.6	31.33 ^a
22	1004.2	158.95 ^a
23	1048.1	409.52 ^a

^aCarrier gas saturated with water vapor.

TABLE 22. Results of experimental determination of $\Delta_f H^\circ(\text{KOH}, \text{g}, 0 \text{ K})$, kJ mol^{-1}

Reference	Method	$\Delta_f H^\circ(0 \text{ K})$		
		2nd law	3rd law	$\Delta_f H^\circ(0 \text{ K})$
Equilibria in flames				
[66JEN/PAD]	Flame photometry, $\text{K}(\text{g}) + \text{H}_2\text{O}(\text{g}) = \text{KOH}(\text{g}) + \text{H}(\text{g})$, 2475 K (one point)	...	155.5	-209.5 ± 12
[67FEU/QUE]	Attenuation of microwaves in K seeded flames, $\text{KOH}(\text{g}) = \text{K}(\text{g}) + \text{OH}(\text{g})$, 2125–2370 K	...	318 ± 20	-189 ± 20
[69COT/JEN]	Flame photometry, $\text{K}(\text{g}) + \text{H}_2\text{O}(\text{g}) = \text{KOH}(\text{g}) + \text{H}(\text{g})$, 1800 K (one point)	...	137.7	-227.3 ± 8
[71KEL/PAD]	Flame photometry, $\text{K}(\text{g}) + \text{H}_2\text{O}(\text{g}) = \text{KOH}(\text{g}) + \text{H}(\text{g})$, 1950–2750 K (32 points)	143.6	144.3	-220.8 ± 11
Mass spectrometric studies of equilibria				
[58POR/SCH]	Knudsen effusion mass spectrometry, $\text{KOH}(\text{cr}) = \text{KOH}(\text{g})$, 626 K (one point)	...	> 166	> -254
[68GUS/GOR]	Knudsen effusion mass spectrometry, $\text{KOH}(\text{cr}) = \text{KOH}(\text{g})$, 598–653 K (13 points)	196.6 ± 6	...	-223.7 ± 7
[82FAR/SRI]	Knudsen effusion mass spectrometry, $\text{KOH}(\text{liq}) = \text{KOH}(\text{g})$, 703–853 K (12 points); Double-boiler experiment, $\text{KOH}(\text{g}) = \text{K}(\text{g}) + \text{OH}(\text{g})$, 1200–1375 K (14 points)	195.6 ± 3.7 354.8 ± 6.5	197.3 ± 0.2 350.5 ± 2.5	-223 ± 10 -221.5 ± 10
[84HAS/ZMB]	Transpiration mass spectrometry, $\text{KOH}(\text{liq}) = \text{KOH}(\text{g})$, Run 1: 840–1060 K (25 points) Run 2: 955–1066 K (26 points)	194.5 ± 6.7 204.3 ± 14	190.6 ± 0.4 188.8 ± 0.4	-229.7 ± 5 -231.5 ± 5
Total vapor pressure measurements				
[21WAR/ALB]	Boiling point, $\text{KOH}(\text{liq}) = \text{KOH}(\text{g})$, 1443–1600 K (nine points)	189.9 ± 6	194.4 ± 2.5	-225.9 ± 5
[21JAC/MOR]	Transpiration, $\text{KOH}(\text{liq}) = \text{KOH}(\text{g})$, 1068 K (nine points)	...	187.6 ± 2	-232.7 ± 5
[69DUB/MIL]	Transpiration, $\text{KOH}(\text{liq}) = \text{KOH}(\text{g})$, 850–1350 K (64 points)	189.2	191.8 ± 0.3	-228.5 ± 4
[74KUD]	Knudsen effusion, $\text{KOH}(\text{liq}) = \text{KOH}(\text{g})$, 760–844 K (6 points)	...	188.7 ± 2.5	-234.3 ± 5
[88KON/COR2]	Transpiration, $\text{KOH}(\text{liq}) = \text{KOH}(\text{g})$, 866.8–1087.0 K (23 points)	185.8 ± 5	193.0 ± 0.8	-227.3 ± 3
Miscellaneous data				
[69GOR/GUS]	Appearance energy measurements, $\text{KOH}(\text{g}) = \text{K}(\text{g}) + \text{OH}(\text{g})$	335 ± 12	...	-206 ± 12
[84DEV/CAR]	$\text{KOH}^*(\text{g})$, electronic emission, $\text{KOH}(\text{g}) = \text{K}(\text{g}) + \text{OH}(\text{g})$	≥ 369	...	≤ -240
[86BAU/LAN]	<i>Ab initio</i> calculation, $\text{KOH}(\text{g}) = \text{K}(\text{g}) + \text{OH}(\text{g})$	348 ± 10	...	-219 ± 10

TABLE 23. Thermodynamic properties at 0.1 MPa: KOH(g)

T/K	C_p°	$-[G^\circ - H^\circ(0K)]/T$	S°	$H^\circ - H^\circ(0K)$	$\Delta_f H^\circ$	$\Delta_f G^\circ$
	J K ⁻¹ mol ⁻¹			kJ mol ⁻¹		
0	0.000	0.000	0.000	0.000	-228.012	-228.012
25	29.101	121.333	150.390	0.726	-228.039	-229.256
50	29.331	141.486	170.591	1.455	-228.533	-230.312
75	31.059	153.331	182.747	2.206	-229.148	-231.066
100	34.162	161.890	192.089	3.020	-229.675	-231.624
150	40.449	174.569	207.179	4.891	-230.474	-232.413
200	44.784	184.304	219.457	7.031	-231.059	-232.968
250	47.504	192.394	229.765	9.343	-231.549	-233.386
300	49.237	199.376	238.591	11.765	-232.018	-233.708
350	50.386	205.538	246.273	14.257	-234.863	-233.859
400	51.179	211.063	253.056	16.797	-235.389	-233.680
450	51.749	216.071	259.118	19.371	-235.871	-233.437
500	52.179	220.654	264.594	21.970	-236.320	-233.142
600	52.805	228.798	274.166	27.221	-237.156	-232.427
700	53.296	235.877	282.344	32.526	-237.945	-231.576
800	53.759	242.141	289.490	37.879	-238.720	-230.613
900	54.230	247.762	295.849	43.279	-239.506	-229.553
1000	54.714	252.862	301.588	48.726	-240.332	-228.403
1100	55.203	257.534	306.826	54.222	-320.088	-222.553
1200	55.687	261.845	311.650	59.766	-319.936	-213.691
1300	56.154	265.850	316.126	65.358	-319.776	-204.843
1400	56.599	269.592	320.304	70.996	-319.606	-196.009
1500	57.017	273.105	324.223	76.677	-319.431	-187.188
1600	57.406	276.416	327.915	82.399	-319.250	-178.376
1700	57.765	79.549	331.407	88.157	-319.068	-169.577
1800	58.095	282.523	334.718	93.951	-318.885	-160.788
1900	58.398	285.354	337.867	99.775	-318.708	-152.011
2000	58.675	288.055	340.870	105.629	-318.537	-143.243
2200	59.159	293.115	346.485	117.414	-318.226	-125.728
2400	59.563	297.781	351.651	129.287	-317.981	-108.239
2600	59.901	302.111	356.432	141.235	-317.827	-90.769
2800	60.186	306.152	360.882	153.244	-317.793	-73.306
3000	60.427	309.941	365.043	165.306	-317.899	-55.841
3200	60.632	313.508	368.949	177.413	-318.170	-38.363
3400	60.807	316.878	372.630	189.557	-318.626	-20.857
3600	60.958	320.073	376.110	201.734	-319.285	-3.325
3800	61.088	323.110	379.410	213.939	-320.167	14.253
4000	61.202	326.004	382.546	226.168	-321.282	31.879
4200	61.302	328.768	385.535	238.419	-322.644	49.574
4400	61.389	331.414	388.389	250.688	-324.266	67.328
4600	61.466	333.951	391.119	262.974	-326.152	85.172
4800	61.535	336.388	393.737	275.274	-328.301	102.100
5000	61.596	338.732	396.250	287.587	-330.720	121.125
5200	61.651	340.991	398.667	299.912	-333.398	139.255
5400	61.700	343.171	400.994	312.247	-336.334	157.481
5600	61.744	345.276	403.239	324.592	-339.509	175.829
5800	61.784	347.313	405.407	336.944	-342.917	194.292
6000	61.820	349.284	407.502	349.305	-346.529	212.881
298.15	49.185	199.133	238.287	11.674	-232.000	-233.698
Uncertainties in Functions						
0	3.000	3.000
300	0.200	0.300	0.500	0.100	3.000	3.000
1000	0.500	0.600	0.800	0.200	3.000	3.000
2000	1.000	0.700	1.200	1.000	3.000	3.000
3000	1.500	0.900	1.600	2.000	4.000	3.000
4000	2.000	1.100	2.000	3.500	5.000	4.000
5000	2.500	1.300	2.500	6.000	7.000	6.000
6000	3.000	1.600	3.000	8.500	9.000	9.000

2.2.3. Potassium Hydroxide Dimer

Molecular Constants of [KOH]₂(g)

[58BAU/DIN]

Bauer *et al.* assumed for K₂O₂H₂ a model consisted of a square planar KOKO part with two hydrogen bridges between the oxygen atoms (the HOHO rhombus is perpendicular to the KOKO square).

[58SPI/MAR]

Spinar and Margrave studied IR spectrum of equilibrium vapors over potassium hydroxide at 690–900 °C and assigned an absorption at 405–410 cm⁻¹ to (KOH)_x where x = 1 or 2. The authors [58SPI/MAR] tentatively attributed this absorption to K–OH stretching vibration.

[59SCH/POR]

Schoonmaker and Porter assumed for K₂O₂H₂ a square planar model without hydrogen bonding, but did not exclude a nonplanar configuration as well.

[67BUE/STA]

Buechler *et al.* studied the deflection of sodium and cesium hydroxides molecular beams in an inhomogeneous electric field and found that the dimeric molecules of these hydroxides are nonpolar. This indicated that at least a M₂O₂ part of the dimers had a planar structure. The authors assumed that the alkali hydroxide dimers from sodium to cesium should have a planar rhomboid configuration.

[69ACQ/ABR]

Acquista and Abramowitz made an unsuccessful attempt at obtaining the IR spectrum of Ar matrix-isolated KOH. They observed several bands below 350 cm⁻¹ which could be ascribed only to polymer species of KOH.

[71BEL/DVO]

Belyaeva *et al.* reported preliminary data obtained in IR spectra of Ar matrix isolated potassium hydroxide at 4.2 K in the range 200–4000 cm⁻¹. The authors analyzed a possibility of either planar or bipyramidal configuration of K₂O₂H₂ (both are of D_{2h} symmetry) and adopted the latter. They assigned the bands at 520, 375, 350, 294, and 272 cm⁻¹ to five B_{1u}, B_{2u}, and B_{3u} fundamentals for this model of K₂O₂H₂. The assignment was supported by force field calculation with estimated values of $r(\text{K-O}) = 2.2 \text{ \AA}$, $r(\text{O-H}) = 1.8 \text{ \AA}$, $\angle (\text{O-K-O}) = 90^\circ$, and $\angle (\text{H-O-K}) = 52^\circ$.

[78BEL] (see also [91BEL])

Belyaeva investigated IR spectra of K₂O₂H₂ and K₂O₂D₂ trapped in the Ne, Ar, Kr, and Xe matrices at 8 K in the range 200–4000 cm⁻¹. Analysis of the spectra was carried out on the assumption that in gaseous phase the alkali hydroxide dimers had a planar rhomboid configuration with the HOOH atoms lying on a straight line (D_{2h} symmetry). Taking into account the isotopic shifts and the spectral data for the other alkali hydroxide dimers, Belyaeva assigned three observed bands in the Ar matrix to two in-plane stretching vibrations K–O in the KOKO ring, ν_{10} (270.5 cm⁻¹) and ν_{12} (294.5 cm⁻¹), and two bending out-of-plane and in-

plane O–H vibrations ν_6 (290 cm⁻¹) and ν_9 (290 cm⁻¹). The ionic model calculation of the geometry and vibrational frequencies $\nu_2 - \nu_{10}$ and ν_{12} of K₂O₂H₂ confirmed the assignment and resulted in the value $r_e(\text{K-O}) = 2.38 \text{ \AA}$ and $\angle (\text{O-K-O}) = 94^\circ$.

[82GUR/VEI]

Gurvich with co-workers accepted a planar D_{2h} configuration for K₂O₂H₂ with structural parameters and vibrational frequencies reported by Belyaeva [78BEL] on the basis of IR spectra in Ar matrix and the ionic model calculation. The value $r(\text{O-H}) = 0.97 \pm 0.03 \text{ \AA}$ and the O–H stretching frequencies ν_1 and ν_{11} (both are $3700 \pm 100 \text{ cm}^{-1}$) were estimated.

[83GIR/VAS] (see also [81GIR/VAS])

Girichev and Vasilleva investigated the structural parameters of dimeric potassium hydroxide molecule in vapor at $720 \pm 50 \text{ }^\circ\text{C}$ using the electron diffraction method. In analysis of the $sM(s)$ function, the authors accepted the molecular constants of the monomeric molecule KOH from the literature data and assumed a planar configuration of K₂O₂H₂ with a rhomboid K₂O₂ part (D_{2h} symmetry). The average structural parameters corresponding to temperature of the experiment (bond lengths r_g and vibrational amplitudes l_g are in \AA) were found as $r_g(\text{K-O}) = 2.419(11)$, $l_g(\text{K-O}) = 0.16(1)$, $r_g(\text{K-K}) = 3.60(2)$, $l_g(\text{K-K}) = 0.18(2)$, $r_g(\text{K-H}) = 3.5(2)$, $l_g(\text{K-H}) = 0.36$, and $\angle (\text{O-K-O}) = 83.8^\circ$.

[85CHA/DAV]

Chase *et al.* selected a C_{2h} configuration for K₂O₂H₂ without hydrogen bonding similar to a model for Li₂O₂H₂ suggested by Berkowitz *et al.* [60BER/MES]. The structural parameters of K₂O₂H₂ and the frequencies corresponding to the K₂O₂ part were estimated by comparison with related molecules including KOH, K₂F₂, and H₂O. The O–H stretching and bending frequencies were taken from [60BER/MES] as estimated for Li₂O₂H₂.

[86GIR/GIR]

Girichev *et al.* reanalyzed the experimental electron diffraction data on the K₂O₂H₂ molecule obtained in [83GIR/VAS] and reported the following values of the effective structural parameters (bond lengths r_g and vibrational amplitudes l_g are in \AA): $r_g(\text{K-O}) = 2.423(8)$, $l_g(\text{K-O}) = 0.160(5)$, $r_g(\text{K-K}) = 3.58(2)$, $l_g(\text{K-K}) = 0.17(1)$, $r_g(\text{O-O}) = 3.10(10)$, $l_g(\text{O-O}) = 0.152$, $r_g(\text{K-H}) = 3.65(10)$ and $l_g(\text{K-H}) = 0.36(1)$. Based on a planar rhomboid configuration (D_{2h} symmetry) and using the IR spectral data [78BEL], Girichev *et al.* calculated the equilibrium structural parameters and fundamentals of the K₂O₂ part.

[89GIR/LAP]

Girichev and Lapshina corrected the analysis made in [86GIR/GIR] for the electron diffraction data on K₂O₂H₂ and obtained somewhat different values of the molecular constants for the K₂O₂ portion of the molecule. Particularly, they calculated $r_e(\text{K-O}) = 2.374(9)$ and $\angle (\text{O-K-O}) = 83.0 \pm 0.1^\circ$.

[89LAP]

In this thesis, summarizing the results of previous electron diffraction investigations of [83GTR/YAS, 86GIR/GIR, 89GIR/LAP], Lapshina reported somewhat different effective parameters of the $K_2O_2H_2$ molecule (bond lengths r_g and vibrational amplitudes l_g are in Å): $r_g(K-O) = 2.43(2)$, $l_g(K-O) = 0.16(1)$, $r_g(K-K) = 3.60(3)$, $l_g(K-K) = 0.17(3)$, $r_g(O-O) = 3.13(25)$, $l_g(O-O) = 0.18(13)$, $r_g(K-H) = 3.51(50)$, and $l_g(K-O) = 0.35(33)$. The equilibrium structural parameters were given as $r_e(K-O) = 2.41(2)$ Å and $\angle(O-K-O) = 83(1)^\circ$.

[90KON]

Konings investigated the IR spectrum of potassium hydroxide vapors at 1015 K in the region 50–609 cm^{-1} and assigned an absorption maxima at 330 ± 8 cm^{-1} to a $K_2O_2H_2$ fundamental.

The molecular constants of $K_2O_2H_2$, measured, calculated, estimated, or accepted in all above-named studies, are listed in Table 24.

Discussion of the Molecular Constants of $[KOH_2](g)$

The possible molecular models of $K_2O_2H_2$ contain a $(KO)_2$ rhombus (square) and differ only in positions of the hydrogen atoms. Bauer *et al.* [58BAU/DIN] assumed a bipyramidal model with bridge hydrogen bonding. In this model, the $(KO)_2$ plane is a square and the $(HO)_2$ plane is a rhombus perpendicular to the $(KO)_2$ plane (D_{2h} symmetry). Chase *et al.* [85CHAS/DAV] accepted a model, proposed by Berkowitz *et al.* [60BER/MES] for $Li_2O_2H_2$ with two H atoms in *trans* position above and below the $(LiO)_2$ rhombus (C_{2h} symmetry), but assumed that the $(KO)_2$ plane is a square. Schoonmaker and Porter [59SCH/POR] adopted a planar rhomboid configuration of $K_2O_2H_2$ without hydrogen bonding (D_{2h} symmetry). The same configuration was predicted by Buechler *et al.* [67BUE/STA] on the basis of the results obtained for the deflection of sodium and cesium hydroxide beams in the inhomogeneous electric field. This configuration was confirmed by the analysis of the IR spectra in inert matrices [78BEL, 91BEL] and by the electron diffraction measurements in vapor [83GIR/VAS, 86GIR/GIR, 89GIR/LAP, 89LAP]. The possibility of the other configurations was considered in [78BEL, 91BEL] and rejected on the basis of the experimental data and the ionic model calculation. It should be noted, however, that a bipyramidal configuration of $K_2O_2H_2$ was considered to be preferable by Belyaeva *et al.* [71BEL/DVO] in preliminary analysis of IR spectra of the potassium hydroxide molecule isolated in Ar matrix.

Structural parameters of $K_2O_2H_2$ vapor were studied by Girichev with co-workers [83GIR/VAS, 86GIR/GIR, 89GIR/LAP, 89LAP] using the electron diffraction method. The values of the same bond lengths for a planar D_{2h} configuration of $K_2O_2H_2$ were slightly changed from one publication of these authors to another because of some corrections in the structural analysis. In addition, it is necessary to emphasize that interdependence between the values of $r(K-O)$, $r(K-K)$, $r(O-O)$, $r(K-H)$, and $\angle(O-K-O)$ in any set

[83GIR/VAS, 86GIR/GIR, 89GIR/IAP, 89LAP] (see Table 24) was sometimes poor. In particular, the value of $r(K-O)$, calculated from $r(K-K)$ and $r(O-O)$, turned out to be 2.38 Å instead of 2.43 Å [89LAP]. Moreover, the value of $r(O-H)$, calculated from $r(K-H)$ and $r(O-O)$, was abnormally large (about 1.5 Å) in comparison with characteristic value 0.97 Å expected for a configuration without hydrogen bonding. Therefore, the reliability of numerical data [83GIR/VAS, 86GIR/GIR, 89GIR/LAP, 89LAP] is doubtful.

The equilibrium structural parameters of $K_2O_2H_2$ were calculated by Belyaeva [78BEL] using the ionic model. The value $r(K-O) = 2.38$ Å, obtained in this calculation, seems to be reliable enough considering the tendency of changing the values $r(M-O)$ for dimeric molecules of alkali metal hydroxides.

The planar $K_2O_2H_2$ molecule of D_{2h} symmetry has 12 nondegenerate fundamental frequencies:

$\nu_1(A_g)$ - O-H stretching;

$\nu_2(A_g)$ - K-O stretching;

$\nu_3(A_g)$ - in-plane ring deformation;

$\nu_4(B_{1g})$ - in-plane O-H bending;

$\nu_5(B_{1g})$ - K-O stretching;

$\nu_6(B_{1u})$ - out-of-plane O-H bending;

$\nu_7(B_{1u})$ - out-of-plane ring deformation;

$\nu_8(B_{2g})$ - out-of-plane O-H bending;

$\nu_9(B_{2u})$ - in-plane O-H bending;

$\nu_{10}(B_{2u})$ - K-O stretching;

$\nu_{11}(B_{3u})$ - O-H stretching;

$\nu_{12}(B_{3u})$ - K-O stretching.

The IR spectral study of $K_2O_2H_2$ inert matrices, performed by Belyaeva [78BEL, 91BEL], provided the assignment of four frequencies, ν_6 , ν_9 , ν_{10} , and ν_{12} . At the same time, Belyaeva [78BEL] calculated the frequencies of $K_2O_2H_2$ (except ν_1 and ν_{11}) using the ionic model. The calculated values for ν_6 , ν_9 , ν_{10} , and ν_{12} are in rather good agreement with the experimental ones. Konings [90KON] attributed a band at 330 ± 8 cm^{-1} in IR spectrum of potassium hydroxide vapor to $K_2O_2H_2$ without an assignment, but this value can hardly match any IR active frequency reported by Belyaeva [78BEL, 81BEL]. Girichev with co-workers [86GIR/GIR, 89GIR/LAP, 89LAP] carried out a combined analysis of their electron diffraction data and the spectral data [78BEL]. The analysis resulted in the values of six frequencies for vibrations of the K_2O_2 ring. Unfortunately, these values are not the same in different publications (like the values of the bond lengths, see above), and cannot be considered as reliable.

The frequency 408 cm^{-1} , found by Spinar and Margrave [58SPI/MAR] in the IR spectrum of potassium hydroxide vapor, is thought to be related to a monomer.

TABLE 24. Bond lengths (Å), angles (deg), and vibrational frequencies (cm⁻¹) of K₂O₂H₂ in the ground electronic state

Constant	[71BEL/DVO] ^a	[78BEL] ^b	[78BEL] ^c	[82GUR/VEI] ^d	[83GIR/VAS] ^e
<i>r</i> (K–O)	2.2	...	2.38	2.38	2.419
<i>r</i> (K–K)	3.60
<i>r</i> (O–O)
<i>r</i> (K–H)	3.5
<i>r</i> (O–H)	1.8	0.97	...
<(O–K–O)	90	...	94	94	83.8
<(K–O–H)	52
ν_1	3700	...
ν_2	362	360	...
ν_3	163	165	...
ν_4	303	300	...
ν_5	250	250	...
ν_6	350	290	308	290	...
ν_7	520	...	122	120	...
ν_8	295	295	...
ν_9	375	290	307	290	...
ν_{10}	272	270.5	275	270	...
ν_{11}	3700	...
ν_{12}	294	294.5	342	294	...
Symmetry	D _{2h}				
	[85CHA/DAV] ^f	[86GIR/GIR] ^g	[89GIR/LAP] ^h	[89LAP] ⁱ	Adopted in present work ^j
<i>r</i> (K–O)	2.43	2.423	2.37	2.43	2.38
<i>r</i> (K–K)	...	3.58	...	3.60	...
<i>r</i> (O–O)	...	3.10	...	3.13	...
<i>r</i> (K–H)	...	3.65	...	3.51	...
<i>r</i> (O–H)	0.96	0.97
<(O–K–O)	90	...	83.0	...	90
<(K–O–H)	110
ν_1	3700	3700
ν_2	273	292	300	295	360
ν_3	150	111	204	203	165
ν_4	1250	300
ν_5	235	304	310	317	250
ν_6	1250	290
ν_7	150	92	120	124	120
ν_8	1250	295
ν_9	1250	290
ν_{10}	255	270.5	291	290	270.5
ν_{11}	3700	3700
ν_{12}	258	294.5	324	317	294.5
Symmetry	C _h	D _{2h}	D _{2h}	D _{2h}	D _{2h}

^aIR spectrum in Ar matrix; the bands are assigned assuming a bipyramidal configuration; the equilibrium structural parameters are calculated using the ionic model.

^bIR spectrum in Ar matrix.

^cIonic model calculation assuming a planar configuration; r_e structure.

^d ν_6 , ν_9 , ν_{10} , and ν_{12} from IR spectra in Ar matrix [78BEL]; equilibrium structural parameters and $\nu_2 - \nu_5$, ν_7 , and ν_8 from the ionic model calculation [78BEL]; r (O–H), ν_1 , and ν_{11} are estimated.

^eElectron diffraction in gas; r_g structure.

^fEstimated.

^gElectron diffraction in gas; r_g structure; the frequencies from combined treatment of electron diffraction data and IR spectral data [C78BEL]; authors [C86GIR/GIR] suppose that ν_3 is overestimated due to separation of the K–O and O–H vibrations and it should be 260 cm⁻¹.

^hElectron diffraction in gas; r_e structure; the frequencies from combined treatment of electron diffraction data and IR spectral data [78BEL]; authors [86GIR/GIR] suppose that ν_5 is overestimated due to separation of the K–O and O–H vibrations and it should be 240 cm⁻¹.

ⁱElectron diffraction in gas; r_g structure; the frequencies from combined treatment of electron diffraction data and IR spectral data [78BEL].

^j ν_6 , ν_9 , ν_{10} , and ν_{12} from IR spectra in Ar matrix [78BEL, 91BEL]; $\nu_2 - \nu_5$, ν_7 , and ν_8 from the ionic model calculation [78BEL]; r (K–O), <(O–K–O), r (O–H), ν_1 , and ν_{11} are estimated.

No excited electronic states of $K_2O_2H_2$ have been detected and none are expected.

The molecular constants of $K_2O_2H_2$ selected in the present work are based on a planar rhomboid configuration of D_{2h} symmetry. This has been proved to be valid for dimeric molecules of all alkali metal hydroxides.

The values of $r(K-O) = 2.38 \text{ \AA}$ and $\angle(O-K-O) = 90^\circ$ are based on the electron diffraction data obtained by Girichev *et al.* [83GIR/VAS, 86GIR/GIR, 89GIR/LAP, 89LAP] and the ionic model calculation by Belyaeva [78BEL]. The O-H bond length is estimated as 0.97 \AA similar to the other alkali metal hydroxide dimeric molecules. The uncertainties are estimated as 0.05 \AA in the bond length of K-O, 0.03 \AA in the bond length of O-H, and 10° in the O-K-O angle. Corresponding value of the product of principal moments of inertia is calculated as $(3.4 \pm 0.3) \cdot 10^{-113} \text{ g}^3 \text{ cm}^6$.

The vibrational frequencies ν_1 and ν_{11} are characteristic O-H stretching frequencies and are estimated as $3700 \pm 100 \text{ cm}^{-1}$ each. The frequencies ν_6 , ν_9 , ν_{10} , and ν_{12} are experimentally based, obtained by Belyaeva [78EL, 91BEL] from analysis of IR spectrum in Ar matrix. For the other frequencies ($\nu_2 - \nu_5$, ν_7 , ν_8), the accepted values are the rounded values calculated by Belyaeva [78BEL] using the ionic model. The uncertainties in the experimental values can be estimated as 10 cm^{-1} and in the calculated ones as 20 cm^{-1} .

The molecular constants of $K_2O_2H_2$ (D_{2h} symmetry) adopted in the present work for calculation of thermal functions are summarized below:

$$r(K-O) = 2.38 \pm 0.05 \text{ \AA}; r(O-H) = 0.97 \pm 0.03 \text{ \AA};$$

$$\angle(O-K-O) = 90 \pm 10^\circ;$$

$$I_A I_B I_C = (3.4 \pm 0.3) \cdot 10^{-113} \text{ g}^3 \text{ cm}^6;$$

symmetry number: $\sigma=4$; statistical weight: $p_x=1$;

$$\nu_1 = 3700 \pm 100 \text{ cm}^{-1}, d_1=1;$$

$$\nu_2 = 360 \pm 20 \text{ cm}^{-1}, d_2=1;$$

$$\nu_3 = 165 \pm 20 \text{ cm}^{-1}, d_3=1;$$

$$\nu_4 = 300 \pm 20 \text{ cm}^{-1}, d_4=1;$$

$$\nu_5 = 250 \pm 20 \text{ cm}^{-1}, d_5=1;$$

$$\nu_6 = 290 \pm 10 \text{ cm}^{-1}, d_6=1;$$

$$\nu_7 = 120 \pm 20 \text{ cm}^{-1}, d_7=1;$$

$$\nu_8 = 295 \pm 20 \text{ cm}^{-1}, d_8=1;$$

$$\nu_9 = 290 \pm 10 \text{ cm}^{-1}, d_9=1;$$

$$\nu_{10} = 270.5 \pm 10 \text{ cm}^{-1}, d_{10}=1;$$

$$\nu_{11} = 3700 \pm 100 \text{ cm}^{-1}, d_{11}=1;$$

$$\nu_{12} = 294.5 \pm 10 \text{ cm}^{-1}, d_{12}=1.$$

Calculation of the $[KOH]_2(g)$ Thermal Functions

The thermal functions of $K_2O_2H_2(g)$ in the standard state are calculated in the "rigid rotor-harmonic oscillator" approximation with low-temperature quantum corrections according to the equations given in [89GUR/VEY]. The molecular constants of $K_2O_2H_2$ used in these calculations are given in the previous subsection. The calculated values of $C_p^\circ(T)$, $\Phi^\circ(T)$, $S^\circ(T)$, and $H^\circ(T) - H^\circ(0)$ at the temperature 0–6000 K are given in Table 28.

The uncertainties in the calculated thermal functions of $K_2O_2H_2(g)$ are due to the uncertainties of the adopted molecular constants, presumably of the calculated vibrational frequencies. At high temperatures, the uncertainties due to the approximate method of calculation become more substantial. These uncertainties are roughly estimated taking into consideration the uncertainties in the thermal functions for monomers. The total uncertainties in the thermal function of $K_2O_2H_2(g)$ are given in Table 28.

The thermal functions of $K_2O_2H_2$ were calculated in earlier reviews [82GUR/VEI] and [85CHA/DAV] in the temperature range 100–6000 K. The comparison of the thermal function for $K_2O_2H_2(g)$ calculated in the present work and in [82GUR/VEI, 85CHA/DAV] is shown in Table 25. The data tabulated in [82GUR/VEI] and in the present work are in good agreement because the molecular constants used in both calculations are practically the same. The large differences, when compared with the early review of [85CHA/DAV], are due to the use of an obsolete structural model and molecular constants.

Enthalpy of Formation of $[KOH]_2(g)$ —Mass Spectrometric Studies

[58POR/SCH], [58POR/SCH2]

Porter and Schoonmaker [58POR/SCH2] carried out a mass spectrometric study of potassium hydroxide vaporization (a preliminary account was published in [58POR/SCH]). Most of the data were obtained in the temperature range between 300 and 400 °C. The major ions observed in the mass spectrum were K^+ , KOH^+ and K_2OH^+ . A small current of K_2O^+ was also detected. K_2OH^+ and

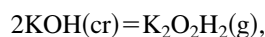
TABLE 25. Differences ($\text{JK}^{-1} \text{ mol}^{-1}$) between the thermal functions of $K_2O_2H_2(g)$ calculated in the present work and in [82GUR/VEI, 85CHA/DAV]

/K	[Present Work]-[82GUR/VEI] ^a			[PresentWork]-[85CHA/DAV] ^b		
	$\Delta C_p^\circ(T)$	$\Delta \Phi^\circ(T)$	$\Delta S^\circ(T)$	$\Delta C_p^\circ(T)$	$\Delta \Phi^\circ(T)$	$\Delta S^\circ(T)$
298.15	0.032	0.081	0.125	24.149	1.743	14.863
1000	0.005	0.121	0.143	7.069	20.660	34.812
2000	0.003	0.132	0.146	2.000	28.663	37.632
3000	0.002	0.138	0.146	0.911	31.765	38.194
4000	0.002	0.139	0.147	0.518	33.401	38.395
5000	0.001	0.141	0.148	0.333	34.410	38.498
6000	0.002	0.142	0.148	0.233	35.094	38.539

^aThe values of $\Phi^\circ(T)$ and $S^\circ(T)$ tabulated in [82GUR/VEI] are recalculated to standard pressure 0.1 MPa.

^bThe values of $\Phi^\circ(T)$ tabulated in [85CHA/DAV] are adjusted to the reference temperature $T = 0$ instead of 298.15 K.

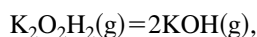
K_2O^+ ions were attributed to ionization of $\text{K}_2\text{O}_2\text{H}_2$ molecules. The existence of stable K_2OH molecules was ruled out. Ion currents K_2OH^+ were measured as a function of the cell temperature for ionizing electron energies of 10 and 20 eV. From the slopes of $\log I[(\text{K}_2\text{OH}^+) \cdot T]$ vs T^{-1} curves average enthalpy of sublimation of dimer was found to be $36 \pm 2 \text{ kcal mol}^{-1}$ ($151 \pm 8 \text{ kJ mol}^{-1}$). From the K_2OH^+ ion current the authors [58POR/SCH2] calculated $\text{K}_2\text{O}_2\text{H}_2$ partial pressure at $T = 626 \text{ K}$: $P(\text{K}_2\text{O}_2\text{H}_2) = 3.9 \cdot 10^{-6} \text{ atm}$. The sensitivity of the apparatus was calibrated from the K^+ ion intensity measurement for potassium evaporation, assuming equal ionization cross sections for $\text{K}(\text{g})$ and $\text{K}_2\text{O}_2\text{H}_2(\text{g})$. Using an estimated value of $\Delta_{\text{s}}S(626) = 32.4 \pm 8 \text{ cal K}^{-1} \text{ mol}^{-1}$ for the reaction



the authors [58POR/SCH2] obtained a rough third-law value for the enthalpy of dimer sublimation: $\Delta_{\text{sub}}H^\circ(626 \text{ K}) = 36 \pm 6 \text{ kcal mol}^{-1}$ ($151 \pm 25 \text{ kJ mol}^{-1}$).

[58POR/SCH3]

For the KOH-NaOH system of unspecified composition, Porter and Schoonmaker obtained partial pressures of $\text{KOH}(\text{g})$ and $\text{K}_2\text{O}_2\text{H}_2(\text{g})$ at temperatures 641 K and 666 K. Using an estimated value $\Delta_{\text{r}}S(666 \text{ K}) = 40 \pm 5 \text{ cal K}^{-1} \text{ mol}^{-1}$ for the reaction

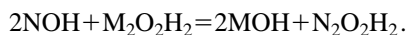


Porter and Schoonmaker obtained an averaged value for the enthalpy of dimer dissociation into monomers: $\Delta_{\text{r}}H^\circ(650 \text{ K}) = 46.5 \pm 5 \text{ kcal mol}^{-1}$ ($194.6 \pm 20 \text{ kJ mol}^{-1}$).

[59SCH/POR]

Schoonmaker and Porter carried out a mass spectrometric study of alkali hydroxide binary mixtures with the aim of obtaining differences in dimerization enthalpies. Effusion cells were constructed of platinum lined with a pressed magnesia or of pure silver. In the case of silver effusion cells the degree of reduction of condensed hydroxide was diminished substantially, and the authors concluded that under these experimental conditions the major portion of M^+ ions was formed by dissociative ionization of MOH molecules.

To determine the difference in the dimerization enthalpies $\Delta_{\text{r}}H^\circ(\text{NOH}) - \Delta_{\text{r}}H^\circ(\text{MOH})$ for the MOH and NOH pair of hydroxides, the equilibrium constant was measured for the gaseous reaction



Equilibrium constant for this reaction was approximately expressed in the form of a combination of ion currents:

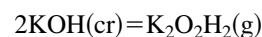
$$K^\circ = \frac{[I(\text{M}^+) + I(\text{MOH}^+)]^2 \cdot I(\text{N}_2\text{OH}^+)}{[I(\text{N}^+) + I(\text{NOH}^+)]^2 \cdot I(\text{M}_2\text{OH}^+)}.$$

For the NaOH-KOH system, four measurements were performed at 883 K; $K^\circ(T)$ values were in the range 12.2–24.3. Using an estimated value $\Delta_{\text{r}}S^\circ(\text{KOH}) - \Delta_{\text{r}}S^\circ(\text{NaOH}) = 1.15 \text{ cal K}^{-1} \text{ mol}^{-1}$ calculated for a planar rhomboid dimer structure, the difference in dimerization enthalpies

was found: $\Delta_{\text{r}}H^\circ(\text{KOH}) - \Delta_{\text{r}}H^\circ(\text{NaOH}) = 6.1 \pm 0.7 \text{ kcal mol}^{-1}$ ($25 \pm 3 \text{ kJ mol}^{-1}$). Combining this result with the value $\Delta_{\text{r}}H^\circ(\text{NaOH}) = -54 \pm 5 \text{ kcal mol}^{-1}$ ($-226 \pm 20 \text{ kJ mol}^{-1}$) previously obtained, Schoonmaker and Porter found the value $\Delta_{\text{r}}H^\circ(\text{KOH}) = -48 \pm 5 \text{ kcal mol}^{-1}$ ($-201 \pm 20 \text{ kJ mol}^{-1}$).

[68GUS/GOR]

Gusarov and Gorokhov carried out a mass spectrometric study of potassium hydroxide vaporization. Results of K_2OH^+ ion intensity measurements in the temperature range 598–653 K were used for calculation of the 2nd-law enthalpy of sublimation of the dimer. The 3rd-law enthalpy of sublimation was calculated using the value $\log[P(\text{KOH})/\text{atm}] = -2.56 \pm 0.28$ for $T = 1068 \text{ K}$, obtained from the data of Jackson and Morgan [21JAC/MOR] on the total vapor pressure of potassium hydroxide. The dimer pressure was calculated using the value $\log[P(\text{d})/P(\text{m})] = -0.40 \pm 0.40$, extrapolated from $T = 646 \text{ K}$. The results of calculations for the reaction



are summarized below:

$$\Delta_{\text{sub}}H^\circ(625 \text{ K}) = 43.9 \pm 1.5 \text{ kcal mol}^{-1} (183.7 \pm 6 \text{ kJ mol}^{-1}),$$

Second law:

$$\Delta_{\text{sub}}H^\circ(0) = 52.9 \pm 1.5 \text{ kcal mol}^{-1} (221.3 \pm 6 \text{ kJ mol}^{-1}),$$

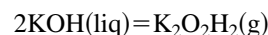
Third law:

$$\Delta_{\text{sub}}H^\circ(0) = 43.8 \pm 1.4 \text{ kcal mol}^{-1} (183.3 \pm 6 \text{ kJ mol}^{-1}).$$

The total errors indicated for 2nd-law values were evaluated as twice standard deviation plus $0.3 \text{ kcal mol}^{-1}$ (an estimate of systematic error). To calculate the $\Delta_{\text{sub}}H^\circ(0 \text{ K})$ values, thermal functions from the 1965 JANAF Tables were used.

[84HAS/ZMB]

Hastie *et al.* carried out a study of vaporization of potassium hydroxide with a transpiration mass spectrometric apparatus. The experimental procedure involved heating the sample in a carrier gas stream (nitrogen) and measuring the intensities of positive ions produced by electron impact from molecules present in supersonic molecular beam. Two separate experiments were performed on potassium hydroxide vaporization as a function of temperature with fixed N_2 pressure: Run 1, $P(\text{N}_2) = 0.2 \text{ atm}$, temperature range 840–1060 K (25 points); Run 2, $P(\text{N}_2) = 0.16 \text{ atm}$, temperature range 955–1066 K (26 points). For the reaction



the authors obtained the following enthalpy values from the 2nd-law analysis of results:

$$\text{Run 1, } \Delta_{\text{vap}}H^\circ(1000 \text{ K}) = 37.9 \pm 1.3 \text{ kcal mol}^{-1} (158.6 \pm 5.4 \text{ kJ mol}^{-1});$$

$$\text{Run 2, } \Delta_{\text{vap}}H^\circ(1000 \text{ K}) = 36.9 \pm 2.7 \text{ kcal mol}^{-1} (154.4 \pm 11 \text{ kJ mol}^{-1}).$$

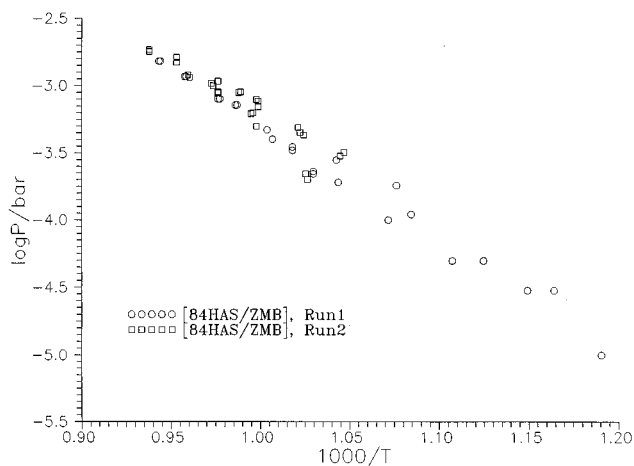


FIG. 8. Partial pressure of $K_2O_2H_2(g)$ over $KOH(liq)$.

The authors recommended the value $\Delta_{\text{vap}}H^\circ(1000 \text{ K}) = 158.6 \pm 5.4 \text{ kJ mol}^{-1}$. The data obtained for $K_2O_2H_2$ pressure are presented in Table 26 and in Fig. 8.

Enthalpy of Formation of $[KOH]_2(g)$ —Experimental Determinations of the Total Vapor Pressure

[21WAR/ALB], [21JAC/MOR], [69DUB/MIL], [74KUD], [88KON/COR2]

Results of the total pressure [21WAR/ALB] and apparent monomer pressure [21JAC/MOR], [69DUB/MIL], [74KUD], [88KON/COR2] measurements for potassium hydroxide were used to calculate dimer partial pressures. The ratios $P(d)/P(m)$ were found as equilibrium constants for the reaction



The calculations were performed with the value $\Delta_f H^\circ(0 \text{ K}) = 16.0 \text{ kJ mol}^{-1}$ adopted for this reaction. The enthalpy of sublimation for the dimer and the enthalpy of formation of

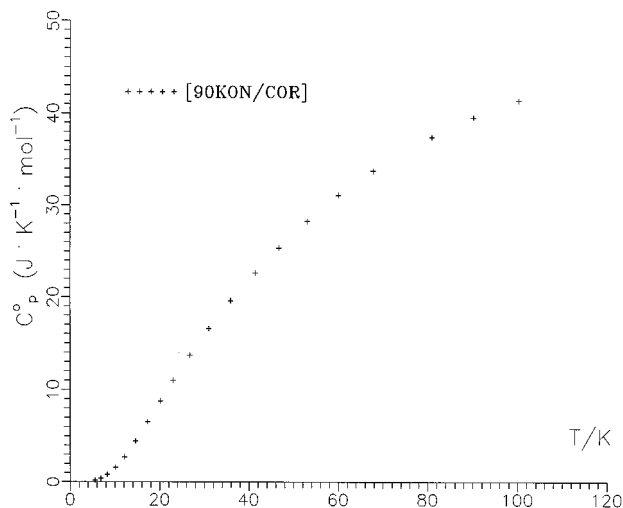
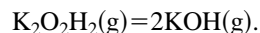


FIG. 9. Heat capacity of $CsOH$ at 5–100 K.

$K_2O_2H_2(g)$ were found from the dimer partial pressure values. The results of calculation are collected in Table 27.

Enthalpy of Formation of $[KOH]_2(g)$ —Miscellaneous Data [89GIR/IAP]

Girichev and Lapshina carried out an electron diffraction investigation of $K_2O_2H_2(g)$ structure. In the process of refining of the theoretical molecular scattering intensity curve $sM(s)$ they obtained the best agreement between theoretical and experimental curves using the value $P(m)/P(d) = 0.67:0.33$, or $P(d)/P(m) = 0.49$ ($T = 990 \pm 20 \text{ K}$). Combining the electron diffraction data on geometry and vibrational frequencies with spectroscopic data for $K_2O_2H_2(g)$, the authors [89GIR/LAP] calculated the 3rd-law enthalpy $\Delta_f H^\circ(0 \text{ K}) = 181.6_{-4.9}^{+7.5} \text{ kJ mol}^{-1}$ for the reaction



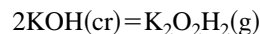
Discussion of the Enthalpy of Formation of $[KOH]_2(g)$

The authors of this review have recalculated all equilibria from the papers annotated in the enthalpy of formation subsections with the thermal functions from this work and from [82GUR/VEI] and [89GUR/VEI].

Similar to the case of $KOH(g)$, two mass spectrometric studies, [68GUS/GOR] and [84HAS/ZMB], appear to be the most important for selection of the $K_2O_2H_2(g)$ enthalpy of formation. Using the data from both papers mentioned, the enthalpy $\Delta_f H^\circ(0 \text{ K}) = 16.0 \pm 3 \text{ kJ mol}^{-1}$ or $\Delta_f H^\circ(298.15 \text{ K}) = 17.1 \pm 3 \text{ kJ mol}^{-1}$ was adopted for the reaction



As was mentioned in the enthalpy of formation subsections, monomer and dimer partial pressures for the data of the boiling point [21WAR/ALB], Knudsen effusion [74KUD] and transpiration measurements [21JAC/MOR], [69DUB/MIL], [88KON/COR2] were calculated with this value. Results of the 2nd- and 3rd-law calculations for the reaction



are presented in Table 27. The 3rd-law values differ from the corresponding values for monomer vaporization by the amount of 16.0 kJ mol^{-1} , as it follows from the method of calculations employed. Hence these calculations are useful only as an illustration of the agreement of the 2nd- and 3rd-law values. In general, agreement between 2nd- and 3rd-law values is good.

Combining the enthalpy of reaction (5) with the enthalpies of formation for $KOH(cr)$ and $KOH(g)$ adopted in this review, the value for the enthalpy of formation of $K_2O_2H_2$ was obtained:

$$\Delta_f H^\circ(K_2O_2H_2, g, 298.15 \text{ K}) = -641.3 \pm 8 \text{ kJ mol}^{-1}.$$

As indicated earlier, results of mass spectrometric studies by Porter and Schoonmaker [58POR/SCH], [58POR/SCH2], [58POR/SCH3] are very informative as to the understanding of the main features of alkali hydroxide vaporization. However, the papers mentioned only contain rough estimates of partial pressures. At the same time, it seems likely that values of differences in dimerization enthalpies presented in the

paper [59SCH/POR] are more reliable due to mutual compensation of possible experimental errors in derivation of the expression for the equilibrium constant. The value of $\text{K}_2\text{O}_2\text{H}_2(\text{g})$ enthalpy of formation was calculated from the data of [59SCH/POR] in combination with the adopted enthalpies of formation for $\text{NaOH}(\text{g})$, $\text{Na}_2\text{O}_2\text{H}_2(\text{g})$, and $\text{KOH}(\text{g})$. The value obtained, $\Delta_f H^\circ(\text{K}_2\text{O}_2\text{H}_2, \text{g}, 298.15 \text{ K}) = -671 \pm 25 \text{ kJ mol}^{-1}$, is in reasonable agreement with that derived above, $\Delta_f H^\circ(\text{K}_2\text{O}_2\text{H}_2, \text{g}, 298.15 \text{ K}) = -641.3 \pm 8 \text{ kJ mol}^{-1}$.

The results of Girichev and Lapshina [89GIR/IAP] are in agreement with the enthalpy of formation obtained from the calculations for reaction (5) in combination with the enthalpies of formation for $\text{KOH}(\text{cr})$ and $\text{KOH}(\text{g})$.

On the basis of the above discussion, the value

$$\Delta_f H^\circ(\text{K}_2\text{O}_2\text{H}_2, \text{g}, 298.15 \text{ K}) = -641 \pm 8 \text{ kJ mol}^{-1}$$

is adopted in this review.

2.2.4. Appendix. Tables of Experimental and Evaluated Data for $[\text{KOH}]_2(\text{g})$

TABLE 26. Partial pressure of $\text{K}_2\text{O}_2\text{H}_2(\text{g})$ over $\text{KOH}(\text{liq})$, [84HAS/ZMB]

No.	Run 1		No.	Run 2	
	T/K	P/atm 10^{-3}		T/K	P/atm 10^{-3}
1	870	0.03	1	955	0.32
2	903	0.05	2	957	0.30
3	929	0.18	3	976	0.43
4	933	0.10	4	978	0.45
5	971	0.22	5	979	0.49
6	971	0.23	6	1002	0.78
7	993	0.40 ^a	7	1002	0.50
8	996	0.47	8	1001	0.69
9	1023	0.79	9	1001	0.76
10	1024	0.79	10	1012	0.88
11	1059	1.50	11	1011	0.89
12	1060	1.50	12	1024	0.87
13	1044	1.16	13	1024	0.89
14	1043	1.16	14	1024	1.07
15	1014	0.71	15	1041	1.14
16	1013	0.71	16	1042	1.19
17	982	0.33	17	1066	1.83
18	982	0.35	18	1066	1.77
19	959	0.28	19	1049	1.60
20	958	0.19	20	1049	1.48
21	958	0.19	21	1028	1.03
22	922	0.11	22	1027	0.99
23	889	0.05	23	1005	0.61
24	859	0.03	24	1004	0.62
25	840	0.01	25	975	0.22
			26	974	0.20

^aA value, corrected for an obvious misprint in [84HAS/ZMB].

TABLE 27. Results of experimental determination of $\Delta_f H^\circ(\text{K}_2\text{O}_2\text{H}_2, \text{g}, 0 \text{ K})$, kJ mol^{-1}

Reference	Method	$\Delta_f H^\circ(0 \text{ K})$		$\Delta_f H^\circ(0 \text{ K})$
		2nd law	3rd law	
Mass spectrometric studies				
[58POR/SCH2]	Knudsen effusion mass spectrometry, $\text{K}_2\text{O}_2\text{H}_2(\text{g})=2\text{KOH}(\text{g})$, 641 and 666 K	...	170.7 ± 5	-626.7 ± 6
[58POR/SCH3]	Knudsen effusion mass spectrometry, $2\text{KOH}(\text{cr})=\text{K}_2\text{O}_2\text{H}_2(\text{g})$, $T(\text{av})=595 \text{ K}$ 626 K (one point)	177 172.9	-664 ± 10 -668 ± 10
[59SCH/POR]	Knudsen effusion mass spectrometry, $2\text{NaOH}(\text{g})+\text{K}_2\text{O}_2\text{H}_2(\text{g})=$ $2\text{KOH}(\text{g})+\text{Na}_2\text{O}_2\text{H}_2(\text{g})$, 883 K (four points)	...	-32.3 ± 5	-662 ± 8
[68GUS/GOR]	Knudsen effusion mass spectrometry, $2\text{KOH}(\text{cr})=\text{K}_2\text{O}_2\text{H}_2(\text{g})$, 598–653 K (13 points) $\text{K}_2\text{O}_2\text{H}_2(\text{g})=2\text{KOH}(\text{g})$, 600–770 K (14 points)	211.3 ± 6 176.7 ± 2	-629.4 ± 6 -632.7 ± 3
[84HAS/ZMB]	Transpiration mass spectrometry, $2\text{KOH}(\text{liq})=\text{K}_2\text{O}_2\text{H}_2(\text{g})$, Run 1: 840–1060 K (25 points) Run 2: 955–1066 K (26 points)	223.6 ± 9 201.6 ± 14	207.1 ± 0.7 204.3 ± 0.4	-633.6 ± 6 -636.4 ± 6
Total vapor pressure measurements				
[21WAR/ALB]	Boiling point, $2\text{KOH}(\text{liq})=\text{K}_2\text{O}_2\text{H}_2(\text{g})$, 1443–1600 K (nine points)	205.9	210.4 ± 3	-630.3 ± 6
[21JAC/MOR]	Transpiration, $2\text{KOH}(\text{liq})=\text{K}_2\text{O}_2\text{H}_2(\text{g})$, 1068 K (nine points)	...	203.6	-637.1 ± 6
[69DUB/MIL]	Transpiration, $2\text{KOH}(\text{liq})=\text{K}_2\text{O}_2\text{H}_2(\text{g})$, 850–1350 K (64 points)	205.2	207.8 ± 0.3	-632.9 ± 6
[74KUD]	Knudsen effusion, $\text{KOH}(\text{liq})=\text{KOH}(\text{g})$, 760–844 K (six points)	...	204.7 ± 4	-637.9 ± 6
[88KON/COR2]	Transpiration, $2\text{KOH}(\text{liq})=\text{K}_2\text{O}_2\text{H}_2(\text{g})$ 866.8–1087.0 K (23 points)	201.9 ± 5	209.0 ± 1.0	-631.7 ± 5
Miscellaneous data				
[89GIR/LAP]	Electron diffraction, $\text{KOH}(\text{g})=2\text{KOH}(\text{g})$, 990 K	...	181.6 ± 7.5 -4.9	-638 ± 10

TABLE 28. Thermodynamic properties at 0.1 MPa: $K_2O_2H_2(g)$

T/K	$C_p^\circ - [G^\circ - H^\circ(0K)]/T$		S	$H^\circ - H^\circ(0K)$	$\Delta_f H^\circ$	$\Delta_f G^\circ$
	J K ⁻¹ mol ⁻¹					
0	0.000	0.000	0.000	0.000	-632.061	-632.061
25	33.714	154.815	188.128	0.833	-632.734	-632.352
50	39.453	178.213	212.900	1.734	-634.279	-631.423
75	50.543	192.846	230.859	2.851	-635.894	-629.634
100	63.312	204.407	247.159	4.275	-637.152	-627.347
150	83.268	223.728	276.925	7.980	-638.786	-622.051
200	94.902	240.324	302.630	12.461	-639.755	-616.315
250	101.621	255.039	324.594	17.389	-640.432	-610.371
300	105.714	268.245	343.513	22.580	-641.023	-604.301
350	108.352	280.202	360.021	27.936	-646.341	-597.950
400	110.141	291.109	374.613	33.401	-647.007	-590.990
450	111.411	301.125	387.663	38.942	-647.578	-583.953
500	112.357	310.378	399.452	44.537	-648.079	-576.857
600	113.715	326.990	420.065	55.845	-648.945	-562.528
700	114.759	341.575	437.675	67.270	-649.709	-548.064
800	115.722	354.569	453.062	78.794	-650.440	-533.493
900	116.688	366.287	466.748	90.415	-651.191	-518.830
1000	117.673	376.960	479.093	102.132	-652.021	-504.079
1100	118.664	386.764	490.355	113.949	-810.708	-480.008
1200	119.640	395.835	500.722	125.865	-809.575	-449.993
1300	120.583	404.277	510.336	137.876	-808.429	-420.074
1400	121.478	412.177	519.305	149.980	-807.261	-390.246
1500	122.318	419.602	527.715	162.170	-806.083	-360.501
1600	123.099	426.609	535.635	174.441	-804.893	-330.832
1700	123.821	433.244	543.119	186.788	-803.699	-301.240
1800	124.484	439.547	550.216	199.204	-802.505	-271.716
1900	125.091	445.551	556.963	211.683	-801.320	-242.261
2000	125.647	451.283	563.394	224.220	-800.148	-212.869
2200	126.618	462.030	575.416	249.450	-797.866	-154.252
2400	127.429	471.945	586.469	274.857	-795.715	-95.835
2600	128.108	481.153	596.696	300.412	-793.748	-37.595
2800	128.678	489.750	606.212	326.093	-792.018	20.501
3000	129.161	497.814	615.106	351.878	-790.569	78.484
3200	129.571	505.408	623.456	377.752	-789.450	136.384
3400	129.923	512.586	631.322	403.702	-788.700	194.227
3600	130.225	519.391	638.757	429.718	-788.356	252.032
3800	130.487	525.860	645.805	455.790	-788.458	309.836
4000	130.715	532.026	652.504	481.910	-789.026	367.648
4200	130.914	537.916	658.886	508.074	-790.089	425.515
4400	131.089	543.555	664.981	534.274	-791.670	483.420
4600	131.244	548.962	670.811	560.508	-793.781	541.431
4800	131.382	554.156	676.400	586.771	-796.415	599.539
5000	131.504	559.154	681.766	613.060	-799.590	657.762
5200	131.614	563.969	686.925	639.372	-803.284	716.141
5400	131.712	568.616	691.895	665.704	-807.494	774.645
5600	131.801	573.105	696.686	692.056	-812.183	833.325
5800	131.881	577.446	701.313	718.424	-817.334	892.191
6000	131.954	581.650	705.785	744.808	-822.897	951.233
298.15	105.593	267.780	342.859	22.385	-641.000	-604.528
Uncertainties in Functions						
0	9.000	9.000
300	3.000	2.500	5.000	0.800	9.000	9.000
1000	4.000	6.000	8.000	3.000	10.000	7.000
2000	6.000	8.000	10.000	4.000	10.000	12.000
3000	8.000	10.000	12.000	6.000	11.000	25.000
4000	10.000	12.000	15.000	12.000	15.000	40.000
5000	12.000	13.000	18.000	20.000	20.000	60.000
6000	15.000	15.000	20.000	25.000	30.000	80.000

3. Rubidium Hydroxide

3.1. Rubidium Hydroxide in Condensed Phases

At ambient pressure RbOH has three crystalline modifications: orthorhombic (α)—stable below 265 K, monoclinic (β)—stable at 265–508 K, and cubic (γ)—stable above 508 K, see Table 1, Part I. There are experimental data on the enthalpies of formation, transition, and fusion of RbOH, but no experimental data on the heat capacity and the enthalpy content are available for RbOH. Thus the thermal functions of RbOH were calculated using the estimated values of the heat capacity, enthalpy, and entropy of this substance.

3.1.1. Heat Capacity and Enthalpy Measurements for RbOH(cr&liq)

Since no experimental values of heat capacity, enthalpy, and entropy of RbOH are available at the present time, the corresponding values estimated in the literature are listed below.

[61DRO]

Drozin estimated the entropy of RbOH at 298.15 K based on the principle of Berthelot and obtained the value $S^\circ(298.15 \text{ K}) = 19.9 \text{ cal K}^{-1} \text{ mol}^{-1} = 83.3 \text{ J K}^{-1} \text{ mol}^{-1}$. This value is highly underestimated.

[71KRA/FIL]

Krasnov and Filippenko estimated the heat capacity values of RbOH (and CsOH) as well as the enthalpy increment $H^\circ(298.15 \text{ K}) - H^\circ(0 \text{ K})$ extrapolating the experimental data in the series LiOH–NaOH–KOH–... They obtained for RbOH(cr): $H^\circ(298.15 \text{ K}) - H^\circ(0 \text{ K}) = 15.8 \text{ kJ mol}^{-1}$, $C_p^\circ(298.15 \text{ K}) = 71.1 \text{ J K}^{-1} \text{ mol}^{-1}$, $C_p^\circ(T) = 48.95 + 74.6 \cdot 10^{-3}T$ ($298 < T < 574 \text{ K}$), and for RbOH(liq): $C_p^\circ(T) = 92 \text{ J K}^{-1} \text{ mol}^{-1}$. Comparison of the corresponding values estimated in [71KRA/FIL] for CsOH with the experimental data shows that estimated values are 5%–20% higher than obtained in [90KON/COR].

[77KUB/UNA]

Kubaschewski and Unal suggested an empirical method for estimation of the heat capacity of ionic inorganic compounds at 298.15 K. They calculated the heat capacity increments for ions Rb^+ and Cs^+ ($26.4 \text{ J K}^{-1} \text{ mol}^{-1}$) as well as for OH^- ($31.0 \text{ J K}^{-1} \text{ mol}^{-1}$). The values for the heat capacity of RbOH and CsOH at 298.15 K were equal $57.4 \text{ J K}^{-1} \text{ mol}^{-1}$ and are about $12.5 \text{ J K}^{-1} \text{ mol}^{-1}$ lower than the experimental one for CsOH [90KON/COR].

[79RIC/VRE]

Richter and Vreuls estimated the entropy of RbOH (and CsOH) at 298.15 K based on the linear dependence of the entropy on the radius of the cation constituent of the compound. They determined the entropy increments of ions (in $\text{J K}^{-1} \text{ mol}^{-1}$): Rb^+ (55.9), Cs^+ (62.1), and OH^- (25.1) and obtained for RbOH $S^\circ(298.15 \text{ K}) = 81.0 \text{ J K}^{-1} \text{ mol}^{-1}$. This value is highly underestimated. For CsOH the estimated value is about $17 \text{ J K}^{-1} \text{ mol}^{-1}$ less than the experimental one [90KON/COR].

[82MED/BER], [82GUR/VEI]

In these books the heat capacity, enthalpy, and entropy of RbOH were estimated using the various empirical methods and the experimental data for Li, Na, and K hydroxides. For α -RbOH the following values were received: $S^\circ(298.15 \text{ K}) = 92 \pm 8 \text{ J K}^{-1} \text{ mol}^{-1}$, $H^\circ(298.15 \text{ K}) - H^\circ(0 \text{ K}) = 14.5 \pm 1.0 \text{ kJ mol}^{-1}$, $C_p^\circ(298.15 \text{ K}) = 69 \text{ J K}^{-1} \text{ mol}^{-1}$, and $C_p^\circ(T) = (51.24 + 59.566 \cdot 10^{-3} T) \text{ J K}^{-1} \text{ mol}^{-1}$ at $298.15 < T < 508 \text{ K}$. The constant values of the heat capacity, 80 ± 6 and $83 \pm 8 \text{ J K}^{-1} \text{ mol}^{-1}$ were accepted for γ -RbOH and RbOH(liq), respectively. Similarly, estimated values for CsOH were in good agreement with the experimental data obtained later.

Discussion of Heat Capacity and Enthalpy Data

The heat capacity, enthalpy, and entropy values of RbOH estimated in the literature differ significantly (see Table 29). The accurate measurements of the CsOH heat capacity and enthalpy [90KON/COR] (6–683 K) and more accurate determination of the heat capacity of KOH [88WHI/PER] (15–340 K) permit us to define these values for RbOH by the interpolation. Thus we obtained $C_p^\circ(298.15 \text{ K}) = 69 \pm 2 \text{ J K}^{-1} \text{ mol}^{-1}$, $S^\circ(298.15 \text{ K}) = 94 \pm 3 \text{ J K}^{-1} \text{ mol}^{-1}$, and $H^\circ(298.15 \text{ K}) - H^\circ(0 \text{ K}) = 13.5 \pm 0.3 \text{ kJ mol}^{-1}$. The heat capacity of monoclinic modifications of KOH and CsOH in the range $298 \text{ K} - T_{\text{trs}}$ are very similar to each other (in the limits 1%–2 and fit satisfactorily by the linear equations. Therefore, the analogous equation:

$$C_p^\circ(T)/\text{J K}^{-1} \text{ mol}^{-1} = 54.792 + 47.653 \cdot 10^{-3}T \quad (298.15 - 508 \text{ K}),$$

was derived for RbOH, using the value $C_p^\circ(298.15 \text{ K})$ (see above) and estimated value $C_p^\circ(508 \text{ K}) = 79 \text{ J K}^{-1} \text{ mol}^{-1}$.

The value $76 \pm 4 \text{ J K}^{-1} \text{ mol}^{-1}$ was adopted for the heat capacity of cubic modification of RbOH. It is the average value between the experimental heat capacities of cubic modifications of KOH and CsOH. For the heat capacity of liquid RbOH the value $86 \pm 5 \text{ J K}^{-1} \text{ mol}^{-1}$ was adopted, the average between the experimental heat capacities of liquid KOH ($87 \text{ J K}^{-1} \text{ mol}^{-1}$) and liquid CsOH ($85 \text{ J K}^{-1} \text{ mol}^{-1}$).

Phase Equilibrium Data

[10HEV], [10HEV2]

Hevesy determined the temperatures and enthalpies of transition and fusion by a thermal analysis method. Unfortunately, he studied a commercial sample of RbOH (“Kahlbaum”) which was highly contaminated by Rb_2CO_3 (–5.2%). The sample was dehydrated in a silver container at $\sim 450^\circ\text{C}$ “for many hours.” The cooling curves made with the rate $12^\circ\text{C}/\text{min}$ gave the transition and fusion temperatures $245 \pm 0.5^\circ\text{C} = 518 \text{ K}$ and $301 \pm 0.9^\circ\text{C} = 574 \text{ K}$, respectively. The latter value is about 80° lower than the value adopted in this review on the base of experimental studies. The enthalpy of transition and fusion of

RbOH ($16.8 \text{ cal g}^{-1} = 7.12 \text{ kJ mol}^{-1}$ and $15.8 \text{ cal g}^{-1} = 6.75 \text{ kJ mol}^{-1}$) were determined by quantitative thermal analysis.

[54BOG]

Bogart measured the density of molten RbOH in the temperature range from $400 \text{ }^\circ\text{C}$ to $850 \text{ }^\circ\text{C}$ and the melting point of RbOH. The sample of RbOH, which contained 2.1% Rb_2CO_3 , was dehydrated by heating in a nickel crucible at $\sim 500 \text{ }^\circ\text{C}$. The fusion temperature ($T_{\text{fus}} = 383 \text{ }^\circ\text{C} = 656 \text{ K}$) was ‘‘more accurately’’ determined by thermal analysis. The temperature was measured by means of two chromel-alumel thermocouples that were immersed directly into the RbOH melt. The cooling curves were made with the rate about $1 \text{ }^\circ\text{C/min}$. The author noted that in an earlier study [10HEV2] the sample of RbOH was not completely dehydrated.

[58ROL/COH], [59ROL/COH]

Rollet *et al.* prepared a sample by electrolysis of RbOH water solution in a stream of hydrogen, then purified it from CO_3^- , Cl^- and ClO_3^- ions and dehydrated up to the constant fusion temperature. After purification the sample contained about 0.5% Rb_2CO_3 only. The authors of [58ROL/COH] investigated the system RbOH– H_2O and obtained for RbOH $T_{\text{trs}} = 235 \text{ }^\circ\text{C} = 508 \text{ K}$ and $T_{\text{fus}} = 380 \pm 1 \text{ }^\circ\text{C} = 653 \text{ K}$ by DTA. In [59ROL/COH] the temperature was measured with a copper - constantan thermocouple that was calibrated by the melting points of Sn ($231.85 \text{ }^\circ\text{C}$) and of Zn ($419.45 \text{ }^\circ\text{C}$) with an uncertainty $0.3 \text{ }^\circ\text{C}$. From cooling and heating curves $T_{\text{trs}} = 235 \text{ }^\circ\text{C} = 508 \text{ K}$, and $T_{\text{fus}} = 382 \text{ }^\circ\text{C} = 655 \text{ K}$ were obtained.

[59RES/UNZ]

Reshetnikov and Unzhakov prepared a sample by evaporation of the solution mixture Rb_2SO_4 and $\text{Ba}(\text{OH})_2$ and by dehydration of RbOH in a stream of dry H_2 at $450 \text{ }^\circ\text{C}$. The sample of RbOH was not analyzed chemically for impurities. The fusion point was determined as $T_{\text{fus}} = 301 \text{ }^\circ\text{C} = 574 \text{ K}$ by thermal analysis.

[61COH/MIC]

Cohen–Adad *et al.* studied the system RbOH– Rb_2CO_3 and obtained for pure RbOH the values: $T_{\text{trs}} = 235 \text{ }^\circ\text{C} = 508 \text{ K}$ and $T_{\text{fus}} = 382 \text{ }^\circ\text{C} = 655 \text{ K}$.

[67RES/BAR], [69RES/BAR]

Reshetnikov and Baranskaya investigated a sample of RbOH containing about 98.5% RbOH, 0.46% Rb_2CO_3 and 0.1% H_2O . They obtained the values $T_{\text{trs}} = 225 \text{ }^\circ\text{C} = 498 \text{ K}$ and $T_{\text{fus}} = 385 \pm 1 \text{ }^\circ\text{C} = 658 \text{ K}$ by DTA. The enthalpy of transition ($1.29 \text{ kcal mol}^{-1} = 5.4 \text{ kJ mol}^{-1}$) and the enthalpy of fusion ($2.12 \text{ kcal mol}^{-1} = 8.9 \text{ kJ mol}^{-1}$) were determined by quantitative DTA.

[690ST/ITK], [75ITK/POR]

Itkina *et al.* studied the system RbOH–LiOH and obtained for RbOH the values: $T_{\text{trs}} = 235 \text{ }^\circ\text{C} = 508 \text{ K}$ and $T_{\text{fus}} = 380 \text{ }^\circ\text{C} = 653 \text{ K}$. Determinations of the transformation temperatures were carried out in a gold container by DTA (heating curves were made with a heating rate 10 K min^{-1}).

[87JAC/MAC]

Jacobs *et al.* measured the temperatures and the enthalpies of transitions and fusion of RbOH by DSC. Preparation of the sample was described earlier [85JAC/KOC]. According to the chemical analysis, the sample contained 83.3% Rb (calculated 83.4%) and 16.5% OH^- ions (calculated 16.6%). The data concerning impurities in the sample were not given. A Perkin–Elmer calorimeter, DSC2, was used for measurements in the temperature range 15–637 K. The thermocouples were calibrated by the melting points of H_2O , In (429.8 K), Pb (600.3 K), and Zn (692.7 K) with an accuracy $\pm 0.2 \text{ K}$. The measurements of the enthalpies of phase transitions were based on the enthalpy of fusion (3.26 kJ mol^{-1}). The following values for the temperatures and the enthalpies of phase transformations of RbOH and RbOD were measured and are summarized in the table:

		α – β	?	β – γ		
RbOH	T_{trs}/K	265	367	511	$T_{\text{fus}}/\text{K} = 637$	
	$\Delta_{\text{trs}}H/\text{kJ mol}^{-1}$	0.3	0.36	4.4	$\Delta_{\text{fus}}H/\text{kJ mol}^{-1} = 3.6$	
RbOD	T_{trs}/K	300	369	513		
	$\Delta_{\text{trs}}H/\text{kJ mol}^{-1}$	0.1	1.17	3.6		

No information was given on the accuracy of listed values. The results of x-ray investigations of RbOH modifications are given in Table 1, Part I. The authors of [87JAC/MAC] noted that the thermal effects at 367 K for RbOH and at 369 K for RbOD were not accompanied by the changes in the structure and the lattice parameters.

[89HEN/LUT]

Henning, Lutz *et al.* studied the phase transitions of RbOH (and RbOD) measuring the temperature dependence of the IR and Raman spectra in the range 100–370 K. A sample of RbOH was prepared by the reaction of $\text{RbOH}\cdot\text{H}_2\text{O}$ with RbNH_2 in liquid ammonia in an autoclave as was described in [87JAC/MAC]. The temperature of α – β transition of RbOH at 265 K was confirmed by the temperature shift of frequency ν_{OH} ; the analogous transition of RbOD was detected at 300 K.

A shift of frequency ν_{OH} was also detected at 367 K. The authors interpreted it as due to order–disorder transition of the monoclinic modification of RbOH. The analogous anomaly of RbOD was obtained at 369 K.

Discussion of Phase Equilibrium Data

The α – β polymorphic transition from orthorhombic to monoclinic modification of RbOH at 265 K and the enthalpy of this transition, 0.3 kJ mol^{-1} , were originally measured by DSC [87JAC/MAC]. The accuracy of these values was not estimated. Based on similar measurements for CsOH by the same authors [87JAC/MAC2], one can estimate the error of measurements of T_{trs} as $\pm 3 \text{ K}$. The value of T_{trs} , obtained from the frequency shifts dependence upon temperature in IR and Raman spectra [89HEN/LUT], being less accurate, does not contradict to the [87JAC/MAC] measurements.

The thermal effect at 367 K for RbOH (and at 369 K for RbOD) was determined in [87JAC/MAC] by DSC. However, the authors [87JAC/MAC] found that the parameters of

the monoclinic lattice of RbOH have not been changed at this temperature. The thermal effect at 367 K for RbOH (and at 369 K for RbOD) may be caused by fusion of RbOH–RbOH·H₂O eutectic. Presence of H₂O (or D₂O) impurity in RbOH sample is confirmed by the fact that the obtained fusion point (637 K) is about 20 K lower than the more precise value 658 ± 3 K (see below).

Measurements of the temperature of RbOH monoclinic–cubic (β – γ) transition (see Table 30) result in the values ranging from 498 to 518 K. The average value of the data obtained by DTA in [58ROL/COH, 61COH/MIC, 73PAP/BOU, 73TOU, 75ITK/POR] is equal 508 ± 3 K. The value $T_{\text{trs}} = 511$ K obtained by DSC [87JAC/MAC] is in satisfactory agreement with the above mentioned, but the purity of the sample of RbOH in [87JAC/MAC] is doubtful (see below).

There is a large scattering of the measured values of T_{fus} because of difficulties in dehydration of the samples. Indeed, heating at 400–450 °C does not result in complete dehydration of RbOH. H₂O admixture may reach up to 10% in this case [73ITK]. Therefore, we do not consider the results of several studies [10HEV, 59RES/UNZ, 87JAC/MAC], in which only partially dehydrated samples were investigated and the corresponding values were 20–80 K underestimated. The other eight studies (see Table 31) yielded the T_{fus} in the range 653–658 K. In the present review an average value 655 ± 3 K is adopted. This value coincides with that found in [59ROL/COH, 61COH/MIC, 71TOU].

The enthalpy of α – β transition (orthorhombic - monoclinic) of RbOH, $\Delta_{\text{trs}}H(265 \text{ K}) = 0.3 \text{ kJ mol}^{-1}$, was determined in only one study [87JAC/MAC]. The information about the uncertainty of this value obtained by DSC was not given.

The “transition” within the monoclinic modification of RbOH at 367 K with $\Delta_{\text{trs}}H = 0.36 \text{ kJ mol}^{-1}$ [87JAC/MAC] was not taken into consideration in this review because this thermal effect may be explained by fusion of RbOH–RbOH·H₂O eutectic (see above). The literature data [10HEV], [67RES/BAR], [87JAC/MAC] concerning the enthalpy of β – γ transition (monoclinic–cubic) and the enthalpy of fusion (see Tables 32 and 33) are in poor agreement (approximately twofold divergence takes place). Data [10HEV2] and [67RES/BAR] were determined by quantitative DTA which is not precise. The sample of RbOH investigated in [10HEV2] was not completely dehydrated. Its melting point was about 80° below correct value. The DSC-data of [87JAC/MAC] are also not accurate enough. The measurements of enthalpy of transformations of CsOH made in [87JAC/MAC2] by the same method may be compared with the more precise calorimetric data of Konings *et al.* [90KON/COR]. The enthalpy of transition of CsOH at 511 K obtained in the former study (7.12 kJ mol^{-1}) is 30% higher than that obtained in [90KON/COR] (5.4 kJ mol^{-1}). On the contrary, the enthalpy of CsOH fusion (7.4 kJ mol^{-1}) obtained in [87JAC/MAC2] is 5% lower than the more accurate value 7.78 kJ mol^{-1} [90KON/COR].

The results of measurements of the β – γ transition and

fusion enthalpy of RbOH in [87JAC/MAC] seem to be greatly underestimated because the samples of RbOH contained essential amount of water (see above). For that reason, we prefer to assume the value that have been estimated on the basis of accurate calorimetric data for KOH and CsOH (see the table, the estimated values are in brackets):

Substance	$T_{\text{trs}}/$ K	$\Delta_{\text{trs}}H$ kJ mol ⁻¹	$\Delta_{\text{trs}}S$ J K ⁻¹ mol ⁻¹	$T_{\text{fus}}/$ K	$\Delta_{\text{fus}}H$ kJ mol ⁻¹	$\Delta_{\text{fus}}S$ J K ⁻¹ mol ⁻¹
KOH	517	5.6	10.83	679	7.9	11.63
RbOH	508	(5.5)	(10.83)	658	(8.0)	(12.1)
CsOH	498.2	5.4	10.83	615.5	7.78	12.64

The uncertainties of these adopted (for RbOH) values have been estimated as 0.5 kJ mol^{-1} and 1.0 kJ mol^{-1} for $\Delta_{\text{fus}}H$ and $\Delta_{\text{trs}}H$, respectively.

Calculation of Thermal Functions of RbOH(cr&liq)

The thermal functions of RbOH(cr&liq) at the temperatures 298.15–2000 K (Table 35) were calculated using the adopted values and equations presented in the previous section. The uncertainties of the tabulated values are given in the Table 35.

The following values are adopted:

$$C_p^\circ(298.15 \text{ K}) = 69 \pm 2 \text{ J K}^{-1} \text{ mol}^{-1},$$

$$S^\circ(298.15 \text{ K}) = 94 \pm 3 \text{ J K}^{-1} \text{ mol}^{-1},$$

$$H^\circ(298.15 \text{ K}) - H^\circ(0) = 13500 \pm 300 \text{ J K}^{-1} \text{ mol}^{-1}.$$

Heat Capacity Equations (in the following temperature ranges):

$$\beta\text{-cr, (298.15–508 K): } C_p^\circ/\text{J K}^{-1} \text{ mol}^{-1} = 54.792 + 47.653 \cdot 10^{-3}T,$$

$$\gamma\text{-cr, (508–658 K): } C_p^\circ/\text{J K}^{-1} \text{ mol}^{-1} = 76.0,$$

$$\text{liq, (658–2000 K): } C_p^\circ/\text{J K}^{-1} \text{ mol}^{-1} = 86.0.$$

Phase Equilibrium Data:

$$\alpha\text{-}\beta \text{ transition: } T_{\text{trs}}/\text{K} = 265 \text{ and } \Delta_{\text{trs}}H/\text{J mol}^{-1} = 300,$$

$$\beta\text{-}\gamma \text{ transition: } T_{\text{trs}}/\text{K} = 508 \pm 3 \text{ and } \Delta_{\text{trs}}H/\text{J mol}^{-1} = 5500 \pm 500,$$

$$\text{Fusion: } T_{\text{fus}}/\text{K} = 658 \pm 3 \text{ and } \Delta_{\text{fus}}H/\text{J mol}^{-1} = 8000 \pm 1000.$$

The calculated values of thermal functions of RbOH(cr&liq) differ from those listed in the earlier review [82GUR/VEI], (see Table 34), due to the use of different estimation schemes for the heat capacity, entropy and enthalpies of transition and fusion.

3.1.2. Enthalpy of Formation of RbOH(cr)

The enthalpy of formation of crystalline rubidium hydroxide can be obtained from its enthalpy of solution in water and appropriate auxiliary data. The enthalpy of solution of RbOH(cr) in water was determined by Forcrand [06FOR] only.

Experimental Study
[06FOR]

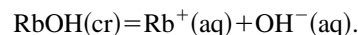
Forcrand measured the enthalpy of solution of RbOH(cr) in water in a calorimeter at 288.15 K (one experiment). For

the reaction $\text{RbOH}(\text{cr}) + 111\text{H}_2\text{O}(\text{l}) = \text{RbOH}(\text{soln}, 111\text{H}_2\text{O})$, the author obtained: $\Delta_{\text{aq}}H^\circ(298.15 \text{ K}) = -59.7 \text{ kJ mol}^{-1}$. Parker [65PAR] recalculated this value taking into account the changes of atomic weights and the corrections for transition to a standard temperature and infinite dilution. For reaction $\text{RbOH}(\text{cr}) = \text{RbOH}(\text{soln}, \infty\text{H}_2\text{O})$ it was obtained: $\Delta_{\text{aq}}H^\circ(298.15 \text{ K}) = -62.3 \pm 0.8 \text{ kJ mol}^{-1}$. Information on the purity of the RbOH sample and other experimental details was not given.

Discussion of the Enthalpy of Formation Data

The enthalpy of formation of $\text{RbOH}(\text{cr})$ was calculated using CODATA data ($\Delta_f H^\circ(\text{OH}^-, \text{aq}, 298.15 \text{ K}) = -230.015 \pm 0.040 \text{ kJ mol}^{-1}$ and $\Delta_f H^\circ(\text{Rb}^+, \text{aq}, 298.15 \text{ K}) = -251.12 \pm 0.10 \text{ kJ mol}^{-1}$ [89COX/WAG]). The uncertainty of the values was recalculated by authors of this review and was increased to $\pm 1.5 \text{ kJ mol}^{-1}$. The latter value was evaluated by a comparison of the results of Forcrand measurements for hydroxides of other alkali metals with the data of more accurate and modern measurements. Thus we obtained the value $\Delta_f H^\circ(\text{RbOH}, \text{cr}, 298.15 \text{ K}) = -418.8 \pm 1.5$

kJ mol^{-1} from the Forcrand data for reaction



We also approximately calculated the enthalpy of formation of $\text{RbOH}(\text{cr})$ using the equation $\Delta_f H^\circ(\text{MOH}, \text{cr}, 298.15 \text{ K}) = f(N)$, where N is atomic number of alkali metal (M) in the Periodical System of Elements; Me = Na, K, Rb and Cs. The value $\Delta_f H^\circ(\text{RbOH}, \text{cr}, 298.15 \text{ K}) = -420 \text{ kJ mol}^{-1}$ was obtained by a graphic interpolation from the data adopted for $\text{NaOH}(\text{cr})$, $\text{KOH}(\text{cr})$, and $\text{CsOH}(\text{cr})$ in this review. The uncertainty of this value was estimated as $\pm 4 \text{ kJ mol}^{-1}$ ($\sim \pm 1\%$). The value obtained is in satisfactory agreement with the value calculated from Forcrand measurements.

The value of the enthalpy of formation of $\text{RbOH}(\text{cr})$ is based on the Forcrand [06FOR] data. This value is

$$\Delta_f H^\circ(\text{RbOH}, \text{cr}, 298.15 \text{ K}) = -418.8 \pm 1.5 \text{ kJ mol}^{-1}.$$

This value and the values recommended in other reviews are compared in Table 29.

3.1.3. Appendix. Tables of Experimental and Evaluated Data for $\text{RbOH}(\text{cr})$

TABLE 29. Comparison of the heat capacity, enthalpy, entropy, and enthalpy of formation values for $\text{RbOH}(\text{cr})$ at 298.15 K

Reference	$C_p^\circ(298.15 \text{ K})$ $\text{J K}^{-1} \text{ mol}^{-1}$	$S^\circ(298.15 \text{ K})$ $\text{J K}^{-1} \text{ mol}^{-1}$	$H^\circ(298.15 \text{ K}) - H^\circ(0 \text{ K})$ J mol^{-1}	$\Delta_f H^\circ(298.15 \text{ K})$ kJ mol^{-1}
61DRO	...	83.3
71KRA/FIL	71.1	...	15800	...
79KUB/UNA	57.4
79RIC/VRE	...	81.0
82MED/BER	69 ± 4	92 ± 8	14500 ± 800	-418.7 ± 1.7
82GUR/VEI	69	92 ± 8	14500 ± 1000	-418.8 ± 4.0
82WAG/EVA	-418.19
89KON/COR	-418.8 ± 1.0
Adopted	69 ± 2	94 ± 3	13500 ± 300	-418.8 ± 1.5

TABLE 30. Temperatures of phase transformations of RbOH

Reference	$t_{\text{trs}}/^\circ\text{C}$	T/K	Comments
Original Studies			
10HEV2	245 ± 0.5	518	Thermal analysis
58ROL/COH, 59ROL/COH	235	508	Thermal analysis (DTA)
61COH/MAC	235	508	Thermal analysis (DTA)
67RES/BAR	225	498	Thermal analysis (DTA)
690ST/ITK, 75ITK/POR	235	508	Thermal analysis (DTA)
73PAP/BOU	235 ± 2	508	Thermal analysis (DTA)
73TOU	235 ± 2	508	Thermal analysis
87JAC/MAC	...	265	(rh-monI, $\alpha - \beta$) DSC-method
	...	367	(monI-monII) DSC-method
	...	511	(monII-cub, $\beta - \gamma$) DSC-method
Reviews			
82MED/BER, 82GUR/VEI	...	508 ± 2	Based on several studies
Adopted	...	$265 \pm 3(\alpha - \beta)$	Based on 87JAC/MAC
	...	$508 \pm 3(\beta - \gamma)$	Based on 58ROL/COH, 73TOU, 61COH/MIC, 73PAP/BOU, 75ITK/POR

TABLE 31. Temperature of fusion of RbOH

Reference	$t_{\text{fus}}/^\circ\text{C}$	T_{fus}/K	Comments
Original studies			
10HEV, 10HEV2	301 ± 1	574	Thermal analysis
54BOG	383	656	Thermal analysis
58ROL/COH	380 ± 1	653	Thermal analysis (DTA)
59ROL/COH	382	655	Thermal analysis (DTA)
61COH/MIC	382	655	Thermal analysis (DTA)
67RES/BAR	385 ± 1	658	Thermal analysis (DTA)
69TSE/DOB	380	653	Thermal analysis (DTA)
690ST/ITK, 75ITK/POR	380	653	Thermal analysis (DTA)
71TOU	382 ± 2	655	Thermal analysis (DTA)
87JAC/MAC	...	637	DSC-method
Reviews			
81MED/BER, 82GUR/VEY	...	658 ± 3	Based on [67RES/BAR]
Adopted	...	655 ± 3	Based on eight studies (see text)

TABLE 32. Enthalpy of β - γ transformation of RbOH

Reference	$\Delta_{\text{tr}}H^\circ$, J mol ⁻¹	Comments
Original studies		
10HEV	7120	Thermal analysis (DTA)
67RES/BAR	5400	Thermal analysis (DTA)
87JAC/MAC2	4400	DSC-method
Estimation (this study)	5500	Estimation based on $\Delta_{\text{tr}}S$, see text
Reviews		
82MED/BER,	5400 ± 500	Based on 67RES/BAR
82GUR/VEY		
Adopted	5500 ± 500	Based on estimation, this study

TABLE 33. Enthalpy of fusion of RbOH

Reference	$\Delta_{\text{fus}}H^\circ$, J mol ⁻¹	Comments
Original studies		
10HEV, 10HEV2	6750	Thermal analysis (DTA)
67RES/BAR	8900	Thermal analysis (DTA)
87JAC/MAC	3600	DSC-method
Estimation (this study)	8000	Estimation based on $\Delta_{\text{fus}}S$ (see text)
Reviews		
82MED/BER,	8900 ± 800	Based on 67RES/BAR
82GUR/VEY		
Adopted	8000 ± 1000	Based on estimation in this study

TABLE 34. Differences (J K⁻¹ mol⁻¹) between the thermal functions of RbOH(cr,liq) calculated in the present work and in [82GUR/VEY]

T/K	$\Delta C_p^\circ(T)$	$\Delta \Phi^\circ(T)$	$\Delta S^\circ(T)$
298.15	0.0	5.354	2.000
500	-2.405	3.917	1.432
1000	3.0	2.079	0.443
1500	3.0	1.750	1.659
2000	3.0	1.840	2.523

TABLE 35. Thermodynamic properties at 0.1 MPa: RbOH(cr&liq)

T/K	C_p°	$-[G^\circ - H^\circ(0K)]/T$	S°	$H^\circ - H^\circ(0K)$	$\Delta_f H^\circ$	$\Delta_f G^\circ$
		J K ⁻¹ mol ⁻¹			kJ mol ⁻¹	
0	0.000	0.000	0.000	0.000	-416.237	-416.237
300	69.088	49.001	94.427	13.628	-418.784	-373.592
350	71.471	56.280	105.256	17.142	-420.503	-365.832
400	73.853	63.018	114.955	20.775	-419.897	-358.062
450	76.236	69.287	123.791	24.527	-419.169	-350.375
500	78.618	75.150	131.947	28.398	-418.327	-342.776
508 cr, β	79.000	76.054	133.198	29.029	-418.181	-341.568
508 cr, γ	76.000	76.054	144.025	34.529	-412.681	-341.568
600	76.000	87.473	156.675	41.521	-411.292	-328.808
658 cr, γ	76.000	93.887	163.688	45.929	-410.441	-320.876
658 liq	86.000	93.887	175.846	53.929	-402.441	-320.876
700	86.000	98.966	191.167	57.541	-401.416	-315.702
800	86.000	109.974	192.651	66.141	-399.023	-303.620
900	86.000	119.734	202.780	74.741	-396.697	-291.835
1000	86.000	128.500	211.841	83.341	-466.141	-277.835
1100	86.000	136.455	220.038	91.941	-462.895	-259.163
1200	86.000	143.736	227.521	100.541	-459.687	-240.783
1300	86.000	150.450	234.404	109.141	-456.519	-222.671
1400	86.000	156.677	240.777	117.741	-453.387	-204.799
1500	86.000	162.484	246.711	126.341	-450.293	-187.151
1600	86.000	167.923	252.261	134.941	-447.235	-169.708
1700	86.000	173.039	257.475	143.541	-444.212	-152.455
1800	86.000	177.868	262.391	152.141	-441.224	-135.380
1900	86.000	182.440	267.040	160.741	-438.273	-118.468
2000	86.000	186.781	271.452	169.341	-435.360	-101.713
298.15	69.000	48.721	94.000	13.500	-418.800	-373.871
Uncertainties in Functions						
0	1.500	1.500
300 cr, β	2.000	3.000	3.000	0.300	1.500	1.800
500 cr, β	3.000	4.000	4.000	1.000	1.800	2.500
1000 liq	4.000	6.000	8.000	3.000	3.500	6.000
1500	6.000	8.000	10.000	6.000	6.000	12.000
2000	8.000	10.000	12.000	10.000	10.000	20.000

3.2. Rubidium Hydroxide in Gaseous Phase

3.2.1. Rubidium Hydroxide Monomer

Molecular Constants of RbOH(g)

[53SMI/SUG]

Smith and Sugden estimated the molecular constants of RbOH, assuming a linear model of the molecule with $r(\text{O}-\text{H}) = 0.97 \text{ \AA}$. The value of $r(\text{Rb}-\text{O})$ was taken in the same way as that for the RbO molecules estimated by Brewer and Mastick [49BRE/MAS]. The value of $\nu(\text{Rb}-\text{O})$ was estimated by comparison with the vibrational frequencies for diatomic metal oxides listed by Herzberg [39HER]; the value of $\nu(\text{Rb}-\text{O}-\text{H})$ was calculated in the ionic model approximation.

[58SPI/MAR]

Spinar and Margrave studied IR spectrum of equilibrium vapors over rubidium hydroxide at 690–900 °C and assigned an absorption at 362–368 cm^{-1} to $(\text{RbOH})_x$ where $x = 1$ or 2. The authors [58SPI/MAR] tentatively attributed this absorption to Rb–OH stretching vibration of the linear RbOH molecule and defined $\nu(\text{Rb}-\text{O}) = 365 \pm 20 \text{ cm}^{-1}$.

[66JEN/PAD]

Jensen and Padley estimated molecular constants of RbOH assuming a bent configuration with $\angle(\text{Rb}-\text{O}-\text{H}) = 114^\circ$.

[69ACQ/ABR]

Acquista and Abramowitz observed the IR spectra of RbOH and RbOD isolated in Ar matrix and attributed two strong absorption features at 354.4 and 309.0 cm^{-1} to the Rb–O stretching (ν_1) and Rb–O–H bending (ν_2) fundamentals, respectively, of the RbOH molecule. The assignments were made on the basis of the temperature dependence of the band intensities and on the values of isotopic shifts in conformity with a linear configuration of the molecule.

[69LID/MAT]

Lide and Matsumura applied a new approach to the vibration-rotation interaction in linear triatomic molecules to explain the anomalies found in the microwave spectrum of RbOH [69MAT/LID]. The authors concluded that a linear equilibrium configuration is very probable for all alkali hydroxides. The value $\nu_3 = 3600 \text{ cm}^{-1}$ was assumed for harmonic force field calculation. The refined values of the equilibrium bond lengths were found as $r(\text{Rb}-\text{O}) = 2.301 \pm 0.002 \text{ \AA}$ and $r(\text{O}-\text{H}) = 0.957 \pm 0.01 \text{ \AA}$.

[69MAT/LID]

Matsumura and Lide investigated the microwave spectra of the RbOH and RbOD molecules and observed $J = 2 \rightarrow 3$ as well as some other transitions. The rotational constants of $^{85}\text{RbOH}$ were calculated as $B_0 = 6290.15 \text{ MHz}$ (0.209817 cm^{-1}) and $D_0^\circ = 0.006 \text{ MHz}$ ($2 \cdot 10^{-7} \text{ cm}^{-1}$). Corresponding values of the bond distances of $r(\text{Rb}-\text{O})$ and $r(\text{O}-\text{H})$ (in \AA) were, respectively, 2.316 and 0.913 (from B_0) and 2.305 and 0.965 (from B_e).

[69TIM/KRA]

Timoshinin and Krasnov listed the molecular constants of

linear RbOH using the data [58SPI/MAR] for ν_1 and some estimates.

[70JEN]

Jensen estimated $\nu_3 = 3610 \text{ cm}^{-1}$ for a linear configuration of RbOH and accepted the other molecular constants from literature data.

[71KEL/PAD]

Kelly and Padley accepted the bond lengths and vibrational frequencies of linear RbOH from literature data.

[78BEL] (see also [91BEL2])

Belyaeva investigated IR spectra of RbOH and RBOD, trapped in Ne, Ar, Kr, and Xe matrices at 8 K, in the range 200–4000 cm^{-1} . The spectra was analyzed on the assumption that the rubidium hydroxide molecules are linear. The bands in the Ar matrix at 354.5/352(shoulder) and 310/303/299.5 cm^{-1} were assigned, respectively, to the Rb–O stretching (ν_1) and the Rb–O bending (ν_2) frequencies of RbOH.

[78LOV]

Lovas in the review of microwave spectra recommended the structural parameters of linear RbOH obtained in [69LID/MAT].

[80NEM/STE]

Nemukhin and Stepanov applied the diatomics-in-molecules approach to calculating the ground-state equilibrium geometry and vibrational frequencies of the RbOH molecule. The structure of the molecule was found to be linear. The values of the vibrational frequencies were obtained using two sets of parameters for the potential surface.

[81PIE/BLU]

Pietro *et al.* calculated *ab initio* equilibrium geometry of the RbOH molecule using extended STO-3G minimal basis set.

[82GUR/VEI]

Gurvich with co-workers adopted a linear molecular model for calculating the thermal functions of RbOH(g) and selected the rotational constant B_0 from [69MAT/LID], ν_1 from [69ACQ/ABR], and ν_2 from [78BEL]. The value of ν_3 was estimated as in the other alkali metal hydroxides.

[86BAU/LAN]

Bauschlicher *et al.* calculated *ab initio* the values of $r(\text{Rb}-\text{O})$, $\nu(\text{Rb}-\text{O})$, and $D_0^\circ(\text{Rb}-\text{OH})$ of RbOH in the linear ground electronic state assuming the rigid OH subunit with a fixed O–H bond distance 0.9472 \AA . The calculations were made using both the self-consistence field (SCF) and singles plus doubles configuration (CISD) levels and extended Gaussian basis set of at least triple-zeta plus double polarization quality.

[86LUT/HEM] (see also [82LUT/ECK])

Lutz *et al.* investigated the IR and Raman spectra of solid RbOH and RbOD at 95 and 300 K in the range 200–4000 cm^{-1} and assigned the O–H(D) stretching frequencies of these molecules.

TABLE 36. Bond lengths (Å), angle (deg), and vibrational frequencies (cm⁻¹) of RbOH in the ground electronic state

Reference	$r(\text{Rb-O})$	$r(\text{O-H})$	$\angle(\text{Rb-O-H})$	ν_1	$\nu_2(3)$	ν_3	Note
53SMI/SUG	2.37	0.97	180	350	330	...	a
58SPI/NAR	365	b
66JEN/PAD	2.60	0.86	114	369	1300	3610	c
69ACQ/ABR	180	354.4	309.0	...	d
69LID/MAT	2.301	0.957	180	e
69MAT/LID	2.316	0.913	150	e
69TIM/KRA	2.30	0.97	180	365	375	3740	f
70JEN	2.31	...	150	354	309	3610	g
71KEL/PAD	2.31	0.96	180	354.4	309	3600	g
78BEL	180	354.5	304	...	d
78LOV	2.301	180	g
80NEM/STE	2.39	0.968	180	335	716	3809	h
80NEM/STE	2.39	0.968	180	332	676	3805	i
81PIE/BLU	2.308	1.000	180	j
82GUR/VEI	2.316	0.913	180	354	309	3700	k
86BAU/LAN	2.349	0.9472	180	380	l
86BAU/LAN	2.323	0.9472	180	398	m
86LUT/HEM	180	3598	n
87ALI/VEN	2.301	0.957	180	354	309	3700	g
Adopted in present work	2.316	0.913	180	354	309	3700	k

^aEstimated.

^bIR spectrum of vapor.

^cEstimated for a bent configuration; ν_2 is nondegenerate.

^dIR spectrum in Ar matrix.

^eMicrowave spectrum.

^f ν_1 from [58SPI/MAR]; other constants are estimated.

^gLiterature data.

^hDiatomics-in molecules method; parameters of potential surface are calculated using the [66BUE/PEY] approach.

ⁱDiatomics-in molecules method; parameters of potential surface are calculated using an alternative approach.

^j*Ab initio* STO-3G calculation.

^kBond lengths from [69MAT/LID]; ν_1 and ν_2 from [69ACQ/ABR, 78BEL]; ν_3 estimated.

^lSCF *ab initio* calculation.

^mCI(SD) *ab initio* calculation.

ⁿIR spectrum of solid.

[87AL'VEN]

Al'tman *et al.* in the review of geometry and vibrational frequencies for triatomic molecules recommended the molecular constants of RbOH selected from literature data.

The molecular constants of RbOH, measured, calculated, estimated, or accepted in above-named studies, are given in Table 36.

Discussion of the Molecular Constants of RbOH(g)

Smith and Sugden [53SMI/SUG] were apparently the first who assumed a linear structure for the RbOH molecule and estimated its bond lengths and vibrational frequencies. On the other hand, Jensen and Padley [66JEN/PAD] on analogy with an early JANAF Thermochemical Tables recommendation for KOH adopted $\angle(\text{Rb-O-H}) = 114^\circ$. However, later Jensen [70JEN] revised this point of view, and after the results of microwave investigations [69MAT/LID, 69LID/MAT], adopted a linear configuration of the molecule. Matsuura and Lide [69MAT/LID] obtained experimental evidence of the RbOH linearity from the microwave spectral

investigation. They found that the molecule had an essentially linear structure with a rather low-frequency bending vibration. In the subsequent publication [69LID/MAT] the same authors applied a new formulation of the vibration-rotation interactions in linear triatomic molecules to the microwave data [69MAT/LID] and refined the values of the bond lengths. Theoretical calculations for the Rb-O bond length in the linear molecule [80NEM/STE, 81PIE/BLU, 86BAU/LAN] as well as the estimation [53SMI/SUG] yielded somewhat exaggerated values.

The investigation of IR spectra of RbOH (and RbOD) isolated in Ar matrix was performed by Acquista and Abramowitz [69ACQ/ABR] and Belyaeva [78BEL, 91BEL]. The spectra were interpreted for a linear model of the molecule. The assignments of the Rb-O stretching frequency, ν_1 , and the Rb-O-H bending frequency, ν_2 , are in excellent agreement between both studies. The value of $\nu(\text{Rb-O})$, tentatively attributed by Spinar and Margrave [58SPI/MAR] to the RbOH molecule when investigating IR spectrum of rubidium hydroxide vapor, is consistent within the limits of experimental errors with ν_1 for RbOH according to [69ACQ/ABR, 78BE1, 91BEL]. The theoretically calculated [80NEM/STE, 86BAU/LAN] and estimated [53SMI/SUG, 69TIM/KRA] values of ν_1 and ν_2 are less reliable, though the estimate of ν_1 by Smith and Sugden [53SMI/SUG] is very close to the experimental value. The O-H stretching frequency, ν_3 , of RbOH was observed only in solid state spectra (see, for example, [82LUT/ECK], [86LUT/HEN]). There are several known estimates [69TIM/KRA, 70JEN, 82GUR/VEI, 87ALI/VEN] which predict the value of ν_3 in the range characteristic for this frequency, 3610–3740 cm⁻¹.

The ground electronic state of linear RbOH is $^1\Sigma^+$. Similar to the other alkali metal hydroxides, low-lying excited electronic states of RbOH are not known, nor expected.

A linear configuration of RbOH with $r_o(\text{Rb-O}) = 2.316 \pm 0.002$ and $r_o(\text{O-H}) = 0.913 \pm 0.010$ Å is accepted in the present work according to [69MAT/LID]. The corresponding value of the moment of inertia is $(13.36 \pm 0.02)10^{-39}$ g cm². The values of $\nu_1 = 354 \pm 10$ cm⁻¹ and $\nu_2 = 309 \pm 10$ cm⁻¹ are taken as average of the IR spectral data [69ACQ/ABR, 78BE1, 91BEL] and $\nu_3 = 3700 \pm 100$ cm⁻¹ is estimated.

The molecular constants of RbOH adopted in the present work for calculation of the thermal functions are summarized below:

$$r_o(\text{Rb-O}) = 2.316 \pm 0.002 \text{ \AA}; r_o(\text{O-H}) = 0.913 \pm 0.010 \text{ \AA};$$

$$\angle(\text{Rb-O-H}) = 180^\circ;$$

$$I = (13.36 \pm 0.02)10^{-39} \text{ g/cm}^2;$$

$$\text{symmetry number: } \sigma = 1; \text{ statistical weight: } p_x = 1;$$

$$\nu_1 = 354 \pm 10 \text{ cm}^{-1}, d_1 = 1;$$

$$\nu_2 = 309 \pm 10 \text{ cm}^{-1}, d_2 = 2;$$

$$\nu_3 = 3700 \pm 100 \text{ cm}^{-1}, d_3 = 1.$$

TABLE 37. Differences ($\text{J K}^{-1} \text{mol}^{-1}$) between the thermal functions of RbOH(g) calculated in the present work and in [82GUR/VEI]

T/K	[Present Work]-[82GIUR/VEI] ^a		
	$\Delta C_p^\circ(T)$	$\Delta \Phi^\circ(T)$	$\Delta S^\circ(T)$
298.15	0.001	0.007	0.005
1000	0.001	0.006	0.007
2000	0.001	0.006	0.007
3000	0.001	0.007	0.007
4000	0.001	0.006	0.008
5000	0.001	0.007	0.008
6000	0.001	0.007	0.008

^aThe values of $\Phi^\circ(T)$ and $S^\circ(T)$ tabulated in [82GUR/VEI] are recalculated to standard pressure 0.1 MPa.

Calculation of the RbOH(g) Thermal Functions

The thermal functions of RbOH(g) in the standard state are calculated in the ‘‘rigid rotor–harmonic oscillator’’ approximation with low-temperature quantum corrections according to the equations given in [89GUR/VEY]. The molecular constants of RbOH used in calculating the thermal functions are given in previous subsections. The calculated values of $C_p^\circ(T)$, $\Phi^\circ(T)$, $S^\circ(T)$, and $H^\circ(T) - H^\circ(0)$ in the temperature range 0–6000 K are given in Table 36.

The uncertainties in the calculated thermal functions of RbOH(g) are mainly due to uncertainties in the molecular constants. At high temperatures the uncertainties, because of the approximate method of calculation, become more substantial. These uncertainties are estimated on the basis of the differences between the thermal functions for the linear triatomic molecules (N_2O , CO_2 , CS_2 , OCS , HCN , FCN , and ClCN), calculated in [89GUR/VEY, 91GUR/VEY] in the ‘‘nonrigid rotor –anharmonic oscillator’’ approximation, and those calculated in the ‘‘rigid rotor–harmonic oscillator’’ approximation. Since the value of the constant of centrifugal distortion of RbOH is known [69MAT/LID], it is possible to estimate the corresponding contribution to the thermal functions. It amounts to from 0.001 to $0.1 \text{ J K}^{-1} \text{mol}^{-1}$ in $\Phi^\circ(T)$ at $T = 298.15$ and 6000 K, respectively. The total uncertainties in the thermal functions of RbOH(g) are presented in Table 36.

The thermal functions of RbOH(g) were calculated earlier in [82GUR/VEI] (100–6000 K). Since the molecular constants adopted in the present work are practically identical with those in [82GUR/VEI], the differences between both calculations are negligible (see Table 37) if one takes into consideration different values of standard pressure (1 atm in [82GUR/VEI]).

Enthalpy of Formation of RbOH(g)—Experimental Investigations of Equilibria in Flames

[66JEN/PAD], [70JEN]

Jensen and Padley performed photometric measurements of rubidium hydroxide formation in hydrogen–oxygen–nitrogen flames. The analysis of the suppressed-ionization logarithmic plot of the rubidium resonance doublet emission intensity against $1/T$ was analogous to that for the potassium data but more complicated, since greater proportions of ru-

bidium were present as ions and hydroxide molecules. In addition to photometric measurements, a procedure based on the electron concentration determination was employed to obtain a $[\text{RbOH}]/[\text{Rb}]$ value. The mean value of $[\text{RbOH}]/[\text{Rb}] = 0.38 \pm 0.1$ was finally adopted ($T = 2475 \pm 15 \text{ K}$). This value corresponds to the equilibrium constant value $K^\circ(2475 \text{ K}) = 0.012$ for the reaction



Third-law calculation performed in [66JEN/PAD] using a bent hydroxide molecule model resulted in the value $D_0^\circ(\text{Rb-OH}) = 83 \pm 2 \text{ kcal mol}^{-1}$ ($347 \pm 8 \text{ kJ mol}^{-1}$). Later Jensen [70JEN] calculated the $D_0^\circ(\text{Rb-OH})$ value from the equilibrium data obtained by Jensen and Padley using a linear model of MOH molecules. The results of calculations for both models were close and he finally recommended the value $D_0^\circ(\text{Rb-OH}) = 347 \pm 9 \text{ kJ mol}^{-1}$.

[69COT/JEN]

Cotton and Jenkins determined dissociation energy $D_0^\circ(\text{Rb-OH})$ using atomic absorption spectroscopic measurements of the concentration of rubidium atoms as a function of hydrogen atom concentration in hydrogen-rich, hydrogen–oxygen–nitrogen flames. The mean value $K^\circ(1570 \text{ K}) = 5.3 \cdot 10^{-4}$ was obtained for the equilibrium constant of reaction (6). Third-law calculations were made with the data from JANAF Tables (see [71STU/PRO]) for a bent model of RbOH molecule. The following value of dissociation energy with the total error limit was obtained: $D_0^\circ(\text{Rb-OH}) = 87 \pm 2 \text{ kcal mol}^{-1}$ ($364 \pm 8 \text{ kJ mol}^{-1}$).

[71KEL/PAD]

Kelly and Padley carried out flame photometric studies of Rb emission in $\text{H}_2 + \text{O}_2 + \text{CO}_2$ and $\text{H}_2 + \text{O}_2 + \text{N}_2$ flames in the temperature range 1950–2750 K. To suppress ionization of rubidium atoms, cesium chloride was introduced in flames together with the rubidium salt. Thirty-two values of the equilibrium constant for reaction (6) were obtained. The data in [71KEL/PAD] were presented on the graph. The graph shows pronounced deviation from linearity for 13 points at temperatures exceeding $\approx 2400 \text{ K}$. This deviation was attributed to unsuppressed ionization of rubidium atoms. Kelly and Padley fitted the equilibrium constant values for reaction (6) with the equation

$$K^\circ(T) = A \exp[-\Delta_r H^\circ(2350 \text{ K})/RT],$$

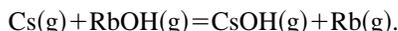
where $\log A = 1.70$, $\Delta_r H^\circ(2350 \text{ K}) = 160 \text{ kJ mol}^{-1}$. They regarded this equation as appropriate to the whole temperature range 1950–2750 K.

From the enthalpy of reaction (6) at the mean temperature of the range, $T = 2350 \text{ K}$, Kelly and Padley calculated the 2nd- and 3rd-law values of dissociation energy $D_0^\circ(\text{Rb-OH})$ for linear and bent models of this molecule (kJ mol^{-1}): 360 ± 12 (2nd law, linear); 362 (3rd law, linear); 352.5 (2nd law, bent); 343 (3rd law, bent). They recommended as the best value $D_0^\circ(\text{Rb-OH}) = 362 \text{ kJ mol}^{-1}$, based on the 2nd- and 3rd-law treatment for the linear model.

Enthalpy of Formation of RbOH(g)—Mass Spectrometric Studies of Equilibria in Flames

[75PAN]

Panchenkov carried out a mass spectrometric measurement of the equilibrium constant for the reaction



From the value $K^\circ(1243 \text{ K}) = 9.01$, the third-law enthalpy for this reaction was calculated: $\Delta_f H^\circ(0 \text{ K}) = -5.1 \pm 2.4 \text{ kcal mol}^{-1}$ ($-21.3 \pm 10 \text{ kJ mol}^{-1}$). Combining this value with the value $D_0^\circ(\text{Cs-OH}) = 90.5 \pm 2 \text{ kcal mol}^{-1}$ selected in the same work [75PAN] as the most reliable, the value $D_0^\circ(\text{Rb-OH}) = 85.4 \pm 3.3 \text{ kcal mol}^{-1}$ ($357.3 \pm 14 \text{ kJ mol}^{-1}$) was obtained. Thermal functions used in the third-law calculation were taken from materials prepared for and later included in the reference book [82GUR/VEI].

Enthalpy of Formation of RbOH(g)—Ab Initio Calculation

[86BAU/LAN]

Bauschlicher *et al.* calculated dissociation energies of the alkali hydroxide molecules MOH into M^+ and OH^- ions by *ab initio* methods. As the “best,” Bauschlicher *et al.* have chosen the value $D_0^\circ(\text{Rb-OH}) = 3.58 \pm 0.10 \text{ eV}$ ($345 \pm 10 \text{ kJ mol}^{-1}$) obtained from the value $D_e(\text{Rb-OH}) = 3.60 \text{ eV}$ (CI(SD) level) with zero-point correction taken equal to -0.06 eV and a correction of 0.04 eV based upon the errors in the computed bond lengths. The computed bond lengths were larger than those experimentally determined and the bond energies turned out to be slightly underestimated.

Discussion of the Enthalpy of Formation of RbOH(g)

The authors of this review have recalculated all equilibria from the papers previously discussed with the thermal func-

tions from this work and with auxiliary data from [82GUR/VEI] and [89GUR/VEY]. The recalculated values of enthalpies of reactions and the values of enthalpy of formation of RbOH(g) are collected in Table 38. The mean value from all data presented is $\Delta_f H^\circ(\text{RbOH,g}, 0 \text{ K}) = -232.7 \pm 5 \text{ kJ mol}^{-1}$. The value $D_0^\circ(\text{Rb-OH}) = 356.0 \pm 5 \text{ kJ mol}^{-1}$ corresponds to this enthalpy of formation. In contrast to other alkali hydroxides, in the case of rubidium the data for the equilibria between condensed and gaseous phase are lacking. Under these circumstances, it appears expedient to draw additional information for obtaining the most reliable enthalpy of formation. In particular, it is helpful to compare dissociation energies of alkali hydroxides and related alkali halides. The comparison shows that (i) $D_0^\circ(\text{M-OH})$ values are systematically lower than $D_0^\circ(\text{M-F})$ for approximately constant amount for all alkali metals [89GOR/MIL]; (ii) $D_0^\circ(\text{Rb-F})$ and $D_0^\circ(\text{Rb-Cl})$ values are several kJ mol^{-1} lower than $D_0^\circ(\text{K-F})$ and $D_0^\circ(\text{K-Cl})$. *Ab initio* calculations [86BAU/LAN] support these observations. Using the value $D_0^\circ(\text{K-OH}) = 357 \text{ kJ mol}^{-1}$ corresponding to the adopted value for KOH(g) enthalpy of formation the value $D_0^\circ(\text{Rb-OH}) = 355 \pm 5 \text{ kJ mol}^{-1}$ is selected as the most satisfactory choice conforming to regularities described. It is very close to the mean value $D_0^\circ(\text{Rb-OH}) = 356 \text{ kJ mol}^{-1}$. The following enthalpies of formation correspond to the selected value: $\Delta_f H^\circ(\text{RbOH,g}, 0 \text{ K}) = -233.7 \pm 5 \text{ kJ mol}^{-1}$; $\Delta_f H^\circ(\text{RbOH,g}, 298.15 \text{ K}) = -238.0 \pm 5 \text{ kJ mol}^{-1}$.

On the basis of the above discussion, the values

$$\Delta_f H^\circ(\text{RbOH,g}, 298.15 \text{ K}) = -238.0 \pm 5 \text{ kJ mol}^{-1};$$

$$D_0^\circ(\text{Rb-OH}) = 355 \pm 5 \text{ kJ mol}^{-1}$$

are adopted in this review.

3.2.2. Appendix. Tables of Experimental and Evaluated Data for RbOH(g)

TABLE 38. Results of determination of $\Delta_f H^\circ(\text{RbOH,g}, 0 \text{ K})$, kJ mol^{-1}

Reference	Method	$\Delta_f H^\circ(0 \text{ K})$		$\Delta_f H^\circ(0 \text{ K})$
		2nd law	3rd law	
[66JEN/PAD]	Flame photometry, $\text{Rb(g)} + \text{H}_2\text{O(g)} = \text{RbOH(g)} + \text{H(g)}$, 2475 K (one point)	...	145.0 ± 8	-227.8 ± 8
[69COT/JEN]	Flame photometry, $\text{Rb(g)} + \text{H}_2\text{O(g)} = \text{RbOH(g)} + \text{H(g)}$, 1570 K (six points)	...	124.5 ± 6	-248.3 ± 6
[71KEL/PAD]	Flame photometry, $\text{Rb(g)} + \text{H}_2\text{O(g)} = \text{RbOH(g)} + \text{H(g)}$, 1950–2750 K (32 points)	...	133.6 ± 6	-239.2 ± 6
[75PAN]	Knudsen effusion mass spectrometry, $\text{Cs(g)} + \text{RbOH(g)} = \text{CsOH(g)} + \text{Rb(g)}$, 1243 K, (one point)	...	-31.8 ± 10	-224.3 ± 10
[86BAU/LAN]	<i>Ab initio</i> calculation, $\text{RbOH(g)} = \text{Rb(g)} + \text{OH(g)}$...	345 ± 10	-224 ± 10

TABLE 39. Thermodynamic properties at 0.1 MPa: RbOH(g)

T/K	C_p°	$-[G^\circ - H^\circ(0K)]T$	S°	$H^\circ - H^\circ(0K)$	$\Delta_f H^\circ$	$\Delta_f G^\circ$
	J K ⁻¹ mol ⁻¹			kJ mol ⁻¹		
0	0.000	0.000	0.000	0.000	-233.697	-233.697
25	29.101	131.053	160.120	0.727	-233.825	-235.102
50	29.314	151.210	180.317	1.455	-234.420	-236.172
75	31.098	163.055	192.471	2.206	-235.083	-236.902
100	34.388	171.617	201.849	3.023	-235.633	-237.502
150	40.925	184.331	217.088	4.914	-236.445	-238.126
200	45.265	194.121	229.507	7.077	-237.033	-238.594
250	47.912	202.268	239.916	9.412	-237.525	-238.925
300	49.569	209.302	248.809	11.852	-238.020	-239.142
350	50.654	215.510	256.537	14.359	-240.746	-239.023
400	51.398	221.073	263.353	16.912	-241.220	-238.744
450	51.930	226.115	269.439	19.496	-241.660	-238.408
500	52.330	230.726	274.932	22.103	-242.082	-238.024
600	52.914	238.916	284.527	27.367	-242.906	-237.134
700	53.379	246.032	292.720	32.682	-243.735	-236.108
800	53.823	252.324	299.876	38.042	-244.582	-234.960
900	54.281	257.968	306.242	43.447	-245.451	-233.706
1000	54.756	263.087	311.986	48.898	-318.044	-229.882
1100	55.238	267.774	317.227	54.398	-317.898	-221.074
1200	55.716	272.099	322.054	59.946	-317.742	-212.278
1300	56.179	276.116	326.532	65.541	-317.579	-203.496
1400	56.621	279.868	330.712	71.181	-317.407	-194.726
1500	57.036	283.390	334.632	76.864	-317.230	-185.970
1600	57.422	286.709	338.326	82.587	-317.049	-177.226
1700	57.780	289.849	341.818	88.348	-316.865	-168.492
1800	58.108	292.829	345.130	94.142	-316.683	-159.770
1900	58.410	295.665	348.280	99.968	-316.506	-151.056
2000	58.685	298.371	351.283	105.823	-316.338	-142.353
2200	59.168	303.440	356.900	117.610	-316.036	-124.968
2400	59.570	308.114	362.066	129.485	-315.807	-107.610
2600	59.908	312.450	366.848	141.434	-315.683	-90.265
2800	60.192	316.496	371.298	153.445	-315.693	-72.928
3000	60.432	320.290	375.459	165.508	-315.866	-55.582
3200	60.636	323.861	379.366	177.615	-316.233	-38.221
3400	60.811	327.236	383.047	189.760	-316.820	-20.829
3600	60.961	330.434	386.528	201.937	-317.654	-3.391
3800	61.091	333.474	389.827	214.143	-318.759	14.093
4000	61.205	336.370	392.964	226.373	-320.156	31.649
4200	61.304	339.137	395.952	238.624	-321.869	49.282
4400	61.391	341.785	398.806	250.894	-323.915	66.997
4600	61.468	344.324	401.537	263.180	-326.306	84.822
4800	61.537	346.763	404.154	275.480	-329.046	102.753
5000	61.598	349.109	406.668	287.794	-332.142	120.804
5200	61.652	351.369	409.085	300.119	-335.587	138.997
5400	61.701	353.550	411.412	312.455	-339.376	157.318
5600	61.746	355.657	413.657	324.799	-343.488	175.788
5800	61.785	357.695	415.825	337.153	-347.909	194.404
6000	61.822	359.668	417.920	349.513	-352.606	213.185
298.15	49.520	209.058	248.502	11.760	-238.000	-239.135
Uncertainties in Functions						
0	5.000	5.000
300	0.300	0.400	0.700	0.150	5.000	5.000
1000	0.500	0.700	1.000	0.300	5.000	5.000
2000	1.000	0.800	1.300	1.000	5.000	5.000
3000	1.500	1.000	1.700	2.000	6.000	5.000
4000	2.000	1.200	2.000	3.000	6.000	6.000
5000	2.500	1.400	2.500	5.500	8.000	8.000
6000	3.000	1.700	3.000	8.500	10.000	10.000

3.2.3. Rubidium Hydroxide Dimer

Molecular Constants of [RbOH]₂(g)

[58SPI/MAR]

Spinar and Margrave studied the IR spectrum of equilibrium vapors over rubidium hydroxide at 690–900 °C and assigned an absorption at 362–368 cm⁻¹ to (RbOH)_x where x = 1 or 2. The authors [58SPI/MAR] tentatively ascribed this absorption to the Rb–OH stretching vibration of the linear monomer.

[59SCH/POR]

Schoonmaker and Porter assumed that the Rb₂O₂H₂ molecule was of a square planar configuration without hydrogen bonding but did not exclude a nonplanar model.

[67BUE/STA]

Buechler *et al.* studied the deflection of sodium and cesium molecular beams in an inhomogeneous electric field and found that the Na₂O₂H₂ and Cs₂O₂H₂ molecules are nonpolar. This indicated that at least the M₂O₂ part of the dimeric molecules should be planar. In the authors' opinion, it was likely that the alkali hydroxide dimers from sodium to cesium have a planar rhomboid configuration in analogy to lithium halide dimers.

[69ACQ/ABR]

Acquista and Abramowitz observed the IR spectra of RbOH and RbOD trapped in the Ar matrix and detected two strong absorption features at 285 and 299.5 cm⁻¹. These features were presumably ascribed to polymeric species of rubidium hydroxide, but the authors [69ACQ/ABR] could not make definite assignments.

[78BEL] (see also [91BEL])

Belyaeva investigated IR spectra of Rb₂O₂H₂ and Rb₂O₂D₂ in inert gas matrices at 8 K in the range 50–4000 cm⁻¹. The analysis of the spectra was made on the assumption of a planar rhomboid configuration (D_{2h} symmetry) of the rubidium hydroxide dimer.

Taking into account the isotopic shifts and the spectral data obtained in different inert matrices and for the other alkali hydroxide dimers, Belyaeva assigned the observed bands to five fundamentals of Rb₂O₂H₂. The assignments are the following: one out-of-plane bending and two in-plane stretching vibrations of Rb–O–Rb–O ring, ν_7 (99/92 cm⁻¹), ν_{10} (247.5/241 cm⁻¹), and ν_{12} (253.5 cm⁻¹), and two out-of-plane and in-plane bending O–H vibrations, ν_6 (278 cm⁻¹) and ν_9 (284.5 cm⁻¹). The ionic model calculation of vibrational frequencies confirmed the assignment and resulted in the equilibrium structural parameters $r_e(\text{Rb–O}) = 2.50 \text{ \AA}$ and $\angle(\text{O–Rb–O}) = 93^\circ$.

[82GUR/VEI]

Gurvich with co-workers accepted for Rb₂O₂H₂ a planar rhomboid configuration of D_{2h} symmetry with equilibrium structural parameters $r_e(\text{Rb–O})$ and $\angle(\text{O–Rb–O})$ calculated by Belyaeva [78BEL] using the ionic model approximation. The vibrational frequencies ν_6 , ν_7 , ν_9 , ν_{10} , and ν_{12} were taken from the IR spectral data [78BEL]. The adopted values of ν_2 – ν_5 and ν_8 were calculated in [78BEL] using the ionic

model. The values of $r(\text{O–H})$, ν_1 , and ν_{11} were estimated in [82GUR/VEI].

[89GIR/LAP]

On the basis of the data on $r_e(\text{M–O})$ obtained for K₂O₂H₂ and Cs₂O₂H₂ from electron diffraction investigation, Girichev and Lapshina estimated $r_e(\text{Rb–O}) = 2.52 \text{ \AA}$ for Rb₂O₂H₂ of planar D_{2h} configuration.

[90GIR/LAP] (see also [89LAP])

Girichev *et al.* investigated saturated rubidium hydroxide vapor at 873 ± 10 K by the electron diffraction method. The least-square analysis of the experimental function $s(M)S$ was carried out accepting the molecular constants of RbOH obtained in the spectral studies [69LID/MAT, 69ACQ/ABR, 78BEL] and assuming a planar D_{2h} configuration for the Rb₂O₂H₂ molecule. The following effective structural parameters of Rb₂O₂H₂ were found (the bond lengths r_g and vibrational amplitudes l_g values are in Å): $r_g(\text{Rb–O}) = 2.49$ (2), $l_g(\text{Rb–O}) = 0.14$ (1), $r_g(\text{Rb–Rb}) = 3.73$ (3), $l_g(\text{Rb–Rb}) = 0.21$ (2), $r_g(\text{O–O}) = 2.59$ (43), $l_g(\text{O–O}) = 0.21$ (1), $r_g(\text{Rb–H}) = 3.10$ (33), and $l_g(\text{Rb–H}) = 0.34$ (2). Combined analysis of their electron diffraction data and spectral data [78BEL] in the harmonic force field approximation resulted in the values of the equilibrium structural parameters $r_e(\text{Rb–O}) = 2.50$ (2) Å, $\angle(\text{O–Rb–O}) = 83$ (2)°, and six vibrational frequencies of the Rb₂O₂ part of the Rb₂O₂H₂ molecule.

The molecular constants of Rb₂O₂H₂, measured, calculated, estimated, or accepted in abovenamed studies, are listed in Table 40.

Discussion of the Molecular Constants of [RbOH]₂(g)

Schoonmaker and Porter [59SCH/POR] assumed for the Rb₂O₂H₂ molecule a square planar model without hydrogen bonding, but did not exclude a nonplanar configuration. According to Buechler *et al.* [67BUE/STA], the Rb₂O₂H₂ molecule, like the other dimers of alkali metal hydroxides, should have a planar rhomboid configuration. That was confirmed by Belyaeva [78BEL, 91BEL] in analysis of IR spectra in Ar matrix and by Girichev with co-workers [89LAP, 90GIR/LAP] in electron diffraction measurements.

Structural parameters of Rb₂O₂H₂, reported by Girichev with co-workers [89LAP, 90GIR/LAP] on the basis of electron diffraction measurements in vapor, contain an obvious inconsistency. The values of $r(\text{Rb–H})$, $r(\text{Rb–Rb})$, and $r(\text{O–O})$, obtained in these studies, yield $r(\text{O–H})$ about 1.2 Å which is unusually large for a D_{2h} configuration without hydrogen bonding. The values of $r(\text{Rb–Rb})$ and $r(\text{O–O})$, obtained in [89LAP, 90GIR/LAP], actually result in $\angle(\text{O–Rb–O}) = 69.5^\circ$ and $r(\text{Rb–O}) = 2.27 \text{ \AA}$ instead of 83° and 2.49 Å, respectively, according to [89LAP, 90GIR/LAP]. Similar to the other alkali hydroxide dimers, the Rb₂O₂H₂ molecule has 12 nondegenerate vibrational frequencies. Five of six frequencies of Rb₂O₂H₂, active in IR spectrum, were assigned to ν_6 , ν_7 , ν_9 , ν_{10} , and ν_{12} by Belyaeva [78BEL, 91BEL] in Ar matrix spectrum. In addition, Belyaeva [78BEL] carried out the ionic model calculation and obtained the frequencies of Rb₂O₂H₂ (except ν_1 and

TABLE 40. Bond lengths (Å), angles (deg), and vibrational frequencies (cm⁻¹) of Rb₂O₂H₂ in the ground electronic state

Constant	[78BEL] ^a	[78BEL] ^b	[82GUR/VEI] ^c	[891AP,90GIR/LAP] ^d	Adopted in present work ^e
<i>r</i> (Rb–O)	...	2.50	2.50	2.49	2.49
<i>r</i> (Rb–Rb)	3.73	...
<i>r</i> (O–O)	2.59	...
<i>r</i> (Rb–H)	3.10	...
<i>r</i> (O–H)	0.97	...	0.97
<(O–Rb–O)	...	93	93	83	90
ν_1	3700	...	3700
ν_2	...	306	306	265	300
ν_3	...	111	111	92	110
ν_4	...	290	290	...	290
ν_5	...	218	218	269	220
ν_6	278	308	278	...	278
ν_7	96	106	100	98	96
ν_8	...	296	295	...	290
ν_9	284.5	290	284	...	284.5
ν_{10}	244	251	244	267	244
ν_{11}	3700	...	3700
ν_{12}	253.5	279	253	274	253.5
Symmetry	D _{2h}	D _{2h}	D _{2h}	D _{2h}	D _{2h}

^aIR spectrum in Ar matrix.^bIonic model calculation.^c ν_6 , ν_7 , ν_9 , ν_{10} and ν_{12} from IR spectrum in Ar matrix [78BEL]; *r*_c (Rb–O), < (O–Rb–O), and ν_2 - ν_5 , ν_8 from ionic model calculation [78BEL]; *r*(O–H) and ν_1 , ν_{11} estimated.^dElectron diffraction in gas; *r*_g structure; frequencies from combined analysis of electron diffraction data and IR spectral data in Ar matrix [78BEL].^e ν_6 , ν_7 , ν_9 , ν_{10} and ν_{12} from IR spectrum in Ar matrix [78BEL, 91BEL]; and ν_2 - ν_5 , ν_8 from ionic model calculation [78BEL]; *r*(Rb–O), < (O–Rb–O), *r*(O–H) and ν_1 , ν_{11} estimated.

ν_{11} , the O–H stretching frequencies) which are in agreement with experimental ones. Six frequencies, belonging to Rb₂O₂H₂ part (ν_2 , ν_3 , ν_5 , ν_7 , ν_{10} , and ν_{12}), were evaluated by Girichev with co-workers [89LAP, 90GIR/LAP] from combined analysis of their electron diffraction data and IR spectral data [78BEL]. However, because of the above-mentioned inconsistency in their results of their structural analysis, these values of frequencies are scarcely reliable, though they are not in disagreement with those obtained in [78BEL] except the value of ν_5 (269 cm⁻¹). By the way, in their earlier investigations of K₂O₂H₂ and Cs₂O₂H₂, Girichev and co-workers recognized that the values of ν_5 calculated for these molecules were overestimated and recommended lower values.

Two bands at 285 and 299.5 cm⁻¹ in IR spectra of rubidium hydroxide isolated in Ar matrix, observed by Acquista and Abramowitz [69ACQ/ABR] and presumably ascribed to polymeric species, can be possibly assigned to ν_6 and ν_9 of Rb₂O₂H₂.

The band at 362–268 cm⁻¹, observed by Spinar and Margrave [58SPI/NAR] and tentatively assigned to ν (Rb–O), probably did not belong to dimer.

There are no data on any excited electronic states of Rb₂O₂H₂, nor are any expected.

A planar rhomboid configuration of D_{2h} symmetry is adopted for Rb₂O₂H₂ in the present work. The adopted structural parameters *r*(Rb–O) = 2.49 Å and < (O–Rb–) = 90°

are based on the results of the electron diffraction data [89LAP, 89GIR/LAP, 90GIR/LAP] and the ionic model calculations [78BEL, 91BEL]. The values of ν_6 , ν_7 , ν_9 , ν_{10} , and ν_{12} are taken from the analysis of IR spectra in Ar matrix [78BEL, 91BEL]. The vibrational frequencies ν_2 – ν_5 and ν_8 are taken from the results of the ionic model calculation by Belyaeva [78BEL]. The values of *r*(OH), ν_1 , and ν_{11} are estimated. The uncertainties in the molecular constants of Rb₂O₂H₂ can be estimated as 0.05 Å and 0.03 Å in *r*(Rb–O) and *r*(O–H), respectively, 10° in < (O–Rb–O), 10 cm⁻¹ in experimental values, 20 cm⁻¹ in calculated probably did values, and 100 cm⁻¹ in estimated values of frequencies.

The molecular constants of Rb₂O₂H₂ (D_{2h} symmetry) adopted in the present work for calculation of the thermal functions are summarized below:

$$r(\text{Rb-O}) = 2.49 \pm 0.05 \text{ \AA}; \quad r(\text{O-H}) = 0.97 \pm 0.03 \text{ \AA};$$

$$\angle(\text{O-Rb-O}) = 90 \pm 10^\circ;$$

$$I_A I_B I_C = (1.8 \pm 0.3) 10^{-112} \text{ g}^3 \text{ cm}^6;$$

$$\text{symmetry number: } \sigma = 4; \text{ statistical weight: } p_x = 1;$$

$$\nu_1 = 3700 \pm 100 \text{ cm}^{-1}, \quad d_1 = 1;$$

$$\nu_2 = 300 \pm 20 \text{ cm}^{-1}, \quad d_2 = 1;$$

TABLE 41. Differences ($\text{J K}^{-1} \text{mol}^{-1}$) between the thermal functions of $\text{Rb}_2\text{O}_2\text{H}_2(\text{g})$ calculated in the present work and in [82GUR/VEI]

T/K	[Present Work]-[82GUR/VEI] ^a		
	$\Delta C_p^\circ(T)$	$\Delta \Phi^\circ(T)$	$\Delta S^\circ(T)$
298.15	0.092	0.422	0.601
1000	0.011	0.572	0.647
2000	0.004	0.611	0.652
3000	0.002	0.625	0.653
4000	0.002	0.633	0.654
5000	0.002	0.637	0.655
6000	0.002	0.640	0.654

^aThe values of $\Phi^\circ(T)$ and $S^\circ(T)$ tabulated in [82GUR/VEI] are recalculated to standard pressure 0.1 MPa.

$$\nu_3 = 110 \pm 20 \text{ cm}^{-1}, d_3 = 1;$$

$$\nu_4 = 290 \pm 20 \text{ cm}^{-1}, d_4 = 1;$$

$$\nu_5 = 220 \pm 20 \text{ cm}^{-1}, d_5 = 1;$$

$$\nu_6 = 278 \pm 10 \text{ cm}^{-1}, d_6 = 1;$$

$$\nu_7 = 96 \pm 10 \text{ cm}^{-1}, d_7 = 1;$$

$$\nu_8 = 290 \pm 20 \text{ cm}^{-1}, d_8 = 1;$$

$$\nu_9 = 284.5 \pm 10 \text{ cm}^{-1}, d_9 = 1;$$

$$\nu_{10} = 244 \pm 10 \text{ cm}^{-1}, d_{10} = 1;$$

$$\nu_{11} = 3700 \pm 100 \text{ cm}^{-1}, d_{11} = 1;$$

$$\nu_{12} = 253.5 \pm 10 \text{ cm}^{-1}, d_{12} = 1.$$

Calculation of the $[\text{RbOH}]_2(\text{g})$ Thermal Functions

The thermal functions of $\text{Rb}_2\text{O}_2\text{H}_2(\text{g})$ in the standard state are calculated in the "rigid rotor-harmonic oscillator" approximation with the low-temperature quantum corrections according to the equations given in [89GUR/VEY]. The molecular constants of $\text{Rb}_2\text{O}_2\text{H}_2$ used in the calculation are given in previous subsections. The calculated values of $C_p^\circ(T)$, $\Phi^\circ(T)$, $S^\circ(T)$, and $H^\circ(T) - H^\circ(0)$ at the temperatures 0–6000 K are given in Table 43.

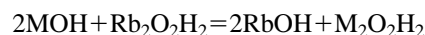
The uncertainties in the calculated thermal functions of $\text{Rb}_2\text{O}_2\text{H}_2(\text{g})$ arise from the uncertainties of the adopted molecular constants; the calculated vibrational frequencies and the angle $\angle(\text{O}-\text{Rb}-\text{O})$. At high temperatures the uncertainties due to the approximate method of calculation become more substantial. These uncertainties are roughly estimated taking into consideration the uncertainties in the thermal functions for monomers. The total uncertainties in the thermal function of $\text{Rb}_2\text{O}_2\text{H}_2(\text{g})$ are presented in Table 43.

The thermal functions of $\text{Rb}_2\text{O}_2\text{H}_2$ were calculated earlier in [82GUR/VEI] (100–6000 K). The data presented in that reference book and calculated in the present work (see Table 41) are in good agreement because the molecular constants, used in both calculations, practically coincide.

Enthalpy of Formation of $[\text{RbOH}]_2(\text{g})$ —Experimental Investigations

[59SCH/POR]

Schoonmaker and Porter carried out a mass spectrometric study of alkali hydroxide binary mixtures with the aim to obtain differences in dimerization; enthalpies of pairs of hydroxides. A silver effusion cell was used in experiments with rubidium hydroxide. The measurements of the equilibrium constants for the gaseous reaction



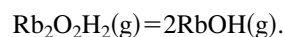
were performed for $\text{M} = \text{Na}, \text{K},$ and Cs at temperatures 823 K, 774–790 K, and 673 K, respectively. The following differences in dimerization enthalpies were obtained from the third-law treatment of data:

$$\begin{aligned} &\Delta_r H^\circ(\text{NaOH}) - \Delta_r H^\circ(\text{RbOH}) \\ &= 10.5 \pm 0.7 \text{ kcal mol}^{-1} (43.9 \pm 3 \text{ kJ mol}^{-1}); \\ &\Delta_r H^\circ(\text{KOH}) - \Delta_r H^\circ(\text{RbOH}) \\ &= 3.0 \pm 0.2 \text{ kcal mol}^{-1} (12.6 \pm 0.8 \text{ kJ mol}^{-1}); \\ &\Delta_r H^\circ(\text{RbOH}) - \Delta_r H^\circ(\text{CsOH}) \\ &= 4.5 \pm 0.3 \text{ kcal mol}^{-1} (18.8 \pm 1.3 \text{ kJ mol}^{-1}). \end{aligned}$$

Estimated values of entropies of dimerization were used in calculations. From all data obtained, Schoonmaker and Porter selected the dimerization enthalpy $\Delta_r H^\circ(\text{RbOH}) = -45 \pm 5 \text{ kcal mol}^{-1}$ ($-188 \pm 20 \text{ kJ mol}^{-1}$).

[90GIR/LAP]

Girichev, Lapshina, and Tumanov carried out an investigation of $\text{Rb}_2\text{O}_2\text{H}_2(\text{g})$ structure by the method of electron diffraction. In the process of refining of the theoretical molecular scattering intensity curve $sM(s)$ they obtained the best agreement between theoretical and experimental curves for the dimer relative concentration of $45_{-14}^{+50} \text{ mol } \%$, or $P(\text{d})/P(\text{m}) = 0.82$ ($T = 873 \pm 10 \text{ K}$). Combining the geometry data obtained from electron diffraction and vibrational frequencies from spectroscopic data for $\text{Rb}_2\text{O}_2\text{H}_2(\text{g})$, the authors calculated the third-law enthalpy $\Delta_r H^\circ(0 \text{ K}) = 159_{-14}^{+41} \text{ kJ mol}^{-1}$ for the reaction



An estimated value of the total vapor pressure of rubidium hydroxide was used in the calculation.

Discussion of the Enthalpy of Formation of $[\text{RbOH}]_2(\text{g})$

The authors of this review have recalculated equilibria from the papers previously discussed with the thermal functions from this work and with auxiliary data from [82GUR/VEI] and [89GUR/VEY]. The recalculated values of enthalpies of reactions and the values of enthalpy of formation of $\text{Rb}_2\text{O}_2\text{H}_2(\text{g})$ are presented in Table 42. The data [59SCH/POR] for the $\text{KOH}-\text{RbOH}$ and $\text{CsOH}-\text{RbOH}$ systems appear to be the most reliable. Taking into account more accurate values of the enthalpy of formation for potassium hydroxide monomer and dimer, a weighted mean value

$\Delta_f H^\circ(\text{Rb}_2\text{O}_2\text{H}_2, \text{g}, 0 \text{ K}) = -630 \pm 10 \text{ kJ mol}^{-1}$ is selected. The value $\Delta_f H^\circ(\text{Rb}_2\text{O}_2\text{H}_2, \text{g}, 298.15 \text{ K}) = -639 \pm 10 \text{ kJ mol}^{-1}$ corresponds to the selected one.

In the case of the NaOH–RbOH system, a substantially more negative value of enthalpy of formation was obtained, analogously to the NaOH–KOH system. Data [90GIR/LAP] cannot be regarded as reliable due to uncertainty in estimation of the total vapor pressure of rubidium hydroxide and large error limits.

On the basis of the above discussion the value

$$\Delta_f H^\circ(\text{Rb}_2\text{O}_2\text{H}_2, \text{g}, 298.15 \text{ K}) = -639 \pm 10 \text{ kJ mol}^{-1}$$

is adopted in this review.

3.2.4. Appendix. Tables of Experimental and Evaluated Data for $[\text{RbOH}]_2(\text{g})$

TABLE 42. Results of determination of $\Delta_f H^\circ(\text{Rb}_2\text{O}_2\text{H}_2, \text{g}, 0 \text{ K})$, kJ mol^{-1}

Reference	Method	$\Delta_f H^\circ(0 \text{ K})$		
		2nd law	3rd law	$\Delta_f H^\circ(0 \text{ K})$
[59SCH/POR]	Knudsen effusion mass spectrometry, $2\text{NaOH}(\text{g}) + \text{Rb}_2\text{O}_2\text{H}_2(\text{g}) = 2\text{RbOH}(\text{g}) + \text{Na}_2\text{O}_2\text{H}_2(\text{g})$, 823 K (three points)	...	-52.1 ± 6	-654 ± 20
	$2\text{KOH}(\text{g}) + \text{Rb}_2\text{O}_2\text{H}_2(\text{g}) = 2\text{RbOH}(\text{g}) + \text{K}_2\text{O}_2\text{H}_2(\text{g})$, 774–790 K (three points)	...	-12.9 ± 4	-631 ± 8
	$2\text{RbOH}(\text{g}) + \text{Cs}_2\text{O}_2\text{H}_2(\text{g}) = 2\text{CsOH}(\text{g}) + \text{Rb}_2\text{O}_2\text{H}_2(\text{g})$, 673 K (three points)	...	-18.1 ± 5	-628 ± 12
[90GIR/LAP]	Electron diffraction, $\text{Rb}_2\text{O}_2\text{H}_2(\text{g}) = 2\text{RbOH}(\text{g})$, 873 K	...	159 +41 –14	–626 +41 –14

TABLE 43. Thermodynamic properties at 0.1 MPa: $\text{Rb}_2\text{O}_2\text{H}_2(\text{g})$

T/K	C_p°	$-[G^\circ - H^\circ(0\text{K})/T]$	S°	$H^\circ - H^\circ(0 \text{ K})$	$\Delta_f H$	$\Delta_f G^\circ$
	$\text{J K}^{-1} \text{ mol}^{-1}$			kJ mol^{-1}		
0	0.000	0.000	0.000	0.000	–630.281	–630.281
25	34.881	169.291	202.823	0.838	–631.153	–630.770
50	43.637	193.233	229.471	1.812	–632.825	–629.771
75	55.975	208.719	249.401	3.051	–634.414	–627.886
100	68.929	221.158	267.311	4.615	–635.584	–625.683
150	87.747	241.997	299.169	8.576	–637.028	–620.140
200	98.127	259.740	325.983	13.249	–637.857	–614.375
250	103.957	275.309	348.564	18.314	–638.447	–608.431
300	107.453	289.166	367.852	23.606	–639.025	–602.340
350	109.686	301.629	384.596	29.038	–644.059	–595.646
400	111.191	312.940	399.347	34.563	–644.587	–588.693
450	112.258	323.285	412.508	40.150	–645.048	–581.677
500	113.053	332.811	424.379	45.784	–645.472	–574.614
600	114.207	349.849	445.099	57.150	–646.282	–560.366
700	115.125	364.749	462.774	68.618	–647.103	–545.983
800	116.004	377.987	478.204	80.174	–647.960	–531.478
900	116.912	389.898	491.920	91.819	–648.863	–516.864
1000	117.855	400.728	504.286	103.558	–793.213	–497.205
1100	118.815	410.663	515.564	115.391	–792.088	–467.661
1200	119.767	419.843	525.943	127.320	–790.942	–438.217
1300	120.691	428.379	535.566	139.344	–789.783	–408.871
1400	121.572	436.359	544.543	151.457	–788.606	–379.611
1500	122.400	443.855	552.959	163.656	–787.419	–350.440
1600	123.171	450.924	560.884	175.935	–786.223	–321.349
1700	123.884	457.615	568.372	188.288	–785.025	–292.329
1800	124.541	463.967	575.472	200.710	–783.827	–263.383
1900	125.142	470.014	582.222	213.195	–782.640	–234.498
2000	125.693	475.787	588.655	225.737	–781.471	–205.683
2200	126.656	486.602	600.682	250.975	–779.203	–148.211
2400	127.461	496.576	611.738	276.389	–777.081	–90.942
2600	128.135	505.833	621.968	301.950	–775.170	–33.843
2800	128.702	514.472	631.485	327.636	–773.527	23.114
3000	129.181	522.573	640.381	353.425	–772.210	79.969
3200	129.589	530.199	648.732	379.303	–771.279	136.746
3400	129.939	537.405	656.599	405.257	–770.789	193.483
3600	130.239	544.236	664.034	431.276	–770.792	250.205
3800	130.499	550.728	671.083	457.350	–771.340	306.935
4000	130.726	556.915	677.783	483.473	–772.471	363.710
4200	130.924	562.823	684.166	509.639	–774.234	420.571
4400	131.099	568.479	690.261	535.841	–776.663	477.507
4600	131.253	573.901	696.092	562.077	–779.782	534.592
4800	131.390	579.110	701.681	588.341	–783.597	591.815
5000	131.512	584.121	707.047	614.632	–788.126	649.205
5200	131.621	588.948	712.207	640.945	–793.353	706.814
5400	131.718	593.606	717.176	667.279	–799.269	764.617
5600	131.807	598.105	721.968	693.632	–805.829	822.660
5800	131.886	602.457	726.595	720.001	–813.009	880.932
6000	131.959	606.670	731.067	746.386	–820.739	939.479
298.15	107.351	288.680	367.188	23.407	–639.000	–602.566
Uncertainties in Functions						
0	10.000	10.000
300	1.000	1.500	2.000	0.200	10.000	10.000
1000	2.000	2.000	3.000	1.000	10.000	10.000
2000	3.000	3.000	4.000	5.000	11.000	11.000
3000	4.000	4.000	7.000	10.000	14.000	14.000
4000	6.000	5.000	9.000	15.000	18.000	20.000
5000	8.000	6.000	10.000	20.000	22.000	30.000
6000	10.000	8.000	12.000	25.000	30.000	50.000

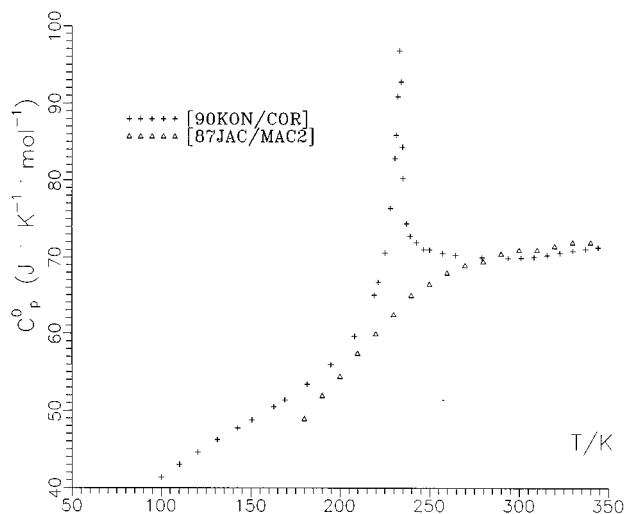


FIG. 10. Heat capacity of CsOH at 100–340 K.

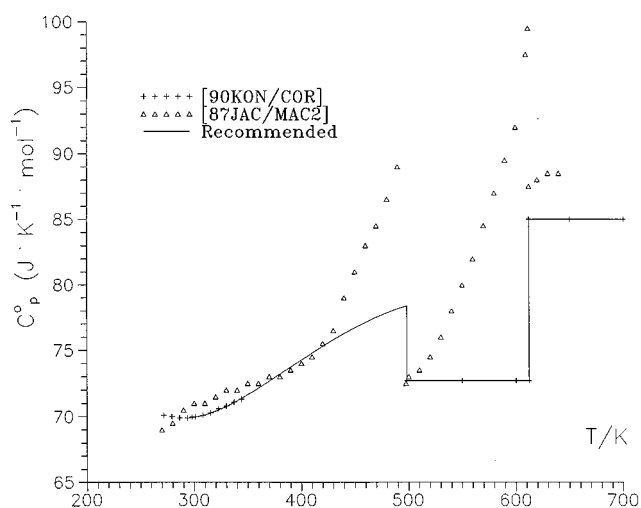


FIG. 11. Heat capacity of CsOH at 298–700 K.

4. Cesium Hydroxide

4.1. Cesium Hydroxide in Condensed Phases

At atmospheric pressure CsOH exists in three crystal phases: low-temperature orthorhombic modification, space group Pmnb (α -CsOH), stable below 234 K; room temperature orthorhombic modification, space group Bmmb (β -CsOH), stable at 234–498.2 K; and high-temperature cubic modification, space group Fm3ml (γ -CsOH), stable at 498.2–615.5 K, see Table 1 Part I.

4.1.1. Heat Capacity and Enthalpy Measurements of CsOH(cr&liq)

[87JAC/MAC2]

Jacobs *et al.* measured the heat capacity of CsOH by DSC at 180–640 K. The sample was prepared by reaction of CsOH–H₂O with CsNH₂ in liquid ammonia in an autoclave at 443 K and 900 bar during six days. The only information given about this sample is that it looked like a white powder of long needles. No information concerning the purity of the sample was given. A Perkin–Elmer DSC calorimeter was used for measurements [87JAC/MAC]; the uncertainties of the heat capacity obtained were estimated as about 2%.

The results were presented as smooth heat capacity values (10 K increments), see Table 44 and Figs. 9–11. The heat capacity of the orthorhombic modification rose sharply from 49 to 69 J K⁻¹ mol⁻¹ in the range 180–270 K, remained nearly constant in the range 270–400 K, and then rose again with acceleration from 74 to 89 J K⁻¹ mol⁻¹ in the range 400–497.5 K. Heat capacity of the cubic modification of CsOH was increased almost linearly from $C_p^\circ(497.5 \text{ K}) = 72.5$ to $C_p^\circ(600 \text{ K}) = 92$ J K⁻¹ mol⁻¹. The heat capacity of liquid CsOH was determined in the narrow temperature interval 612–640 K; it was nearly constant (from 87.5 to 88.5 J K⁻¹ mol⁻¹) within the limits of the experimental uncertainties. In addition, the temperatures and enthalpies transition and fusion were determined.

[90KON/COR]

This study of Konings *et al.* consists of two parts. The first part dealt with the measurements of low-temperature heat capacity made in the University of Michigan, USA; the second part was devoted to determination of the enthalpy increments for the solid and liquid CsOH made in Netherlands Energy Research Foundation.

The preparation of CsOH from cesium metal was made by the method described before [88KON/COR]. Three different samples were used: CsOH-1 contained 0.27% Cs₂CO₃; CsOH-2 and CsOH-3 contained less than 0.02% Cs₂CO₃.

The heat capacity of CsOH-1 sample (21.4469 g) at 5–344 K was measured in the Mark XIII adiabatic calorimeter [68WES/FUR]. The accuracy of measurements was about 0.5% in the range 10–15 K, increasing to about 0.1% between 30 and 350 K. The results of these measurements are listed in Table 45 and shown in Figs. 9–11. A reversible λ -type transition with a wide peak (maximum at 233.96 K) was observed in the heat capacity of CsOH. This transition is connected with antiferroelectric ordering. The authors [90KON/COR] calculated the following values of thermodynamic functions of CsOH at 298.15 K:

$$\begin{aligned} C_p^\circ(298.15 \text{ K}) &= 69.96 \pm 0.10 \text{ J K}^{-1} \text{ mol}^{-1}, \\ S^\circ(298.15 \text{ K}) &= 104.22 \pm 0.08 \text{ J K}^{-1} \text{ mol}^{-1}, \\ H^\circ(298.15 \text{ K}) - H^\circ(0) &= 14103 \text{ J mol}^{-1}. \end{aligned}$$

The high-temperature enthalpy was measured from 440 to 683 K by drop calorimeter. An isothermal diphenyl-ether calorimeter described in [79COR/MUI] was used. The samples CsOH-2 (7.81521 g) and CsOH-3 (4.90927 g) were enclosed in aspherical silver ampoules with a 0.25 mm wall thickness. The ampoules were heated in a furnace whose temperature was measured by Pt–Pt/Rh thermocouples with accuracy ± 0.1 K. The calibration of the calorimeter was made with the USA NBS reference material synthetic sapphire. The results of 6 measurements for orthorhombic modification (β -CsOH, 439.5–488.3 K), 11 measurements for cubic modification (γ -CsOH, 508–597.7 K), and nine

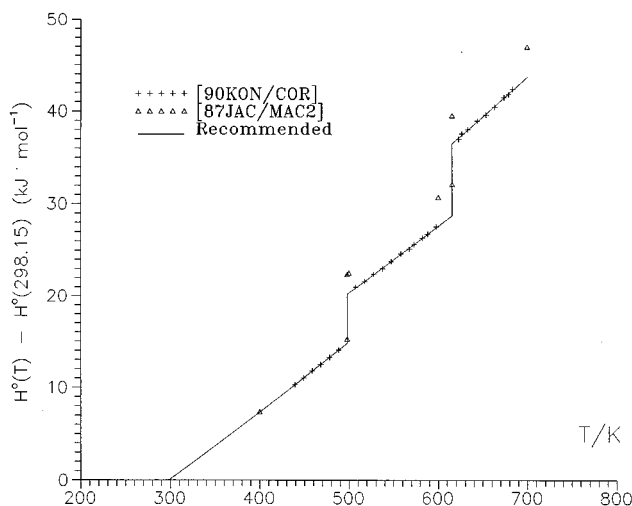


FIG. 12. Enthalpy $H^\circ(T) - H^\circ(298.15)$ for solid and liquid CsOH at 298–700 K.

measurements for liquid CsOH (622.8–683.4 K) are listed in Table 46 and shown in Fig. 12.

These data were fitted by the following equations (in J mol^{-1}):

$$\beta\text{-cr, (298.15–498.2 K): } H^\circ(T) - H^\circ(298.15 \text{ K}) = 57.8256T + 20.3495 \cdot 10^{-3}T^2 - 19049.6,$$

$$\gamma\text{-cr, (498.2–615.5 K): } H^\circ(T) - H^\circ(298.15 \text{ K}) = 72.676T - 15997.7,$$

$$\text{liq, (615.5–683 K): } H^\circ(T) - H^\circ(298.15 \text{ K}) = 85.027T - 15816.7.$$

The authors did not discuss the accuracy of their measurements. The maximum deviations of the experimental points from the values calculated using these equations were 0.25%, 0.5%, and 0.4%, respectively, and the average deviations were 0.14%, 0.20%, and 0.22%, respectively.

Discussion of Heat Capacity and Enthalpy Data

Figures 9 and 10 show the low-temperature heat capacity values obtained in the range 5.63–344 K [90KON/COR], and the values obtained by DSC in the range 180–340 K [87JAC/MAC2]. There are considerable differences between these data. The heat capacity data [87JAC/MAC2] are lower than those obtained in [90KON/COR]. In the range 180–260 K, the differences are about 3%–7%. At higher temperatures the heat capacity curves [87JAC/MAC2] and [90KON/COR] cross each other at 285 K and then the curve [87JAC/MAC2] goes about 1%–2% higher than another one. The results [87JAC/MAC2] did not confirm the phase transformation, which was detected in earlier work of Jacobs *et al.* [81JAC/HAR] (at 232 K) and then confirmed in [90KON/COR] (at 233.96 K). The authors [87JAC/MAC2] did not comment on this contradiction with the data [81JAC/HAR]. The transition in CsOH is connected with antiferroelectric ordering, with the anomaly in heat capacity being very broad, about 210 K. The calculated values of transition entropy and enthalpy are $4.095 \text{ J K}^{-1} \text{ mol}^{-1}$ and $958 \text{ J K}^{-1} \text{ mol}^{-1}$, respectively [90KON/COR]. The low-temperature heat capacity data

[90KON/COR] are adopted in this review. In the vicinity of $T=294 \text{ K}$, the heat capacity undergoes a smooth-minimum [90KON/COR]. The minimum is caused by the fact that the decreasing of the anomaly part of heat capacity CsOH (maximum of λ -curve is at 234 K) becomes comparative with the increasing of the lattice heat capacity. The fitting of the data [90KON/COR] by using a spline procedure [94LUT/GUR] results in $C_p^\circ(294 \text{ K}) = 69.92 \text{ J K}^{-1} \text{ mol}^{-1}$ and $C_p^\circ(298.15 \text{ K}) = 69.93 \text{ J K}^{-1} \text{ mol}^{-1}$. The latter value is a little less than that given in [90KON/COR] ($69.96 \text{ J K}^{-1} \text{ mol}^{-1}$). Calculation of the integral values using the spline method yields about the same results as given in [90KON/COR] $S^\circ(298.15 \text{ K}) = 104.20 \text{ J K}^{-1} \text{ mol}^{-1}$ and $H^\circ(298.15 \text{ K}) - H^\circ(0 \text{ K}) = 14102 \text{ J mol}^{-1}$. In the present work the values of [90KON/COR] are adopted for the range 5–298.15 K (see Table 52), except a value $C_p^\circ(298.15 \text{ K})$: 69.93 instead the value $69.96 \text{ J K}^{-1} \text{ mol}^{-1}$. The value 69.93 is used for the fitting of heat capacity of β -CsOH data by the equation (see below). The values of thermodynamic functions at 298.15 K adopted in this review are compared with those recommended in different reference books in Table 47.

Figure 11 shows the heat capacity data of solid and liquid measured in [87JAC/MAC2] (298–640 K), and calculated in [90KON/COR] using the experimental enthalpy data (439.5–683.4 K). The enthalpy data taken from [90KON/COR] and calculated using the heat capacity and the enthalpies of transformations from [87JAC/MAC2] are shown in Fig. 12. In the range 298–400 K, the heat capacity data reported in these two studies are in sufficient agreement (about 1%–2%), but above 400 K the heat capacity data [87JAC/MAC2] were considerably higher than that from [90KON/COR]. The discrepancies are about 20% near the transition temperature (498 K), and about 26% near the fusion temperature (600 K). The corresponding deviations of the enthalpy increments (see Fig. 12) are about 5% at 500 K and 8% at 650 K.

The reason for such large differences is unknown. It is possible that sharp increase in the heat capacity curves for β -CsOH and γ -CsOH in [87JAC/MAC2] is connected with impurities in the sample. On the other hand, the values of T_{fus} obtained in [87JAC/MAC2] and [90KON/COR] are close to each other. This last fact permits us to conclude that the samples of CsOH used in both studies contained either minor impurities or similar amounts of them. Most probably, the above-mentioned deviations of the data from these two works are caused by imperfection of the DSC-calorimetric method used in [87JAC/MAC2]. Besides, comparably small systematic errors in calorimetric measurements of the enthalpy increments [90KON/COR] may result in significant distortions of the heat capacity curves obtained by differentiation of the enthalpy data. The authors [87JAC/MAC2] noted that sharp growing of the heat capacity is typical for solid compounds containing molecular anions.

The result of the measurements of the enthalpy of the β - γ transition is strong evidence in favor of the data [90KON/COR]. The value $\Delta_{\text{trs}}H = 7.12 \text{ kJ mol}^{-1}$ obtained in [87JAC/MAC2] is 30% larger than value 5.4 kJ mol^{-1} obtained in [90KON/COR]. The higher reliability of the lat-

ter value measured calorimetrically is obvious. Thus the data [90KON/COR] are adopted in the present review. The equation for heat capacity of β -CsOH

$$C_p^\circ(T)/\text{J K}^{-1} \text{ mol}^{-1} = -46.557 + 395.682 \cdot 10^{-3}T + 24.848 \cdot 10^5 T^2 - 331.165 \cdot 10^{-6} T^2$$

was derived by approximation of the data [90KON/COR] for enthalpy increments (six points, 439.5–488.3 K) and for heat capacity of β -CsOH at 260–340 K (eight points of $H^\circ(T)$ - $H^\circ(298.15 \text{ K})$ obtained by integration of the heat capacity measured in [90KON/COR]). This equation fits the experimental heat capacity values [90KON/COR] at 300–340 K within 0.1%, while the linear equation for heat capacity of β -CsOH derived in [90KON/COR] fits the ones within 0.5% only. For the heat capacity of cubic modification (γ -CsOH) the rounded value $72.7 \text{ J K}^{-1} \text{ mol}^{-1}$ is adopted. This value was calculated from 11 enthalpy points [90KON/COR] (508–597.7 K).

The heat capacity of liquid CsOH obtained in these two studies were in satisfactory agreement: $85.027 \text{ J K}^{-1} \text{ mol}^{-1}$ from the enthalpy data [90KON/COR] in the range 622.8–683.4 K, (nine points), and about $88.0 \text{ J K}^{-1} \text{ mol}^{-1}$ [87JAC/MAC2] measured by DSC in the range 612–640 K. The rounded value $85.0 \text{ J K}^{-1} \text{ mol}^{-1}$ [90KON/COR] is adopted in this review.

Phase Equilibrium Data

[10HEV2]

Hevesy determined the temperatures and enthalpies of transition and fusion by a thermal analysis method. A commercial sample of CsOH (“Kahlbaum”) that had no impurity of Cs_2CO_3 was studied. The dehydration of the sample was made in a silver apparatus at about 450°C “for many hours.” The cooling curves made with the rate $12^\circ\text{C}/\text{min}$ gave the transition temperature $223 \pm 0.5^\circ\text{C} = 496 \text{ K}$ and the fusion temperature $272.3 \pm 0.3^\circ\text{C} = 545.45 \text{ K}$. The last value is about 70° lower than the one adopted in this review. The enthalpy of transition ($11.8 \text{ cal g}^{-1} = 7.4 \text{ kJ mol}^{-1}$) and the enthalpy of fusion ($10.7 \text{ cal g}^{-1} = 6.7 \text{ kJ mol}^{-1}$) were determined by quantitative thermal analysis.

[48HAC/THO]

Hackspill and Thomas measured the fusion temperature of a commercial sample of CsOH by the thermal analysis and detected the value $T_{\text{fus}} = 272^\circ\text{C} = 545 \text{ K}$.

[63ROL/COH]

Rollet *et al.* investigated the system CsOH– H_2O and measured by DTA for the pure CsOH the following values: $T_{\text{trs}} = 215^\circ\text{C} = 488 \text{ K}$ and $T_{\text{fus}} = 346^\circ\text{C} = 619 \text{ K}$.

[64COH/RUB], [66COH/RUB]

Cohen-Adad and Ruby investigated the systems CsOH– Cs_2CO_3 and CsOH–CsF. The pure CsOH was prepared by electrolysis of Cs_2CO_3 water solution in a stream of dry nitrogen and then was dehydrated up to constant melting point. The authors detected the transition temperature $215^\circ\text{C} = 488 \text{ K}$ and the fusion temperature $346^\circ\text{C} = 619 \text{ K}$, using thermal analysis.

[65RES/BAR], [67RES/BAR]

In the first study, Reshetnikov and Baranskaya investigated the system CsOH– CsNO_3 . The sample of CsOH was prepared by reaction Cs_2SO_4 with $\text{Ba}(\text{OH})_2$ in a water solution. Dehydration of CsOH was carried out by heating at 450 – 470°C in a silver container. According to the chemical analysis, the sample contained 99.5% CsOH and 0.3% Cs_2CO_3 . The authors [65RES/BAR] detected the following values: $T_{\text{trs}} = 223^\circ\text{C} = 496 \text{ K}$ and $T_{\text{fus}} = 316^\circ\text{C} = 589 \text{ K}$.

In the second work, slightly different values $T_{\text{trs}} = 220 \pm 1^\circ\text{C} = 493 \text{ K}$ and $T_{\text{fus}} = 315 \pm 1^\circ\text{C} = 588 \text{ K}$ were obtained. The enthalpy of transition $1.45 \text{ kcal mol}^{-1} = 6.07 \text{ kJ mol}^{-1}$ and the enthalpy of fusion $1.09 \text{ kcal mol}^{-1} = 4.56 \text{ kJ mol}^{-1}$ were measured by quantitative thermal analysis.

[74POR/ITK], [75ITK/POR]

Portnova and Itkina investigated the system CsOH–LiOH. The sample of CsOH was dehydrated in a stream of dry and CO_2 -free argon at 400 – 450°C during 12 h. For the pure CsOH $T_{\text{trs}} = 220^\circ\text{C} = 493 \text{ K}$ and $T_{\text{fus}} = 340^\circ\text{C} = 613 \text{ K}$ were detected by DTA.

[74TOU]

Touzain investigated the system CsOH–Cs. For a sample of CsOH that contained about 2% Cs_2CO_3 , the following values were detected by the thermal analysis: $T_{\text{trs}} = 220 \pm 3^\circ\text{C} = 493 \text{ K}$ and $T_{\text{fus}} = 340 \pm 4^\circ\text{C} = 613 \text{ K}$.

[81JAC/HAR]

Jacobs and Harbrecht reported for the first time that CsOH has a low-temperature transition. The temperatures of α – β and β – γ transitions were obtained at 232 K and 497 K by DTA.

[87BAS/ELC]

Bastow *et al.* confirmed the low-temperature transition of CsOH at 232 K by DTA and by measurements of the temperature dependence of the dielectric constant. Structural parameters obtained from high resolution neutron powder diffraction data demonstrated that transition of CsOH at 232 K is an antiferroelectric ordering. For CsOD the transition temperature 262 K was detected in the same investigation.

[87JAC/MAC2]

Jacobs *et al.* measured the heat capacity, temperatures, and enthalpies of transition and fusion of CsOH by DSC. For the polymorphic transition of CsOH (orthorhombic–cubic) they determined $T_{\text{trs}} = 497.5 \text{ K}$ and $\Delta_{\text{trs}}H = 7.12 \text{ kJ mol}^{-1}$, and for fusion $T_{\text{fus}} = 612 \text{ K}$ and $\Delta_{\text{fus}}H = 7.4 \text{ kJ mol}^{-1}$. The uncertainties of these data were not estimated in the study. The authors also investigated the crystal structures of CsOH (and CsOD) modifications using the x-ray analysis, neutron diffraction experiments, IR and Raman spectroscopic measurements.

[90KON/COR]

Konings *et al.* measured the temperatures and the enthalpies of phase transformations. The transition and the melting temperatures were recorded directly in a Mettler DSC apparatus (type TA-13) by heating the sample in a sealed silver crucible at a heating rate 5 K min^{-1} . The T_{trs} and T_{fus} were

obtained as sharp and reproducible peaks at 498.2 ± 0.5 K and 615.5 ± 0.5 K, respectively. Listed uncertainties are the standard deviation of a number of DSC runs. The enthalpy of transformations $\Delta_{\text{trs}}H = 5.4 \text{ kJ mol}^{-1}$ and $\Delta_{\text{fus}}H = 7.783 \text{ kJ mol}^{-1}$ were calculated from the equations for enthalpies of β -, γ - and liquid CsOH.

Discussion of Phase Equilibrium Data

The antiferroelectric transition of CsOH (α - β) at 232 K was detected for the first time in [81JAC/HAR] by DTA and was confirmed in [87BAS/ELC]. More detailed investigation of this transition was made by calorimetric measurements of the low-temperature heat capacity [90KON/COR]. The authors detected λ -type anomaly with a peak maximum at 233.96 K. The width of this λ -anomaly is very broad, about 200 K, indicating a non-isothermal effect.

The results of different measurements of the temperature of orthorhombic-cubic (β - γ) transition were in the range from 488 to 498.2 K (see Table 48). The value adopted in this review, $T_{\text{trs}} = 498.2 \pm 1.0$ K, is based on the data by Konings *et al.* and was detected by the Mettler DSC-apparatus for a pure sample of CsOH, see above. This value is in a good agreement with the value 497.5 K detected in [87JAC/MAC2]. The results of other determinations of T_{trs} are less accurate.

As in the case of RbOH, there is great scattering in the measured values of the melting point of CsOH (from 545 up to 619 K), see Table 49. We do not consider the measurements with the samples of CsOH that were not completely dehydrated [10HEV2, 48HAC/THO, 65RES/BAR, 67RES/BAR]. The results of the other eight studies gave the values of T_{fus} from 612 to 619 K. In this review we adopt the value 615.5 ± 1.0 , which is based on the data by Konings *et al.* [90KON/COR]. These authors suggested that an uncertainty of their determination is ± 0.5 K. As they did not give the amounts of water and other impurities in the sample, we have increased the uncertainty of fusion temperature up to ± 1.0 K.

The enthalpy of antiferroelectric transition (α - β) ($\Delta_{\text{trs}}H = 958 \text{ J mol}^{-1}$) was derived from integration of the excess heat capacity in the range of λ -anomaly centered at 233.96 K [90KON/COR]. The integration of the excess function C_p°/T gave the value of entropy of transition $\Delta_{\text{trs}}S = 4.095 \text{ J K}^{-1} \text{ mol}^{-1}$. Both values were taken into account for calculating the thermodynamic functions below 400 K.

The data concerning the enthalpy of β - γ transition (orthorhombic-cubic) and the enthalpy of fusion (see Tables 50 and 51) are in poor agreement. All these data except [90KON/COR] were measured by insufficiently precise methods—DTA and DSC. More exact were the measurements of the enthalpy increments for the β -, γ -modifications and liquid CsOH [90KON/COR]. The values $\Delta_{\text{trs}}H = 5.4 \text{ kJ mol}^{-1}$ and $\Delta_{\text{fus}}H = 7.78 \text{ kJ mol}^{-1}$ were adopted in this review with uncertainties 0.3 and 0.4 kJ mol^{-1} , respectively.

Calculation of Thermal Functions of CsOH(cr&liq)

The thermal functions of CsOH(cr) at the temperatures 5–298.15 K (Table 52) were taken from the data [90KON/COR]. The thermal functions of CsOH(cr&liq) for the temperatures 0–2000 K (Table L56) were calculated using the adopted values and equations presented in the previous section and the data of Table 52. The uncertainties of the tabulated values are listed in Table 56.

The following values are adopted:

$$\begin{aligned} C_p^\circ(298.15 \text{ K}) &= 69.93 \pm 0.10 \text{ J K}^{-1} \text{ mol}^{-1}, \\ S^\circ(298.15 \text{ K}) &= 104.22 \pm 0.10 \text{ J K}^{-1} \text{ mol}^{-1}, \\ H^\circ(298.15 \text{ K}) - H^\circ(0) &= 14103 \pm 10 \text{ J mol}^{-1}. \end{aligned}$$

Heat Capacity Equations (in the following temperature ranges):

$$\begin{aligned} \beta\text{-cr, (298.15–498.2 K): } C_p^\circ/\text{J K}^{-1} \text{ mol}^{-1} &= 46.557 \\ &+ 395.682 \cdot 10^{-3}T + 24.848 \cdot 10^5 T^{-2} - 331.165 \cdot 10^{-6}T^2, \\ \gamma\text{-cr, (498.2–615.5 K): } C_p^\circ/\text{J K}^{-1} \text{ mol}^{-1} &= 72.7, \\ \text{liq, (615.5–2000 K): } C_p^\circ/\text{J K}^{-1} \text{ mol}^{-1} &= 85.0. \end{aligned}$$

Phase Equilibrium Data:

$$\alpha\text{-}\beta \text{ transition: } T_{\text{trs}}/\text{K} = 233.96 \text{ and } \Delta_{\text{trs}}H/\text{J mol}^{-1} = 958,$$

$$\beta\text{-}\gamma \text{ transition: } T_{\text{trs}}/\text{K} = 498.2 \pm 1.0 \text{ and } \Delta_{\text{trs}}H/\text{J mol}^{-1} = 5400 \pm 300,$$

$$\text{Fusion: } T_{\text{fus}}/\text{K} = 615.5 \pm 1.0 \text{ and } \Delta_{\text{fus}}H/\text{J mol}^{-1} = 7780 \pm 400.$$

The calculated values of thermal functions of CsOH(cr&liq) differ from those listed in earlier reviews [82GUR/VEI] and [85CHA/DAV] (see Table 53), due to the use of new experimental data [90KON/COR] for the heat capacities and the enthalpies of transition and fusion of CsOH.

4.1.2. Enthalpy of Formation of CsOH(cr)

Two methods have been used for determination of the enthalpy of formation of CsOH(cr). One is based on calorimetric measurements of the enthalpies of solution of CsOH(cr) in water. The results of such studies (three works) are presented in the Table 54. The second method was used in the work [88KON/COR] only. It is based on calorimetric measurements of the enthalpy of reaction $\text{CsOH}(\text{cr}) + \text{HCl}(\text{soln}) = \text{CsCl}(\text{soln}) + \text{H}_2\text{O}(\text{soln})$ and the enthalpy of solution of CsCl (cr) in the solution obtained after indicated reaction (see Table 53).

Experimental Studies

[1892BEK]^b

Beketov measured the enthalpy of solution of CsOH(cr) in water in a calorimeter at 289.15 K (one experiment). No information regarding a purity of cesium hydroxide sample and other important experimental details was given in the paper.

[06FOR]^b

Forcand carried out one measurement of the enthalpy of solution of CsOH(cr) in water at 288.1 K. Information on the experimental details (purity of the CsOH sample, the method

of analysis of final solution, a precision of temperature measurements and so on) was not given.

[88KON/COR]

Konings *et al.* have used two methods for determination of the enthalpy of formation of CsOH(cr). One method is based on calorimetric measurements of the enthalpy of solution of cesium hydroxide in water. Four experiments were carried out for determination of $\Delta_{\text{aq}}H^\circ(\text{CsOH,cr},298.15\text{ K})$ (see Table 54). The second method was based on the results of measurements of the enthalpies of processes 1 and 2 (corresponding reaction scheme is given in the Table 55). The precise isoperibol calorimeter was used. Its energy equivalent was determined electrically. The precision of temperature measurements was $\pm 0.0002^\circ$. The cesium hydroxide sample was prepared from elemental Cs (trade mark "Merk, reinst"). The cesium metal was heated at 525 K in argon saturated with water vapor (partial pressure was about 1.3 kPa). The product was subsequently heated under high vacuum at 700 and 605 K to yield anhydrous CsOH (without CsOH-hydrates). The Cs content in the CsOH sample was found to be 88.41 ± 0.06 mass% (the calculated value is 88.65%). The CsCl sample was prepared from CsCO_3 (trade mark "Merck, p.a.11) and contained 79.00 ± 0.04 mass% of cesium (the calculated value is 78.94%). The x-ray powder-diffraction analysis showed that other phases (except CsOH and CsCl accordingly) were absent in the samples prepared. The chemical analysis also proved that the samples were free from impurities apart from a small amount of Cs_2CO_3 (0.27 ± 0.06 mass%) in the CsOH sample. The CO_3^{2-} amount was determined by titration with standard HCl(aq). The presence of Cs_2CO_3 -impurity was taken into account in calculations. The 0.10095 molar HCl solution was used as solvent in calorimetric measurements.

The $\Delta_f H^\circ(\text{CsOH,cr},298.15\text{ K})$ values obtained by Konings *et al.* are $-416.45 \pm 0.55\text{ kJ mol}^{-1}$ (first method) and $-416.42 \pm 0.63\text{ kJ mol}^{-1}$ (second method). (The former value included a small mistake, see the next subsection.) Taking the weighted mean of two results, the authors [88KON/COR] recommended the value $\Delta_f H^\circ(\text{CsOH,cr},298.15\text{ K}) = -416.44 \pm 0.41\text{ kJ mol}^{-1}$.

Discussion of the Enthalpy of Formation Data

The results obtained by Beketov [1892BEK] and Forcrand [06FOR] have only a historical interest because at that time experimental techniques, methods and materials were of a poor quality. Moreover, many important details of measurements were not given in their papers. The data obtained by Konings *et al.* [88KON/COR] appear to be the most reliable. These authors used a precise isoperibol calorimeter, and their CsOH and CsCl samples were rather pure and carefully characterized. Corrections for the presence of Cs_2CO_3 impurity in the samples were taken into account. Two methods were

used in this study to determine the enthalpy of formation of CsOH(cr), and the results obtained were very close.

Some small corrections were inserted by the authors of this review in the results of Konings *et al.* [88KON/COR]: (1) The value [$\Delta_{\text{aq}}H^\circ(\text{CsOH, cr} \rightarrow 5500\text{H}_2\text{O}, 298.15\text{ K}) - \Delta_{\text{aq}}H^\circ(\text{CsOH,cr} \rightarrow \text{H}_2\text{O}, 298.15\text{ K})$] was estimated to be equal $+ (0.18 \pm 0.10)\text{ kJ mol}^{-1}$ as the average from the Parker's [65PAR] data on corresponding enthalpies of dilution of MOH (soln, 5500H₂O), where M = Li, Na and K. Konings *et al.* [88KON/COR] erroneously estimated this value as equal $- (0.15 \pm 0.03)\text{ kJ mol}^{-1}$; therefore, their data were recalculated. (2) The uncertainties of all [88KON/COR] experimental results were also recalculated using the Student's criterion.

After these recalculations, two new values were obtained: $\Delta_f H^\circ(\text{CsOH,cr},298.15\text{ K}) = -416.1 \pm 0.6\text{ kJ mol}^{-1}$ (first method) and $\Delta_f H^\circ(\text{CsOH,cr},298.15\text{ K}) = -416.4 \pm 0.9\text{ kJ mol}^{-1}$ (second method). The weighted mean of these two values is $-416.2 \pm 0.5\text{ kJ mol}^{-1}$.

The adopted value of enthalpy of formation of crystalline cesium hydroxide is the weighed mean of the two values obtained from the studies by Konings *et al.* [88KON/COR] with the use of two experimental methods (see Tables 54, 55, and the previous subsection):

$$\Delta_f H^\circ(\text{CsOH,cr},298.15\text{ K}) = -416.2 \pm 0.5\text{ kJ mol}^{-1}.$$

This value and the values recommended in the other reviews are compared in Table 47.

4.1.3. Appendix. Tables of Experimental and Evaluated Data for CsOH(cr)

TABLE 44. Smoothed heat capacity of CsOH [87JAC/MAC2]

T/K	$C_p^\circ, \text{J K}^{-1} \text{mol}^{-1}$	T/K	$C_p^\circ, \text{J K}^{-1} \text{mol}^{-1}$	T/K	$C_p^\circ, \text{J K}^{-1} \text{mol}^{-1}$
180	49.0	350	72.5	500	73.0
190	52.0	360	72.5	510	73.5
200	54.5	370	73.0	520	74.5
210	57.5	380	73.0	530	76.0
220	60.0	390	73.5	540	78.0
230	62.5	400	74.0	550	80.0
240	65.0	410	74.5	560	82.0
250	66.5	420	75.5	570	84.5
260	68.0	430	76.5	580	87.0
270	69.0	440	77.5	590	89.5
280	69.5	450	79.0	600	92.0
290	70.5	460	81.0	610	(97.5)
300	71.0	470	83.0	612(γ)	(99.5)
310	71.0	480	84.5	612(liq)	87.5
320	71.5	490	86.5	620	88.0
330	72.0	497.5(β)	89.0	630	88.5
340	72.0	497.5(γ)	72.5	640	88.5

^bThe results were recalculated by Parker [65PAR] taking into account the changes of atomic weights and the corrections for transition to a standard temperature (298.15 K) and infinite dilution (see Table 54, column 6).

TABLE 45. Experimental heat capacity values of CsOH [90KON/COR]

N	T/K	$C_p^{\circ}/\text{J K}^{-1} \text{mol}^{-1}$	N	T/K	$C_p^{\circ}/\text{J K}^{-1} \text{mol}^{-1}$
1	5.63	0.172	53	162.95	50.53
2	6.20	0.250	54	169.09	51.42
3	6.86	0.380	55	175.23	52.37
4	7.55	0.563	56	181.63	53.44
5	8.28	0.805	57	188.28	54.63
6	9.13	1.137	58	194.93	55.97
7	10.12	11.586	59	201.56	57.61
8	11.11	2.115	60	208.18	59.66
9	12.13	2.724	61	214.77	62.39
10	13.30	3.519	62	219.22	65.03
11	14.60	4.469	63	221.25	66.52
12	15.93	5.489	64	221.41	66.65
13	17.30	6.563	65	221.54	66.73
14	18.70	7.660	66	223.24	68.17
15	20.12	8.776	67	225.28	70.62
16	21.57	9.892	68	227.36	73.80
17	23.04	11.00	69	228.39	76.40
15	24.79	12.28	70	228.88	76.70
19	26.80	13.71	71	229.87	78.48
20	28.83	15.09	72	230.84	82.87
21	31.05	16.57	73	231.79	85.90
22	33.47	18.11	74	232.70	90.91
23	35.90	19.58	75	233.58	96.78
24	38.53	21.10	76	234.45	92.80
25	41.36	22.63	77	235.16	84.35
26	44.21	24.11	78	235.38	80.27
27	46.71	25.36	79	236.36	76.25
28	49.63	26.75	80	237.37	74.43
29	53.01	28.25	81	238.39	73.16
30	56.39	29.66	82	239.41	72.80
31	60.03	31.07	83	240.92	72.41
32	63.93	32.46	84	242.57	72.06
33	67.85	33.74	85	242.92	71.96
34	72.04	34.99	86	244.92	71.46
35	76.49	36.23	87	246.93	71.06
36	80.95	37.42	88	248.94	71.02
37	5.42	38.51	89	249.10	71.09
38	90.17	39.55	90	250.22	71.01
39	95.20	40.50	91	257.53	70.56
40	100.23	41.37	92	264.81	70.27
41	105.27	42.22	93	272.09	70.10
42	110.33	43.05	94	279.36	70.02
43	115.40	43.86	95	286.62	69.95
44	120.49	44.65	96	293.88	69.91
45	125.83	45.43	97	301.14	69.95
46	131.42	46.24	98	308.37	70.05
47	137.03	47.02	99	315.60	70.30
48	142.64	47.77	100	322.82	70.58
49	144.81	48.04	101	330.06	70.84
50	148.29	48.52	102	337.29	71.07
51	150.68	48.82	103	344.04	71.32
52	156.81	49.67			

TABLE 46. Experimental enthalpy values $H^{\circ}(T) - H^{\circ}(298.15 \text{ K})$ of CsOH [90KON/COR]

N	T/K	$H^{\circ}(T) - H^{\circ}(298.15 \text{ K})$
		J mol ⁻¹
1	439.5	10305
2	449.3	11033
3	458.9	11774
4	468.4	12474
5	478.5	13268
6	488.3(β)	14074
7	508.0(γ)	20999
8	517.8	21605
9	527.8	22394
10	537.8	23019
11	547.5	23789
12	558.4	24628
13	567.9	25149
14	573.2	25620
15	582.4	26350
16	588.3	26756
17	597.7(γ)	27533
18	622.8(liq)	36995
19	626.3	37569
20	633.1	38060
21	643.5	38994
22	653.4	39643
23	663.4	40478
24	673.5	41492
25	678.7	41829
26	683.4	42389

TABLE 47. Comparison of the heat capacity, enthalpy, entropy, and enthalpy of formation values for CsOH(cr) at 298.15 K

Reference	$C_p^\circ(298.15\text{ K})$	$S^\circ(298.15\text{ K})$	$H^\circ(298.15\text{ K}) - H^\circ(T)$	$\Delta H_f^\circ(298.15\text{ K})$
	$\text{J K}^{-1}\text{ mol}^{-1}$	$\text{J K}^{-1}\text{ mol}^{-1}$	J mol^{-1}	kJ mol^{-1}
82MED/BER	73.2±4.0	102.5±8.0	15900±800	-416.56±1.67
82WAG/EVA	-417.23
A				
82GUR/VEI	73.0	102.0±2.0	16000±1000	-416.6±4.0
85CHA/DAV	67.872	98.7±4.2	...	-416.73±0.8
89KON/COR	-416.44±0.41
90KON/COR	69.96±0.1	104.22±0.08	14103	...
Adopted	69.93±0.1	104.22±0.10	14103±10	-416.2±0.5

TABLE 48. Temperature of phase transformations of CsOH

Reference	$t_{\text{trs}}/^\circ\text{C}$	T_{trs}/K	Comments
Original studies			
10HEV2	223±0.5	496	Thermal analysis
63ROL/COH	215	488	Thermal analysis (DTA)
64COH/RUB,	215	488	Thermal analysis (DTA)
66COH/RUB			
65RES/BAR	223	496	Thermal analysis (DTA)
67RES/BAR	220±1	493	Thermal analysis (DTA)
74POR/ITK,	220	493	Thermal analysis (DTA)
75ITC/POR			
74TOU	220±3	493	Thermal analysis
81JAC/HAR	...	232($\alpha-\beta$)	Thermal analysis
		497($\beta-\gamma$)	Thermal analysis
87BAS/ELC	...	232($\alpha-\beta$)	Thermal analysis
87JAC/MAC2	...	497.5($\beta-\gamma$)	DSC method
90KON/COR	...	233.96($\alpha-\beta$)	Calorimetric
		498.2±0.5($\beta-\gamma$)	DSC method
Reviews			
82MED/BER		493±3($\beta-\gamma$)	Based on 67RES/BAR
82GUR/VEI		497±1($\beta-\gamma$)	Based on 81JAC/HAR
85CHA/DAV		493±1($\beta-\gamma$)	Based on 67RES/BAR
Adopted		233.96($\alpha-\beta$)	Based on 90KON/COR
		498.2±1($\beta-\gamma$)	Based on 90KON/COR

TABLE 49. Temperature of fusion of CsOH

Reference	$t_{\text{fus}}/^\circ\text{C}$	T_{fus}/K	Comments
Original studies			
10HEV2	272.3±0.3	545.45	Thermal analysis
48HAC/THO	272	545	Thermal analysis
63ROL/COH	346	619	Thermal analysis (DTA)
64COH/RUB,	346	619	Thermal analysis (DTA)
66COH/RUB			
65RES/BAR	316	589	Thermal analysis (DTA)
67RES/BAR	315±1	588	Thermal analysis (DTA)
74POR/ITK,	340	613	Thermal analysis (DTA)
75ITK/POR			
74TOU	340±4	613	Thermal analysis
87JAC/MAC2	...	612	DSC method
90KON/COR	...	615.5±0.5	DSC method
Reviews			
82MED/BER,	...	616±3	Based on 6 studies
82GUR/VEI			
85CHA/DAV	...	588±1	Based on 67RES/BAR
Adopted	...	615.5±1	Based on 90KON/COR

TABLE 50. Enthalpy of $\beta-\gamma$ transition of CsOH

Reference	$\Delta_t H, \text{kJ mol}^{-1}$	Comments
Original studies		
10HEV2	7400	Thermal analysis (DTA)
67RES/BAR	6070	Thermal analysis (DTA)
81JAC/HAR	7100	DSC method
87JAC/MAC2	7120	DSC method
90KON/COR	5400	Enthalpy measurements
Reviews		
82MED/BER	6100±600	Based on 67RES/BAR
82GUR/VEI	7100±500	Based on 81JAC/HAR
85CHA/DAV	6070±630	Based on 67RES/BAR
Adopted	5400±300	Based on 90KON/COR

TABLE 51. Enthalpy of fusion of CsOH

Reference	$\Delta_t H, \text{kJ mol}^{-1}$	Comments
Original studies		
10HEV2	6700	Thermal analysis (DTA)
67RES/BAR	4560	Thermal analysis (DTA)
81JAC/HAR	7300	DSC method
87JAC/MAC2	7400	DSC method
90KON/COR	7783	Enthalpy measurements
Reviews		
82MED/BER	4560±600	Based on 67RES/BAR
82GUR/VEI	7300±500	Based on 81JAC/HAR
85CHA/DAV	4560±420	Based on 67RES/BAR
Adopted	7780±400	Based on 90KON/COR

TABLE 52. Thermal functions of CsOH(cr) below 298.15

T/K	$C_p^\circ(T)$ $\text{J K}^{-1} \text{mol}^{-1}$	$H^\circ(T) - H^\circ(0)$ J mol^{-1}	$S^\circ(T)$ $\text{J K}^{-1} \text{mol}^{-1}$
5	0.125	0.00016	0.058
10	1.513	0.00338	0.449
15	4.773	0.01853	1.638
20	8.680	0.05214	3.542
25	12.43	0.1051	5.887
30	15.88	0.1760	8.464
35	19.03	0.2630	11.156
40	21.90	0.3659	13.890
45	24.53	0.4820	16.616
50	26.92	0.6106	19.320
60	31.04	0.9012	24.610
70	34.40	1.2289	29.660
80	37.19	1.5873	34.440
90	39.49	1.9710	38.922
100	41.36	2.3755	43.220
120	44.56	3.2353	51.040
140	47.42	4.1555	58.140
160	50.10	5.1309	64.640
180	53.15	6.1619	70.710
200	57.19	7.2627	76.500
210	60.32	7.8488	79.360
220	65.55	8.4758	82.280
225	70.36	8.8144	83.785
230	79.27	9.1865	85.420
233.96	98.00	9.534	86.918
235	84.97	9.630	87.328
240	72.38	10.007	88.870
260	70.51	11.430	94.630
280	69.97	12.834	99.830
298.15	69.93	14.103	104.220

TABLE 53. Differences ($\text{J K}^{-1} \text{mol}^{-1}$) between the thermal functions of CsOH(cr,liq) calculated in the present work and in [82GUR/VEI, 85CHA/DAV]

T/K	[82GUR/VEI]			[85CHA/DAV]	
	$\Delta C_p^\circ(T)$	$\Delta \Phi^\circ(T)$	$\Delta S^\circ(T)$	$\Delta C_p^\circ(T)$	$\Delta S^\circ(T)$
298.15	-3.070	8.582	2.220	2.058	5.478
500	-7.300	5.591	-2.890	-10.980	0.567
1000	2.000	1.188	-2.645	3.412	4.921
1500	2.000	0.055	-1.834	3.412	6.305
2000	2.000	-0.342	-1.259	3.412	7.285

TABLE 54. The enthalpy of formation of CsOH(cr) from measurements of the enthalpies of solution of cesium hydroxide in water

Authors	Moles of $\text{H}_2\text{O}, n^a$	T/K	No. of measurements	$\Delta_{\text{aq}}H^\circ, ^a$ kJ mol^{-1}	$\Delta_{\text{aq}}H^\circ, ^b$ at 298.15 K kJ mol^{-1}	$\Delta_f H^\circ(\text{KOH}, \text{cr},$ 298.15 K) ^c kJ mol^{-1}
1892BEK	325	289.15	1	-66.4	-69.0 ^d	-419.0
06FOR	111	288.15	1	-68.7	-71.5 ^d	-416.5
88KON/COR	5500	298.15	4	$-71.7_2 \pm 0.3_5^e$	-71.9 ± 0.4^f	-416.1 ± 0.6

^aReaction is $\text{CsOH}(\text{cr}) + n\text{H}_2\text{O}(1) = \text{CsOH}(\text{soln}, n\text{H}_2\text{O})$.

^bReaction is $\text{CsOH}(\text{cr}) + \infty\text{H}_2\text{O}(1) = \text{CsOH}(\text{soln}, \infty\text{H}_2\text{O})$.

^cThe CODATA values ($\Delta_f H^\circ(\text{OH}^-, \text{soln}, \infty\text{H}_2\text{O}, 298.15 \text{ K}) = -230.015 \pm 0.04 \text{ kJ mol}^{-1}$ and $\Delta_f H^\circ(\text{Cs}^+, \text{soln}, \infty\text{H}_2\text{O}, 298.15 \text{ K}) = -258.00 \pm 0.50 \text{ kJ mol}^{-1}$ [89COX/WAG]) were used in treatment of experimental data. The uncertainty was calculated as a square root from the sum of squares of uncertainties of the $\Delta_{\text{aq}}H^\circ_\infty(298.15 \text{ K})$, $\Delta_f H^\circ(\text{OH}^-, \text{soln}, \infty\text{H}_2\text{O}, 298.15 \text{ K})$ and $\Delta_f H^\circ(\text{Cs}^+, \text{soln}, \infty\text{H}_2\text{O}, 298.15 \text{ K})$ values.

^dRecalculated by Parker [65PAR] (see Sec. 4.1).

^eRecalculated by authors of this study, using the Student's criterion; the original value is $-71.7_2 \pm 0.2_3 \text{ kJ mol}^{-1}$.

^fRecalculated by authors of this study (see Sec. 4.1); the original value is $-71.5_7 \pm 0.2_3 \text{ kJ mol}^{-1}$.

TABLE 55. Reaction scheme and results of determination of the enthalpy of formation of CsOH(cr), obtained in the study [88KON/COR] (second method)

Reaction	No. of measurements	$\Delta_f H^\circ(298.15 \text{ K})$, kJ mol ⁻¹	References
1. CsOH(cr)+HCl(soln)= =CsCl(soln)+H ₂ O(soln) ^a	3	-127.68±0.76 ^b	88KON/COR
2. CsCl(cr)+(soln)=CsCl(soln)	3	17.73±0.10 ^b	88KON/COR
3. Cs(cr)+0.5Cl ₂ (g)=CsCl(cr)	...	-442.27±0.51 ^c	82GUR/VEI, 89COX/WAG
4. 0.5H ₂ (g)+0.5Cl ₂ (g)=HCl(soln)	...	-166.26±0.10 ^d	82WAG/EVA, 89COX/WAG
5. H ₂ (g)+0.5O ₂ (g)=H ₂ O(soln)	...	-285.830±0.040 ^e	89COX/WAG
6. Cs(cr)+0.5O ₂ (g)+0.5H ₂ (g)=CsOH(cr); $\Delta H_6 = -\Delta H_1 + \Delta H_2 + \Delta H_3 - \Delta H_4 + \Delta H_5$		-416.42±0.93 (the original value is -416.42±0.63 kJ mol ⁻¹)	

^aThe authors [88KON/COR] assumed that the enthalpy of process {CsCl+H₂O}(soln)=CsCl(soln)+H₂O(soln) was equal to zero. It seems to be well-founded because corresponding solutions are very diluted.

^bThe original values of uncertainties were recalculated, using the Student's criterion.

^cThe value was calculated from $\Delta_{\text{aq}} H^\circ(\text{CsCl}, \text{cr} \rightarrow \infty \text{H}_2\text{O}, 298.15 \text{ K})$ as evaluated by Gurvich *et al.* [82GUR/VEI] and the CODATA selections for the standard enthalpies of formation of OH⁻(soln, ∞H₂O) and Cs⁺(soln, ∞H₂O) [89COX/WAG].

^dThe value was calculated from the CODATA selection for the enthalpy of formation of Cl⁻(soln, ∞H₂O) [89COX/WAG] and the enthalpy of dilution of HCl(soln, 556H₂O) to infinite dilution [82WAG/EVA].

^eIt was taken in the paper [88KON/COR] that $\Delta_f H^\circ(\text{H}_2\text{O}, \text{l}, 298.15 \text{ K}) = \Delta_f H^\circ(\text{H}_2\text{O}, \text{soln}, 298.15 \text{ K})$. It could not be a source of errors because the solution was very diluted and its composition was H₂O(soln, 5400 H₂O · 10HCl · CsCl).

TABLE 56. Thermodynamic properties at 0.1 MPa: CsOH(cr&liq)

T/K	C_p°	$-[G^\circ - H^\circ(0\text{ K})]/T$	S°	$H^\circ - H^\circ(0\text{ K})$	$\Delta_f H^\circ$	$\Delta_f G^\circ$
0	0.000	0.000	0.000	0.000	-414.018	-414.018
25	12.430	1.687	5.887	0.105	-414.842	-412.099
50	26.920	7.100	19.320	0.611	-415.698	-409.017
75	35.820	13.347	32.080	1.405	-416.333	-405.528
100	41.360	19.460	43.220	2.376	-416.742	-401.865
150	48.720	30.543	61.450	4.636	-417.199	-394.312
200	57.190	40.185	76.500	7.263	-417.337	-386.652
250	71.020	48.936	91.820	10.721	-416.727	-379.018
300	69.952	57.211	104.653	14.232	-416.185	-371.523
350	71.648	64.783	115.541	17.765	-417.838	-363.777
400	74.259	71.746	125.276	21.412	-417.281	-356.090
450	76.710	78.195	134.169	25.188	-416.582	-348.482
498.2 cr, β	78.387	83.997	142.065	28.929	-415.794	-341.228
498.2 cr, γ	72.700	83.997	152.904	34.329	-410.394	-341.228
500	72.700	84.246	153.167	34.460	-410.373	-340.978
600	72.700	96.871	166.421	41.730	-409.193	-327.209
615.5 cr, γ	72.700	98.646	168.276	42.857	-409.007	-325.094
615.5 liq	85.000	98.646	180.916	50.637	-401.227	-325.094
700	85.000	109.251	191.851	57.820	-399.164	-314.777
800	85.000	120.301	203.201	66.320	-396.730	-302.888
900	85.000	130.079	213.212	74.820	-394.338	-291.302
1000	85.000	138.848	222.168	83.320	-459.765	-276.280
1100	85.000	146.797	230.269	91.820	-456.619	-258.085
1200	85.000	154.066	237.665	100.320	-453.512	-240.174
1300	85.000	160.762	244.469	108.820	-450.444	-222.521
1400	85.000	166.968	250.768	117.320	-447.413	-205.101
1500	85.000	172.753	256.633	125.820	-444.422	-187.899
1600	85.000	178.169	262.118	134.320	-441.469	-170.894
1700	85.000	183.260	267.271	142.820	-438.554	-154.071
1800	85.000	188.063	272.130	151.320	-435.679	-137.420
1900	85.000	192.610	276.726	159.820	-432.848	-120.927
2000	85.000	196.926	281.085	168.320	-430.063	-104.584
298.15	69.930	56.918	104.220	14.103	-416.200	-371.798
Uncertainties in Functions						
0	0.500	0.500
300	0.100	0.100	0.100	0.010	0.500	0.500
500	1.000	0.500	0.800	0.300	0.600	0.600
1000	2.500	2.000	3.000	2.000	2.000	2.000
1500	5.000	4.000	5.000	4.000	4.000	6.000
2000	7.000	6.000	7.000	8.000	8.000	12.000

4.2. Cesium Hydroxide in Gaseous Phase

4.2.1. Cesium Hydroxide Monomer

Molecular Constants of CsOH(g)

[53SMI/SUG]

As with the other alkali metal hydroxides, Smith and Sugden assumed a linear model and estimated molecular constants of CsOH.

[59SCH/POR]

Schoonmaker and Porter accepted a linear configuration of CsOH but did not exclude a nonlinear one.

[66JEN/PAD]

Jensen and Padley assumed a nonlinear configuration and estimated molecular constants for CsOH.

[66KUC/LID]

Kuczkowski *et al.* reported preliminary results of investigations of the microwave spectrum of CsOH. They obtained the evidence for an effective linear geometry of the mol-

ecule, though did not exclude the possibility of a quasi linear structure. Assuming $0.95 \pm 0.05 \text{ \AA}$ for the O–H distance, they obtained the Cs–O distance of $2.40 \pm 0.01 \text{ \AA}$.

[67LID/KUC]

Lide and Kuczkowski studied the microwave spectra of gaseous CsOH and CsOD. The spectra were interpreted in terms of a linear molecule or nonlinear one with a large-amplitude low-frequency bending vibration. The ν_2 bending mode was assumed to be in the range $250\text{--}350 \text{ cm}^{-1}$ with a high degree of anharmonicity; the ν_1 stretching mode was estimated as $400 \pm 80 \text{ cm}^{-1}$. For CsOH, the rotational constant $B_0 = 5501.08 \text{ MHz}$ (0.183496 cm^{-1}) and corresponding bond distances $r_0(\text{Cs–O}) = 2.403 \text{ \AA}$ and $r_0(\text{O–H}) = 0.920 \text{ \AA}$ were calculated. The equilibrium values were calculated as 2.395 \AA and 0.969 \AA , respectively.

[68ACQ/ABR] (see also [67ACQ/ABR])

Acquista *et al.* investigated the IR spectra of CsOH and CsOD in the Ar matrix and assigned a band at 335.6 cm^{-1} to

the Cs–O stretching mode and a band at 309.8/304.2(shoulder)/302.4 cm^{-1} to the Cs–O–H bending mode of a linear CsOH. The frequency of the O–H stretching vibration was estimated in the neighborhood of 3600 cm^{-1} .

[69LID/MAT]

Lide and Matsumura applied a new approach to the vibration-rotation interaction in linear triatomic molecules to explain the anomalies found in the microwave spectrum of CsOH [67LID/KUC] and refined the values of the equilibrium bond lengths in the molecule: $r(\text{Cs–O}) = 2.391(2)$ Å and $r(\text{O–H}) = 0.960(10)$ Å.

[69TIM/KRA]

Timoshinin and Krasnov estimated molecular constants using empirical approaches and literature data.

[70HOU/BUN]

Hougen *et al.* derived an expression of the vibration-rotation Hamiltonian for any triatomic molecule. The procedure was applied for the microwave data on CsOH and CaOD [67LID/KUC] and it resulted in the calculation of force constants, harmonic frequencies and bending vibration-rotation constants for four various approximations of the force field.

[70JEN]

Jensen reinterpreted the equilibrium data [66JEN/PAD] assuming a linear configuration for CsOH with the molecular constants from [67LID/KUC] and [68ACQ/ABR].

[71KEL/PAD]

Kelly and Padley accepted a linear structure and selected molecular constants from literature data.

[78BEL] (see also [91BEL2])

Belyaeva investigated the IR spectra of CsOH and CsOD in the Ne, Ar, Kr, and Xe matrices at 8 K in the range 200–4000 cm^{-1} . Analysis of the spectra was carried out on the assumption that in gaseous phase there are linear monomeric molecules of cesium hydroxide. The assignment was made for the stretching Cs–O [a band at 336/334(shoulder) cm^{-1}], bending Cs–O–H (a band at 310/304.5/302 cm^{-1}), and stretching O–H (a band at 3705 cm^{-1}) vibrations.

[78LOV]

Lovas in his review of microwave spectra recommended equilibrium bond lengths $r_e(\text{Cs–O}) = 2.391(2)$ Å and $r_e(\text{O–H}) = 0.960(10)$ Å according to [69LID/MAT].

[82GUR/VEI]

Gurvich *et al.* adopted a linear structure. The rotational constant B_0 was taken from [67LID/KUC], the vibrational frequencies were selected on the basis of IR Ar matrix spectral data [68ACQ/ABR, 78BEL].

[84OGD/BOW]

Ogden and Bowsher briefly reported the results of matrix isolation IR spectral studies performed on CsOH. The bands at 316, 310, and 304 cm^{-1} in Ar matrix and 330 and 316 cm^{-1} in N matrix were detected.

[85CHA/DAV]

Chase *et al.* adopted a linear configuration with the equi-

librium bond lengths obtained by Lide and Matsumura [69LID/MAT] from microwave spectrum and vibrational frequencies ν_1 and ν_2 obtained by Acquista *et al.* [69ACQ/ABR] from IR spectra in Ar matrix. The value of ν_3 was taken as estimated by Jensen [70JEN].

[86BAU/LAN]

Bauschlicher *et al.* calculated *ab initio* the values of $r(\text{Cs–O})$, $\nu(\text{Cs–O})$, and $D_0^\circ(\text{Cs–OH})$ of CsOH in the linear ground electronic state assuming the rigid OH subunit with a fixed O–H distance 0.9472 Å. The calculations were made using both the self-consistent field (SCF) and singles-plus-doubles configuration (CISD) levels and extended Gaussian basis set of at least triple-zeta plus double polarization quality.

[86LUT/HEN] (see also [82LUT/ECK])

Lutz *et al.* investigated the IR and Raman spectra of solid CsOH and CsOD at 95 and 300 K in the range 200–4000 cm^{-1} and assigned the O–H(D) stretching frequencies of these molecules.

[87ALL/VEN]

Alltman *et al.* in the review on molecular constants of triatomic molecules recommended for CsOH the geometry and vibrational frequencies from the literature data.

[90KON]

Konings investigated the IR spectrum of CsOH vapors at 875 K in the region 50–609 cm^{-1} . Two strong absorption maxima at 336 ± 2 and 230 ± 1 cm^{-1} were assigned to ν_1 (Cs–O stretching) and ν_2 (Cs–O–H bending) fundamentals of linear CsOH.

[91KON/BOO]

Konings *et al.* investigated IR spectra of CsOH and CsOD at 875 K in the range 50–600 cm^{-1} . The strong adsorption band observed for each molecule at 340–360 cm^{-1} could not be interpreted straight forwardly, but the authors came to the conclusion that $\nu_1 = 360 \pm 10$ cm^{-1} (the Cs–O stretching mode) and $\nu_2 = 320 \pm 20$ cm^{-1} (the Cs–O–H bending mode).

The molecular constants of CsOH, measured, calculated, estimated, or accepted in above-named studies, are listed in Table 57.

Discussion of the Molecular Constants of CsOH(g)

Prior to experimental and theoretical investigations of the molecular constants of CsOH, some empirical estimates were made, particularly by Smith and Sugden [53SMI/SUG] for a linear structure and by Jensen and Padley [66JEN/PAD] for a nonlinear one (later Jensen [70JEN] adopted a linear structure). Lide with co-workers [66KUC/LID, 67LID/KUC, 69LID/MAT] carried out a thorough study of the microwave spectra of CsOH and CsOD and came to the conclusion that the molecule is linear. This conclusion was supported by the theoretical analysis made by Hougen *et al.* [70HOU/BUN]. The result of an *ab initio* calculation [86BAU/LAN] for the Cs–O bond length satisfactorily agrees with the microwave data. As for the O–H distance, which is suspiciously short in the ground vibrational state (0.920 Å), the authors [67LID/

KUC] connected that with an unusual large amplitude of the bending mode.

The vibrational frequencies were determined both in vapor [90KON, 91KON/BOO] and in Ar matrix [67ACQ/ABR, 68ACQ/ABR, 78BEL, 91BEL]. The assignments of the Cs–O stretching frequency, ν_1 , made in [67ACQ/ABR, 68ACQ/ABR] (335.6 cm^{-1}), [78BEL, 91BEL] (336 cm^{-1}), and [90KON] (336 cm^{-1}), practically coincide. The values of the Cs–O–H bending frequency, ν_2 , found in the Ar matrix studies [67ACQ/ABR, 68ACQ/ABR] (302.4 cm^{-1}) and [78BEL, 91BEL] (306 cm^{-1}), are also in good agreement. These values of ν_1 and ν_2 are well supported by the results of matrix isolation spectral investigation performed by Ogden and Bowsher [84OGD/BOW]. The assignment of the band at 230 cm^{-1} to ν_2 made in [90KON], was obviously incorrect because this value does not match with those for the other alkali metal hydroxides. The later investigation of IR spectra of CsOH and CsOD vapors [91KON/BOO] did not provide more reliable results. The authors [91KON/BOO] interpreted a wide absorption band as overlapping ν_1 and ν_2 and estimated $\nu_1 = 360\text{ cm}^{-1}$ and $\nu_2 = 320\text{ cm}^{-1}$ without many grounds for that. The values of ν_1 and ν_2 reported in [67LID/KUC] on the basis of the microwave spectral data, also should be considered as rough estimates. The values of ν_1 for CsOH, calculated by Bauschlicher *et al.* [86BAU/LAN] in two *ab initio* levels, are somewhat overestimated similar to the other alkali hydroxide molecules. As to the O–H stretching frequency, ν_3 , which was never observed in matrices or vapor for the other alkali metal hydroxides due to overlapping strong H_2O spectrum, Belyaeva [78BEL, 91BEL] apparently succeeded in assigning a very weak band at 3705 cm^{-1} in Ar matrix spectrum to this frequency.

Selection of the molecular constants of CsOH for calculation of the thermal functions in the present work is entirely based on reliable experimental data. The structural parameters are determined in the microwave spectral investigations by Lide with co-workers [66KUC/LID, 67LID/KUC, 69LID/MAT]; the vibrational frequencies are taken from the IR spectral studies in Ar matrix [67ACQ/ABR, 69ACQ/ABR, 78BEL, 91BEL]. These values of the molecular constants were supported by the sophisticated force field calculations performed by Hougen *et al.* [70HOU/BUM].

The ground electronic state of linear CsOH ($C_{\infty v}$ symmetry) is $^1\Sigma^+$. There are no data on the existence of low-lying excited electronic states of CsOH, nor are any expected.

The molecular constants of CsOH, adopted in the present work for calculation of the thermal functions, are summarized below:

$$r_o(\text{Cs–O}) = 2.403 \pm 0.002 \text{ \AA}; r_o(\text{O–H}) = 0.920 \pm 0.10 \text{ \AA};$$

$$\angle(\text{Cs–O–H}) = 180^\circ;$$

$$I = (15.255 \pm 0.030) 10^{-39} \text{ g cm}^2;$$

symmetry number: $\sigma = 1$; statistical weight: $p_x = 1$;

$$\nu_1 = 335.6 \pm 10 \text{ cm}^{-1}, d_1 = 1;$$

$$\nu_2 = 306 \pm 10 \text{ cm}^{-1}, d_2 = 2;$$

$$\nu_3 = 3705 \pm 100 \text{ cm}^{-1}, d_3 = 1.$$

Calculation of the CsOH(g) Thermal Functions

The thermal functions of CsOH(g) in the standard state are calculated in the ‘‘rigid rotor harmonic oscillator’’ approximation with low-temperature quantum corrections according to the equations given in [89GUR/VEY]. The molecular constants of CsOH used in calculation are given in the previous subsection. The calculated values of $C_p^\circ(T)$, $\Phi^\circ(T)$, $S^\circ(T)$, and $H^\circ(T) - H^\circ(0)$ at the temperatures 0–6000 K are given in Table 63.

The uncertainties in the calculated thermal functions of CsOH(g) are due to the uncertainties in the adopted molecular constants. At high temperatures the uncertainties due to the approximate method of calculation become more substantial. These uncertainties are estimated on the basis of the differences between the thermal functions for the linear triatomic molecules (N_2O , CO_2 , CS_2 , OCS , HCN , FCN , and ClCN), calculated in [89GUR/VEY, 91GUR/VEY] in the ‘‘nonrigid rotor–anharmonic oscillator’’ approximation, and those calculated in the ‘‘rigid rotor–harmonic oscillator’’ approximation. The total uncertainties in the thermal function of CsOH(g) are presented in Table 63.

The thermal functions of CsOH(g) were calculated earlier in [82GUR/VEI] and [85CHA/DAV] in the range 100–6000 K. The comparison of the thermal function calculated in the present work and in [82GUR/VEI] and [85CHA/DAV] for CsOH(g) is shown in Table 58. The differences are very small when compared with [82GUR/VEI] and slightly larger for [85CHA/DAV]. These differences are due to insignificant discrepancies between the adopted molecular constants in the calculations.

Enthalpy of Formation of CsOH(g)—Experimental Investigations of Equilibria in Flames

[53SMI/SUG]

Smith and Sugden calculated the difference in dissociation energies of lithium and cesium hydroxides from the $([\text{LiOH}]/[\text{Li}])/([\text{CsOH}]/[\text{Cs}])$ temperature dependence in flames with alkali compounds added: $D_0^\circ(\text{Li–OH}) - D_0^\circ(\text{Cs–OH}) = 11.0\text{ kcal mol}^{-1}$. Using the value $D_0^\circ(\text{Li–OH}) = 102 \pm 1\text{ kcal mol}^{-1}$ obtained in the same work, they selected as the most probable the value $D_0^\circ(\text{Cs–OH}) = 91 \pm 1\text{ kcal mol}^{-1}$ ($381 \pm 4\text{ kJ mol}^{-1}$).

[66JEN/PAD], [70JEN]

Jensen and Padley performed measurements of potassium hydroxide formation in $\text{H}_2 + \text{O}_2 + \text{N}_2$ flames. The suppressed-ionization techniques used in the case of sodium and potassium appeared inappropriate to obtain $[\text{CsOH}]/[\text{Cs}]$ value: even at the highest concentration of rubidium introduced into the flame, together with cesium, the ionization of the latter was not sufficiently suppressed. Hence, it was not possible to obtain the hydroxide concentration as a difference between total concentration of cesium in a flame and photometrically measured concentration of cesium atoms. Instead, the experimental evidence was used that H, Cs^+ and

TABLE 57. Bond lengths (Å), angle (deg), and vibrational frequencies (cm⁻¹) of CsOH in the ground electronic state

Reference	<i>r</i> (Cs–O)	<i>r</i> (O–H)	<(Cs–O–H)	<i>ν</i> ₁	<i>ν</i> ₂ (2)	<i>ν</i> ₃	Note
[53SMI/SUG]	2.78	0.97	180	300	300	...	a
[66JEN/PAD]	2.75	0.96	117	330	1300	3610	a
[66KUC/LID]	2.40	0.95	180	b
[67LID/KUC]	2.403	0.920	180	400	300	...	c
[68ACQ/ABR]	180	335.6	306	36000	d
[69LID/MAT]	2.391	0.967	180	b
[69TIM/KRA]	2.40	0.97	180	...	355	3740	e
[0HOU/BUN]	180	335.5	307.7	3548.5	f
[70HOU/BUN]	180	335.5	306.1	3500.7	f
[70HOU/BUN]	180	322.6	307.7	3728.1	f
[70HOU/BUN]	150	351.8	307.7	3704.2	f
[70JEN]	2.40	...	180	336	310	34120	a
[71KEL/PAD]	2.40	0.96	180	333.6	309.8	3600	a
[78BEL]	180	336	305.5	3705	d
[78LOV]	2.391	0.960	180	g
[82GUR/VEI]	2.403	0.920	180	336	306	3705	h
[85CHA/DAV]	2.391	0.96	180	306.5	306	3610	i
[86BAU/LAN]	2.448	0.9472	180	350	i
[86BAU/LAN]	2.419	0.9472	180	378	k
[86LUT/HEM]	3562	l
[87ALI/VEN]	2.391	0.960	180	336	306	3705	m
[90KON]	180	336	230	...	n
[91KON/BOO]	180	360	320	...	n
Accepted in present work	2.403	0.920	180	335.6	306	3705	o

^aEstimated using literature data.^bMicrowave spectrum; *r*_e structure.^cMicrowave spectrum; *r*₀ structure; *ν*₁ and *ν*₂ are estimated.^dIR spectrum in Ar matrix.^eBond lengths from [66KUC/LID]; *ν*₂ and *ν*₃ are estimated.^fForce field calculation in four approximations using experimental data [67LID/KUC] and [68ACQ/ABR].^gFrom [69LID/MAT].^h*r*₀ structure from [69LID/KUC]; frequencies from [78BEL].ⁱ*r*_e structure from [67LID/KEJC]; *ν*₁ and *ν*₂ from [58ACQ/ABR]; *ν*₃ estimated in [70JEN].^jSCF *ab initio* calculation.^kCI(SD) *ab initio* calculation.^lIR and Raman spectrum of crystal.^mFrom literature data.ⁿIR spectrum of gas.^o*r*₀ structure from [69LID/KUC]; *ν*₁ and *ν*₂ from [68ACQ/ABR]; *ν*₃ from [78BEL].

Cs concentrations all achieved almost steady values at a height of about 3 cm above the reaction zone of principal flame (designated 3.4/1/2), and were therefore very close to their equilibrium values. Electron concentration (equal to Cs⁺ concentration) was measured by means of a resonant cavity. Cesium concentration was calculated from the ionization equilibrium constant and the value (CsOH/[Cs] = 2.1 ± 0.6) was obtained. To this value corresponds the equilibrium constant *K*^o(2475 K) = 0.065 for the reaction



A third-law calculation performed in [66JEN/PAD] using a bent hydroxide molecule model resulted in the value *D*₀^o(Cs–OH) = 91 ± 3 kcal mol⁻¹ (381 ± 12 kJ mol⁻¹).

Jensen [70JEN] recalculated the *D*₀^o(Cs–OH) value using a linear model for the CsOH molecule. He found results of

TABLE 58. Differences (J K⁻¹ mol⁻¹) between the thermal functions of CsOH(g) calculated in the present work and in [82GUR/VEI, 85CHA/DAV]

<i>T</i> /K	[Present Work]-[82GUR/VEI] ^a			[Present Work]-[85CHA/DAV] ^b		
	$\Delta C_p^o(T)$	$\Delta \Phi^o(T)$	$\Delta S^o(T)$	$\Delta C_p^o(T)$	$\Delta \Phi^o(T)$	$\Delta S^o(T)$
298.15	0.003	0.005	0.008	0.000	0.056	-0.052
1000	0.006	0.009	0.012	-0.099	0.052	0.028
2000	0.007	0.011	0.017	-0.123	0.015	-0.061
3000	0.004	0.013	0.019	-0.078	-0.018	-0.102
4000	0.002	0.015	0.020	-0.050	-0.041	-0.120
5000	0.002	0.017	0.020	-0.034	-0.058	-0.130
6000	0.001	0.017	0.021	-0.025	-0.007	-0.135

^aThe values of $\Phi^o(T)$ and $S^o(T)$ tabulated in [82GUR/VEI] are recalculated to standard pressure 0.1 MPa.^bThe values of $\Phi^o(T)$ tabulated in [85CHA/DAV] are adjusted to the reference temperature *T* = 0 instead of 298.15 K.

calculations for both models to be close and recommended the value $D_0^\circ(\text{Cs-OH}) = 380 \pm 12 \text{ kJ mol}^{-1}$.

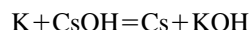
[69COT/JEN]

Cotton and Jenkins determined $D_0^\circ(\text{Cs-OH})$ value using measurements of the concentration of cesium atoms by atomic absorption spectroscopy as a function of hydrogen atom concentration in a set of six isothermal hydrogen-rich, hydrogen-oxygen-nitrogen flames of different composition. Equilibrium constant values for reaction (7) were evaluated from the slope-to-intercept ratio of a linear fit of relative metal atom vs hydrogen-atom concentration. The mean value $K^\circ(1570 \text{ K}) = 9.0 \cdot 10^{-4}$ was obtained for the equilibrium constant of reaction (7). Third-law calculations carried out with the data from the JANAF Tables (1961) for a bent model of CsOH molecule resulted in the value $D_0^\circ(\text{Cs-OH}) = 90 \pm 2 \text{ kcal mol}^{-1}$ ($377 \pm 8 \text{ kJ mol}^{-1}$).

Enthalpy of Formation of CsOH(g)—Mass Spectrometric Studies of Equilibria

[69GOR/GUS], see also [70GOR/GUS]

Gorokhov *et al.* studied the gaseous equilibrium



at temperatures 795, 997, and 1044 K (12 points). K^+ , KOH^+ , Cs^+ , and CsOH^+ ion currents were measured at 50 eV electron energy for the temperatures 997 and 1044 K. In the case of measurements at 795 K, the electron energy was reduced to 6 eV, to eliminate fragmentation of KOH and CsOH molecules with formation of atomic ions. Thermal functions for KOH and CsOH calculated by Dr. Yungman for a linear model of MOH molecules were used in the third-law treatment of data. The following value was obtained: $D_0^\circ(\text{Cs-OH}) - D_0^\circ(\text{K-OH}) = 7.63 \pm 1.1 \text{ kcal mol}^{-1}$ ($31.9 \pm 4.6 \text{ kJ mol}^{-1}$). The total uncertainty indicated was calculated taking into account twice standard deviation and uncertainties in ionization cross sections and in temperature measurements. The equilibrium constant values are listed in Table 59.

Combining the value $D_0^\circ(\text{Cs-OH}) - D_0^\circ(\text{K-OH}) = 7.63 \pm 1.1 \text{ kcal mol}^{-1}$ with that from appearance energy measurements, $6 \pm 1 \text{ kcal mol}^{-1}$, a slightly rounded value $7 \pm 1 \text{ kcal mol}^{-1}$ was recommended in [69GOR/GUS]. Combining this value with the dissociation energy recommended, $D_0^\circ(\text{KOH}) = 82 \pm 3 \text{ kcal mol}^{-1}$, the authors [69GOR/GUS] adopted the value $D_0^\circ(\text{CsOH}) = 89 \pm 3 \text{ kcal mol}^{-1}$ ($372 \pm 12 \text{ kJ mol}^{-1}$) as the most reliable.

[88BLA/JOH]

Blackburn and Johnson carried out a mass spectrometric study of cesium hydroxide vaporization. The sensitivity calibration of the apparatus was performed through the weight loss measurement of the sample in the Knudsen effusion experiment with the simultaneous measurements of Cs^+ , CsOH^+ , and Cs_2OH^+ ion currents at ionizing electron energy of 30 eV. The ratio of dimer to monomer ionization cross sections was assumed to be 2. Partial pressures of CsOH(g) were obtained in the range 654–772 K (13 points). Using thermal functions from the JANAF Tables [74CHA/

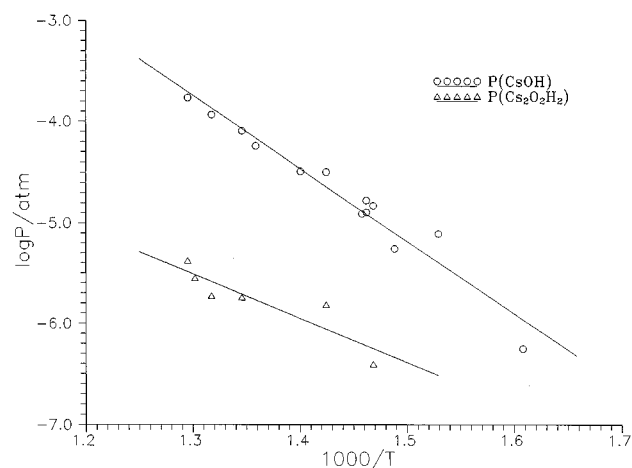


Fig. 13. Partial pressures of monomer and dimer over CsOH(liqu) [88BLA/JOH].

CUR] the enthalpy of monomer vaporization and the enthalpy of formation of CsOH(g) were obtained: $\Delta_s H^\circ(298.15 \text{ K}) = 36.330 \pm 0.448 \text{ kcal mol}^{-1}$ ($152.00 \pm 1.87 \text{ kJ mol}^{-1}$); $\Delta_f H^\circ(\text{CsOH}, \text{g}, 298.15 \text{ K}) = -60.7 \pm 0.5 \text{ kcal mol}^{-1}$ ($-254.0 \pm 2 \text{ kJ mol}^{-1}$). The partial pressures of CsOH(g) are listed in Table 60 and are presented in Fig. 13.

Enthalpy of Formation of CsOH(g)—Experimental Determinations of the Total Vapor Pressure

[88KON/COR2]

Konings and Cordfunke measured vapor pressure of cesium hydroxide using the transpiration method. In several experiments the carrier gas (argon) was saturated with water vapor. 31 measurements were carried out in the temperature range 675.7–975.6 K. The authors [88KON/COR2] found that the presence of water vapor had no influence on the CsOH vapor pressure, thus indicating the congruent vaporization of the hydroxide. Assuming only gaseous monomeric species to be present, the vapor pressure over liquid CsOH was represented with the equation:

$$\log(P/\text{Pa}) = -(6414 \pm 148) \cdot (T/\text{K})^{-1} + (9.769 \pm 0.180).$$

The third-law enthalpy of sublimation was calculated in [88KON/COR2] using thermal functions from the reference book [82GUR/VEI]: $\Delta_s H^\circ(298.15 \text{ K}) = 158.2 \pm 0.7 \text{ kJ mol}^{-1}$. The vapor pressure values are listed in Table 61 and are presented in Fig 14.

Enthalpy of Formation of CsOH(g)—Miscellaneous Data

[67EME/GUS]

Emelyanov *et al.* studied the ionization of cesium hydroxide molecules by electron impact. Cesium peroxide sample contaminated with cesium hydroxide was used as a source of cesium hydroxide vapors. Cesium peroxide was obtained by thermal decomposition of partly hydrolyzed cesium superoxide directly in the platinum effusion cell. Beginning from the temperature $\approx 400 \text{ }^\circ\text{C}$, Cs^+ (8), CsOH^+ (1), Cs_2^+ (0.1), Cs_2O^+ (0.1), and Cs_2OH^+ (1.0) ions were detected in the

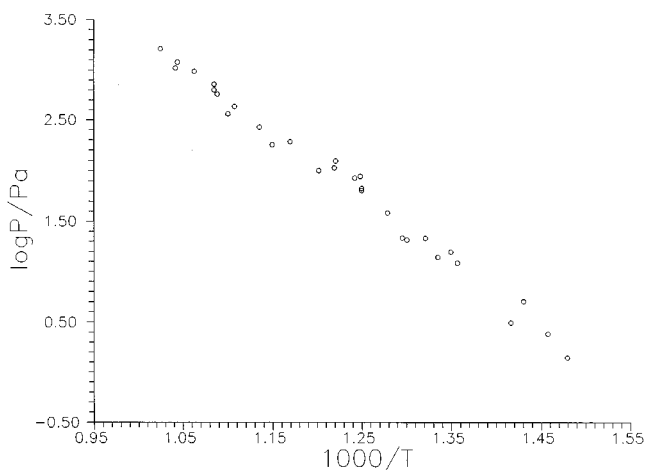


FIG. 14. Apparent pressure of CsOH(g) over CsOH(liq) [88KON/COR2].

mass spectrum (relative intensities are given in parentheses). Formation of Cs^+ ions with the appearance energy of 7.46 ± 0.14 eV was attributed to fragmentation of CsOH molecules under electron impact:



Combining this value of appearance energy with the ionization energy of atomic cesium (3.89 eV), the value $D_0^\circ(\text{Cs}-\text{OH}) = 3.57 \pm 0.14$ eV = 82 ± 3 kcal mol⁻¹ (344 ± 12 kJ mol⁻¹) was calculated.

[69GOR/GUS], see also [70GOR/GUS]

Gorokhov *et al.* performed mass spectrometric measurements of appearance energies of ions in mass spectra of potassium and cesium hydroxides. The value $D_0^\circ(\text{Cs}-\text{OH}) = 86 \pm 3$ kcal mol⁻¹ (358 ± 12 kJ mol⁻¹) was calculated from the appearance energy of Cs^+ ion, $\text{AE}(\text{Cs}^+/\text{CsOH}) = 7.6 \pm 0.15$ eV. Combining this dissociation energy with the value $D_0^\circ(\text{K}-\text{OH}) = 80 \pm 3$ kcal mol⁻¹ obtained in the same work, the authors [69GOR/GUS] adopted the value $D_0^\circ(\text{Cs}-\text{OH}) - D_0^\circ(\text{K}-\text{OH}) = 6 \pm 1$ kcal mol⁻¹ (23 ± 4 kJ mol⁻¹). Uncertainty in the difference of dissociation energies was assumed to be close to reproducibility error, 0.05 eV, due to close values of appearance energies for K^+ and Cs^+ ions and mutual compensation of systematic errors.

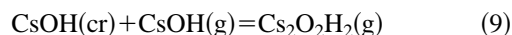
[86BAU/LAN]

Bauschlicher *et al.* calculated dissociation energies of the alkali hydroxide molecules MOH into M^+ and OH^- ions by *ab initio* methods at both the self-consistent-field (SCF) and singles plus doubles configuration-interaction level (CI(SD)) using extended Gaussian basis sets of at least triple zeta plus double polarization quality. As the "best," $D_0^\circ(\text{Cs}-\text{OH}) = 3.78 \pm 0.10$ eV (365 ± 10 kJ mol⁻¹) was chosen, as calculated from the value $D_e(\text{Cs}-\text{OH}) = 3.77$ eV (CI(SD) level) with zero-point correction taken equal to -0.06 eV and a correction of 0.07 eV based upon the errors in the computed bond lengths. (The computed bond lengths were slightly too long and bond energies were slightly underestimated.)

Discussion of the Enthalpy of Formation of CsOH(g)

The authors of this review have recalculated all equilibria from the papers discussed in the previous with the thermal functions from this work and with auxiliary data from [82GUR/VEI] and [89GUR/VEY]. The recalculated values of enthalpies of reactions and the values of enthalpy of formation of CsOH(g) are collected in Table 62.

Similar to the case of KOH(g), the high temperatures employed in studies of equilibria in flames ([53SMI/SUG], [66JEN/PAD], and [69COT/JEN]) resulted in a significant increase of uncertainties for the 3rd-law enthalpies of reactions. Results of the condensed phase-gas equilibria studies [88BLA/JOH] and [88KON/COR2], performed at substantially lower temperatures, seem to be more appropriate for selecting the enthalpy of formation. To calculate the enthalpy of sublimation from the results of transpiration measurements, it is necessary to have information on the dimer to monomer ratio in the vapor of cesium hydroxide. This information can be gained from the mass spectrum of cesium hydroxide vapor. The following ratios of ion intensities $\text{Cs}^+ : \text{CsOH}^+ : \text{Cs}_2\text{OH}^+$ were obtained for $T \approx 700$ K: 5.3:1.0:6.8 [59SCH/POR]; 8:1:1 [67EME/GUS]; 50:1:0.06 [88BLA/JOH]. Taking into account that Cs^+ and CsOH^+ ions result from CsOH fragmentation and assuming the ratio of ionization cross sections $\sigma(d)/\sigma(m) = 1.5$, the following estimates of $P(d)/P(m)$ values were obtained: [59SCH/POR], 0.7; [67EME/GUS], 0.07; [88BIA/JOH], $\approx 10^{-3}$. The ion intensity ratio from the [88BLA/JOH] seems to be significantly distorted, probably due to mass discrimination effects of the quadrupole mass analyzer. The value $P(d)/P(m) = \approx 0.03$ employed in [88BLA/JOH] was apparently calculated from the $\text{Cs}_2\text{OH}^+ : \text{CsOH}^+$ ion intensity ratio, without taking into account Cs^+ ion intensity. Very probably the spectrum obtained in [67EME/GUS] corresponds to unsaturated vapor, because a partially hydrolyzed cesium peroxide was used as a source of cesium hydroxide vapor. At the same time the value $P(d)/P(m) = 0.7$ seems to be too high on the ground of comparison with the potassium hydroxide vapor composition. As a compromise, the value $P(d)/P(m) = 0.2$ was accepted, corresponding to the geometrical mean of the minimum and maximum values, 0.07 and 0.7. The third-law value $\Delta_r H^\circ(0) = 21.2 \pm 5$ kJ mol⁻¹ for the enthalpy of reaction



was calculated using this estimate of $P(d)/P(m)$.

The value of $\Delta_r H^\circ(0 \text{ K})$ so obtained was employed in calculation of monomer and dimer partial pressures from the data of transpiration experiments [88KON/COR2]. The enthalpy of sublimation for the monomer $\Delta_r H^\circ(0 \text{ K}) = 162.5 \pm 5$ kJ mol⁻¹, is in good agreement with the value $\Delta_r H^\circ(0 \text{ K}) = 163.9 \pm 5$ kJ mol⁻¹ calculated from the data [88BLA/JOH] corrected for the dimer content [due to low relative concentration of the dimer the enthalpy of sublimation for the monomer depends very weakly on the $P(d)/P(m)$ value]. From the papers annotated, results [88KON/COR2] and [88BLA/JOH] are the most reliable. A rounded mean value

of the CsOH enthalpy of sublimation from these papers is $\Delta_s H^\circ(0\text{ K}) = 163.0 \pm 5\text{ kJ mol}^{-1}$. To this value corresponds $\Delta_s H^\circ(298.15\text{ K}) = 160.7 \pm 5\text{ kJ mol}^{-1}$. Combining this latter value with the adopted enthalpy of formation of CsOH(cr), the enthalpy of formation $\Delta_f H^\circ(\text{CsOH,g}, 298.15\text{ K}) = 255.5 \pm 5\text{ kJ mol}^{-1}$ was obtained. Corresponding value for $T = 0\text{ K}$ is $\Delta_f H^\circ(\text{CsOH,g}, 0\text{ K}) = -251.0 \pm 5\text{ kJ mol}^{-1}$. Most other values in Table 67 are in good agreement with that given above. A more negative value calculated from exchange reaction between K(g) and CsOH(g) [69GOR/GUS] is probably due to difficulties in evaluation of equilibrium constants from ion intensities, especially for molecules inclined to deep fragmentation under electron impact. Measurements of appearance energy of ions [67EME/GUS] resulted in a more positive value $\Delta_f H^\circ(\text{CsOH,g}, 0\text{ K}) = -226 \pm 12\text{ kJ mol}^{-1}$ possibly because of some errors in calibration of electron energy scale using a standard (Xe^+) with the appearance energy substantially higher than that for ions under study (Cs^+). Results of appearance energy measurements [69GOR/GUS] and of *ab initio* calculation [86BAU/LAN] are in good agreement with the most reliable data [88KON/COR2] and [88BLA/JOH].

On the basis of the above discussion, the values

$$\Delta_f(\text{CsOH,g}, 298.15\text{ K}) = -256.0 \pm 5\text{ kJ mol}^{-1};$$

$$D_0^\circ(\text{Cs-OH}) = 368.6 \pm 5\text{ kJ mol}^{-1}$$

are adopted in this review.

4.2.2. Appendix. Tables of Experimental and Evaluated Data for CsOH(g)

TABLE 59. Equilibrium constant values for the reaction $\text{Cs(g)} + \text{KOH(G)} = \text{K(g)} + \text{CsOH(g)}$, [69GOR/GUS]

No.	T/K	K°
1	795	71.3
2	795	65.0
3	795	70.0
4	795	126
5	997	58.4
6	997	77.0
7	997	59.1
8	997	78.1
9	997	86.6
10	997	128
11	1044	46.6
12	1044	80.4

TABLE 60. Partial pressure of CsOH(g) over CsOH(liq), [88BLA/JOH]

No.	T/K	P/(atm 10^5)
1	654	0.782
2	684	1.68
3	684	1.28
4	686	1.24
5	714	3.23
6	622	0.0560
	13	772
7	672	0.553
8	736	5.70
9	759	11.6
10	702	3.19
11	681	1.49
12	743	8.04
13	772	17.1

TABLE 61. Apparent vapor pressure over cesium hydroxide, [88KON/COR2]

No.	T/K	P/Pa
1	675.7	1.40
2	686.4	2.42
3	699.1	5.08
4	705.6	3.13
5	737.3	12.22
6	756.9	21.50
7	769.4	20.73
8	781.6	38.34
9	799.6	67.16
10	801.3	88.29
11	804.8	85.09
12	819.4	124.57
13	820.0	106.76
14	854.6	191.77
15	880.5	267.36
16	902.6	432.60
17	919.4	575.43
18	922.2	723.88
19	922.3	720.23
20	922.4	633.74
21	940.8	972.77
22	958.1	1199.93
23	975.6	1627.13
24	741.4	15.71 ^a
25	748.8	13.96 ^a
26	771.6	21.62 ^a
27	800.0	64.03 ^a
28	832.4	100.38 ^a
29	869.8	178.96 ^a
30	909.3	364.59 ^a
31	959.7	1048.40 ^a

^aCarrier gas saturated with water vapor.

TABLE 62. Results of determination of $\Delta_f H^\circ(\text{CsOH}, \text{g}, 0 \text{ K})$, kJ mol^{-1}

Reference	Method	$\Delta_f H^\circ(0 \text{ K})$		$\Delta_f H^\circ(0 \text{ K})$
		2nd law	3rd law	
Equilibria in flames				
[53SMI/SUG]	Ionization in flames, $\text{Cs}(\text{g}) + \text{LiOH}(\text{g}) = \text{Li}(\text{g}) + \text{CSOH}(\text{g})$	42	...	-265 ± 10
[66JEN/PAD]	Flame photometry, $\text{Cs}(\text{g}) + \text{H}_2\text{O}(\text{g}) = \text{CsOH}(\text{g}) + \text{H}(\text{g})$, 2475 K (one point)	...	112.3	-264.6 ± 10
[69COT/JEN]	Flame photometry, $\text{Cs}(\text{g}) + \text{H}_2\text{O}(\text{g}) = \text{CsOH}(\text{g}) + \text{H}(\text{g})$, 1570 K (six points)	...	119.0	-257.9 ± 8
Mass spectrometric studies of equilibria				
[69GOR/GUS]	Knudsen effusion mass spectrometry, $\text{Cs}(\text{g}) + \text{KOH}(\text{g}) = \text{CsOH}(\text{g}) + \text{H}(\text{g})$ (12 points)	-4 ± 13	-32.5 ± 2.5	-272 ± 10
[88BLA/JOH]	Knudsen effusion mass spectrometry, $\text{CsOH}(\text{liq}) = \text{CsOH}(\text{g})$, 622–772 K (13 points)	168 ± 20	163.9 ± 1.1	-250.1 ± 8
Total vapor pressure measurements				
[88KON/COR2]	Transpiration, $\text{CsOH}(\text{liq}) = \text{CsOH}(\text{g})$, 675.7–975.6 K (31 points)	156.1 ± 8	162.5 ± 0.6	-251.5 ± 10
Miscellaneous data				
[67EME/GUS]	Appearance energy of ions, $\text{CsOH}(\text{g}) = \text{Cs}(\text{g}) + \text{OH}(\text{g})$ (three points)	344 ± 12		-226 ± 12
[69GOR/GUS]	Appearance energy of ions, $\text{CsOH}(\text{g}) = \text{Cs}(\text{g}) + \text{OH}(\text{g})$ (13 points)	358 ± 12		-241 ± 12
	Appearance energy of ions, $\text{Cs}(\text{g}) + \text{KOH}(\text{g}) = \text{CSOH}(\text{g}) + \text{K}(\text{g})$	-23 ± 4		-263 ± 10
[86BAU/LAN]	<i>Ab initio</i> calculation, $\text{CsOH}(\text{g}) = \text{Cs}(\text{g}) + \text{OH}(\text{g})$	365 ± 10		-248 ± 10

TABLE 63. Thermodynamic properties at 0.1 MPa: CsOH(g)

T/K	C_p°	$-[G^\circ - H^\circ(0\text{ K})]/T$	S°	$H^\circ - H^\circ(0\text{ K})$	$\Delta_f H^\circ$	$\Delta_f G^\circ$
	J K ⁻¹ mol ⁻¹			kJ mol ⁻¹		
0	0.000	0.000	0.000	0.000	-251.549	-251.549
25	29.101	136.896	165.968	0.727	-251.751	-253.011
50	29.344	157.056	186.169	1.456	-252.384	-254.046
75	31.280	168.907	198.361	2.209	-253.060	-254.726
100	34.722	177.488	207.813	3.032	-253.617	-255.199
150	41.328	190.261	223.210	4.942	-254.424	-255.800
200	45.602	200.113	235.736	7.125	-255.006	-256.169
250	48.174	208.315	246.212	9.474	-255.505	-256.394
300	49.771	215.394	255.147	11.926	-256.022	-256.509
350	50.813	221.639	262.903	14.442	-256.692	-256.207
400	51.525	227.233	269.738	17.002	-259.222	-255.816
450	52.034	232.301	275.837	19.591	-259.710	-255.361
500	52.415	236.934	281.340	22.203	-260.161	-254.853
600	52.974	245.159	290.949	27.474	-260.980	-253.713
700	53.423	252.300	299.149	32.794	-261.721	-252.443
800	53.856	258.613	306.311	38.158	-262.423	-251.069
900	54.305	264.273	312.680	43.566	-263.123	-249.607
1000	54.774	269.406	318.426	49.020	-331.596	-244.369
1100	55.251	274.104	323.669	54.521	-331.449	-235.654
1200	55.725	278.438	328.497	60.070	-331.293	-226.952
1300	56.186	282.463	332.975	65.666	-331.129	-218.264
1400	56.625	286.222	337.155	71.306	-330.958	-209.587
1500	57.039	289.750	341.076	76.990	-330.783	-200.925
1600	57.424	293.074	344.770	82.713	-330.607	-192.273
1700	57.780	296.219	348.262	88.474	-330.431	-183.633
1800	58.108	299.203	351.574	94.268	-330.262	-175.003
1900	58.409	302.043	354.724	100.094	-330.105	-166.381
2000	58.684	304.753	357.727	105.949	-329.965	-157.769
2200	59.166	309.827	363.344	117.736	-329.753	-140.558
2400	59.569	314.505	368.510	129.610	-329.67	-123.362
2600	59.906	318.846	373.291	141.559	-329.787	-106.170
2800	60.190	322.895	377.742	153.569	-330.130	-88.956
3000	60.430	326.692	381.903	165.632	-330.752	-71.710
3200	60.634	330.266	385.809	177.739	-331.696	-54.413
3400	60.809	333.643	389.491	189.884	-332.995	-37.046
3600	60.960	336.843	392.971	202.061	-334.682	-19.589
3800	61.090	339.884	396.270	214.266	-336.782	-2.024
4000	61.203	342.783	399.407	226.496	-339.310	15.655
4200	61.303	345.551	402.395	238.747	-342.282	33.475
4400	61.390	348.200	405.249	251.016	-345.703	51.444
4600	61.467	350.740	407.980	263.302	-349.570	69.584
4800	61.536	353.180	410.597	275.602	-353.867	87.898
5000	61.597	355.527	413.111	287.916	-358.579	106.400
5200	61.652	357.789	415.528	300.241	-363.677	125.099
5400	61.701	359.971	417.855	312.576	-369.131	143.995
5600	61.745	362.078	420.100	324.921	-374.892	163.111
5800	61.785	364.117	422.267	337.274	-380.927	182.423
6000	61.821	366.090	424.363	349.634	-387.177	201.965
298.15	49.724	215.148	254.840	11.834	-256.000	-256.506
Uncertainties in Functions						
0	5.000	5.000
300	0.300	0.400	0.700	0.150	5.000	5.000
1000	0.500	0.700	1.000	0.300	5.000	5.000
2000	1.000	0.800	1.300	1.000	5.000	5.000
3000	1.500	1.000	1.700	2.000	6.000	5.000
4000	2.000	1.200	2.000	3.000	6.000	6.000
5000	2.500	1.400	2.500	6.000	8.000	8.000
6000	3.000	1.700	3.000	9.000	10.000	10.000

4.2.3. Cesium Hydroxide Dimer

Molecular Constants of [CsOH]₂(g)

[67BUE/STA]

Buechler *et al.* studied the deflection of Cs₂O₂H₂ molecular beam in an inhomogeneous electric field at 500 °C and found that the molecule was nonpolar which indicated a planar structure for at least the Cs₂O₂ part. On the basis of the similar result for sodium hydroxide, it was assumed that the alkali hydroxide dimers from sodium to cesium should have a planar rhomboid configuration.

[68ACQ/ABR] (see also [67ACQ/ABR])

Acquista *et al.* observed the IR spectra of CsOH and CsOD isolated in the Ar matrix and detected the absorption features which presumably were attributed to polymeric species of Cs₂O₂H₂. The authors [68ACQ/ABR] could not make definite assignments of these bands.

[78BEL] (see also [91BEL2])

Belyaeva investigated the IR spectra of Cs₂O₂H₂ and Cs₂O₂D₂ in the Ar matrix at 8 K in the range 50–4000 cm⁻¹ on the assumption that the cesium hydroxide dimer has a planar rhomboid configuration (D_{2h} symmetry). Taking into account the isotopic shifts and the data on spectra of the other alkali hydroxide dimers, Belyaeva assigned the observed bands to five fundamentals of the Cs₂O₂H₂ molecule. These are an out-of-plane bending and two in-plane stretching vibrations in the Cs–O–Cs–O ring, ν_7 (B_{1u}), ν_{10} (B_{2u}), and ν_{12} (B_{3u}), and two out-of-plane and in-plane bending O–H vibrations, ν_6 (B_{1u}) and ν_9 (B_{2u}). The ionic model calculation of the structural parameters and vibrational frequencies confirmed the assignment.

[82GUR/VEI]

Gurvich *et al.* adopted for Cs₂O₂H₂ a planar rhomboid configuration of D_{2h} symmetry with equilibrium structural parameters $r(\text{Cs–O})$ and $\angle(\text{O–Cs–O})$ as well as the frequencies $\nu_2 - \nu_5$ and ν_8 calculated by Belyaeva [78BEL] using the ionic model approximation. The frequencies ν_6 , ν_7 , ν_9 , ν_{10} , and ν_{12} were taken as measured in Ar matrix IR spectra [78BEL]. The values of $r(\text{O–H})$, ν_1 and ν_{11} were estimated.

[85CHA/DAV]

Chase *et al.* selected a C_{2h} configuration for Cs₂O₂H₂ similar to the model for Li₂O₂H₂ suggested by Berkowitz *et al.* [60BER/MES]. The O–H stretching and bending frequencies were taken the same as estimated in [60BER/MES] for Li₂O₂H₂. The other molecular constants of Cs₂O₂H₂ were estimated by comparison with related molecules including CsOH, Cs₂F₂, and H₂O.

[89GIR/LAP] (see also [89LAP])

Girichev and Lapshina investigated the structural parameters of the cesium hydroxide dimer, Cs₂O₂H₂ in vapor at 803 ± 10 K using the electron diffraction method. In analysis of the $sM(s)$ function the authors [89GIR/LAP] accepted the data on molecular constants of the monomeric molecule CsOH known in literature and assumed a planar configuration of Cs₂O₂H₂ with a rhomboid Cs₂O₂ part (D_{2h} symme-

try). The recommended effective structural parameters of Cs₂O₂H₂ were (bond lengths r_g and vibrational amplitudes l_g in Å): $r_g(\text{Cs–O}) = 2.62(11)$, $l_g(\text{Cs–O}) = 0.13(2)$, $r_g(\text{Cs–Cs}) = 3.95(3)$, $l_g(\text{Cs–Cs}) = 0.22(2)$, $r_g(\text{O–O}) = 2.87(58)$, $l_g(\text{O–O}) = 0.22(20)$, $r_g(\text{Cs–H}) = 3.28$, and $l_g(\text{Cs–H}) = 0.34(20)$. Using the IR spectral data [78BEL], the authors [89 GIR/LAP] calculated the equilibrium structural parameters and the fundamentals of the Cs₂O₂ part.

[91KON/BOO]

Konings *et al.* investigated the IR spectra of CsOH and CsOD at 875 K in the range 50–600 cm⁻¹ and assigned an adsorption feature at 230 cm⁻¹ to the in-plane Cs–O stretching mode, ν_{12} (B_{3u}), of Cs₂O₂H₂.

The molecular constants of Cs₂O₂H₂, measured, calculated, estimated, or accepted in above-named studies, are listed in Table 64.

Discussion of the Molecular Constants of [CsOH]₂(g)

A rhomboid planar configuration without hydrogen bonding was assumed for the Cs₂O₂H₂ molecule by Schoonmaker and Porter [59SCH/POR] although these authors did not exclude the possibility of a nonplanar configuration. Buechler *et al.* [67BUE/STA] studied the deflection of the Cs₂O₂H₂ molecular beam in an inhomogeneous electric field and came to the conclusion that at least a Cs₂O₂ part of the molecule was planar. The authors [67BUE/STA] predicted a planar rhomboid configuration for the molecule as a whole. This planar configuration of D_{2h} symmetry was confirmed by Belyaeva [78BEL, 91BEL] in the analysis of IR spectra of Cs₂O₂H₂ and Cs₂O₂D₂ in Ar matrix, supported by the ionic model calculation. Girichev and Lapshina [89GIR/LAP, 89LAP] came to the same conclusion as a result of the electron diffraction investigation of Cs₂O₂H₂ vapor. It should be noted however that the structural parameters of Cs₂O₂H₂, obtained in [89GIR/LAP, 89LAP], are not consistent with each other. The values of $r(\text{Cs–Cs})$ and $r(\text{O–O})$ (see Table 64) actually yield $\angle(\text{O–Cs–O}) = 72^\circ$ instead of 81.3° and $r(\text{Cs–O}) = 2.44$ Å instead of 2.62 Å. An overestimated value of $r(\text{O–H})$ (about 1.2 Å) is obtained from the value of $r(\text{Cs–H})$ given in [89GIR/LAP]. Nevertheless, the equilibrium value of $r(\text{Cs–O})$, calculated in [78BEL] and [89GIR/LAP, 89LAP], are in good agreement.

The Cs₂O₂H₂ molecule of D_{2h} symmetry similar to K₂O₂H₂ has 12 nondegenerate vibrational frequencies six of which are active in IR spectrum.

Belyaeva [78BEL, 91BEL] investigated IR spectrum of Cs₂O₂H₂ isolated in Ar matrix and assigned five bands to ν_6 , ν_7 , ν_9 , ν_{10} and ν_{12} . It should be noted that the assigned value of ν_7 for Cs₂O₂H₂ is unexpectedly larger than for Rb₂O₂H₂. There is no reasonable explanation of this anomaly (if the assignment was correct) but the matrix effect. In addition, Belyaeva [78BEL] calculated the frequencies of Cs₂O₂H₂ (except the O–H stretching frequencies, ν_1 and ν_{11}) using the ionic model.

The frequencies of the Cs₂O₂H₂ part (ν_2 , ν_3 , ν_5 , ν_7 , ν_{10} , and ν_{12}) were calculated by Girichev and Lapshina [89GIR/LAP, 89LAP] from a combined analysis of their

TABLE 64. Bond lengths (Å), angles (deg), and vibrational frequencies (cm⁻¹) of Cs₂O₂H₂ in the ground electronic state

Constant	[78BEL] ^a	[78BEL] ^b	[82GUR/VEI] ^c	[85CHA/DAV] ^d	[89GIR/LAP] ^e
<i>r</i> (Cs–O)	...	2.61	2.61	2.63	2.62
<i>r</i> (Cs–Cs)	3
<i>r</i> (O–O)	2.87
<i>r</i> (Cs–H)	3.28
<i>r</i> (O–H)	0.97	0.96	...
<(Cs–O–)	110	...
<(O–Cs–O)	...	92	92	90	81.3
$\nu_1(A_g)$	3700	3700	...
ν_2	...	275	275	299	251
ν_3	...	85.8	86	110	71
ν_4	...	275	275	1250	...
ν_5	...	185	185	210	282
ν_6	272	291	272	1250	...
ν_7	113	97.1	113	120	85
ν_8	...	281	281	1250	...
ν_9	278.5	278	278	1250	...
ν_{10}	227	217	227	220	253
ν_{11}	3700	3700	...
ν_{12}	235	238	235	230	255
Symmetry	D _{2h}	D _{2h}	D _{2h}	D _{2h}	D _{2h}
Constant	[91KON/BOO] ^f	Adopted in present work ^g			
<i>r</i> (Cs–O)	...	2.60			
<i>r</i> (Cs–Cs)			
<i>r</i> (O–O)			
<i>r</i> (Cs–H)			
<i>r</i> (O–H)	...	0.97			
<(Cs–O–H)			
<(O–Cs–O)	...	90			
$\nu_1(A_g)$...	3700			
ν_2	...	275			
ν_3	...	85			
ν_4	...	275			
ν_5	...	185			
ν_6	...	272			
ν_7	...	113			
ν_8	...	280			
ν_9	...	278.5			
ν_{10}	...	227			
ν_{11}	...	3700			
ν_{12}	...	235			
Symmetry	D _{2h}	D _{2h}			

^aIR spectrum in Ar matrix.^bIonic model calculation.^c ν_6 , ν_7 , ν_9 , ν_{10} and ν_{12} from IR spectrum in Ar matrix [78BEL]; ν_2 - ν_5 , ν_8 and structural parameters from ionic model calculation [78BEL]; ν_1 , ν_{11} , and *r*(O–H) are estimated.^dEstimated.^e r_g structure from electron diffraction measurements; the frequencies from combined treatment of electron diffraction data and IR spectral data [78BEL]; authors [86GIR/GIR] suppose that ν_5 is overestimated due to separation of the K–O and O–H vibrations and it should be 200 cm⁻¹.^fIR spectrum of vapor.^g ν_6 , ν_7 , ν_9 , ν_{10} , and ν_{12} from IR spectrum in Ar matrix [78BEL, 91BEL]; ν_2 - ν_5 , ν_8 from ionic model calculation [78BEL]; structural parameters and ν_1 , ν_{11} are estimated.

electron diffraction data and the IR spectral data in Ar matrix [78BEL]. Reliability of these frequencies is rather questionable although the discrepancies from corresponding IR spectral data [78BEL, 91BEL] are not very large.

The value of ν_{12} for $\text{Cs}_2\text{O}_2\text{H}_2$ obtained by Konings *et al.* [91KON/BOO] from the analysis of the IR spectra of cesium hydroxide vapor, is in excellent agreement with value observed in Ar matrix [78BEL, 91BEL].

Acquista *et al.* [68ACQ/ABR] observed in IR spectrum of CsOH isolated in Ar matrix, several bands below 300 cm^{-1} whose relative intensities decreased with increasing the temperature. These bands were evidently due to polymeric species of CsOH (most probably to dimer), but it was not possible to make definite assignments.

There are no data on the existence of low-lying excited electronic states of $\text{Cs}_2\text{O}_2\text{H}_2$, nor are any expected.

A planar rhomboid configuration of $\text{Cs}_2\text{O}_2\text{H}_2$ (D_{2h} symmetry) is adopted in the present work. The structural parameters of the molecule, $r(\text{Cs}-\text{O}) = 2.62 \pm 0.05\text{ \AA}$, $r(\text{O}-\text{H}) = 0.97 \pm 0.03\text{ \AA}$, and $\angle(\text{O}-\text{Cs}-\text{O}) = 90 \pm 10^\circ$ are based on the electron diffraction data by Girichev and Lapshina [89GIR/LAP, 89LAP] and the ionic model calculation by Belyaeva [78BEL]. The corresponding value of the product of principal moments of inertia is $(5.4 \pm 0.5)10^{-112}\text{ g}^3\text{ cm}^6$. The vibrational frequencies ν_6 , ν_7 , ν_9 , ν_{10} , and ν_{12} are those measured in IR spectra in matrix [78BEL, 91BEL]; their uncertainties are estimated as 10 cm^{-1} . The values of ν_2 – ν_5 and ν_8 are accepted from an ionic model calculation [78BEL] with average uncertainties about 20 cm^{-1} . The values of ν_1 and ν_{11} are estimated.

The molecular constants of $\text{Cs}_2\text{O}_2\text{H}_2$ (D_{2h} symmetry) adopted in the present work for calculation of thermal functions are summarized below:

$$r(\text{Cs}-\text{O}) = 2.62 \pm 0.05\text{ \AA}; r(\text{O}-\text{H}) = 0.97 \pm 0.03\text{ \AA};$$

$$\angle(\text{O}-\text{Cs}-\text{O}) = 90 \pm 10^\circ;$$

$$I_A I_B I_C = (5.4 \pm 0.5)10^{-112}\text{ g}^2\text{ cm}^6;$$

symmetry number: $\sigma=4$; statistical weight: $p_x=1$;

$$\nu_1 = 3700 \pm 100\text{ cm}^{-1}, d_1=1;$$

$$\nu_2 = 275 \pm 20\text{ cm}^{-1}, d_2=1;$$

$$\nu_3 = 85 \pm 10\text{ cm}^{-1}, d_3=1;$$

$$\nu_4 = 275 \pm 20\text{ cm}^{-1}, d_4=1;$$

$$\nu_5 = 185 \pm 20\text{ cm}^{-1}, d_5=1;$$

$$\nu_6 = 272 \pm 10\text{ cm}^{-1}, d_6=1;$$

$$\nu_7 = 113 \pm 20\text{ cm}^{-1}, d_7=1;$$

$$\nu_8 = 280 \pm 20\text{ cm}^{-1}, d_8=1;$$

$$\nu_9 = 278.5 \pm 10\text{ cm}^{-1}, d_9=1;$$

$$\nu_{10} = 227 \pm 10\text{ cm}^{-1}, d_{10}=1;$$

$$\nu_{11} = 3700 \pm 100\text{ cm}^{-1}, d_{11}=1;$$

TABLE 65. Differences ($\text{J K}^{-1}\text{ mol}^{-1}$) between the thermal functions of $\text{Cs}_2\text{O}_2\text{H}_2(\text{g})$ calculated in the present work and in [82GUR/VEI, 85CHA/DAV]

T/K	[Present Work]-[82GUR/VEI] ^a			[Present Work]-[85CHA/DAV] ^b		
	$\Delta C_p^\circ(T)$	$\Delta \Phi^\circ(T)$	$\Delta S^\circ(T)$	$\Delta C_p^\circ(T)$	$\Delta \Phi^\circ(T)$	$\Delta S^\circ(T)$
298.15	0.006	0.243	0.266	25.484	5.352	20.512
1000	0.001	0.261	0.268	7.206	26.058	41.128
2000	0.001	0.264	0.263	2.029	34.537	43.996
3000	-0.001	0.263	0.261	0.921	37.804	44.566
4000	0.001	0.262	0.260	0.523	39.524	44.758
5000	0.000	0.262	0.260	0.260	40.589	44.863
6000	0.000	0.261	0.259	0.233	41.301	44.914

^aThe values of $\Phi^\circ(T)$ and $S^\circ(T)$ tabulated in [82GUR/VEI] are recalculated to standard pressure 0.1 MPa.

^bThe values of $\Phi^\circ(T)$ tabulated in [85CHA/DAV] are adjusted to the reference temperature $T = 0$ instead of 298.15 K.

$$\nu_{12} = 235 \pm 10\text{ cm}^{-1}, d_{12}=1;$$

Calculation of the $[\text{CsOH}]_2(\text{g})$ Thermal Functions

The thermal functions of $\text{Cs}_2\text{O}_2\text{H}_2(\text{g})$ in the standard state are calculated in the “rigid rotor–harmonic oscillator” approximation with low-temperature quantum corrections according to the equations given in [89GUR/VEY]. The molecular constants of $\text{Cs}_2\text{O}_2\text{H}_2$ used in calculation are given in the previous subsection. The calculated values of $C_p^\circ(T)$, $\Phi^\circ(T)$, $S^\circ(T)$, and $H^\circ(T) - H^\circ(0)$ at the temperature range 0–6000 K are given in Table 68.

The uncertainties in thus calculated thermal functions of $\text{Cs}_2\text{O}_2\text{H}_2(\text{g})$ are because of the uncertainties of the adopted molecular constants, presumably of the calculated vibrational frequencies and structural parameters. At high temperatures the uncertainties due to the approximate method of calculation become more substantial. These uncertainties are roughly estimated taking into consideration the uncertainties in the thermal functions for monomers. The total uncertainties in the thermal function of $\text{Cs}_2\text{O}_2\text{H}_2(\text{g})$ are presented in Table 68.

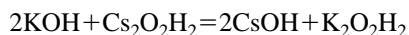
The comparison of the thermal function for $\text{Cs}_2\text{O}_2\text{H}_2(\text{g})$ calculated in [82GUR/VEY] and [85CHA/DAV] is shown in Table 65. There is a good agreement of the data presented in this work and reference book [82GUR/VEI]. Small differences between the values of $\Phi^\circ(T)$ and $S^\circ(T)$ are mainly due to a slight correction of the value of $I_A I_B I_C$ in the present work. Large differences when compared with the reference book [85CHA/DAV] are due to selection of an obsolete model of the $\text{Cs}_2\text{O}_2\text{H}_2$ molecule and molecular constants.

Enthalpy of formation of $[\text{CsOH}]_2(\text{g})$ —Experimental Investigations

[59SCH/POR]

Schoonmaker and Porter carried out mass spectrometric study of alkali hydroxide binary mixtures with the aim to obtain differences in dimerization enthalpies of pairs of hydroxides. A silver effusion cell was used in experiments with

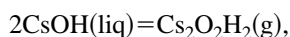
cesium hydroxide. For the KOH–CsOH, system measurements of the equilibrium constants for the gaseous reaction



were performed at 692 K. Equilibrium constant values were in the range 51–68.5. The difference in dimerization enthalpies $\Delta_f H^\circ(\text{CsOH}) - \Delta_f H^\circ(\text{KOH}) = 6.3 \pm 0.2 \text{ kcal mol}^{-1}$ ($26 \pm 0.8 \text{ kJ mol}^{-1}$) was found using an estimated value $\Delta_f S^\circ(\text{CsOH}) - \Delta_f S^\circ(\text{KOH}) = 1.0 \text{ cal K}^{-1} \text{ mol}^{-1}$. Similar measurements were made for the RbOH–CsOH system at 673 K. Equilibrium constant values were in the range 18.9–27. Using $\Delta_f S^\circ(\text{CsOH}) - \Delta_f S^\circ(\text{RbOH}) = 0.45 \text{ cal K}^{-1} \text{ mol}^{-1}$ the value $\Delta_f H^\circ(\text{CsOH}) - \Delta_f H^\circ(\text{RbOH}) = 4.5 \pm 0.3 \text{ kcal mol}^{-1}$ ($18.9 \pm 1.2 \text{ kJ mol}^{-1}$) was obtained. Combining the differences found with the dimerization enthalpy of KOH ($-48 \pm 5 \text{ kcal mol}^{-1}$) and RbOH ($-45 \pm 5 \text{ kcal mol}^{-1}$), Schoonmaker and Porter selected the value $\Delta_f H^\circ(\text{CsOH}) = 40 \pm 5 \text{ kcal mol}^{-1}$ ($-167 \pm 20 \text{ kJ mol}^{-1}$).

[88BLA/JOH]

Blackburn and Johnson performed a mass spectrometric study of cesium hydroxide vaporization. Partial pressure values of $\text{Cs}_2\text{O}_2\text{H}_2(\text{g})$ were obtained in the temperature range 681–772 K (six points). Using thermal functions from the JANAF Tables [74CHA/CUR] the third-law enthalpy of dimer vaporization and the enthalpy of formation of $\text{Cs}_2\text{O}_2\text{H}_2(\text{g})$ were obtained:



$$\Delta_v H^\circ(298.15 \text{ K}) = 37.199 \pm 0.727 \text{ kcal mol}^{-1} \\ \times (155.64 \pm 3.04 \text{ kJ mol}^{-1});$$

$$\Delta_f H^\circ(\text{Cs}_2\text{O}_2\text{H}_2, \text{g}, 298.15 \text{ K}) = -156.9 \pm 3 \text{ kcal mol}^{-1} \\ \times (-656.5 \pm 3 \text{ kJ mol}^{-1}).$$

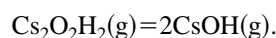
The partial pressures of $\text{Cs}_2\text{O}_2\text{H}_2(\text{g})$ are listed in Table 66 and are presented in Fig. 13.

[88KON/COR2]

Konings and Cordfunke measured total (apparent) vapor pressure of cesium hydroxide using transpiration technique. The authors of this review estimated vapor composition of cesium hydroxide and calculated the enthalpy of formation of $\text{Cs}_2\text{O}_2\text{H}_2(\text{g})$ from the dimer partial pressure. The results are presented in Table 67.

[89GIR/IAP]

Girichev and Lapshina carried out an investigation of $\text{Cs}_2\text{O}_2\text{H}_2(\text{g})$ structure by the method of electron diffraction. In the process of refining of the theoretical molecular scattering intensity curve $sM(s)$ they obtained the best agreement between theoretical and experimental curves for the dimer relative concentration of $31^{+18}_{-6} \text{ mol}\%$, or $P(\text{d})/P(\text{m}) = 0.45$ ($T = 803 \pm 10 \text{ K}$). Combining the electron diffraction data obtained on geometry and vibrational frequencies with spectroscopic data for $\text{Cs}_2\text{O}_2\text{H}_2(\text{g})$, the authors [89GIR/LAP] calculated the third-law enthalpy $\Delta_f H^\circ(0) = 146^{+14}_{-11} \text{ kJ mol}^{-1}$ for the reaction

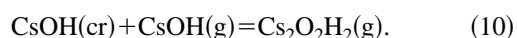


An estimated value of the total vapor pressure of cesium hydroxide was used in the calculation of the equilibrium constant for this reaction.

Discussion of the Enthalpy of Formation of $[\text{CsOH}]_2(\text{g})$

The authors of this review have recalculated all equilibria from the papers discussed in the subsections with the thermal functions from this work and with auxiliary data from [82GUR/VEI] and [89GUR/VEY]. The recalculated values of enthalpies of reactions and the values of enthalpy of formation of $\text{Cs}_2\text{O}_2\text{H}_2(\text{g})$ are collected in Table 67.

In an earlier subsection the authors of this review calculated the enthalpy $\Delta_f H^\circ(0 \text{ K}) = 21.2 \pm 5 \text{ kJ mol}^{-1}$ for the reaction



Recalculation to $T = 298.15 \text{ K}$ resulted in the value $\Delta_f H^\circ(298.15 \text{ K}) = 19.2 \pm 5 \text{ kJ mol}^{-1}$. Combining this value with the adopted enthalpies of formation of $\text{CsOH}(\text{cr})$ and $\text{CsOH}(\text{g})$ the enthalpy of formation was calculated: $\Delta_f H^\circ(\text{Cs}_2\text{O}_2\text{H}_2, \text{g}, 298.15 \text{ K}) = -653.0 \pm 8 \text{ kJ mol}^{-1}$. The data [59SCH/POR] are in good agreement with this value. The data [88BLA/JOH], as was expected, give more positive value of enthalpy of formation, due to low $P(\text{d})/P(\text{m})$ ratio. The data [89GIR/LAP] are also in agreement with the results obtained using the reaction (9). They cannot be regarded as reliable, however, due to use of roughly estimated total vapor pressure of cesium hydroxide.

From the discussions on the enthalpy of formation of $\text{CsOH}(\text{g})$ and $\text{Cs}_2\text{O}_2\text{H}_2(\text{g})$ it follows that the adopted value for $\text{Cs}_2\text{O}_2\text{H}_2(\text{g})$ is to be obtained from a combination of the enthalpy of reaction (9) with the adopted values of enthalpies of formation of $\text{CsOH}(\text{cr})$ and $\text{CsOH}(\text{g})$. On the basis of these discussions the value

$$\Delta_f H^\circ(\text{Cs}_2\text{O}_2\text{H}_2, \text{g}, 298.15 \text{ K}) = -653.0 \pm 8 \text{ kJ mol}^{-1}$$

is adopted in this review.

4.2.4. Appendix. Tables of Experimental and Evaluated Data for $[\text{CsOH}]_2(\text{g})$

TABLE 66. Partial pressure of $\text{Cs}_2\text{O}_2\text{H}_2(\text{g})$ over $\text{CsOH}(\text{liq})$, [88BIA/JOH]

No.	T/K	P/(atm 10^6)
1	759	1.88
2	702	1.53
3	681	0.394
4	743	1.81
5	768	4.21
6	772	2.81

TABLE 67. Results of determination of $\Delta_f H^\circ(\text{Cs}_2\text{O}_2\text{H}_2, \text{g}, 0 \text{ K})$, kJ mol^{-1}

Reference	Method	$\Delta_f H^\circ(0 \text{ K})$		$\Delta_f H^\circ(0 \text{ K})$
		2nd law	3rd law	
[59SCH/POR]	Knudsen effusion mass spectrometry, $2\text{KOH}(\text{g}) + \text{Cs}_2\text{O}_2\text{H}_2(\text{g}) =$ $2\text{CsOH}(\text{g}) + \text{K}_2\text{O}_2\text{H}_2(\text{g})$, 692 K (four points)	...	-26.2 ± 8	-653 ± 10
[88BIA/JOH]	Knudsen effusion mass spectrometry, $2\text{CsOH}(\text{liq}) = \text{Cs}_2\text{O}_2\text{H}_2(\text{g})$ 681–772 K (six points)	141 ± 60	197 ± 1.1	-631 ± 20
[88KON/COR]	Transpiration, $2\text{CsOH}(\text{liq}) = \text{Cs}_2\text{O}_2\text{H}_2(\text{g})$, 675.7–975.6 K (31 points)	178 ± 10	183.7 ± 0.6	-644.4 ± 10
[89GIR/LAP]	Electron diffraction, $\text{Cs}_2\text{O}_2\text{H}_2(\text{g}) = 2\text{CsOH}(\text{g})$, 803 K	...	146_{-11}^{+14}	-649 ± 20

TABLE 68. Thermodynamic properties at 0.1 MPa: Cs₂O₂H₂(g)

T/K	C_p°	$-[G^\circ - H^\circ(0\text{ K})]/T$	S°	$H^\circ - H^\circ(0\text{ K})$	$\Delta_f H^\circ$	$\Delta_f G^\circ$
	J K ⁻¹ mol ⁻¹			kJ mol ⁻¹		
0	0.000	0.000	0.000	0.000	-644.367	-644.367
25	35.332	178.629	212.276	0.841	-645.384	-644.911
50	45.159	202.764	239.517	1.838	-647.111	-643.793
75	58.731	218.563	260.322	3.132	-648.675	-641.778
100	72.020	231.381	279.090	4.771	-649.796	-639.307
150	90.227	252.953	312.110	8.874	-651.126	-633.734
200	99.886	271.277	339.534	13.651	-651.879	-627.817
250	105.217	287.285	362.450	18.791	-652.436	-621.720
300	108.385	301.478	381.937	24.138	-653.027	-615.494
350	110.398	314.204	398.807	29.611	-657.926	-608.508
400	111.750	325.726	413.642	35.167	-658.549	-601.405
450	112.707	336.242	426.863	40.779	-659.091	-594.228
500	113.421	345.910	438.776	46.433	-659.563	-586.996
600	114.467	363.169	459.553	57.831	-660.345	-572.406
700	115.316	378.234	477.263	69.320	-660.979	-557.698
800	116.149	391.598	492.715	80.893	-661.537	-542.904
900	117.026	403.610	506.446	92.552	-662.094	-528.041
1000	117.946	414.523	518.823	104.300	-798.201	-505.718
1100	118.888	424.525	530.108	116.142	-797.067	-476.526
1200	119.827	433.762	540.493	128.078	-795.916	-447.436
1300	120.741	442.347	550.121	140.106	-794.753	-418.444
1400	121.614	450.369	559.101	152.224	-793.573	-389.539
1500	122.435	457.902	567.520	164.427	-792.388	-360.723
1600	123.201	465.003	575.446	176.710	-791.198	-331.983
1700	123.910	471.722	582.937	189.066	-790.013	-303.317
1800	124.563	478.100	590.038	201.490	-788.839	-274.723
1900	125.162	484.170	596.789	213.976	-787.691	-246.190
2000	125.710	489.963	603.224	226.520	-786.576	-217.721
2200	126.670	500.814	615.251	251.761	-784.485	-160.937
2400	127.472	510.818	626.309	277.178	-782.666	-104.333
2600	128.144	520.100	636.539	302.742	-781.218	-47.870
2800	128.709	528.761	646.057	328.428	-780.239	8.499
3000	129.188	536.880	654.954	354.219	-779.818	64.822
3200	129.595	544.524	663.305	380.099	-780.039	121.131
3400	129.943	551.744	671.172	406.054	-780.972	177.482
3600	130.243	558.588	678.608	432.073	-782.681	233.906
3800	130.503	565.092	685.657	458.148	-785.216	290.451
4000	130.729	571.289	692.357	484.272	-788.608	347.148
4200	130.927	577.207	698.740	510.438	-792.889	404.039
4400	131.101	582.871	704.835	536.641	-798.065	461.147
4600	131.255	588.301	710.666	562.877	-804.136	518.522
4800	131.392	593.517	716.255	589.142	-811.064	576.173
5000	131.514	598.535	721.621	615.433	-818.825	634.125
5200	131.622	603.369	726.782	641.747	-827.357	692.416
5400	131.720	608.032	731.751	668.081	-836.601	751.036
5600	131.808	612.537	736.543	694.434	-846.461	810.019
5800	131.888	616.893	741.170	720.804	-856.866	869.355
6000	131.960	621.111	745.642	747.189	-867.702	929.075
298.15	108.293	300.981	381.267	23.937	-653.000	-615.725
Uncertainties in Functions						
0	8.000	8.000
300	1.000	1.500	2.000	0.200	8.000	8.000
1000	2.000	2.000	3.000	1.000	8.000	8.000
2000	3.000	3.000	4.000	5.000	10.000	9.000
3000	4.000	4.000	7.000	10.000	13.000	13.000
4000	5.000	5.000	9.000	15.000	17.000	20.000
5000	6.000	6.000	10.000	20.000	22.000	30.000
6000	8.000	8.000	12.000	25.000	26.000	50.000

5. Recommendations for Future Measurements

Based on our critical review of thermodynamic and spectroscopic properties of the potassium, rubidium and cesium hydroxides, we recommend the following investigations.

- (1) Measurement of the heat capacity of KOH at low temperatures, especially at $T < 60$ K, the heat capacity or the enthalpy increments of γ -KOH (517–679 K) and liquid KOH (in the region of 300–500 K above the fusion temperature).
- (2) Measurement of the heat capacity of RbOH at low temperatures and the thermal properties of solid and liquid RbOH (including heat capacity, enthalpy increments, enthalpies of transition and of fusion) in the range from 298 to 1000–1200 K.
- (3) Measurements of the thermal properties of solid and liquid CsOH in the range from ~ 500 K to 1000–1200 K.
- (4) Measurements of the enthalpy of formation of RbOH(cr) from its enthalpy of solution in water.
- (5) Mass spectrometric study of potassium, rubidium and cesium hydroxides to obtain reliable quantitative data on vapor composition, including relative concentration of trimeric and possibly tetrameric molecules.
- (6) Measurements of total (apparent) pressure over rubidium hydroxide, e.g., by transpiration and/or Knudsen effusion method.
- (7) To improve the accuracy of the calculated thermal functions of gases, it is desirable that:
 - (a) the structure of dimeric molecules should be defined more explicitly;
 - (b) the vibrational frequencies of the dimeric molecules, active in Raman spectra, should be detected spectroscopically.

6. Acknowledgments

The work described in this paper has been performed under auspices of the Standard Reference Data Program of the National Institute of Standards and Technology. The authors are grateful to Dr. Malcolm W. Chase for his keen interest in this work.

7. References for Potassium, Rubidium, and Cesium Hydroxides

- | | | | |
|----------|--|-----------|---|
| 1875BER | Berthelot M., <i>Ann. Chim. Phys.</i> 4 , 513 (1875). | 06FOR | Forcrand R., <i>Compt. Rend. Acad. Sci.</i> 142 , 1252 (1906). |
| 1875BER2 | Berthelot M., <i>Ann. Chim. Phys.</i> 4 , 74 (1875). | 10HEV | Hevesy G. Von., <i>Z. Anorg. Allgem. Chem.</i> 67 , 242 (1910). |
| 1886THO | Thomsen J., <i>Thermochemische Untersuchungen</i> . Leipzig: Verlag von J. A. Barth, 1882–1886 (1886). | 10HEV2 | Hevesy G. Von., <i>Z. Phys. Chem.</i> 73 , 667 (1910). |
| 1892BEK | Beketoff N., <i>Bull. Acad. Sci. Russ.</i> 34 , 169 (1892). | 15SCA | Scarpa G., <i>Atti Accad. Nazl. Lincei. Classe Sci. Fis., Mat. Natur.</i> 24 II , 476 (1915). |
| | | 15SCA2 | Scarpa G., <i>Atti Accad. Nazl. Lincei. Classe Sci. Fis., Mat. Natur.</i> 24 II , 738 (1915). |
| | | 21JAC/MOR | Jackson D. D., Morgan J., <i>J. Ind. Eng. Chem.</i> 13 , 110 (1921). |
| | | 21WAR/ALB | Wartenberg H. Von., Albrecht P., <i>Z. Electrochem.</i> 27 , 162 (1921). |
| | | 23EWL | Ewles I., <i>Philos. Mag.</i> 45 , 957 (1923). |
| | | 39HER | Herzberg G., 'Molecular Spectra and Molecular Structure. I. Diatomic Molecules.' New York, (1939). |
| | | 39TEI/KLE | Teichert W., Klemm W., <i>Z. Anorg. Allgem. Chem.</i> 243 , 138 (1939). |
| | | 46VOS/PON | Voskresenskaya N. K., Ponomareva K. S., <i>Zh. Fiz. Khim</i> 20 , 433 (1946). |
| | | 47GIN/COR | Ginnings D. C., Corruccini R. J., <i>J. Res. NBS</i> 38 , 593 (1947). |
| | | 48HAC/THO | Hackspill L., Thomas G., <i>Compt. Rend. Acad. Sci.</i> 227 , 797 (1948). |
| | | 49BRE/MAS | Brewer L., Mastick D. F., UCRL-572 (1949). |
| | | 49SEW/MAR | Seward R. P., Martin K. E., <i>J. Am. Chem. Soc.</i> 71 , 3564 (1949). |
| | | 51DIO | Diogenov G. G., <i>Dokl. AN SSSR</i> 78 , 697 (1951). |
| | | 51RED/LON | Redmond R. F., Lones J., U. S. AEC Reports, ORNL-1040, Part 1, 1951. |
| | | 51VED/SKU | Vedeneev A. V., Skuratov S. M., <i>Zh. Fiz. Khim</i> 25 , 837 (1951). |
| | | 52BER/KHI | Bergman A. G., Khitrov V. A., <i>Izv. Sektora Fiz.-Khim. Analiza IONKH AN SSSR.</i> 21 , 199 (1952). |
| | | 52RES/DIO | Reshetnikov N. A., Diogenov G. G., <i>Dokl. AN SSSR</i> 85 , 819 (1952). |
| | | 52SMI/SUG | Smith H., Sugden T. M., <i>Proc. R. Soc. London Ser. A</i> 211 , 58 (1952). |
| | | 53KHI/KHI | Khitrov V. A., Khitrova N. N., Khmellkov V. F., <i>Zh. Obshch. Khim.</i> 23 , 1630 (1953). |
| | | 53SMI/SUG | Smith H., Sugden T. M., <i>Proc. R. Soc. London Ser. A</i> 219 , 204 (1953). |
| | | 54BER/RES | Bergman A. G., Reshetnikov N. A., <i>Izv. Sektora Fiz.-Khim. Analiza IONKH AN SSSR.</i> 25 , 208 (1954). |
| | | 54BOG | Bogart D., <i>J. Phys. Chem.</i> 58 , 1168 (1954). |
| | | 54KET/WAL | Ketchen E. E., Wallace W. E., <i>J. Am. Chem. Soc.</i> 76 , 4736 (1954). |
| | | 54KHI | Khitrov V. A., <i>Izv. Sektora Fiz.-Khim. Analiza IONKH AN SSSR.</i> 25 , 236 (1954). |

- 54POW/BLA Powers W. D., Blalock G. C., U. S. AEC Reports. ORNL-1653-1, 1954.
- 56COH/MIC Cohen-Adad R., Michaud M., *Compt. Rend. Acad. Sci.* **242**, 2569 (1956).
- 58BAU/DIN Bauer S. H., Diner R. M., Porter R. F., *J. Chem. Phys.* **29**, 901 (1958).
- 58GUN/GRE Gunn S. R., Green L. G., *J. Am. Chem. Soc.* **80**, 4782 (1958).
- 58LEE Lee H. S., thesis, 1958.
- 58POR/SCH Porter R. F., Schoonmaker R. C., *J. Phys. Chem.* **62**, 234 (1958).
- 58POR/SCH2 Porter R. F., Schoonmaker R. C., *J. Phys. Chem.* **62**, 486 (1958).
- 58POR/SCH3 Porter R. F., Schoonmaker R. F., *J. Chem. Phys.* **28**, 168 (1958).
- 58RES/VIL Reshetnikov N. A., Vilutis N. I., *Zh. Neorg. Khim.* **3**, 366 (1958).
- 58ROL/COH Rollet A. P., Cohen-Adad R., Michaud M., Tranquard A., *Compt. Rend. Acad. Sci.* **246**, 3249 (1958).
- 58SPI/MAR Spinar L. H., Margrave J. L., *Spectrochim. Acta* **12**, 244 (1958).
- 59BER/RES Bergman A. G., Reshetnikov N. A., *Izv. Fiz.-Khim. NII Pri Irkutskom Un-te* **4**, 9 (1959).
- 59BUC Buchanan R. A., *J. Chem. Phys.* **31**, 870 (1959).
- 59RES/UNZ Reshetnikov N. A., Unzhakov G. M., *Izv. Fiz.-Khim. NII Pri Irkutskom Un-te* **4**, 41 (1959).
- 59ROL/COH Rollet A. P., Cohen-Adad R., Choucroun J., *Bull. Soc. Chim. France* **1**, 146 (1959).
- 59SCH/POR Schoonmaker R. C., Porter R. F., *J. Chem. Phys.* **31**, 830 (1959).
- 60BER/MES Berkowitz J., Meschi D. J., Chupka W. A., *J. Chem. Phys.* **33**, 533 (1960).
- 60SNY/KUM Snyder R. G., Kumamoto J., Ibers J. A., *J. Chem. Phys.* **33**, 1171 (1960).
- 61COH/MIC Cohen-Adad R., Michaud M., Said J., Rollet A. P., *Bull. Soc. Chim. France* **2**, 356 (1961).
- 61DRO Drozin N. N., *Zh. Fiz. Khim* **35**, 1789 (1961).
- 61MIC Michaud M., *Compt. Rend. Acad. Sci.* **253**, 1947 (1961).
- 61RES Reshetnikov N. A., *Zh. Neorg. Khim.* **6**, 682 (1961).
- 61RES/ROM Reshetnikov N. A., Romanova E. V., *Zh. Neorg. Khim.* **6**, 1381 (1961).
- 61WIL Wilmshurst J. K., *J. Chem. Phys.* **35**, 1800 (1961).
- 63LUX/BRA Lux P., Brandl F., *Z. Anorg. Allgem. Chem.* **326**, 25 (1963).
- 630ET/MCD Oetting F. L., McDonald R. A., *J. Phys. Chem.* **167**, 2737 (1963).
- 63ROL/COH Rollet A. P., Cohen-Adad R., Ferlin C., *Compt. Rend. Acad. Sci.* **256**, 5580 (1963).
- 64COH/RUB Cohen-Adad R., Ruby C., *Compt. Rend. Acad. Sci. C* **258**, 6163 (1964).
- 65PAR Parker V. B., *NSRDS-NBS* **2**, 66 (1965).
- 65RES/BAR Reshetnikov N. A., Baranskaya E. V., *Zh. Neorg. Khim.* **10**, 183 (1965).
- 66BER/MOR Berdichevskii N. I., Morachevskii A. G., *Zh. Prikl. Khim.* **39**, 791 (1966).
- 66BUE/PEY Buenker R. L., Peyerimhoff S. D., *J. Chem. Phys.* **45**, 3682 (1966).
- 66COH/RUB Cohen-Adad R., Ruby C., *Compt. Rend. Acad. Sci. C* **263**, 1014 (1966).
- 66JEN/PAD Jensen D. E., Padley P. J., *Trans. Faraday Soc.* **62**, 2132 (1966).
- 66KUC/LID Kuczkowski R. L., Lide D. R. Jr., Krisher L. C., *J. Chem. Phys.* **44**, 3131 (1966).
- 66MIT/GRO Mitkevich E. M., Grot L. S., *Zh. Neorg. Khim.* **11**, 902 (1966).
- 67ACQ/ABR Acquista N., Abramowitz S., Lide D. R., *INBS Report. No. 9601, Ch. 4* (1967).
- 67BUE/STA Buechler A., Stauffer J. L., Klemperer W., *J. Chem. Phys.* **46**, 605 (1967).
- 67EME/GUS Emel'yanov A. M., Gusarov A. V., Gorokhov L. N., Sadovnikova N. A., *Teoret. i Eksperim. Khimiya* **3**, 226 (1967).
- 67LID/KUC Lide D. R. Jr., Kuczkowski R. L., *J. Chem. Phys.* **46**, 4768 (1967).
- 67MIC Michaud M., *Compt. Rend. Acad. Sci. C* **264**, 1939 (1967).
- 67RES/BAR Reshetnikov N. A., Baranskaya E. V., *Izv. Vuzov. Khimiya i Khim. Tekhnol.* **10**, 496 (1967).
- 67RUB Ruby C., *Compt. Rend. Acad. Sci. C* **264**, 1172 (1967).
- 67TSE/ROG Tsentsiper A. B., Rogozhnikova T. I., Bakulina V. M., *Izv. AN SSSR. Khim.* **9**, 2073 (1967).
- 68ACQ/ABR Acquista N., Abramowitz S., Lide D. R., *Chem. Phys.* **49**, 780 (1968).
- 68DUB/MIL Dubois J., Millet J., *Compt. Rend. Acad. Sci. C* **266**, 852 (1968).
- 68FEU/QUE Feugier A., Queraud A., 'Electricity from MHD.1,' Vienna: AEA, IV, 2130 (1968).
- 68GUS/GOR Gusarov A. V., Gorokhov L. N., *Zh. Fiz. Khim* **42**, 860 (1968).
- 68MIC Michaud M., *Rev. Chim. Miner.* **5**, 89 (1968).
- 68RUB/SEB Ruby C., Sebaoun A., Vouillon J.-C., *Compt. Rend. Acad. Sci. C* **267**, 1043 (1968).
- 68WES/FUR Westrum E. F., Furukawa G. T., McCullough J. P., 'Experimental Thermodynamics,' Editors: Scott D. W., McCullough J. P., Butterworths, 1 (1968).

- 69ACQ/ABR Acquista N., Abramowitz S., *J. Chem. Phys.* **51**, 2911 (1969).
- 69COT/JEN Cotton J. H., Jenkins D. R., *Trans. Faraday Soc.* **65**, 1537 (1969).
- 69DUB/MIL Dubois J., Millet J., *Compt. Rend. Acad. Sci. C* **269**, 1336 (1969).
- 69GOR/GUS Gorokhov L. N., Gusarov A. V., Panchenkov I.G., *VINITI*, No.1298-Dep. Moskva, (1969).
- 69LID/MAT Lide D. R. Jr., Matsumura Ch., *J. Chem. Phys.* **50**, 3080 (1969).
- 69MAT/LID Matsumura Ch., Lide D. R. Jr., *J. Chem. Phys.* **50**, 71 (1969).
- 690ST/ITK Ostrovityanova S. E., Itkina L. S., *Zh. Neorg. Khim.* **14**, 577 (1969).
- 69RES/BAR Reshetnikov N. A., Baranskaya E. V., 'Nauchnye trudy Irkutskogo med. in-tA.,' *Irkutsk* **95**, 135 (1969).
- 69TIM/KRA Timoshinin V. S., Krasnov K. S., *Zh. Strukt. Khim.* **10**, 101 (1969).
- 69TSE/DOB Tsentsiper A. B., Dobrolyubova M. S., 'Redkie shchelochnye elementy. 1, Perm': *Permskii politekhn. in-t*, 147 (1969).
- 70GOR/GUS Gorokhov L. N., Gusarov A. V., Panchenkov I. G., *Zh. Fiz. Khim* **44**, 269 (1970).
- 70HOU/BUN Hougen J. T., Bunker P. R., Johns J. W. C., *J. Mol. Struct.* **34**, 136 (1970).
- 70JEN Jensen D. E., *J. Phys. Chem.* **74**, 207 (1970).
- 70STU/HIL Stull D. R., Hildenbrand D. L., Oetting F. L., Sinke G. C., *J. Chem. Eng. Data* **15**, 52 (1970).
- 71BEL/DVO Belyaeva A. A., Dvorkin M. I., Shcherba L. D., *Opt. Spektrosk.* **31**, 392 (1971).
- 71GIN Ginzburg D. M., *Zh. Fiz. Khim* **45**, 2937 (1971).
- 71GIN/GUB Ginzburg D. M., Guba N. I., Kochkolda V. E., *Zh. Fiz. Khim* **45**, 2939 (1971).
- 71KEL/PAD Kelly R., Padley P. J., *Trans. Faraday Soc.* **67**, 740 (1971).
- 71KRA/FIL Krasnov K. S., Filippenko N. V., *Izv. Vuzov. Khimiya i Khim. Tekhnol.* **14**, 1435 (1971).
- 71STU/PRO Stull D. R., Prophet H., *JANAF Thermochemical Tables*, 2nd ed., Washington: NSRDS-NBS N37 (1971).
- 72FEU Feugier A., these doct. Sci. Phys. Fac. Sci. Univ. Paris., 1 1972.
- 72KAM/MAE Kamisuki T., Maeda S., *Bull. Chem. Soc. Jpn.* **45**, 1345 (1972).
- 73BAR/KNA Barin I., Knacke O., 'Thermochemical properties of inorganic substances,' Berlin, Heidelberg: Springer-Verlag (1973).
- 73CAN Cantor S., *Inorg. Nucl. Chem. Lett.* **9**, 1275 (1973).
- 73ITK Itkina L. S., *Gidroksidy litiya, rubidiya i tseziya*, Moskva: izd-vo Nauka, (1973).
- 73PAP/BOU Papin G., Bouaziz R., *Compt. Rend. Acad. Sci. C* **277**, 771 (1973).
- 73PEA/TRU Pearson E. F., Trueblood M. B., *J. Chem. Phys.* **58**, 826 (1973).
- 73TOU Touzain P., *Compt. Rend. Acad. Sci. C* **276**, 1583 (1973).
- 74BEC/COU Bec C., Counioux J. J., Papin G., Sebaoun A., *Compt. Rend. Acad. Sci. C* **278**, 1193 (1974).
- 74CHA/CUR Chase M. W., Curnutt J. L., Hu A. T., Prophet H., Syverud A. N., Walker L. C., *JANAF Thermochemical Tables*, 1974 Supplement, *J. Phys. Chem. Ref. Data* **3**, (1974).
- 74KUD Kudin L. S., thesis, Ivanovo, 1974.
- 74POR/ITK Portnova S. M., Itkina L. S., *Zh. Neorg. Khim.* **19**, 1624 (1974).
- 74TOU Touzain P., *Compt. Rend. Acad. Sci. C* **279**, 41 (1974).
- 74VAS/KUN Vasillev V. P., Kunin B. T., *Zh. Neorg. Khim.* **19**, 1217 (1974).
- 75ITK/POR Itkina L. S., Portnova S. M., Ostrovitianjva S. E., *Proc. 4th Intern. Conf. Therm. Anal.* 1974, Budapesti, 603 (1975).
- 75KUI/TOR Kuijpers P., Topping T., Dymanus A., *Z. Naturforsch. A* **30**, 1256 (1975).
- 75PAN Panchenkov I. G., thesis, Moscow, 1975.
- 76PEA/WIN Pearson E. F., Winnewisser B. P., Trueblood M. B., *Z. Naturforsch. A* **31**, 1259 (1976).
- 77BAR/KNA Barin I., Knacke O., Kubaschewski O., *Thermochemical Properties of Inorganic Substances. Supplement. 1*, Berlin: Springer-Verlag, 1 (1977).
- 77ENG England W. B., Report prepared for the 16th symposium on engineering aspects of MHD.1, Pittsburgh, PA (1977).
- 77KUB/UNA Kubaschewski O., Unal H., *High Temp. High Pressures* **9**, 361 (1977).
- 78BEL Belyaeva A. A., thesis, Leningrad, 1978.
- 78ENG England W. B., *J. Chem. Phys.* **68**, 4896 (1978).
- 78LOV Lovas F. J., *J. Phys. Chem. Ref. Data* **7**, 1445 (1978).
- 79BON/HAS Bonnell D. W., Hastie J. W., *Proceedings of the 10th Materials Research Symposium*, NBS Special Publication 226 SP-561/1, 1, 357 (1979).
- 79COR/MUI Cordfunke E. H. P., Muis R. P., Prins G., *J. Chem. Thermodyn.* **11**, 819 (1979).
- 79RIC/VRE Richter J., Vreuls W., *Ber. Bunsenges. Phys. Chem.* **83**, 1023 (1979).
- 79KOR/MUI Cordfunke E. H. P., Muis R. P., Prins G., *J. Chem. Thermodyn.* **11**, 819 (1979).
- 79RIC/VRE Richter J., Vreuls W., *Ber. Busenges. Phys. Chem.* **83**, 1023 (1979).

- 80BAI Baikov Yu. M., Zh. Eksperim. i Teor. Fiz. **78**, 2266 (1980).
- 80BAI/SHA Baikov Yu. M., Shalkova E. K., Kinetika i Kataliz **21**, 1426 (1980).
- 80NEM/STE Nemukhin A. V., Stepanov N. F., J. Mol. Struct. **67**, 81 (1980).
- 80PIE/LEV Pietro W. J., Levi B. A., Hehre W. J., Stewart R. F., Inorg. Chem. **19**, 2225 (1980).
- 81AKU/IKE Akutsu N., Ikeda H., J. Phys. Soc. Jpn. **50**, 2865 (1981).
- 81GIR/VAS Girichev G. V., Vasilleva S. B., Krasnov K. S., Tezisy dokladov 14-go Vsesoyuznogo Chugaevskogo soveshchaniya po khimii koordinatsionnykh soedinenii., Ivanovo, **2**, 511 (1981).
- 81JAC/HAR Jacobs H., Harbrecht B., Z. Kristallogr. **156**, 59 (1981).
- 81JAC/HAR2 Jacobs H., Harbrecht B., Z. Naturforsch. B **36**, 270 (1981).
- 81PIE/BLU Pietro W. J., Blurock E. S., Hout R. F., Hehre W. J., Defrees D. J., Stewart R. F., Inorg. Chem. **20**, 3650 (1981).
- 82FAR/SRI Farber M., Srivastava R. D., Moyer J. W., J. Chem. Thermodyn. **14**, 1103 (1982).
- 82GUR/VEI Gurvich L. V., Veits I. V., Medvedev V. A., Bergman G. A., Yungman V. S., Khachkuruzov G. A. *et al.*, 'Termodinamicheskie svoistva individualnykh veshchestv. Spravochnoe izdanie v 4-kh tomakh,' Editors: Glushko V. P. *et al.*, Moskva: Nauka **4**, 1 (1982).
- 82JAC/KOC Jacobs H., Kockelkorn J., Schardey A., Z. Kristallogr. **159**, 63 (1982).
- 82LUT/ECK Lutz H. D., Eckers W., Haeuseler H., J. Mol. Struct. **80**, 221 (1982).
- 82MED/BER Medvedev V. A., Bergman G. A., Vasillev V. P., Kolesov V. P., Gurvich L. V., Yungman V.S. *et al.*, *Termicheskie konstanty veshchestv*, Editors: Glushko V. P. *et al.*, Moskva: VINITI 10(2), 1 (1982).
- 82WAG/EVA Wagman D. D., Evans W. H., Parker V. B., Schumm R. H., Halow I., Bailey S. M., Churney K. L., Nuttall R. L., J. Phys. Chem. Ref. Data **11**, 1 (1982).
- 83BAI Baikov Yu. M., Kinetika i kataliz **24**, 243 (1983).
- 83FAR/SRI Farber M., Srivastava R. D., Moyer J. W., Leeper J. D., Eng. Aspects Magnetohydrodynamics **1**, 5.1.1 (1983).
- 83GIR/VAS Girichev G. V., Vasilleva S. B., Izv. vuzov. Khim. Khim. Tekhnol. **26**, 1137 (1983).
- 83HAS/ZMB Hastie J., Zmbov K. F., Bonnell D., Proc. Symp. High Temp. Mater. Chem. **4**, (1983).
- 84DEV/CAR Dever D. F., Cardelino B., Gole J. L., High Temp. Sci. **18**, 159 (1984).
- 84HAS/ZMB Hastie J., Zmbov K. F., Bonnell D., High Temp. Sci. **17**, 333 (1984).
- 84HYN/STE Hynes A. J., Steinberg M., Schofield K., J. Chem. Phys. **80**, 2585 (1984).
- 84KAN/KAW Kanesaka I., Kawahara H., Kawai K., J. Raman Spectrosc. **15**, 165 (1984).
- 84OGD/BOW Ogden J. S., Bowsher B. R., Report. No. AEEW-R-1700 Harwell: AERE (1984).
- 84WHI White M. A., Thermochim. Acta **74**, 55 (1984).
- 85CHA/DAV Chase M. W., Davies C. A., Downey J. R., Frurip D. J., McDonald R. A., Syverud A. N., 'JANAF Thermochemical Tables. third edition,' J. Phys. Chem. Ref. Data **14**, Suppl. 1 (1985).
- 85JAC/KOC Jacobs H., Kockelkorn J., Tacke T., Z. Anorg. Allgem. Chem. **531**, 119 (1985).
- 85KAN/HIR Kanno H., Hiraishi J., Bull. Chem. Soc. Jpn. **58**, 2701 (1985).
- 86BAS/ELC Bastow T. J., Elcombe M. M., Howard C. I., Solid State Commun. **59**, 257 (1986).
- 86BAU/LAN Bauschlicher C. W. Jr., Langhoff S. R., Partridge H., J. Chem. Phys. **84**, 901 (1986).
- 86GIR/GIR Girichev G. V., Giricheva N. I., Lapshina S. Yu., Danilova T. G. Issledovanie struktury i energetiki molekul.1, Ivanovo, 74 (1986).
- 86IOR/TOL Iorish V. S., Tolmach P. S., Zh. Fiz. Khim **60**, 2583 (1986).
- 86LUT/HEN Lutz H. D., Henning J., Jacobs H., Mach B., J. Mol. Struct. **145**, 277 (1986).
- 87ALI/VEN Alitman A. B., Veniaminova G. I., Tolmachev S. M., Dep. VNIKI Gosstandarta SSSR 17.02.87.1 No. 295 (1987).
- 87BAS/ELC Bastow T. J., Elcombe M. M., Howard C. J., Solid State Commun. **62**, 149 (1987).
- 87JAC/MAC Jacobs H., Mach B., Lutz H.-D., Henning J., Z. Anorg. Allgem. Chem. **544**, 28 (1987).
- 87JAC/MAC2 Jacobs H., Mach B., Harbrecht B., Lutz H.-D., Henning J., Z. Anorg. Allgem. Chem. **544**, 55 (1987).
- 87MAC/JAC Mach B., Jacobs H., Schafer W., Z. Anorg. Allgem. Chem. **553**, 187 (1987).
- 87RAW/YAM Raw T. T., Yamamuda T., Gilles C. W., J. Chem. Phys. **87**, 3706 (1987).
- 87SUZ/AND Suzer S., Andrews L., Chem. Phys. Lett. **140**, 300 (1987).
- 88BAI/NIK Baikov Yu. M., Nikolaev B. S., Perevalova

- T. A., Shalkova E. K., Ellkin B. Sh., *Izv. AN SSSR. Neorgan. Materialy* **24**, 615 (1988).
- 88BLA/JOH Blackburn P. E., Johnson C. E., *J. Nuclear Mater.* **154**, 74 (1988).
- 88COR/KON Cordfunke E. H. P., Konings R. J. M., Westrum E. F., *Thermochim. Acta* **128**, 31 (1988).
- 88KON/COR Konings R. J. M., Cordfunke E. H. P., Ouweltjes W., *J. Chem. Thermodyn.* **20**, 777 (1988).
- 88KON/COR2 Konings R. J. M., Cordfunke E. H. P., *J. Chem. Thermodyn.* **20**, 103 (1988).
- 88WHI/PER White M. A., Perrott A., Britten D., Van Oort M. J. M., *J. Chem. Phys.* **89**, 4346 (1988).
- 89COX/WAG 'CODATA Key Values for Thermodynamics,' Editors: Cox J. D., Wagman D. D., Medvedev V. A., New York, Washington: Hemisphere Publ. Corp., 1 (1989).
- 89COR/KON Cordfunke E. H. P., Konings R. J. M., *Thermochim. Acta* **157**, 315 (1989).
- 89GIR/LAP Girichev G. V., Lapshina S. B., *Zh. Struktur. Khimii* **30**, 55 (1989).
- 89GOR/MIL Gorokhov L. N., Milushin M. I., Emelyanov A. M., *High Temp. Sci.* **26**, 395 (1989).
- 89GUR/VEY Gurvich L. V., Veyts I. V., Medvedev V. A., *et al.*, 'Thermodynamic Properties of Individual Substances,' Hemisphere Publ. Corp., New York, Vol. 1, Part 1 (1989).
- 89HEN/LUT Henning J., Jacobs H., Lutz H. D., Mach B., *J. Mol. Struct.* **196**, 113 (1989).
- 89KON/COR Konings R. J. M., Cordfunke E. H. P., *J. Nucl. Mater.* **167**, 251 (1989).
- 89LAP Lapshina S. B., thesis, Ivanovo, 1989.
- 90GIR/IAP Girichev G. V., Lapshina S. B., Tumanov I. V., *Zh. Struktur. Khim.* **31**, 132 (1990).
- 90KON Konings R. J. M., thesis, 1990.
- 90KON/COR Konings R. J. M., Cordfunke E. H. P., Westrum E. F., Shaviv R., *J. Phys. Chem. Solids* **51**, 439 (1990).
- 91BEL Belyaeva A. A., *Opt. Spektrosk.* **71**, 88 (1991).
- 91BEL2 Belyaeva A. A., *Opt. Spektrosk.* **71**, 303 (1991).
- 91GUR/VEY Gurvich L. V., Veyts I. V., Medvedev V. A., *et al.*, 'Thermodynamic Properties of Individual Substances,' Hemisphere Publ. Corp., New York, Vol. 2, Part 1 (1991).
- 91KON/BOO Konings R. J. M., Booij A. S., Cordfunke E. H. P., *Vibr. Spectrosc.* **1**, 383 (1991).
- 94KON Konings R. J. M., private communication (1994).
- 94LYU/GUR Lyutsareva N. S., Gurvich L. V., Yungman V. S., Khomichev S. A., *Zh. Fiz. Khim* **68**, 2100 (1994).